AN INVESTIGATION INTO THE USE OF LIPID MATRICES FOR THE CONTROLLED RELEASE OF THERAPEUTIC AGENTS

by

Nurzalina Abdul Karim Khan

Thesis submitted for the degree of Doctor of Philosophy
in the Faculty of Medicine, University of London

The School of Pharmacy, University of London

November, 2000

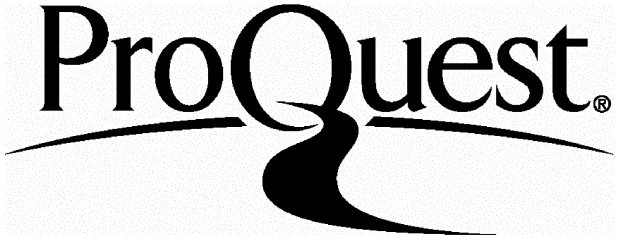

ABSTRACT

The variety of components within Gelucires® can result in complex carrier characteristics ranging from polymorphic changes to the interaction of added drugs with the carrier components. Paracetamol, a weakly acidic drug with a pKa of 9.5 and a 1 in 70 solubility in water together with caffeine, a weakly basic drug with a pKa of 13.9 and a 1 in 60 solubility in water, were incorporated into Gelucire 50/13. The effects of the different drugs and their loadings at 5, 10, 20 and 30% w/w were established.

Hot-Stage Microscopy (HSM) coupled with a Differential Interference Contrast (DIC) facility and Differential Scanning Calorimetry (DSC) showed that the addition of paracetamol caused a marked change to the matrix by stabilising the lowest melting form of the gelucire whereas caffeine did not significantly affect it. Dissolution studies together with erosion and water uptake studies were performed in distilled water at 37°C. A difference in the contributions of erosion and diffusion as mechanisms of drug release arose due to the different drugs added and mathematical fittings of the results correlated well with physical measurements. The loadings of drug did not greatly affect the parameters studied.

The effects of ageing the matrices at 20°C and 37°C after 7, 30, 90 and 180 days storage were also investigated. Storage at the higher temperature tempered the matrices to a more stable form and the drug incorporated also influenced the extent of the ageing effect. Ageing resulted in a lowering of the matrix tensile strength as time progressed and higher drug release rates were obtained during dissolution due to a greater contribution of erosion as the release mechanism. Scanning Electron Microscopy (SEM) studies revealed that the addition of a sterically compatible emulsifier such as sorbitan monostearate inhibited the blooming of stable crystals on the surfaces of the matrices.

Science without religion is lame,

religion without science is blind.

Albert Einstein

ACKNOWLEDGEMENTS

I would like to thank my supervisor Professor Duncan Q. M. Craig for his guidance and Universiti Sains Malaysia, Penang, for generously sponsoring my studies. In addition, I would like to extend my thanks to Gattesfossé for providing the gelucire samples used in the studies.

I am indebted to my colleagues in the Pharmaceutics Department especially Keith and Brian for their technical help and Dr. Basit, Douglas, Rajesh, Kevin, Manisha and Vicky for their friendship and valuable support. I am also very grateful to Dave McCarthy for his assistance and patience with my numerous SEM samples.

On a personal note, I would like to thank my family in Malaysia for their prayers and my friends in London especially Patricia for their warmth and loyalty. Last and certainly not least, a special thank you to Enrico for his unwavering support, constant encouragement and total belief in me, and also for pulling me out of the snow!

TABLE OF CONTENTS

CHAPTER 2 : Investigations into the G50/13 matrix structure using Differential Scanning Calorimetry (DSC)

CHAPTER 3 : Morphological studies using Differential Interference Contrast (DIC) Microscopy

LIST OF FIGURES

CHAPTER 9

LIST OF TABLES

CHAPTER 7

CHAPTER 8

CHAPTER 9

APPENDIX 3

LIST OF PLATES

CHAPTER 7

Part I

Part II

LIST OF SYMBOLS AND ABBREVIATIONS

G50/13	Gelucire 50/13
PEG	polyethylene glycol
HLB	hydrophile-lipophile balance
α, β', β	polymorphic forms of lipids
PLP	fatty acid residues Palmitic-Linoleic-Palmitic (C_{16} - $C_{18:2}$ - C_{16})
E	Elaidic ($C_{18:1}$ *trans*)
O	Oleic ($C_{18:1}$ *cis*)
S	Stearic (C_{18})
PVAc	polyvinyl acetate
HPMC	hydroxypropylmethylcellulose
HPLC	high performance liquid chromatography
DTA	differential thermal analysis
DSC	differential scanning calorimetry
ΔH_f	heat of fusion
L/M/HMF	low/middle/high melting fractions
DIC	differential interference contrast
OPD	optical path difference
HSM	hot stage microscopy
t_{onset}	onset temperature of melting
t_m	end temperature of melting
E-W	east-west orientation
N-S	north-south orientation
SEM	scanning electron microscopy
RH	relative humidity
SMS	sorbitan monostearate
ANOVA	analysis of variance

CHAPTER 1: INTRODUCTION

1.1 Gelucires

Gelucires are a family of inert pharmaceutical excipients consisting of mono-, di- and triglycerides and of mono- and diesters of fatty acids and PEG (polyethylene glycol). In addition, some of the corresponding free fatty acids and PEGs are present in small quantities. Derived from natural food-grade fat and oils, they are well tolerated by the body and thus can be formulated into oral formulations (Gattefossé,1983).

1.1.1 Properties of gelucires

Gelucires are characterised by two numbers. The first is the melting point which is only an approximation since the numerous components of gelucire cause it to melt over a range of temperatures rather than to be in the possession of one sharp melting point. The second is the hydrophile-lipophile balance (HLB) number which reflects the proportion of the water dispersible parts to the fat soluble parts in each gelucire. The nomenclature range is from 33 to 70 for the first number and from 1 to 18 for the second. These ranges are not exhaustive as more gelucires could be manufactured in the future which would extend the variety, and in addition, some glyceridic carriers which are technically gelucires could be classified differently for marketing purposes. For example, G70/02 which is glyceryl tribehenate is also called Compritol 888 (Ratsimbazafy et al, 1997). Some of these gelucires are represented in Figure 1.1.

Table 1.1: The HLB values of gelucires arise from the contributions from individual components (Craig, 1996):

Component	HLB value
triglycerides	1-2
diglycerides	2-3
monoglycerides	3-4
PEG diester of fatty acids	6-15
PEG monoester of fatty acids	10-15

Figure 1.1: Some of the gelucires available (Gattefossé,1983).

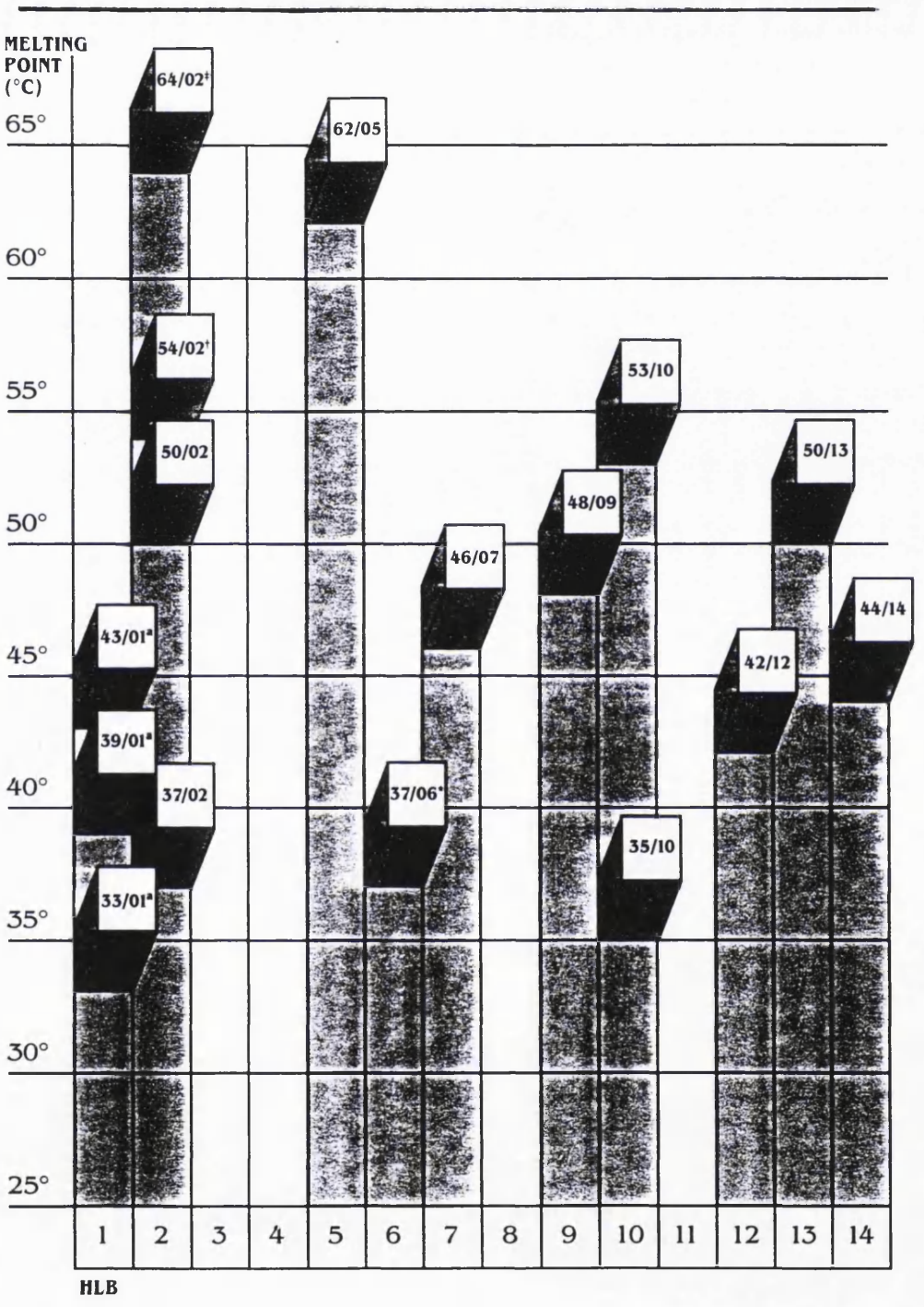

Keys to Figure 1.1:

[a] Semi-synthetic glycerides.

[†] Trade name Precirol (glyceryl palmitostearate).

[‡] Trade name Precirol WL-2155 (glyceryl stearate).

* Trade name Labrafil M-2130BS.

The overall HLB value is the function of the percentage of the component in the gelucire and its HLB value. To illustrate the association between HLB numbers and gelucire constituents which is represented by Table 1.1, G44/01 which has a low HLB number consists of a triglyceride mixture with its fatty acids ranging from C12 to C18. On the other hand, G55/18 has a high HLB number as it is only composed of PEG 6000 esters of fatty acids without any glycerides at all.

The mixture of hydrophilic PEG esters and hydrophobic glycerides confer many favourable properties to these materials. Other lipid based matrices have tended to require the incorporation of soluble surfactants that produce a wetting action in order to improve the release of drugs. When using gelucires however, there is no need for such surfactants due to the amphiphilic nature of the bases. More specifically, the role of surfactant is taken by the mono- and diesters of PEG, while the monoglycerides act as co-surfactants, and the di- and triglycerides act as the oily phase (Roussin and Laforêt, 1997). In addition, the thixotropic nature of the gelucires means that active ingredients which are heat sensitive can be incorporated when the base is kept liquid by stirring and be allowed to set in the dosage forms when removed from the stirrer (Gattefossé, 1983).

1.1.2 The production of gelucires

The two methods used for producing gelucires are direct esterification and alcoholysis. Gelucires are manufactured mainly through the latter by hydrolysing coconut/palm/palm kernel oil, followed by fractional distillation of the free fatty acids produced (Chow, 2000). Hydrolysis can be autocatalytic, catalysed by metals or the enzyme lipase (Pike, 1980). The fatty acids are then hydrogenated and esterified with PEG (usually of the molecular weight grades ranging from 300 to 1500) at 230°C under nitrogen atmosphere.

$$\text{Triglycerides} + \text{water} \longrightarrow \text{Fatty acids} + \text{glycerol} \qquad (1)$$

$$\text{Fatty acids} + \text{PEG} \longrightarrow \text{PEG esters of fatty acids} + \text{water} \qquad (2)$$

Direct esterification involves esterifying palmitic acid, stearic acid and selected fatty acids extracted from directly hydrogenated coconut or palm kernel oil, with glycerol and PEG or by inter-esterification of the hydrogenated oils to form the mixed glyceride component.

Fatty acids + PEG $\longrightarrow$ PEG esters of fatty acids + water (3)

Fatty acids + glycerol $\longrightarrow$ glycerides + water (4)

Structural representation of the processes:

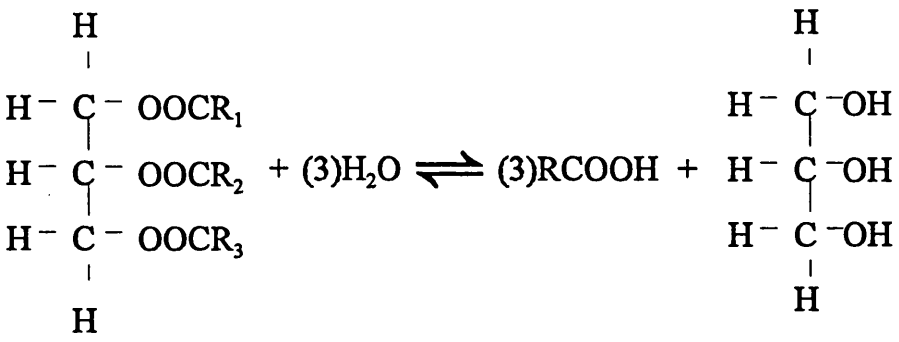

glycerides fatty acid glycerol

R = H or $CH_3(CH_2)_n$ where n is 0,1,2,.....etc. Structure represents a monoglyceride when two of the OCR moieties are replaced by H atoms, a diglyceride when either OC-R_1, R_2 or R_3 is replaced by a H atom and a triglyceride when R_1, R_2 and R_3 are H or $CH_3(CH_2)_n$. For example, in G50/13, n is mainly 10, 12, 14 and 16.

fatty acid PEG PEG monoester of fatty acid

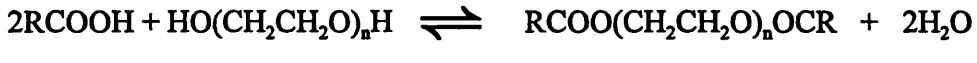

PEG diester of fatty acid

where n = 1,2,3....etc. For example, in G50/13, n = 33 or 34

Direct esterification is used when the gelucire does not contain the PEG component, for example glyceryl palmitostearate (G54/02 or commercially known as Precirol) and the process does not require a catalyst (Armstrong, 2000).

1.1.3 Applications of gelucires

There are many different gelucires available with a wide range of melting points and HLB values giving properties suitable for a breadth of functions. As mentioned before, the behaviour of the gelucires also depends on the proportion of the hydrophilic and lipophilic components within them, with the more lipophilic bases suitable as oily vehicles and ointments, and the more hydrophilic bases suitable as for example, bioavailability enhancers (Table 1.2).

Table 1.2: Some of the uses of gelucires depending on their composition (Gattefossé, 1996).

Types of gelucires	Composition	Uses
33/01 39/01 43/01	glycerol esters of fatty acids	vehicle, oily phase for ointment.
44/14	PEG- glyceryl laurate	emulsifier for solid and semi solid Self MicroEmulsifying Drug Delivery Systems, bioavailability enhancer.
50/13 53/10	PEG-glyceryl palmitostearate PEG- glyceryl stearate	hydrophilic glyceride for semi-solid formulations.
50/02 50/13 54/02 70/02	cetyl palmitate PEG-glyceryl palmitostearate glyceryl palmitostearate glyceryl tribehenate	coating and matrix agents for sustained release formulations.

Gelucires may be prepared as dosage forms via a number of routes, one of the most promising being liquid filled hard gelatin capsules (Waginaire and Glass, 1981; Burns et al, 1996a,b). This type of formulation has several advantages over conventional capsules including the improvement of dose uniformity of high potency drugs and a better control of dust levels (Shah et al, 1996). The number of components in the formulation can be reduced for simplicity as there is no longer a need for functional excipients such as lubricants, glidants, binders and disintegrants. Industrial scale-up is easier to achieve as the conditions that would produce small quantities for research and development would be simple to reproduce in the manufacturing stage (Baykara and Yüksel, 1991). Melt dispersion or melt-fusion technology, as will be used in the current project, on top of being simple and cost effective, also eliminates the danger of working with organic solvents (Flanders et al, 1987; Bodmeier et al, 1992).

Other advantages of using gelucires include those of oily, liquid, unstable or hygroscopic drugs, low apparent density materials and active ingredients that are sensitive to light or air can now be formulated with gelucires and filled into hard gelatin capsules. Doelker et al (1986) incorporated benzonatate (oil-soluble, sensitive to light and air), nicotinic acid (hygroscopic), chloral hydrate (hygroscopic and unstable) and paramethadione (oil soluble and toxic) into various gelucires including G50/13 and filled the mixture into hard gelatin capsules. It was found that depending on the drug, incorporation was more successful with certain gelucires than others. Here, the balance between the melting point and HLB proved critical as the chances of incompatibility of excipients with such drugs are higher. Chloral hydrate for example, reduced the melting points of the gelucires to the extent that leakage from capsules which contained G33/01, G44/14 and G50/13 was observed. Nicotinic acid was not miscible with the low melting point and HLB gelucires, G33/01 and G37/02, and the mass had to be thickened in order to prevent the phases from separating. On the other hand, the very hydrophobic drug paramethadione showed highly favourable dissolution profiles after being incorporated into gelucires. The difference in the gelucire used also gave a range of release rates for the same drug (Figure 1.2).

In gelucires which did not disintegrate in the dissolution medium such as G35/10 and G50/02, very low release of benzonatate was observed. For G35/10, this retardation was

thought to be due to the formation of a hydrated layer around the matrix which impeded the disintegration of the mass. As dissolution progressed, the difference in the release profiles appeared to be associated with the melting points and HLB values as exemplified by G33/01 and G37/02. The gelucire grades with high HLB values such as G44/14 and G50/13, gave elevated rates of drug release and availability, similar to the dissolution profile of the soft capsule formulation already available on market (Tessalon®). Therefore, the different grades of gelucires can provide a choice of controlled release formulations.

Figure 1.2: Release profiles of benzonatate from various grades of gelucires (Doelker et al, 1986).

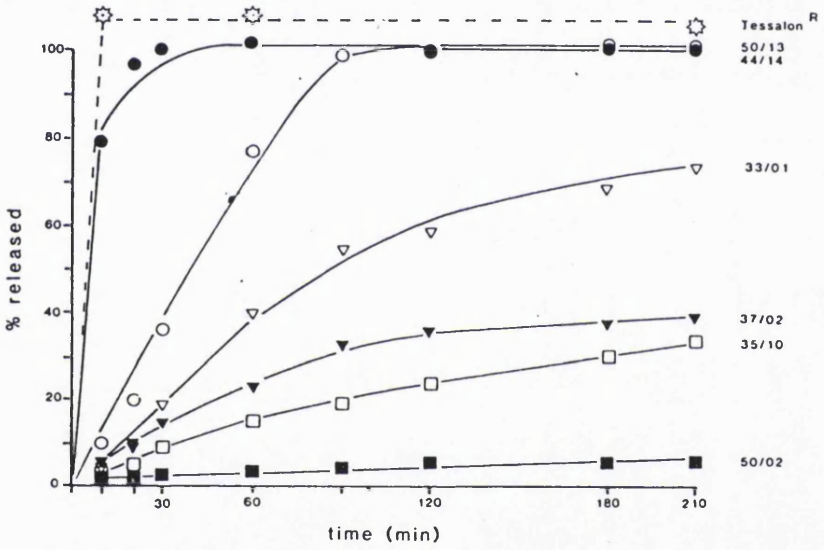

Raising the HLB values and lowering the melting points of gelucires resulted in the elevated release of theophylline derivatives (Ortigosa et al, 1991; Ratsimbazafy and Brossard, 1992). An increase in the melting point by 18°C reduced the kinetics of theophylline dissolution approximately by half. It was then suggested that for a fast-release formulation, a gelucire with a melting point of about 37°C and HLB greater than 10 is required whereas for a sustained-release formulation, melting point of about 50°C and low HLB is required instead (Ortigosa et al, 1991). A first order relationship between the amount of drug released and the HLB values of the gelucires was discovered (Howard and Gould, 1987; Baykara and Yüksel, 1991). This relationship held for the release of water soluble salicylic acid from a series of G48/09 and G62/05 blends that have different HLB values but not for the release of the poorly water soluble tioconazole (Howard and Gould,

1987). Therefore the hydrophobicity of a drug can be the more dominant factor than the HLB value of the vehicle.

1.1.4 Gelucires as excipients in controlled-release formulations

Controlled-release dosage forms are able to give a smoother, more sustained and prolonged drug absorption into the body. This overcomes the recurrent problem of conventional dosage forms, which release the drug very rapidly in the beginning possibly reaching a toxic level followed by a sudden fall in the drug concentration in the blood as biological processes such as metabolism, elimination and excretion come into play. For certain conditions, this leads to a reduction in the pharmacological activity and thus, a sustained therapeutic effect cannot be achieved. Plasma concentration profiles of these dosage forms are compared in Figure 1.3.

Figure 1.3: Diagrammatic illustration of the drug plasma concentration variation with time on ingestion of various oral dosage forms (reproduced from Huet de Barochez et al, 1989).

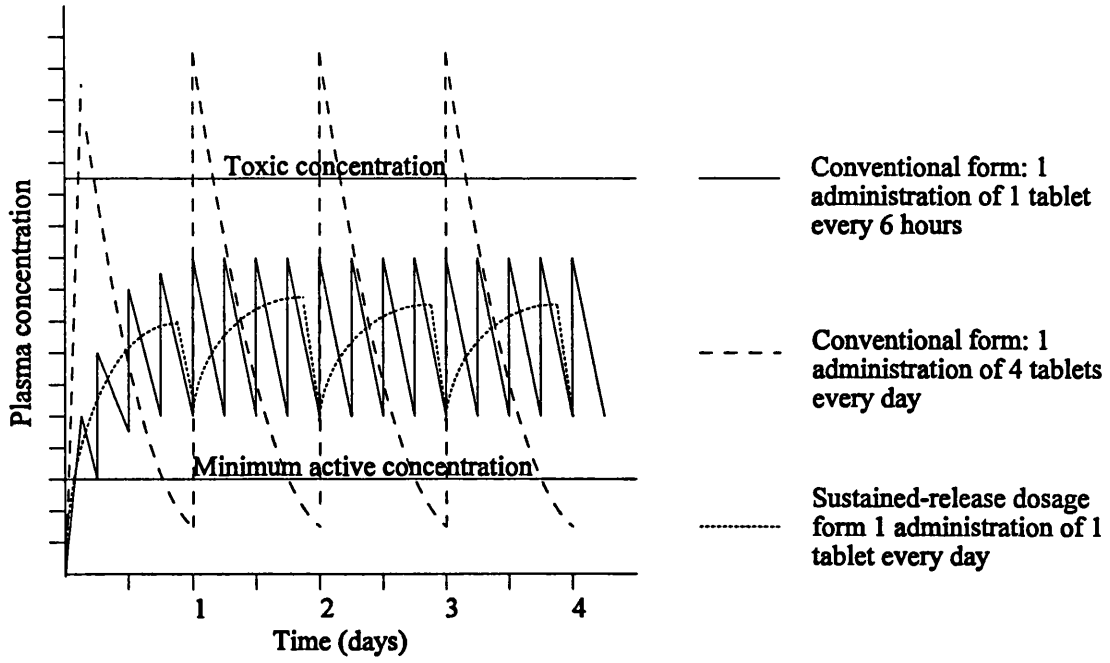

Controlled-release formulations can also remove the need of frequent administration for drugs that have short half-lives due to their rapid elimination from the circulation.

Formulation with gelucires demonstrated that the action of a drug with a short biological half-life, such as nifedipine, was prolonged and in addition, the bioavailability of this poorly water soluble drug was enhanced (Vila-Jato et al, 1990; Remunan et al, 1992a). Such formulations have also been shown to present less fluctuations of the drug concentration in the plasma. Lipophilic drugs dispersed in gelucires will be taken up by the lipoproteins, especially the chylomicrons, into the lymphatic system. The lymphatic system is the usual transport system for fats and fat soluble drugs (Gurr and Harwood, 1991; Charman and Stella, 1991). This system bypasses the liver, hence avoiding metabolism and this is one of the methods thought to be responsible for the enhancement of the bioavailability of such drugs (Aungst and Hussain, 1992; Burns et al, 1996b).

These formulations do not have to be limited to poorly soluble drugs as they can be utilised for the modification of the release of soluble drugs, such as oxprenolol (Baykara and Yüksel, 1991) or salbutamol (Esquisabel et al, 1996). The inconvenience to the patient brought about by repetitive dosing can be abolished as a single dose can release enough drug to sustain the necessary pharmacological effect throughout a long period of time before metabolism and excretion dominate. When the frequency of drug dosing for chronic diseases is reduced, the patient compliance improves (Eraker et al, 1984). Harmful side-effects due to the accumulation of drug when the next dose is given before the plasma concentration of the previous dose has not fallen sufficiently can also be minimised (Linhardt, 1989).

The potential of gelucires as controlled-release matrices has also been demonstrated by other studies. The release rates of lithium sulphate, a water-soluble drug used typically to treat mania, can be decreased by increasing the melting points of the gelucires utilised (Bernasconi et al, 1985; Vial-Bernasconi et al, 1987). G62/05 matrices gave the lowest rate of release followed by G48/09 and G46/07 respectively. In addition, the release rate can be modified by varying the concentration of this water soluble drug, that is, elevating the loading of lithium sulphate resulted in an increase in its release from G46/07 matrices. The release of an unnamed water soluble drug with a short half-life could be controlled by liquid filling it with gelucires into hard gelatin capsules (Huet de Barochez et al, 1989). A slower release was obtained using G50/02 than G50/13 due to the lower hydrophilicity of

the former but the release was even slower with G62/05 due to its higher melting point. More importantly, a sustained release profile had also been shown for poorly water soluble drugs, such as indomethacin (Vial-Bernasconi et al, 1995). A mixture of G33/01 and G46/07 was used and liquid filled into hard gelatin capsules after being melt-fused with the drug. Due to the erosional nature of the release, the gelucire formulation was found to be particularly suitable for poorly water soluble drugs.

The lipid nature of the gelucires can also be exploited for controlled release purposes. Seta et al (1988) demonstrated that the effect of captopril was enhanced in dogs when the drug was formulated in gelucires. This was because the oily matrices decreased the gastrointestinal motility, thus allowing more time for the drug to be taken up at its specific absorption site. A novel delivery system, Hepatic Avoidance using Lymphatic Output (HALO™), uses the principle of lipophilic drugs being able to bypass metabolism by the liver when formulated into lipid matrices, as had been previously mentioned (Barnwell et al, 1994,1996). By adding G50/02 into the sustained-release component of the system, the bioavailability of drugs such as propanolol was not only increased but the lymphatic delivery of the drug was also maintained over a required period of time. This system was also able to produce a biphasic release profile, that is fast release followed by sustained release, by utilising various gelucires in the same formulation (Burns et al, 1996a,b). G33/01 was incorporated into the fast release phase because its solidification prevented the leakage of the phase from the capsules but at the same time was able to melt at the body temperature of 37°C. G50/02 was used as the other phase because its combination of melting point and HLB value allowed it to function as a solid erodible matrix which gave a sustained release profile.

Although the primary use of gelucire is for the liquid filling of hard gelatin capsules, other dosage forms are also possible, as explored by many studies. A variation to this liquid filling into capsule method is the creation of a controlled-release formulation within the hard gelatin capsules, as studied by Bodmeier et al (1990). This gives a good alternative to sustained-release formulations consisting of compressed tablets, which have encountered problems because the compaction energy causes the wax to melt and start to pick and stick. In order to minimise these picking and sticking, dilution of these waxes with inert fillers

is necessary. In the fluidized bed technique, hard gelatin capsules are filled with wax-powder mixture and heated within the capsules. When the melt cools to solid, a sustained-release formulation is obtained, without the need of melt/solvent granulation, the preparation of sustained release beads nor the addition of inert fillers (Bodmeier et al, 1990).

Means of filling the hard gelatin capsules by other techniques were examined. Granules of drug and gelucire could be prepared from either the melt or solvent method and filled into the capsules (Brossard et al,1991). Granules of quinidine sulphate and gelucire made through the solvent method were found to give rapid drug release but the granules made through melt-fusion gave slow and incomplete release instead (Saraiya and Bolton, 1990). However, the same solvent granulation technique was able to produce prolonged release granules for theophylline. Again, the rate was dictated by the amount of gelucire used. The fluid-bed technique can also be used to coat drug granules with gelucire which had been dissolved in a solvent (Delgado-Charro et al, 1991, 1992). This coating led to the prolonged release of amoxycillin and the profile was very sensitive to the amount of gelucire used.

The controlled-release potential of gelucires has also been studied using oral spheres, formed by dispersing the drug in a polymer such as Eudragit and coating the dried resultant spherical beads with liquid gelucire (Magron et al, 1987; Laghoueg et al, 1989). A constant rate of drug delivery in synthetic gastric liquid was obtained from this core and shell type of dosage form for sulfanilamide and sodium salicylate. Moreover, it was discovered that the rate of drug delivery could be controlled by the thickness of the gelucire shell. Oral spheres could also be formed by dispersing the drug in the gelucire itself as the polymer/ co-polymer matrix and forming the spheres from this paste (Bidah and Vergnaud, 1990; Bidah et al, 1991,1992). When sodium salicylate was formulated into these spheres, the rate of release was found to be proportional to the area of the device.

Tablets such as those fabricated by Vila Jato et al (1990) and Remunan et al (1992a) by forming granules using melt or solvent methods and compressing them, are also possible controlled-release dosage forms. Both in vitro and in vivo studies showed that the release of nifedipine could be controlled by incorporating them into these forms. Microparticles

formed by emulsifying drug-gelucire melt in a heated aqueous phase followed by cooling to room temperature to congeal them, could also be compressed into tablets or made into an aqueous sustained release oral suspension dosage form (Bodmeier et al,1992). By this method, it was found that high loadings of water insoluble drugs such as ibuprofen could be incorporated into the microparticles, which were then able to give a yield of more than 90% during release.

1.1.5 Gelucire 50/13

In the current study, G50/13 was chosen as the model gelucire. It has a sufficiently high melting point in order to form a semi-solid matrix and a balance of components which could allow both hydrophobic or hydrophilic drugs to be incorporated into it (Table 1.3).

Table 1.3: Composition of Gelucire 50/13 (Gattefossé data sheet, 1992) (also Appendix1)

The proportions of each G50/13 component	
Monoglycerides	5%
Diglycerides	8%
Triglycerides	8%
PEG monoester	29%
PEG diester	43%
Composition of the fatty acids within the lipid components	
Caprylic acid (C8)	< 3%
Capric acid (C10)	< 3%
Lauric acid (C12)	< 5%
Myristic acid (C14)	< 5%
Palmitic acid (C16)	40 to 50%
Stearic acid (C18)	48 to 58%

Semi-solid matrix (SSM) technology using G50/13 have been shown to improve the bioavailability of poorly water soluble drugs. Bowtle et al (1986) investigated in-vivo the

feasibility of using this base for the release rate control of fenoprofen and found that the half-life of the drug was increased five-fold together with the best drug availability, in comparison with formulations incorporating PEG 2000 and Myverol 18/07. The feasibility of using G50/13 to increase bioavailability was also studied with another short half-life, poorly water soluble drug, ketoprofen (Dennis et al, 1990). The matrix with pure G50/13 was found to release the drug too rapidly in-vitro and thus mixed with G50/02 in 3:1 ratio. Even though this formulation showed good availability when investigated in-vitro, it did not show a similar result in-vivo although the in-vivo result was still comparable to a marketed product.

G50/13 has a HLB value which is high enough to promote drug release. The releases of theophylline and its derivatives from G50/02 and G50/13 were compared in order to eliminate the melting point influence and it was found that as the HLB value rose, the drug release increased correspondingly (Ortigosa et al, 1991; Ratsimbazafy and Brossard, 1992). This could be due to the G50/13 being more hydrophilic which facilitated the diffusion through the matrix of a drug which was not too lipophilic, as shown by the larger apparent diffusion coefficient, D' (Refer to Section 1 in Chapter 4). This hydrophilicity can be ascribed mainly to the PEG component as 80% of G50/13 is made up of PEG esters of fatty acids. Moreover, the PEG component in G50/13 has the nominal molecular weight of 1500. PEG 1500 had been shown to give a release which was in between a rapid release (as did PEG 1000) and a slower release profile (as did PEG 6000) (Shehab et al, 1996a).

Mixing G50/13 and G50/02 together in a matrix further revealed that as the proportion of G50/13 increased, the release not only rose but the mechanism of release also became less diffusional (Kopcha et al, 1991). G50/13 can also increase the availability of the drug for release. In a study whereby a matrix was formulated with various proportions of Precirol ATO-5 (G53/02) to G50/13, it was found that the release of theophylline and propanolol was less than 5% and 20% respectively from pure Precirol ATO-5 matrices even after 24 hours of dissolution. As the proportion of the G50/13 increased, the release of the drugs was boosted and the total release was completed in 8 to 12 hours for pure G50/13 matrices (Bodmeier et al, 1990). The cumulative amount of oxprenolol released was also the highest for G50/13 after 7 hours of dissolution compared to other gelucires of various melting

points and HLB values (Baykara and Yüksel, 1991).

On the other hand, G50/13 has a melting point high enough for controlled release and will not soften at the body temperature of 37°C. Some retardation of sodium salicylate in the urinary excretion of human volunteers was found when aspirin mixed with G50/13 in hard gelatin capsules was administered (Djimbo et al, 1984). As mentioned previously, even though G50/13 has the nominal melting point of 50°C, it would be more accurate to describe it as a melting range due to the existence of the various components. The melting points of just the main fatty acids that make this gelucire up are given below (Table 1.4). In addition, PEG 1500 which is the PEG incorporated into G50/13 has a melting point between 42-45°C (Ford et al, 1984).

Table 1.4: The melting and boiling points of the main G50/13 fatty acids (Gunstone, 1994).

Chain length (C_n)	Systematic name	Trivial name	Acid melting point (°C)	Acid boiling point (°C)
12	dodecanoic	lauric	44.8	130
14	tetradecanoic	myristic	54.4	149
16	hexadecanoic	palmitic	62.9	167
18	octadecanoic	stearic	70.1	184

G50/13 exhibited a gelling ability which meant that even at high temperatures, which were close to its melting range, its matrices were still pliable and able to maintain their integrity which was important for sustaining its controlled-release properties (Kopcha et al, 1991). In an aqueous medium, G50/13 showed a degree of solubilization and disintegration but stayed intact which allowed salbutamol to be completely released in 8 to 10 hours thus achieving a sustained release profile (Esquisabel et al, 1996). This capacity to alter its dimensions whilst still retaining appropriate release behaviour was also demonstrated by its ability to swell about twice more than that shown by G35/10 but without significantly altering the release rates (Prapaitrakul et al, 1991).

Incorporation into a variety of gelucires of a basic drug which existed in two different polymorphic forms showed that the best profile for a prolonged release was demonstrated

by G50/13. The drug which was soluble in G50/13 was also converted to its most stable form in the carrier (Mouricout et al, 1990). Drugs which are normally difficult to formulate such as those which are oily liquids, sensitive to air and light, hygroscopic or deliquescent were found to give the most favourable release profiles when incorporated into G50/13 matrices (Doelker et al, 1986).

1.1.6 Manufacturing factors that affect gelucire behaviour

The properties of gelucires can be affected by the preparation conditions used to manufacture the matrices. Cooling rates appeared not to only affect the structure of the carrier as elucidated from thermal analysis but also the dissolution behaviour (Sutananta et al, 1995b). Theophylline release from G55/18 was shown to be markedly different in samples which were slow-cooled or rapidly-cooled during matrix setting, not only in terms of release rates but also release mechanisms. G50/13 also exhibited a dependence on the cooling rate with the slow-cooled samples giving a greater release than the fast-cooled samples. However, the difference in the G55/18 system was attributed to the variation in the crystal structure of the samples whilst the difference in the G50/13 was associated with the redistribution of constituents within the sample. This demonstrates the need to remove all thermal history from such glyceridic bases by heating them above their melting points so that the performance of new formulations are not affected by previous manufacturing processes.

The melt-fusion process for the fabrication of matrices is the method frequently used for gelucires. One of the first sets of investigators advocating this method was Sekiguchi and Obi (1961) who dispersed the poorly soluble sulphathiazole in the soluble carrier, urea, which resulted in the rapid release of the drug. The dispersion of finer drug crystallites within the matrix could also be achieved by quenching a supersaturated drug/carrier mixture from a high temperature (Chiou and Riegelman, 1971). This type of dispersion would be superior to the fine drug particles produced by grinding, milling, etc. because the latter could exhibit agglomeration and poor wettability in water. One of the drawbacks of this technique is that heating is necessary and for drugs which are volatile or those which readily decompose, fusion at high temperatures is not viable. It is important therefore, to

select a gelucire with a melting range low enough if such drugs are to be incorporated. One advantage that gelucire offers is that it is thixotropic and can remain fluid at low temperatures with constant stirring (Gattefossé, 1983).

1.2 Controlled-release formulations and their mechanisms of drug release

In general terms, controlled release formulations can be divided into three broad categories which reflect the mechanisms that are responsible for their actions; diffusion, osmosis and polymer erosion (Heller, 1984). However, these categories are not exclusive as each formulation can be governed by more than one mechanism. For example, rate of drug release from erosional devices is usually modulated by both diffusion and erosion processes whilst rate of release from osmotic devices is controlled by the diffusion of water across a semi-permeable membrane combined with osmotic forces.

Polymer erosion can be further subdivided according to the mechanisms that change the polymer properties. Type 1 erosion involves the hydrolytic cleavage of water soluble polymers that are made insoluble by covalent cross-links. This cleavage can take place at the cross-links themselves or at the backbone of the chain, thus releasing the water-soluble polymers. Type 2 erosion occurs through the hydrolysis, ionization or protonation of a pendant group which would make the polymer soluble in water. Type 3 erosion is like Type 1 except it occurs not in polymers with covalent cross-links but simple insoluble chains made soluble by backbone cleavages which release small molecules. Again, these classifications are not exclusive and an erosional process can be a combination of the above categories. Erosional processes are designed to give a zero-order rate of release, so that release is constant over a period of time. However, a completely zero-order release is difficult to obtain because frequently, the diffusional process also play a part in drug release in a particular controlled-release matrix.

Diffusional release follows a square-root of time profile, as described by Higuchi (1963). A matrix with a drug dissolved or dispersed in it, when placed in a dissolution medium which is thermodynamically compatible with the polymer, will swell with the formation of a polymeric gel phase (Peppas et al, 1980). Even though such a process is frequently quoted

for hydrophilic polymers such as HPMC, it could also be applied to a certain extent to hydrophilic gelucires like G50/13 because those gelucires are also composed of long repetitive hydrocarbon chains, moreover esterified with PEG chains which give them the hydrophilic character. In addition, many studies concerning gelucires have reported the swelling of matrices incorporated with the carriers. Diffusion can be diagrammatically represented as below (Figure 1.4) if the process is taken to come from a single surface of the matrix, for simplicity.

A is an inert substrate, B is the solvent-free polymer, C is the swollen polymeric gel and D is the surrounding swelling medium. $X_*(t)$ is the position of the polymer/gel interface, L_o is the initial thickness of the matrix tablet and L(t) is the position of gel/medium interface.

Figure 1.4: Diagrammatic representation of drug diffusion in a swellable polymer.

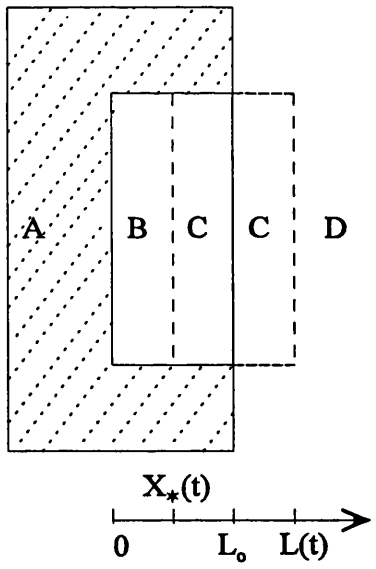

If D_1 and D_2 are the drug diffusion coefficients in the dry polymer and in the gel-like phase respectively, then ϵ is the diffusitivity ratio D_1/D_2. β is a dimensionless constant described by M_sS_0/ρ where M_s is the molecular weight of the medium, S_0 is the initial concentration of the medium and ρ is the density of the medium. ξ_* is the dimensionless position described by X_*/L_0 (see Figure 1.4). C_* is the concentration of the drug at the polymer/gel interface. The relationship between all these parameters is evident in the equation describing the position of the polymer/gel interface (Equation 1.1) (Peppas et al, 1980).

$$\frac{1-\xi_*}{\xi_*} = \frac{C_*(1-\beta)}{2\varepsilon(1-C_*)} \times \frac{1}{\exp(-\pi^2/2\xi_*)} \qquad \text{....Equation 1.1}$$

When a matrix is placed in a liquid medium, the drug within it will diffuse outwards while a countercurrent diffusion of the medium, D, into the matrix occurs. This relaxes the polymer and a gel-like swollen layer is formed. The interface between the dry polymer and the gel phase is a constantly moving front. As dissolution progresses, the interface recedes and the gel layer thickens. The drug now has a longer distance to travel with the added tortuosity and therefore, the release is slightly retarded, giving the square-root of time kinetics. More details of these erosional and diffusional processes will be given in Section 1 of Chapters 4 and 5.

1.3 Fatty acids and glycerides

Although gelucires have already been used for a variety of purposes, comparatively little is known regarding their physical and performance characteristics. This is partly due to the wide range of different components making up the gelucires, as exemplified by G50/13 (Table 1.3), resulting in physical and chemical complexity. Even small concentrations of the minor constituents can influence the solidification and melting characteristics of a fat which is made up of several components (Dimick, 1991).

The different components can exert individual effects or interact between each other to influence the characteristics of the gelucire matrix. Moreover, the glyceride and fatty acid components may show polymorphism which can have additional effects on the matrix behaviour. The occurrence of polymorphism in lipids will be discussed in the following section.

1.3.1 Polymorphism in fatty acids and glycerides

Polymorphism is a phenomenon that has long been established to occur in fatty acids. It is defined as "the ability to reveal different unit cell structures in crystal, originating from a variety of molecular conformations and molecular packings" (Sato and Garti, 1988) or in other words, the ability of a substance to exist in more than one crystalline form. The

existence of polymorphs is an important factor to consider in the formulation of fatty materials, as the individual forms also exhibit unique melting points and stabilities which can affect properties such as dissolution rates and bioavailability of drugs incorporated in these fat matrices. In some cases, these characteristics can be exploited and a certain polymorphic form with a particular dissolution rate or stability for example, is formulated into a dosage form.

Polymorphism in lipids arises from the molecular packing adjustments of the fat components (Chapman, 1962). One dimensional polymorphism caused exclusively by a different stacking sequence of the long chain lamellae in a particular direction is called polytypism. These phenomena are controlled by external conditions and also thermodynamic stability. The thermodynamic stability is determined by a relationship that includes the Gibbs energy;

$$G = H - TS \qquad \text{....}\textit{Equation 1.2}$$

where G is the Gibbs free energy, H is the enthalpy, S is the entropy and T is the absolute temperature in Kelvin. At the most stable state, that is the equilibrium state, Gibbs energy is at its lowest (Wunderlich, 1990). Each polymorph in polymorphic substances has its own Gibbs free energy curve as a function of temperature (Aronhime, 1988). The polymorph with the lower Gibbs energy is the stable form at that particular temperature. At a temperature of transition, two phases are in contact and at an equilibrium therefore the stability of both phases must be equal. This means that the G values per mole of each phase must also be equal at the given temperature and pressure.

There are two types of polymorphism:

i) enantiotropic ii) monotropic.

The transformation and crystallisation processes of, for example, a simple fatty acid with only two polymorphic forms, A and B are illustrated below (Sato and Garti, 1988):

i) Enantiotropic- when each form is thermodynamically stable in a definite range of temperature and pressure;

a) the more stable forms will crystallise at all temperature when the Gibbs energies of A

and B, G(A) and G(B), cross at T_o and a reversible solid state transformation occurs (Figure 1.5).

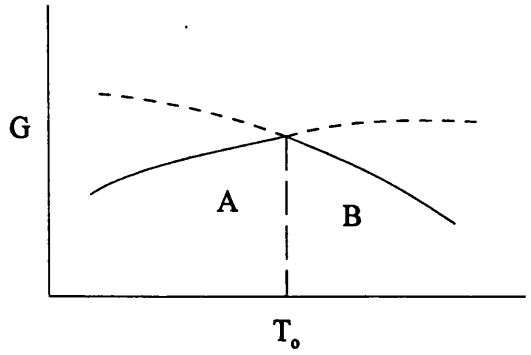

Figure 1.5

b) both forms can crystallise at temperatures where unstable forms can metastabilise, when G(A) and G(B) cross at T_o but irreversible solid-solid transformation from both A to B ($T > T_o$) and B to A ($T < T_o$) are kinetically hindered. If the solid state transformation from A to B occurs below the melting point of B during melt crystallisation, then B solidifies; if not A or B can solidify (Figure 1.6). In the usual case, A converts to B at T'_o below the melting point of B.

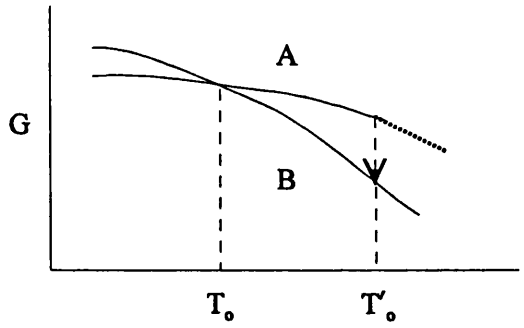

Figure 1.6

ii) monotropic - one of two forms is thermodynamically unstable. Either A or B can form below both their melting points due to competition between crystallisation and transformation if G(A) and G(B) do not cross. In melt-mediated transformation, B will recrystallise from the melt formed by rapid melting of A (Figure 1.7).

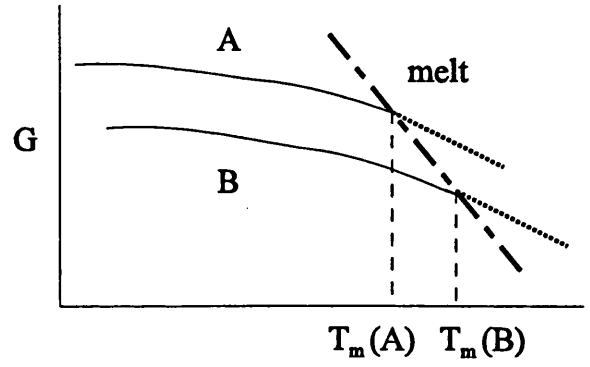

Figure 1.7

Although enantiotropic transformations show endothermic reactions during heating, monotropic transformations can also display exotherms during heating, that is, when the more stable form has a lower heat content than the transforming form (Aronhime, 1988). The phase transitions in lipids are usually monotropic. For triglycerides however, the transition is always monotropic, that is, it occurs from the less stable to the more stable polymorph (Bailey, 1950).

Phase transitions can also be of a first or second order (Hagemann, 1988). In first order transition, the free energy curves are discontinuous. Most triglyceride transitions fall under this category. In second order transitions, only the heat capacity curve is discontinuous because only the molecular movement is increased. There is no heat evolution during the process nor large changes to the crystal structure. This type of transition can occur over a wider temperature range than the first order.

The polymorphs of lipids can exist in forms which are commonly labelled α, β' and β forms, in the order of increasing stability and melting points (Lutton, 1950; Chapman, 1962; Garti et al, 1985). Transformations of one polymorphic form to another also take place in that order (Hoerr, 1960). α is obtained first when the melt of a fat is cooled quickly. The α form then will melt upon heating it slowly but will resolidify in an exothermic reaction into the β' form. Heating this form further will cause it to melt and resolidify finally as the stable β form. Most fats will have the unstable α form and either/ both β' and β forms in the equilibrium state of the lipids (Yoshino et al, 1984). The subcells of α are arranged in a hexagonal, β' in an orthorhombic and β in a triclinic packing in order of increasing density (Hagemann and Rothfus, 1983) (refer to Section 1.3.2 for more details on structural arrangements).

The mechanisms which govern which of the polymorphic forms should crystallise or dominate are complex. In fatty acids, the polymorphic and crystallisation behaviours are dominated by the strong hydrogen bonding between the carboxylic groups, and the packing of the aliphatic chains has a lesser influence (Aronhime et al, 1990). Therefore, transformations occur in solution as it is the interaction between the solvents and the fatty acids that determines the polymorphism. Polymorphism in triglycerides on the other hand,

is dominated by van der Waal interactions and the packing density of the aliphatic chains. Due to the low energy barrier, the transformations for triglycerides can occur through the solid or melt state, and solvent crystallisation here will eliminate polymorphism resulting in only one polymorph being stabilised.

Another of the factors that affect polymorphic transformations is the heating rate and this is related to the postulation that the transformation process occurs in two stages (Aronhime et al, 1987,1988b). One is the liquefaction of the α-form which is affected by slow heating rates, the other is the crystallisation into β-form, which extent is affected by fast heating rates. During a slow heating of fats, a bigger portion of the α-form would undergo solid-state transformation than during faster rates and this is reflected by a decrease in the ΔH_{α}. When faster rates are used, the α-form melts before it could undergo a solid-state transformation and since the succeeding β-form is crystallised from this melt, the transformation is called melt-mediated. On the other hand, very fast heating rates do not allow enough time for the β-form to crystallise. The hydrocarbon chain length also determines the path of transformation. The shorter chains go through solid state because the lower enthalpy of these chains permits such a transformation (Garti et al, 1985,1989).

Lipids which are very similar to each other and which only differ by a few carbon chain length or degree of unsaturation can nevertheless display different polymorphic behaviour. Yap et al (1989b) found that after temperature cycling, palm stearin followed by palm oil were more likely to form β crystals than hydrogenated palm oil and palm olein, for which the β' form was very stable. Repeated temperature cycling resulted in more of the β form appearing. The same investigators (Yap et al, 1989a,b) also found that by adding one oil to another, for example palm oil to canola oil, a particular form can be stabilised. The time at which the second oil is added to the first oil is also important. When the palm oil is added to the canola oil before hydrogenation, the time taken to obtain the β' form was shorter than if added after hydrogenation.

When mixtures of different chain length triglycerides were investigated for their β' to β transformation (Garti et al, 1989), it was found that the orthorhombic form (β') became predominant, even though the triclinic form (β) is the most thermodynamically stable. This

was probably because the β' to β transformation was sterically hindered by the various chain lengths. This confirmed the observation that the β' form is favoured in a mixture of triglycerides, even when the triglycerides were formed from various saturated or unsaturated fatty acids (Garti et al, 1989; Gunstone,1996). The steric factor plays a role when an emulsifier exerts its effect on polymorphic processes, that is when an emulsifier retards the transformation to the more stable form. In tripalmitin crystallisation, the emulsifier was found to retard the transformation of β' to β more than others and this was thought to be due to a stronger interaction between the emulsifier and β' molecules (Sato and Kuroda, 1987). This interaction could result in the blocking of the 180° rotation of aliphatic chains, necessary for the packing of the most stable form (Aronhime et al, 1990).

This inhibiting effect also depends on the heating rate, being stronger during faster heating rate and weaker during slow heating, indicating a kinetic effect. This effect of the emulsifier is attributed to the 'button syndrome', which was first postulated by Aronhime et al (1988b). It was put forward, through molecular modelling, that surfactant holds triglyceride chains by hydrogen bonds and prevents the transformation of α to β . The emulsifier is incorporated among the hydrocarbon chains of the fat, causing the formation of defects which enhance the mobility freedom of the hydrocarbon chain methyl ends therefore predisposing it to the less stable forms, as demonstrated by structural analysis such as X-ray powder diffraction.

For the hydrogen bonds to occur, there must be steric compatibility between the hydrophilic head of the emulsifier and the polar sites of the triglycerides, so that both hydrophobic and hydrophilic interactions are maximised. For example, with sorbitan monostearate, the two hydroxyl groups of the emulsifier point to the carbonyl groups of the two neighbouring triglycerides molecule, causing hydrogen bonds to form. The hydrophilic moiety of the emulsifier must be small enough to allow the insertion within the crystal lattice but bulky enough to perform the 'button syndrome'. Therefore, the requirements of the emulsifier to be a controller of polymorphic transformation are both structural and chemical. However, the presence of the emulsifier does not dictate the formation of any preferred polymorph but rather controls the mobility freedom of the molecules and their facility to undergo configurational changes.

1.3.2 Structural arrangements and phase diagrams

A triglyceride molecule exists in a tuning fork configuration and these molecules are arranged in pairs, head to tail. The packing can either be double-spacing (-2) when it is two fatty acid chain lengths long or triple spacing (-3) when it is three fatty acid chain lengths long (Figure 1.8).

Figure 1.8: Diagrammatic representation of triglycerides structural arrangements in double chain or triple chain configurations (Jacobsberg and Ho, 1976).

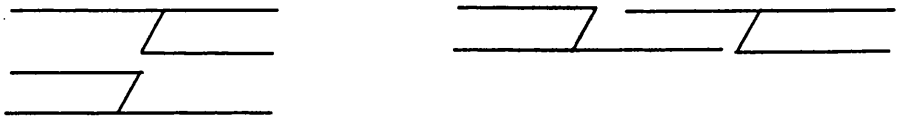

double chain structure triple chain structure

Figure 1.9: Diagrammatic representation of the polymorphs chain arrangement (Timms, 1984, Dimick, 1991).

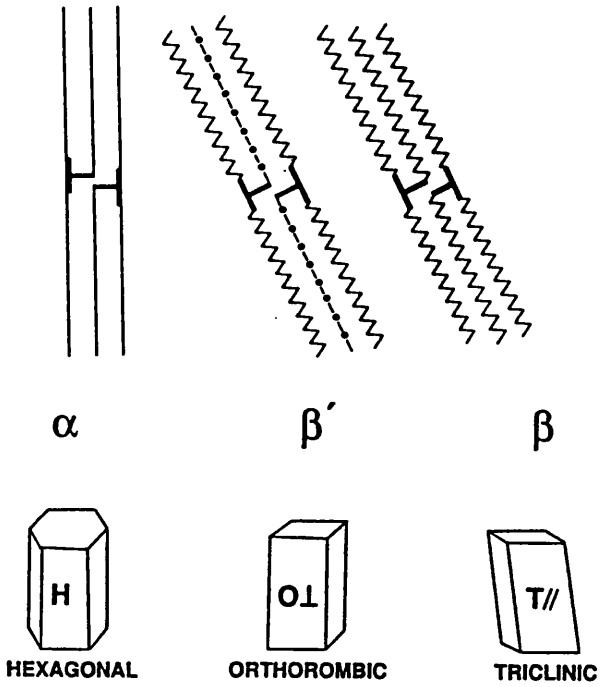

The type of polymorphic form obtained, the rate of crystallisation, the crystal structure and the melting point depend on the way in which these triglyceride molecules pack together (Small, 1985; Aronhime et al, 1990). In addition, the hydrocarbon chains of the fatty acids

are arranged in a regular zig-zag. The arrangement of these zig-zags relative to each other has a role in defining the different polymorphic forms. One zig-zag period is a subcell. The α form which has hexagonal subcells H are made up of fatty acid chains perpendicular to the basal plane. The chains are thought to be oscillating with a high degree of molecular freedom. The β′ form has the orthorhombic subcells $O_{\perp}$.The zig-zag plane of every chain is perpendicular to the zig-zag planes of its neighbours. In the β form which is associated with the triclinic subcell T however, all the zig-zag planes are parallel (Figure 1.9). The terms hexagonal, orthorhombic and triclinic refer to cross-sectional view of unit cell packing of the triglyceride. In order to differentiate the different polymorphs by drawing upon the differences in their packing, X-ray diffraction studies are usually performed (Table 1.5). The spacing characteristics revealed that the density of the packing increases in the order of α, β′, and β which is also the order of increasing stability. This table gives a simplified classification for mixed triglycerides with different saturated chains.

Table 1.5: Nomenclature and assignment of triglyceride polymorphs (Chapman, 1962; Lutton and Fehl, 1970).

Polymorph	X-ray short spacing characteristics
α	A single strong short spacing at 0.415nm
β′	Usually two strong short spacings ca. 0.38nm and 0.42nm or three short spacings at ca. 0.427nm, 0.397nm and 0.371nm
β	A form which does not satisfy the criteria for α or β′ but also usually shows a very strong short spacing at ca. 0.46nm.

Figure 1.10: Planar angles of the α, β and β′ polymorphs of tristearin dimers (Dimick, 1991).

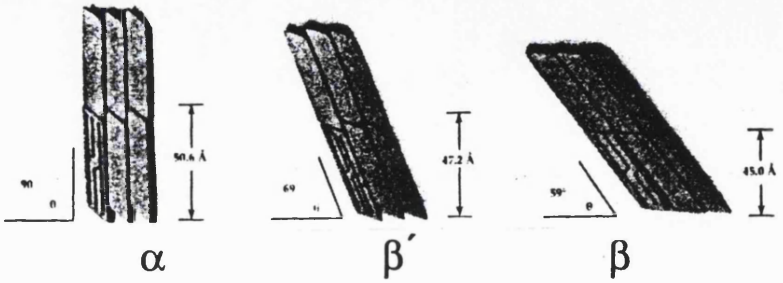

An illustration of the planar angle of triglyceride dimers and the shifts in this angle as the polymorphic transformation occurs between the α, β and β′ as exemplified by tristearin is shown in Figure 1.10. In the β form, the terminal methyl groups of the of the fatty acid chains lie in one plane. As a result of this bilayer packing, a higher melting and more stable crystal is produced (Small, 1986). Triglycerides which have fatty acids of similar chain lengths can have the most efficient packing.

Mixtures of fats not only affect the packing arrangements of the molecules but also the phase behaviours which can be illustrated by phase diagrams. The simplest mixture of triglycerides, that is a binary mixture, can already give rise to 4 different types of phase diagram (Figure 1.11).

Figure 1.11: The phase diagrams for a binary mixture of triglycerides (Timms, 1984).

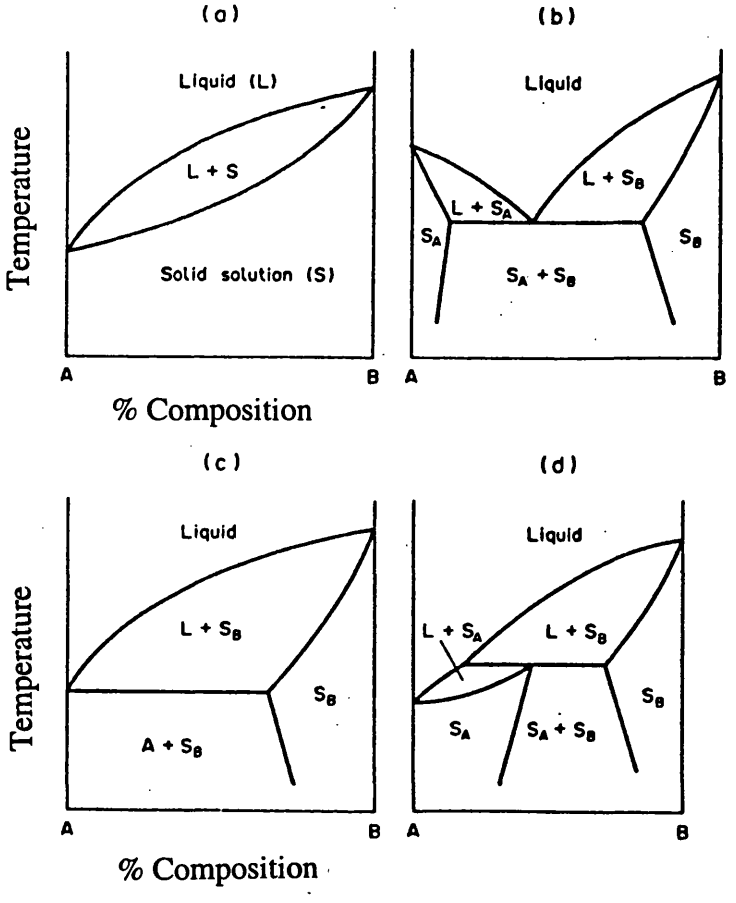

Type (a) phase behaviour with its continuous solid solutions only occur when the two triglycerides are of very similar melting points, molecular volume and polymorph; this

system is monotectic.

Type (b), the eutectic system tend to occur when the triglycerides still have quite similar melting points but different molecular volume or polymorph (S_A and S_B are solid triglyceride A and solid triglyceride B respectively).

Type (c) the monotectic system with its partial solid solutions occur when there are bigger differences in the melting points of the triglycerides and the high melting component dissolves some of the low melting component.

Type (d) the peritectic system occur only in mixed saturated/unsaturated systems where at least one triglyceride has two unsaturated acids.

However, it needs to be understood that in natural fat systems, phase diagrams for a binary system would represent an oversimplification. Even the simplest fats such as cocoa butter is made up of five triglycerides, each with its own polymorphs. The resulting phase diagram would be an extremely complex one. Even so, the binary system highlights several behaviours of the natural fats. For example, as explained for gelucires, the fat tends to melt over a broad range of temperatures rather than one sharp melting point (Kawamura, 1979; Liversidge et al, 1981; De Muynck and Remon, 1992). A simplistic form of explanation would be that of a superimposition of all the binary diagrams in the natural fat system would result in no clear eutectic point being observed. Also, mixtures of β and β' are common even after tempering, and additionally at equilibrium, when both occur in the fat, the highest melting form may not necessarily be the β form although as mentioned before, the β' form would normally be favoured in a system with a variety of molecular sizes and types of triglyceride such as in palm kernel oil, as this form is more flexible in its chain packing, necessary for formation of solid solutions (Rivarola et al, 1987; deMan and deMan, 1994; Gunstone, 1996).

1.3.3 Composition and polymorphic forms of palm oil

Gelucires with a fatty acid and glyceride component are partly derived from palm and palm kernel oil (see Section 1.1.2). Palm oil has a high saturated acid content with 10-15% of it at the 2-position of its triglycerides (Wuidart, 1996). This give rise to its three main types of triglycerides: trisaturated, disaturated and monounsaturated. The various binary phase

diagrams of these triglycerides indicate that they are either eutectics or peritectics. Besides the triglycerides, palm oil also contain some diglycerides, monoglycerides and free fatty acids (Jacobsberg and Ho, 1976; Pike, 1980). The glycerides can interact with each other to produce an unpredicted effect. Eutectic mixtures can arise from molecular size differences, such as for palm oil and palm kernel oil. Also, a mixture of two triglycerides with different polymorphs can transform into one new polymorph, β-2 and this is called a compound formation (Timms, 1984). Compound formation can affect physical properties of the fat such as crystal habit and solid fat content.

The DSC melting profiles are complex due to various effects occurring at about the same time such as polymorphic transformation and intersolubility of different components (Kawamura, 1979, 1980). However, even tempering does not totally eliminate the two-part profile of the DSC curves indicating that the main phase separation is not only due to polymorphic changes (Figure 1.12). The higher melting fraction is solid and classified as stearin, and the lower melting fraction is liquid called olein. The higher melting solid solution of the palm oil was found to be dominated by POP and PPP and the lower melting by POO (Busfield and Proschogo, 1990). Each fraction can undergo α to β′ transformation.

Figure 1.12: The DSC thermal profiles of palm oil during crystallisation (a) and melting (b) (Oh and Berger, 1983). The range of 3-2 in the crystallisation profile (a) indicates the stearin crystallisation peak and 2-1 is the olein crystallisation peak. Likewise, the range 1-2 in the melting profile (b) shows the olein melting peak and 2-3 is the stearin melting peak.

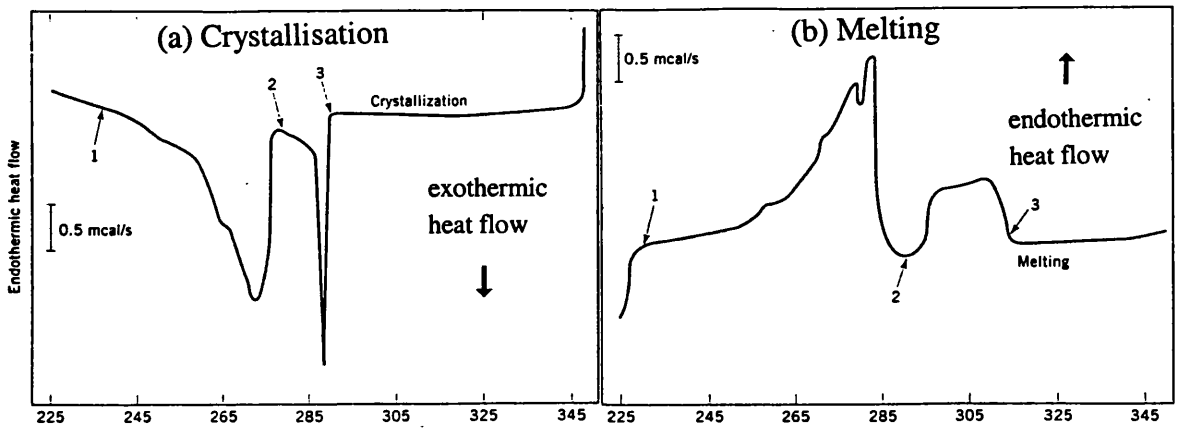

1.3.4 Solid fat content (SFC)

Solid fat content is the measure in percent of the amount of solid fat present at a particular temperature, traditionally determined by NMR or dilatometry (Basiron, 1996). It is now also possible to construct it from DSC data. The DSC thermal profile could be integrated at different temperatures to determine the percentage of fat remaining solid at a particular temperature and this information can be used to compare fats which had undergone various thermal treatments (Lehrian et al, 1980).

Figure 1.13: Solid Fat Content of crude stearin (Basiron, 1996).

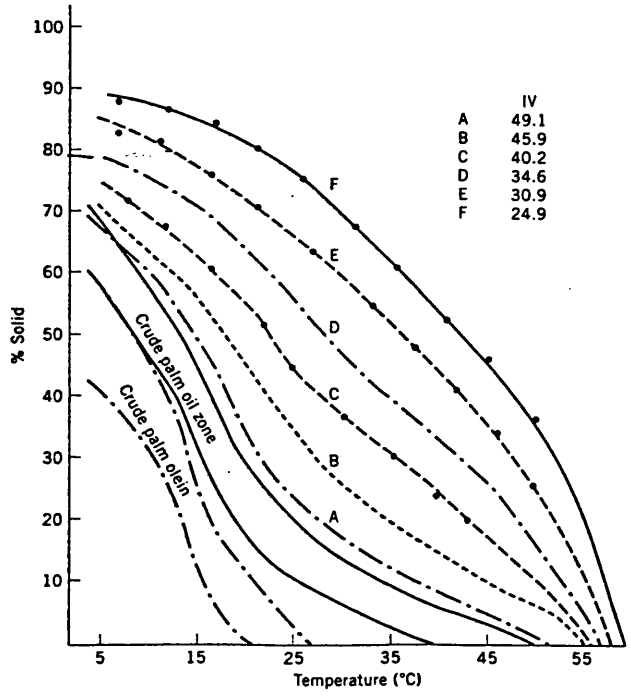

Palm oil is composed of the stearin and olein fractions as indicated previously in Figure 1.12. By controlling the fractionation conditions, stearin or olein of required specifications for a particular use could be produced and SFC curves plotted to characterise these fractions. For example, stearins obtained with various iodine values (IV) gave differing SFC curves with higher IV samples being softer and lower IV samples being harder (Figure 1.13).

The SFC is the more commonly used technique to characterise mixtures of fats since it is very difficult to construct a phase diagram for mixtures of fats (heat changes occur over a

broader range, overlapping of melting and eutectic points, etc.). The 'contours' on the SFC graph can indicate behaviours such as eutectics, compound formations and sharp or broad-range melting. The detection of the eutectic effect is especially important in assessing the compatibility between two different fats. In a compound coating mixture containing lauric hard butter and cocoa butter, the eutectic phenomenon was observed when the SFC of the mixture at various concentrations of the butters was plotted (Laustsen, 1991). At the eutectic composition, the SFC of the mixture is at its lowest. This resulted in liquid fat being formed by the eutectic composition which migrated to the surfaces and recrystallised as bloom. Blooming is the effect that causes the loss of gloss and texture on fat surfaces such as chocolates. Therefore, some edible fats need to be high in their SFC in order to remain stable during storage at ambient temperature and prevent liquid fat from separating out.

Figure 1.14: Incompatibility of the blend of cocoa butter (CB) and refined palm kernel oil (RPKO) (Kristott, 1999).

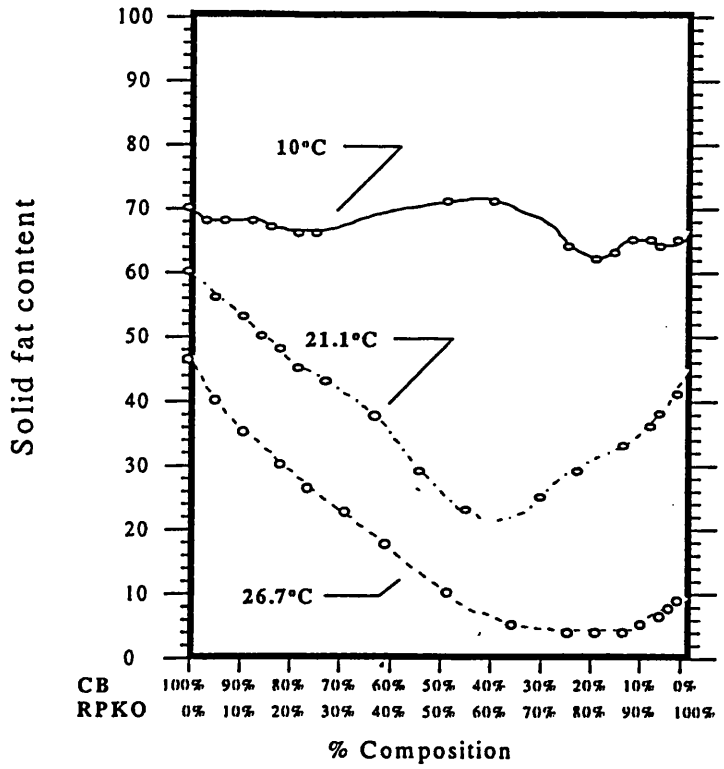

A eutectic composition indicated by the minimum on the curves was also discovered for cocoa butter and palm kernel oil when the SFC diagram of the blends was plotted (Kristott, 1999) (Figure 1.14). Similarly, this minimum was found for the blends of cocoa butter and fully hardened milk fat (Timms, 1984). Knowledge obtained from these diagrams can then

allow the manufacturers to manipulate the composition of fat mixtures and conditions of production. When a certain percentage of solid fat is required to crystallise at a particular temperature, additives can also be mixed into pure oils and DSC can be used to measure the SFC (Yap et al, 1989b). Again, such information would be very useful in choosing the right processes to achieve a certain outcome. For more details on this subject, refer to Section 1 of Chapter 6.

1.3.5 Factors affecting the polymorphism of fatty acids and glycerides

The complexity of the fat system makes it very difficult to predict its physical properties. For example, in order to construct reliable phase diagrams or isosolid diagrams, the molecular composition, together with the polymorphs associated, need to be obtained. However, this is an extremely difficult task due to the complex mixtures of glycerides in the fat (Liversidge et al, 1981). Even though the individual glyceride can be extracted using a technique such as HPLC, for a system such as gelucire, whereby the glycerides are made more complex by the esterification with PEG, the poor understanding of the phase changes has impeded the construction of such diagrams.

Besides the factors that could possibly affect the polymorphism of the fatty acid component in the gelucire which have been mentioned before, such as the types of fatty acid mixture and additives present, preparation conditions also play an important role. Heating rate affected the extent of the production of the different polymorphs (Aronhime, 1988). It is also well known especially in the food industry that cooling rate can influence the hardness of the fat, by causing differences in the crystal size, solid fat content or possibly polymorphism (deMan,1961b). The type of change induced on the fat by the cooling rate is also influenced by the additional processing undergone by it such as interesterification and isomerization (deMan, 1961a). When the original fat was slow cooled, the product was softer than when rapidly cooled. However, after interesterification of the fat, the slow cooled product was much harder whilst isomerization caused an even greater increase in the hardness. The increase in hardness after interesterification was attributed to the elevation in the high melting glycerides whilst for isomerization, it was attributed to the increase in the trans-form.

Interesterification has also produced smaller crystals after slow cooling and bigger crystals after rapid cooling but the reverse is valid for the original fat. Rivarola et al (1987) showed that for hydrogenated sunflowerseed oil, as the rate of cooling increased, the β' form (more unstable) tended to crystallise out. Rapidly cooling the oil produced small, thin needles (1-10μm long) whilst slow cooling produced long needles (20-30μm). Similarly, with sunflower / cotton oil blends, a rapid cooling rate increased the proportion of the solution which crystallised at low temperature. Laine et al (1988) noted that there was more amorphousness in rapidly cooled triglycerides than slow-cooled ones. Further factors that may affect polymorphism are ageing and storage conditions, as will be elaborated below.

1.4 The ageing process

In designing and formulating dosage forms, one of the factors that cannot be overlooked is that the dosage forms are usually stored for a certain period of time before being used. The storage conditions that these forms are subjected to on leaving the manufacturing plant are not always easily controlled and it would be unduly optimistic to predict an absence of temperature fluctuations within their environs. These factors have the potential of altering the performance of the dosage forms (Moës and Jaminet, 1976; Frömming and Hosemann, 1985) and it is essential to attempt to elucidate the mechanisms of change, if any.

1.4.1 Ageing in the fatty acids and glycerides components

Process such as ageing can affect polymorphic transformation as well as the phase distribution in a fat, the rates of phase changes and the crystal size (Timms, 1984). Changes to the fatty matrix after ageing could result in a modification of the in vitro and in vivo release of the incorporated drug (Taylor and Simpkins, 1981; Kahela et al, 1987). A number of the studies on this effect had been centred on the changes in the physical and chemical properties of fatty suppository bases. For example, Liversidge et al (1981) had found that upon storage, the melting point of the bases had increased and this was associated with the α and β' polymorphs converting to the β polymorph. This was shown by the binary mixtures of tripalmitin and tristearin whereby ageing decreased the number of transitions on DTA thermal profiles until the eventual melting point could be seen. They also found

that the rate of this change decreased with increasing chain length of the fatty acid. This could be due to a lower molecular mobility of the longer chains which resulted in a difficulty in reorientating to a more stable polymorph.

One of the implications of a higher melting point lipidic base is a lower release rate of drug (Thoma and Serno, 1982; Müller, 1984). However, this observation was not supported by all the investigators on this subject. Laine et al (1988) did not find any signs of polymorphism upon ageing of fatty suppositories. Instead they attributed the increased hardness of the suppositories upon ageing to the change from layered form to a crystalline one. It is interesting to note that Laine and his colleagues used X-ray diffractogram data to interpret that there was no polymorphism whilst Liversidge et al (1981) who did find polymorphism after ageing utilised the differential thermal analysis (DTA) technique. However, Moes et al (1976) investigated the effect of fatty suppositories ageing on the release of paracetamol also by using X-ray diffractogram and attributed the increase in the melting temperature with the consequent decrease in paracetamol release to the transformation of unstable to more stable polymorph. It seemed that the X-ray diffraction studies data is open to a variety of interpretation.

One of the methods to obtain a particular polymorphic form is by *tempering* the fatty material. Tempering has been described as a process which would produce the optimum quantity and quality of seed crystals from which more of that particular fat form could crystallise out during cooling of the molten fat (DuRoss and Knightly, 1965). For example, Lutton and Fehl (1970) recommended that in order to obtain the most stable form of the even chain triglycerides, β, the fatty material needs to be stored in the temperature range between the α and β melting points. This nucleation process could be induced by thermal and mechanical means (Cebula et al, 1991). The tempering process has been frequently used in the dairy and confectionery industries in order to obtain an acceptable product which will remain unchanged during ageing (Manning and Dimick, 1985). This process was also used in the production of fatty suppositories in order to obtain formulations with particular physical characteristics. Tempering a previously cooled fatty base at 4-5°C above its solidification point resulted in suppositories with the most stable glyceride form that showed little tendency towards brittleness (Müller, 1989). Although tempering is usually

performed at an elevated temperature, it can still occur at lower temperatures but at a lower rate (Hoerr, 1960).

A tempering cycle whereby the molten fat is cooled to initiate crystallisation followed by an elevation of the temperature in order to melt out the less stable crystals is frequently used (Nickless and Sidaway, 1980; Koyano et al, 1990; Seguine, 1991). Using this principle, a continuous tempering apparatus consisting of a series of heat exchangers was developed for convenience and speed (Cebula et al, 1991). Tempering could also be achieved by adding a seed, for example a fatty material previously tempered to a required form, to molten fat (Koyano et al, 1990; Urbanski, 1991). Once crystallised, the fat will predominantly contain that particular form. Addition of foreign oil (Yap et al, 1989a) or surfactants (Aronhime et al, 1990) can delay the transformation of the polymorphs that occur during tempering. The time taken for the transformation during tempering to complete also depends on the type of fats present and the tempering temperature (Samsudin and Rahim, 1996). Characterisation of cocoa butter using microscopy and thermal analysis after the tempering process revealed that the melting points of the crystals produced increased with the tempering temperature (Dimick and Manning, 1987).

1.4.2 Ageing in the PEG component

Besides the fat components, gelucires are also made up of PEG constituents. Although most of the PEG (80%) in G50/13 is esterified with fatty acids, it would still be useful to present the consequence of ageing in the pure PEG form. In the ageing of indomethacin-polyethylene glycol 6000 solid dispersions prepared by melt-fusion (Ford and Rubinstein, 1979), radial aggregates of crystals were observed forming under the microscope. The greater the indomethacin content, the greater the time taken for these structures to completely form. It is possible that together with the more stable extended form, the less stable folded chain crystals of PEG 6000 were also formed initially. This formation of the folded form could be due to the melt crystallising at a temperature lower than a critical point, the delay being caused by the viscous nature of the melt. On ageing, the unstable form converted to the more stable extended form, which was seen as the development of the aggregates.

Together with the crystallization of indomethacin itself, this progressive crystallisation of PEG could be the possible explanation to the decrease in dissolution rate upon ageing. The decrease in dissolution rate was more obvious for the samples stored at a higher humidity environment and/or higher temperature, again probably due to the increase in crystallisation (Ford and Rubinstein, 1979). The method of matrix preparation also has a bearing on the outcome. When the tablets prepared from the melt granulates of this mix were compared to conventional tablets (Ford and Rubinstein,1980), the former tablets had a faster dissolution rate. However, on storage, the hardness of the tablets increased and the dissolution rate had a varied profile over time, first decreasing and then increasing. Again, storing the tablets at a high humidity environment decreased its dissolution rate.

Elevated dissolution rate for melts formulations compared to physical mixes had been shown before previously by the same authors (Ford and Rubinstein, 1977b) for chlorpropamide and urea discs. Ageing up to 28 days for formulations containing lower concentrations of chlorpropamide did not significantly alter their dissolution rate but at higher concentrations (>60%), there was a reduction in the dissolution rate at the beginning of the process, followed by an increase in the dissolution rate as storage continued. The initial decrease was attributed to the crystallisation of the high proportion of chlorpropamide and the subsequent increase to the diffusion of drug molecules within the melt.

The effects of ageing on samples also depend on the rate of cooling during preparation. Sjokvist Saers et al (1993) found that when 10% w/w griseofulvin dispersion in PEG 3000 was slow cooled, the rate of dissolution remained unchanged during storage but on the other hand, the rate decreased during storage for fast cooled samples. X-ray diffractogram and ΔH_f values indicate an increase in the order of PEG. When compared with xylitol as a carrier, the xylitol-griseofulvin dispersion did not show any change in dissolution rate after storage irrespective of the cooling rate. This could indicate that it is the increase in the crystallinity of the PEG itself that is affecting the dissolution rate. However, at higher storage temperature (45°C), ageing of rapidly or slow cooled samples did not significantly change the dissolution rate. On the same note, Sutananta et al (1994b) determined that the tensile strength of G55/18 (which is consisted of only PEG 6000 esters of fatty acids) of

ambient cooled (considered rapid) moulded tablets increased, compared to the aged slow cooled samples which were essentially unchanged. However, the corresponding DSC thermal profiles did not show any significant developments after storage.

1.4.3 Ageing in gelucires

It is not sufficient to just extrapolate data from purely glyceridic or PEG systems to a mixed system such as gelucire. There have been several studies focussing on the effect of ageing on gelucires. Sutananta et al (1994b) investigated the changes caused by storage on various gelucires. They found that the chemical composition was one of the factors influencing the outcome of the ageing process. Differential scanning calorimetry (DSC) data showed that the gelucires which had a high glyceride content tended towards an equilibrium state after ageing. Those with a mixture of glycerides and PEG esters form several segregations of different microscopic regions which were difficult to recombine into a stable equilibrium state. Samples solely containing PEG esters showed only minor changes upon ageing, which were perhaps due to the chain folding event of PEG molecules. Tensile strength studies after ageing revealed that gelucires with only glycerides or only PEG esters increased in strength whilst those with a more mixed composition decreased in strength. The authors postulated that this decrease could be due to the two components changing their distribution with respect to each other rather than just the simple combination of effects of glycerides and PEG esters together.

The effect on the gelucires after ageing also depends on the methods with which they were originally prepared. Fast-cooled samples reached an equilibrium state quicker than slow-cooled samples because slow-cooled samples produced a greater number of segregation which were more difficult to recombine (Sutananta et al, 1994a). The effect of ageing on drugs formulated with gelucire was studied by Remunan et al (1992b) on formulations of nifedipine and G50/13 achieved by tableting the granulates, instead of using the usual melt-dispersion technique. Various storage conditions were looked at and it was found that high humidity can alter the dissolution profile of the drug from the gelucire. Increasing the temperature made this effect more profound. Even though the change was partly attributed to the formation of microcrystals of nifedipine and to structural modifications in gelucire,

there was no evidence to prove as such. Dennis et al (1990) also found that storing a gelucire formulation (ketoprofen dispersed in G50/13:G50/02 mix) affected its release profile. However, the increased rate of drug release in vitro was not significantly repeated in vivo. When fluid-bed G64/02 coated granules of amoxycillin were stored under different conditions of temperature and humidity (Delgado-Charro et al, 1993), the mechanism of release altered but both the rate and mechanism of release did not seem to be influenced by the actual period of storage, that is they were not different after 2 and 4 months ageing.

Since gelucires are mostly formulated in hard gelatin capsules, the effect of the excipient on the capsules upon ageing was investigated by Doelker et al (1986) using different formulations of various gelucires with liquid or deliquescent drugs. After three years of storage at room temperature, the release of benzonatate from still intact capsules was slightly raised. This could be due to the increased crystallinity of the gelucires expelling the drug from within the matrix. It was also found that it was necessary to choose the right gelucire for a particular drug as a wrong combination could result in the gelatin capsules softening, becoming sticky or leakage of contents.

1.5 Objectives of the investigation

Even though gelucires including G50/13 have been used in many types of dosage form which have been formulated through a variety of techniques such as liquid filled hard gelatin capsules (Waginaire and Glass, 1981; Doelker et al, 1986; Baykara et al, 1991; Burns et al, 1996; Shah et al, 1996), granules filled hard gelatin capsules (Brossard et al, 1991; Delgado-Charro and Vila Jato, 1991, 1992), sustained-release formulation through a heated fluidized bed (Bodmeier et al, 1990), oral spheres (Magron et al, 1987; Laghoueg et al, 1989; Bidah et al, 1990, 1991,1992) and compressed tablets from granulates (Vila Jato et al, 1990; Saraiya and Bolton, 1990; Remunan et al, 1992), comparatively little attention has been paid to the characterisation of the gelucires through physical and thermal methods, and the relationship with their performance. The exceptions to this are the studies performed by Sutananta et al (1994, 1995) which revealed an association between the rate of cooling and the behaviour of the gelucires.

Some of the previous studies hypothesised a relationship between the HLB and melting point values of the gelucires with their dissolution behaviour (Howard and Gould, 1987; Ortigosa et al, 1991; Brossard et al, 1991; Ratzimbazafy and Brossard, 1992). Others had formulated mathematical models relating the dimensions of the dosage forms to the release profiles (Magron et al, 1987; Laghoueg et al,1989; Ouriemchi et al, 1994; Aïnaoui and Vergnaud, 1998) or the kinetics of release with the amount of gelucire utilised (Saraiya and Bolton, 1990; Vila Jato et al, 1990; Delgado-Charro and Vila Jato, 1991, 1992). Many of these studies were focussed on obtaining feasible formulations for the drugs studied by using gelucires. Thus, different types of gelucires or series of gelucire blends were investigated for use with a particular drug of interest. On the other hand, different drugs had also been shown to affect formulations containing the same gelucire in dissimilar ways. For example, the release of benzonatate from G50/13 matrices was relatively rapid but the release of chloral hydrate from the same gelucire was retarded due to the formation hard and non-disintegratable mixtures (Doelker et al, 1986). Increasing the loading of paramethadione in G50/13 was discovered to improve the availability of the drug due to a more rapid disintegration of the mass. In this current investigation, the effect of two model drugs with similar solubilities in water on G50/13 was elucidated. G50/13 was chosen as it had previously shown good controlled release profiles with various drugs (see Section 1.1.5). The influence of drug loading on the physical characteristics and release behaviour of the matrices was also examined.

Nevertheless, G50/13 has the potential of being altered by the ageing process as it is partly composed of glycerides and fatty acids. These components have been frequently shown to be affected by storage which could involve changes in the polymorphic forms, fat phases or crystal sizes (see Section 1.4.1). In turn, the changes could lead to melting point or drug release alterations (Moës and Jaminet, 1976; Liversidge et al, 1980; Laine et al, 1988). In addition, the PEG component could also be affected by ageing resulting in modifications to the drug release (see Section 1.4.2). This had been shown by pure PEGs to be due to crystallinity changes during storage (Ford and Rubinstein, 1977, 1980; Sjökvist Saers et al, 1993). Finally, the numerous contituents of the gelucire could undergo redistribution leading to segregation of the components after ageing (Sutananta et al, 1994b). One of the purposes of this current study was to examine any changes to the G50/13 brought about by

the ageing process. These changes could affect the physical structure which may or may not be accompanied by modifications in the release profiles from the matrices.

In addition to the time factor, the components of gelucire could also be affected by the storage temperature that they are subjected to during ageing. The type of incorporated drug may have a bearing on the storage temperature effect. This would have implications in the way that formulations containing G50/13 could be stored without any detrimental effects on the required drug release behaviour. The current study proposed to look at any modifications brought about by storage at two different temperatures, 20°C which is a reasonable average room temperature for a temperate country and the elevated temperature of 37°C, which is the maximum possible without melting the entire carrier and a temperature that could be reached in a hot climate. Preliminary studies had shown that the first melting endotherm had occurred in the region of 36°C. A tempering temperature of 37°C could be expected to melt out unstable gelucire forms and transform them to more stable modifications. The impact of this process on the matrix behaviour could then be assessed.

The techniques utilised for these investigations would allow the physical structure of the matrix to be elucidated at a macromolecular level. The thermal analysis techniques used for this purpose such as differential scanning calorimetry (DSC) and hot-stage microscopy (HSM) had been known to be complementary to each other. Dissolution studies can then reveal any association between the macromolecular structure and the release behaviour, including the mechanisms of release. In short, the objectives of these investigations are to determine whether;

1) Different model drugs would have different effects on the G50/13 and its behaviour as a carrier.
2) Altering the loadings of those drugs would have any bearing on the matrix structure and behaviour.
3) Storing the G50/13 and its drug dispersions at various periods of time will show any modifications.
4) Temperatures of storage have any significance on the performance of the dispersions.

CHAPTER 2: INVESTIGATIONS INTO THE G50/13 MATRIX STRUCTURE USING DIFFERENTIAL SCANNING CALORIMETRY (DSC)

2.1 Introduction

Many materials show characteristic changes when subjected to a thermal signal. Processes such as melting or crystallisation absorb or give out latent heat respectively. By studying these events, modifications to the structure brought on by certain treatments to the substance can be determined. In Differential Thermal Analysis (DTA), the difference in the temperature between the sample and reference positioned in a furnace is measured against temperature or time while the substance is subjected to a programmed temperature. Its function is quite limited as only qualitative data such as phase transitions positions can be detected (Ford and Timmins, 1989).

2.1.1 Principles of DSC

One of the most important techniques in terms of thermal analysis is Differential Scanning Calorimetry (DSC). DSC is often considered to be a more evolved technique than DTA as DSC is able to provide quantitative as well as qualitative data (Ford and Timmins, 1989). In DSC, the differential thermal energy between the sample and reference is measured. When the sample undergoes a transition, a temperature difference develops between the sample and the reference and this temperature difference is converted into a thermoanalytical parameter such as heat flow (Giron, 1986; Griffin and Laye,1992).

There are two common types of DSC, heat-flux and power compensation (Griffin and Laye, 1992). Heat-flux DSC is very similar to DTA. The instrument signal is derived from the temperature difference between the sample, which is put in a small crucible/pan, and reference, which is usually an empty crucible (Figure 2.1). The sample and the reference are placed on two raised platforms on a constantan disc, which besides supplying the heating, also forms part of the temperature-measuring elements. The differential temperature is converted to heat flow using the equation below (Haines et al, 1998):

$$\Delta Q / dt = (T_s - T_r) / R_T \qquad \textit{Equation 2.1}$$

where Q is heat (J), t is time (s), R_T is the thermal resistance of the cell (KW^{-1}), T_s is the temperature of sample (K) and T_r is the reference temperature (K).

Figure 2.1: Diagrammatic representation of a heat-flux DSC similar to the instrument used in the current study (reproduced from Haines, 1995).

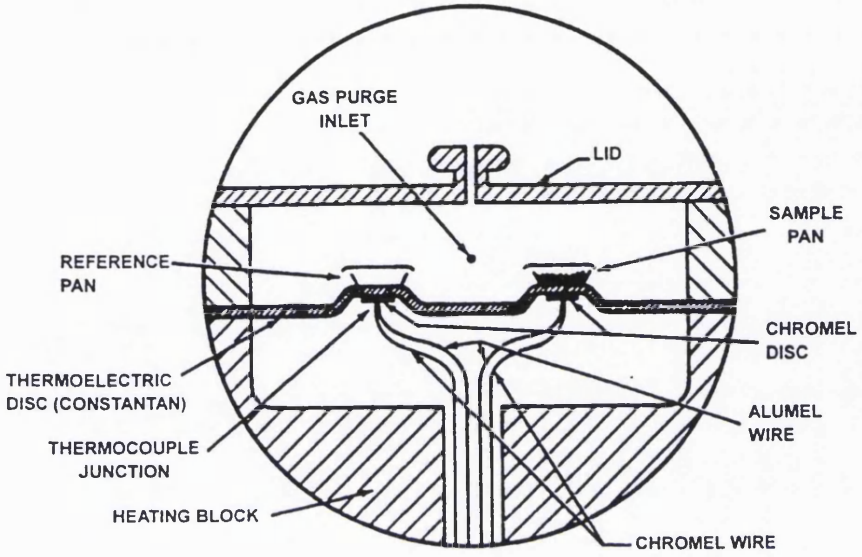

In power compensation DSC, the temperature is controlled so that it is always the same in the sample and the reference, usually via platinum resistance thermometers. The sample and reference are also isolated from each other and have their own heating elements. They are both heated at the same time and once the sample undergoes a change, a temperature difference develops against the reference which is then detected. Depending on the difference, more or less energy is sent to the heaters in order to keep the temperature constant, which is then monitored as the difference in power output to the heaters.

Aspects of the sample which determine its thermal profile are its melting point, chemical reactivity, thermal conductivity and thermal history. Other factors which can affect the measured heat flow are the amount of sample used, the heating environment, for example in air or nitrogen, the sample pans and the heating rate. A larger mass will yield larger peaks but it will also give a greater thermal lag due to poor heat transfer when the heat has to travel larger distances. Heating rates which are very slow can allow near equilibrium conditions to be achieved but have the obvious disadvantage of being time-consuming and can possibly anneal the sample. Moreover, substances which are not stable to heat may degrade during a long scanning process (Coleman and Craig, 1996). Heating rates which are fast, on the other hand, can cause larger thermal lags as the sample cannot keep up with

the external heating and can also decrease the separation of two thermal events. This was exemplified by Lloyd et al (1997a) who found that even though two endothermic peaks were observed when PEG 4000 was scanned at 2°C/min, these were reduced to a shoulder on a main peak at 10°C/min and finally, only a single peak at 40°C/min.

2.1.2 Applications of DSC

2.1.2.1. Characterisation of solid dispersions using DSC

In these current investigations, the model drugs are incorporated into the gelucire matrix to form solid dispersions. Chiou and Riegelman (1971) described the term solid dispersion as 'a dispersion of one or more active ingredients in an inert carrier or matrix at the solid state prepared by a melting (fusion), solvent or melting-solvent method'. Frequently, the term solid solution is also used and this generally implies that the drug is so intimately mixed that it is dispersed in the carrier in a molecular state (Chiou and Niazi, 1971). When the drug is in this state, it is very soluble in an aqueous environment. However, formulation of dosage forms through the formation of solid dispersions can bring certain problems. Certain combination of substances can show eutectic behaviour whereby at certain compositions, the two substances with different melting points can share a common depressed melting point.

DSC is also useful in elucidating whether drug and carrier interacted when fused together (Dordunoo et al,1996). With the knowledge that triamterene had a negligible solubility in PEG when the fusion temperature was 100°C, the expected values of the solidification enthalpies of only the carriers (Equation 2.2) were compared to the observed values.

$$\Delta H_{exp} = \Delta H^{\circ}.P/100 \qquad \text{....}\textit{Equation 2.2}$$

where ΔH_{exp} is the expected enthalpy of the dispersion, ΔH° is the enthalpy of the pure carrier and P is the percentage of the carrier in the dispersion. When the expected values and the experimentally derived values of the dispersions did not greatly differ from one another, it was taken to indicate that the drug and carrier did not interact during fusion.

However, lowered enthalpies of fusion on dispersions prepared at a higher temperature suggested that there was an increase in the amorphous content.

A study with PEG 4000 (Lloyd et al, 1997a) demonstrated that modifications in the DSC thermal profile of a material mixed together with another material may not only be due to the solid state characteristics changes at room temperature. For example, an extinguished peak can no longer be taken to just indicate the formation of a solid solution of the drug with the carrier or a solid state interaction between the two materials during excipient compatibility studies. Increasing the heating rates of the DSC scans resulted in the detection of the paracetamol melting endotherms in the PEG at progressively lower loadings. ΔH_f values became increasingly small due to the broadness of the peaks and could only be approximated. In this case, the slow dissolution of the drug in the carrier did not produce the expected thermal profile. Such studies illustrate the need to be discerning when interpreting DSC data.

Thermal analysis has been used in many investigations to find the solubility and the eutectic composition of drugs in carriers, as had been reported in Ford and Timmins (1989). When 2% chloramphenicol was dispersed in urea, its DTA profile revealed that even at this concentration there was an endotherm for the eutectic melting, indicating that the solubility of chloramphenicol in urea was less than 2%. However, there are times when such information is not directly obtainable. For example, some carriers do not melt easily during thermal analysis, so the solubilities of drugs in such carriers have to be estimated from the plots of drug fusion values against drug content and the solubility value is obtained from intercept of the drug content axis. There are other difficulties in finding the eutectic composition. In eutectics formed between low molecular weight molecules and polymers, Smith and Pennings (1974) put forward expressions to describe the liquidus curves for the two components, assuming that the ratios of the molar volumes of the polymer and diluent are very large and that the temperature dependence of the heats of fusion of the components is negligible:

$$\frac{1}{T_{ml}} - \frac{1}{T^{o}_{ml}} = -\frac{R}{\Delta H_1}\left[\ln\phi_1 - \phi_1 + 1 + \chi\left(1 - \phi_1\right)^2\right] \qquad \text{....Equation 2.3}$$

and

$$\frac{1}{T_{m2}} - \frac{1}{T^{o}_{m2}} = -\frac{R}{\Delta H_u}\frac{V_u}{V_1}\left[-\phi_1 + \chi\phi_1^{\,2}\right] \qquad \text{....Equation 2.4}$$

where T_m is the melting point of the liquidus and T^o_m is the melting point of the pure component. Subscripts 1 and 2 correspond to the diluent and polymer parts respectively, ΔH_1 is the heat of fusion of the diluent, ΔH_u is the heat of fusion per mole of structural units of the polymer, ϕ_1 is the volume fraction of the diluent, χ is the Flory-Huggins interaction parameter, V_u and V_1 are the molar volumes of the structural unit of the polymer and the diluent. Providing that χ is negligible, the eutectic composition, ϕ_1^e, is found at the temperature whereby $T_{m1} = T_{m2}$. Therefore, Equations 2.3 and 2.4 can be combined to give:

$$\phi_1^{\,e} = \exp\left\{\frac{\Delta H_1}{R}\left(\frac{1}{T^{o}_{m1}} - \frac{1}{T^{o}_{m2}}\right) - 1\right\} \qquad \text{....Equation 2.5}$$

Taking this equation into account, for a mixture where the melting point of the polymer is below that of the diluent, such as in PEG-drug systems, the composition and temperature of the eutectic will lean heavily towards the polymer side. A resultant difficulty of this in a system where PEG and similar polymers are the carriers, is that they melt over a wide range of temperature and therefore, the lower temperature endothermic peak due to the melting of the eutectic composition may be masked by the melting endotherm of the excess carrier.

2.1.2.2 Characterisation of polymorphic forms using DSC

When a substance crystallises, it can manifest in several different crystal habits such as prisms, plates or needles. If only the external habits are different, a morphological analysis technique such as microscopy can distinguish between them. However, in polymorphism, not only the habits are dissimilar but also the ways the molecules are arranged in the solids are distinct. This difference can be detected by thermal methods (Lutton and Fehl, 1970; Aronhime, 1988). Gelucires contain fat components that can exhibit polymorphism which can alter amongst others their release behaviour and therefore DSC can be used to study this

phenomenon.

The role of DSC in characterising polymorphs in drugs is well established. DSC scans of gepirone hydrochloride revealed the melting endotherms of the less stable polymorphs and also the more stable polymorphs formed by the solid-solid transition from the former (Behme et al, 1985). It was also postulated that this drug showed enantiotropic polymorphism when the DSC endotherms for the less stable form was removed after the drug was subjected to a heat treatment involving holding the lesser form at temperatures below its melting point.

In characterising the polymorphs by using the DSC, three types of curves may be obtained (Giron, 1986):

i) Where one metastable form of the polymorphs transforms into a more stable form in the solid state before the latter form melts. This is called solid-solid transition and the enthalpy of such transitions are usually small, therefore manifesting itself as a small endotherm before a bigger endotherm of melting. In enantiotropic polymorphism, the transition is reversible whereas in monotropic polymorphism, it is irreversible.

ii) Where one metastable form transforms to the more stable form in the melt state. The less stable form which has a lower melting point, melts and recrystallises as the higher melting point form and this is seen on the DSC scan as an endotherm, followed by the crystallising exotherm and finally a melting endotherm of the more stable form if heating is continued.

iii) Where each crystalline form melts without transforming into another form, whether in the solid or the liquid state. The differences in the melting points and the melting enthalpies of the forms can be widely varied.

The heating rates can also influence the type of transformation observed. Scanning gepirone hydrochloride at low rates produced peaks corresponding to the occurrence of a solid-solid transformation but at higher heating rates, the drug undergoes a melt-transformation indicated by the presence of two endotherms with an exotherm in between them (Behme et al, 1985). In addition, the heating rates can determine the number of polymorphic forms detected, with more peaks being observed at low rates (Liversidge et al, 1981; Ford and Timmins, 1989; Cebula et al, 1992). This is because the less stable polymorphs have more

time at lower heating rates to melt, recrystallise as more stable forms and remelt in these forms.

Besides fat components, gelucires are also made up of PEG esters of fatty acids. Although the behaviour of PEG esterified with other compounds such as fatty acids have not been extensively investigated, the polymer on its own has been studied using the DSC on numerous times. For PEG, its molecular weight often determines its properties (Ford and Timmins, 1989). PEG was found to exist in folded and extended chain form when high molecular weight PEGs exhibited two transitions on their thermal profiles. Similar to polymorphism, an endotherm due to the melting of the unstable folded crystals was followed by an exotherm due to the recrystallisation to the more stable extended form. Furthermore increasing the molecular weight of PEGs decreased their solidification rate and this was also related to their ability to fold (Dordunoo et al, 1996). The DSC thermal profiles can be further complicated by the presence of amorphous PEG. After melting and recrystallising rapidly PEG 6000, a very low temperature endotherm increased in its magnitude compared to an untreated PEG, indicating that the degree of amorphous PEG had increased (Ford and Timmins, 1989).

2.1.2.3 Characterisation of lipids using DSC

In excipients such as gelucires that contain various glycerides and fatty acids in the fat component, the thermal profile is expected to be complex. Overlapping of transitions would be difficult to avoid. For example, G50/13 contains saturated triglycerides which include trilaurin, trimyristin, tripalmitin and tristearin, and in addition, these triglycerides exhibit polymorphism. The individual thermal profile of each triglyceride mentioned are shown below (Figure 2.2) and the melting points and heats of fusion of the polymorphs are given in Table 2.1. It could also be seen from the table that the heat of fusion increases with the increasing stability of the polymorphic form.

To compound this complexity, the triglycerides are not restricted to the monoacid type. There are various permutations of diacid triglycerides made from the fatty acids common to G50/13. The melting points of the polymorphs of some diacid triglycerides are shown

in Table 2.2. In addition, there are also some monoglycerides and the thermal structure data is presented in Table 2.3. From these tables, it could be seen that the G50/13 fat component alone can give rise to various melting ranges. The polymorphs of the glycerides that have similar melting points would have the potential to form mixed crystals or solid solutions with each other.

Figure 2.2: DSC thermal profiles of saturated triglycerides. Heating rates for C12, C14, C16 and C18 were 20, 10, 10 and 5°C/min respectively (Aronhime, 1988).

Key:
C12=trilaurin
C14=trimyristin
C16=tripalmitin
C18=tristearin

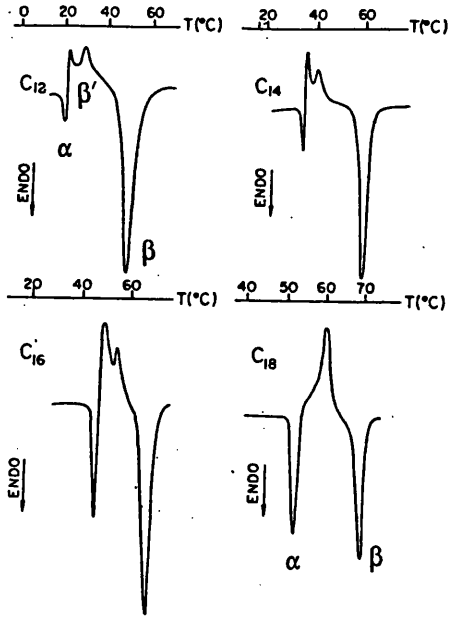

The diagrams indicate that for C12, there was some α melting as shown by the lowest temperature endotherm, followed by an exotherm showing a recrystallisation into the β′ form. This form subsequently melted as shown by the second endotherm and recrystallised into the β form which finally melted as indicated by the highest temperature endotherm. The ΔH_f of α for C12 was small suggesting that a large part of this form changed to the more stable forms via solid-solid transformation. On the other hand, the high ΔH_f of α for C18 reflected that a significant portion of this modification was via melt transformation as solid-solid transformation was hindered by the long aliphatic chains. However, the lower heating rate for C18 (5°C/min) allowed the β form to crystallise from the melt and also by some solid-solid transformation. Increasing the heating rate to 10°C/min or more will prevent the crystallisation of β due to insufficiency of time for the molecular packing to this form to occur (Aronhime, 1988).

Table 2.1: Melting point and heat of fusion values of the more common saturated monoacid triglycerides in G50/13 (fatty acid data from Garti and Sato, 1988).

Fatty acid chain length	Melting point (°C)			Heat of fusion (kJ/mol)		
	α	β′	β	α	β′	β
12	15.2	34	46.5	60.3	81.2	114.3
14	32.8	45	58.5	78.7	100.5	135.2
16	44.7	56.6	66.4	93.4	131.5	163.3
18	54.7	63.2	73.5	109.3	142.8	188.4

Table 2.2: Melting points of some saturated diacid triglycerides of the higher chain lengths most likely to be contained in G50/13 (triglyceride data from Garti and Sato, 1988).

Fatty acid chain length	Melting point (°C)		
	α	β′	β
18-16-18	56	64	68
16-18-18	57	61	65
16-18-16	59	65	68
18-14-18	56	59	62
12-16-16	45	49.5	54

Table 2.3: Melting points of 1-monoglycerides of fatty acids contained in G50/13 (monoglyceride data from Garti and Sato, 1988).

Fatty acid chain length	Melting point (°C)			
	α	β′	β	β (2-monoglyceride)
12	44	59.5	63	51
14	56	67.5	70.5	61.3
16	66.5	74	77	69
18	74	79	81.5	75.2

In this study, the influence of drug loading on the structure of G50/13 will be assessed. In addition, the effect of incorporating different types of drug and the thermal processes during the production of such dispersions will also be investigated.

2.2 Materials and Methods

2.2.1 Preparation of samples

The pure and untreated G50/13 sample was received from the manufacturers in 500g containers. As the molten gelucire was filled into the containers, their large size could have resulted in different cooling environments within the solidifying mass. This could have led to a segregation of components depending on the position of the gelucire in the container, as Sutananta et al (1994a) postulated that various cooling rates caused the emergence of such segregations. Preliminary studies were conducted on the G50/13 obtained from the top, middle and bottom positions of three different batches prior to any heat treatments in order to examine the homogeneity of the sample within the container.

In the other studies, the DSC scans were performed on the previously prepared melt-fused tablets (see Section 2, Chapter 4) as it is better to perform the thermal analysis on the final dispersion rather than on physical mixes, in order to elucidate the real nature of the dispersion. The tablets were equilibrated for 12-24 hours over silica gel after preparation and wholly comminuted in order to get a uniformed sample. This was a reasonable technique to use in order to fit solid fat into the pans. De Muynck and Remon (1992) obtained samples for the DSC from scraping it off from the fracture in the middle of a glyceride suppository. 9-10.5 mg of the sample was then placed in non-hermetic aluminium pans (Perkin-Elmer, Beaconsfield) and their lids were crimped into place. This amount was needed to cover the base of the pan without being too excessive so as to cause a great thermal lag. Preliminary studies of different sample masses of 7.5 to 12.5mg had shown that the smaller masses gave non-reproducible thermal profiles probably due to gaps on the base of the pan whilst the larger masses caused a leakage during melting. This type of pan was chosen as it gave a satisfactory contact with the sample once crimped. A hermetic pan was not ideal as some of the samples were sticky and could not be distributed evenly at the

base. The reference was an empty, crimped pan weighing within 0.01mg of the sample pan.

2.2.2 Scanning conditions

The DSC scans were performed using a TA instruments DSC 2920 (Leatherhead) equipped with a Refrigerated Cooling Accessory (RCS) which would allow the temperature to go below ambient and additionally, stabilise the heating process. This instrument uses the heat-flux principle of DSC (see Section 1.1). The heating rate used for the scan was 2°C/min and the purge gas employed was nitrogen at 40cm^3/min. A similar sample size (6-10mg) and the heating rate of 2°C/min were chosen so that a maximum number of transitions could be detected in the melting profile (Liversidge et al, 1981; De Muynck and Remon, 1992). The relatively slow rate was chosen so that the resolution of the peaks was optimal (see Section 2.1). This would also allow each thermal process to go to completion and the different stages of melting could possibly be correlated to the findings of HSM. A much lower scanning speed however, could anneal the fatty matrix and permit structural reorganisation to occur over the time scale of the experiment. In a previous study using G50/13, the scanning speed of 2°C/min was utilised as no evidence was found to indicate that lower speeds detected recrystallisation into higher melting point forms (Sutananta et al, 1994a). As no exothermic peak was seen between two overlapping endotherms of PEG 4000, it was regarded that the rate was fast enough to only cause the melting of the structures already present at the beginning of the scanning process but not the melting of the folded form, followed by exothermic recrystallisation to the extended form and subsequently the melting of this form, as would happen in the structural reorganisation of the PEG (Lloyd, 1997).

2.2.3 Data collection

The melting temperature was often taken to be the temperature of the endotherm at its most minimum heat flow value (peak), as gelucires do not have a sharp onset but instead melt over a broad range (Serajuddin et al, 1988). During preliminary studies, G50/13 was also found to give a broad melting range and so, the peak of the endotherm as computed by Universal Analysis™ (TA instruments, Leatherhead) rather than onset was taken to be the

melting temperature as it was not always clear where the onset melting temperature was. Moreover, the peak of the endotherm was the temperature at which the rate of melting was at its maximum. This would correspond better to the melting temperature found under Hot Stage Microscopy (see Chapter 3) as the exact temperature at which the gelucire started to melt is difficult to ascertain accurately under microscopy. In addition, the onset that was given by the analysis programme was calculated from the tangent to the first peak and not the point where the deflection from the baseline first occurred. The significance of this onset temperature was incorporated into the calculation of Solid Fat Content (SFC) instead (see below). The onset temperature measured from the tangent would depend on the slope of the leading edge of the endotherm and this slope would also affect the SFC profile.

In other studies where several peaks were detected in the melting profile (Liversidge et al, 1981; De Muynck and Remon, 1992), the temperature of the last peak maximum was taken to be the melting point. In this current study, the melting point was not assigned to any one particular peak as the sizes of the peaks can be altered by certain conditions and so, the choice of the maximum peak could change. Moreover, preliminary studies showed that the peaks towards the end of the melting range were significant enough to not be overlooked even though they were much smaller than the other peaks. Therefore, the melting points of all the peaks are reported here.

The enthalpy or heat of fusion was calculated as the area under the curve from the baseline, using the TA instruments software (Universal Analysis™). The heat flow is given as power (mW or W/g) and the heat of fusion is given in J/g, noting the relationship between power and heat is Watt = Joules/second. The area under the curve was taken between the temperature where the first inflection of the baseline occurred, to the temperature where the endothermic curve returned to the baseline. Projections from the baseline to the point of curve transitions are taken to be the borders of the area under the curve of the mid-range peaks (refer to Appendix 3 for an example of this step). This is analogous to the suggestion that a DSC curve may be integrated in parts when there is an overlapping of peaks, the total enthalpy change thus being the sum of these areas (Wendlandt, 1986). Other suggestions in analysing the enthalpies of complex peaks include the sum of Gaussian peaks or first-order peaks (Haines et al, 1998). The fitting of the Gaussian equation to complex peaks can

be performed by using specialised calorimetry software such as the Origin™ software (Microcal™ Software Inc, USA). These methods are beyond the scope of the current investigation and could be explored in future studies.

Temperature calibrations were performed using n-octadecane (Riedel de Haén, Sigma-Aldrich GmbH, Germany), indium and tin (both are GPR grade supplied with TA instruments DSC cell accessory unit, Leatherhead). Their melting temperatures of 28.24°C, 156.60°C and 231.93°C respectively ensured that the temperature calibrations encompassed the range that is encountered in the current study for accuracy. Heat of fusion calibration was performed using indium (as above) with its standard heat given as 28.71 J/g. All the data generated were analysed using Universal Analysis, converted to ASCII format by the same program and imported into the Excel program (Version 7, Microsoft®) which plotted the profiles shown in Section 2.3.

The Solid Fat Content (SFC) of the samples at a certain temperature was calculated by taking the area under the curve up to that temperature and dividing it with the total area of the temperature range of interest. The SFC is then the percentage of the remaining area to the total area, which therefore gives the indication of the amount of solid matrix left at a certain point when the SFC is plotted against temperature. The integration of the partial areas were performed by using the Origin™ software (Microcal™ Software Inc., USA). A diagrammatic example of this procedure is given in Appendix 4. Some of the details have been discussed in Chapter 1 and more will be covered in Chapter 6. All measurements were performed five times.

2.3 Results and Discussions

2.3.1 Pure G50/13

Preliminary studies revealed that the thermal profiles of the pre-heated G50/13 samples obtained from the various positions of the container were significantly different from each other (Figure 2.3). Such a result suggests that there is a heterogeneity in the composition of the gelucire related to its position within the container. The heterogeneity could have

arisen due to redistribution of components or polymorphic modifications. If polymorphism of the lipid components was the factor, then heating the gelucire until all polymorphs are destroyed should cause the thermal structure to be similar upon recrystallisation under the same cooling condition. However, if the segregation or redistribution of the components was the determinant, then contrasting results in subsequent investigations could be obtained from samples taken from various positions in the container. Therefore, it was decided on this premise that the whole G50/13 block from each container be comminuted down and mixed thoroughly so that the samples acquired for further studies will be homogenous.

Figure 2.3: Thermal profiles of untreated G50/13 taken from various positions in the container

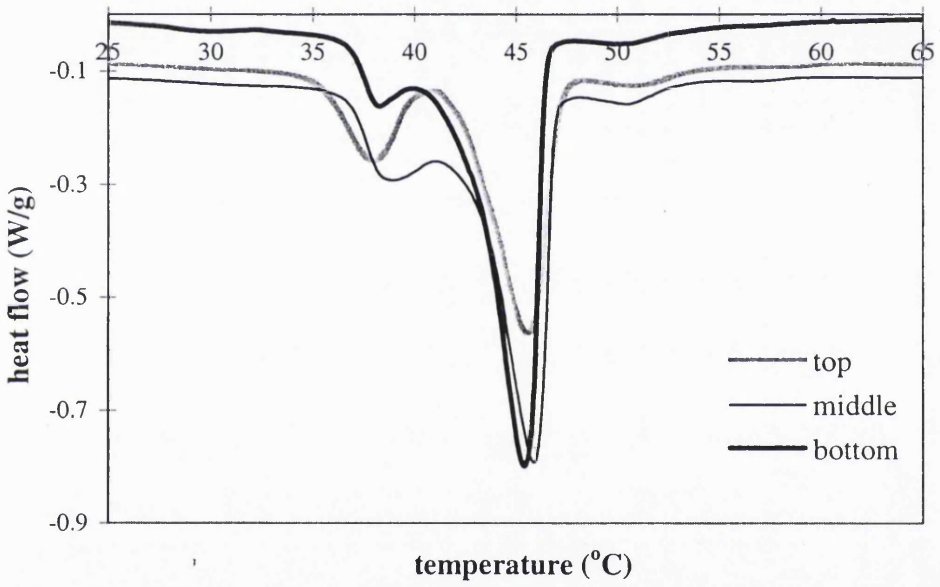

The thermal profiles of the pure G50/13 and the drug dispersions revealed a protracted endotherm comprising several peaks demonstrating the heterogeneity of the components (Figures 2.4 and 2.6). The pure G50/13 profiles in those Figures refer to the data in Table 2.4 obtained from thermally treated samples and are different from the profiles in Figure 2.3 which were acquired from samples as received from the manufacturer, before heat treatments. Mono-, di- and triglycerides have been shown to have a melting profile rather than a sharp melting peak due to the overlap of exothermic and endothermic peaks (Liversidge et al, 1981; De Muynck and Remon, 1992) and such profiles have also been shown previously with gelucires (Serajuddin et al, 1988; Sutananta et al, 1994a). The two lower temperature peaks were distinctive but the two higher temperature peaks were smaller and could probably be better described as shoulders. The peaks will be classified

Peaks 1, 2, 3 and 4 in the order of increasing temperature from now on, which for pure G50/13 are at 36.0°C, 44.0°C, 48.7°C and 55.7°C respectively (Table 2.4, Figures 2.4 and 2.6). These values correspond well to those previously quoted for ambiently cooled G50/13 (Sutananta et al, 1994a).

Table 2.4: Means ± standard deviations of peak temperature values (°C) and heat of fusion values (J/g) of pure G50/13.

	1st peak	*2nd peak*	*3rd peak*	*4th peak*	*Total*
peak temp. (°C)	36.0 ± 0.2	44.0 ± 0.2	48.7 ± 0.4	55.7 ± 0.1	
heat of fusion (J/g)	37.7 ± 1.0	99.6 ± 1.4	7.8 ± 0.2	2.4 ± 0.1	147.6 ± 2.2

The peaks for pure G50/13 range from 36.0°C to 55.7°C (Table 2.4), which is a span of about 20°C. This span only encompasses the peaks which are where the rates of melting are at their highest, but the actual onset of melting occurred earlier and the total completion of the melting process occurred later which means the entire span is more than 20°C. To demonstrate that this broad span is coincidental to the melting of the various components within the gelucire, it can be compared to the melting points and heat of fusion values of some of these pure components as given in Tables 2.1 to 2.3 of Section 1, bearing in mind that mixtures of fat components can lower their usual melting ranges (Small, 1986). Besides the values for the glycerides, the melting range for PEG 1500 is 42-45°C as determined by HSM and on the DSC gave a single melting endotherm (Ford, 1984). G50/13 is made partly from hydrogenated palm oil and consists in its triglyceride component mainly of palmitic and stearic acids triglycerides. Hydrogenation of palm oil results in the production of high amounts of 16-18-18 and 16-18-16 diacid triglycerides which stable form is the β'-2 polymorph (Timms, 1984). The melting points of this form indicate that these triglycerides probably constitute a part of the dominant Peak 2 (Table 2.2).

The composition of the gelucire forms giving rise to the peaks is not thought to be restricted to a single type of polymorph of each component. Exothermic peaks are not visible in the thermal profile of G50/13 which is often interpreted as an absence in the polymorphic transformation of a less stable to a more stable form during the scanning process. However, the DSC thermal profiles could have just revealed the existing polymorphs that were

Figure 2.4: Thermal profiles of paracetamol dispersions in G50/13 at different drug loadings

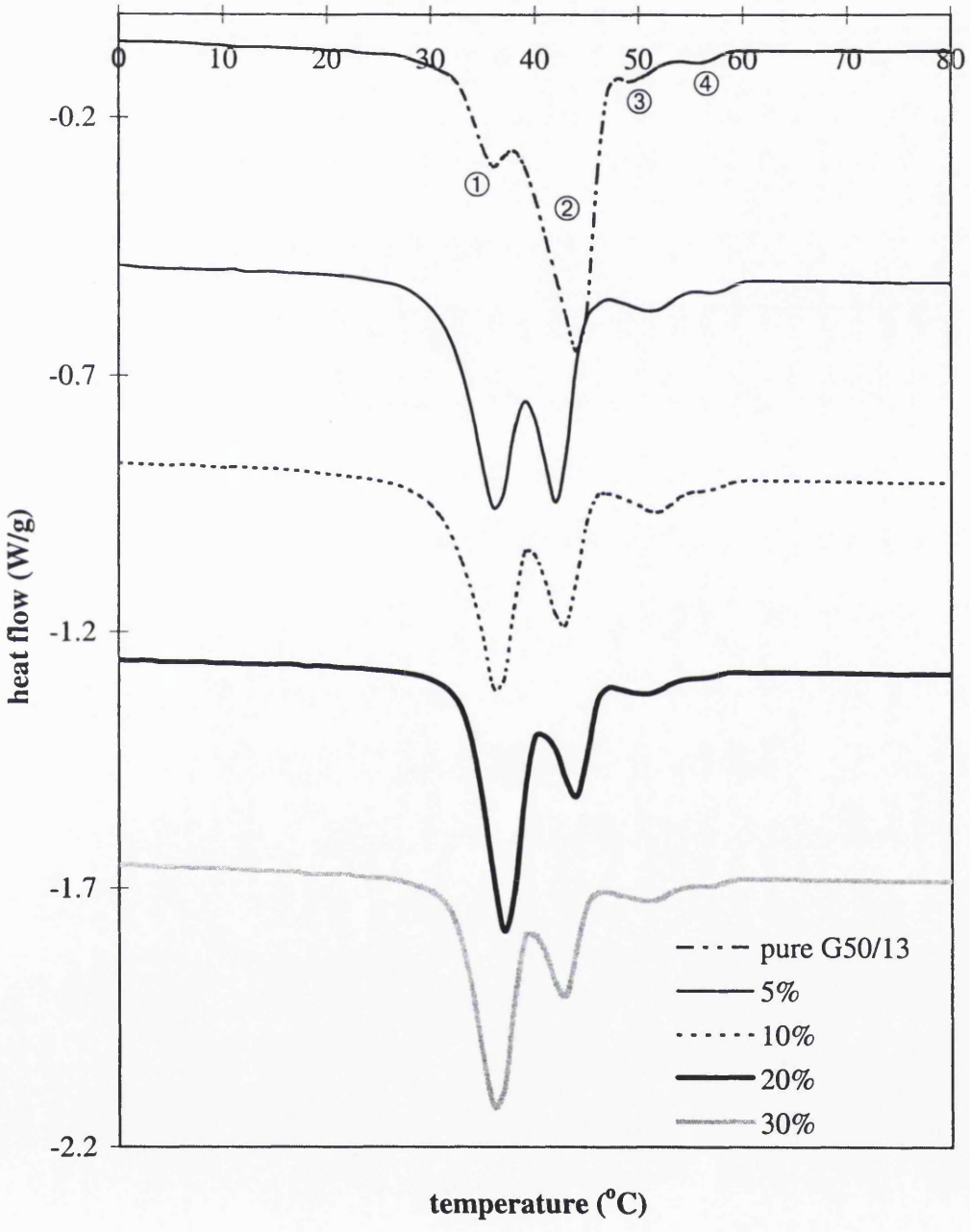

N.B. Endothermic heat flow for all the Figures is in the downwards direction.

The thermal profiles are vertically offset for clarity.

present in the initial solid matrix, with little or no transformation of the molten metastable polymorphs occurring during the scan, such as type (iii) mentioned in Section 1.2.2. Hence, no exothermic peaks associated with melt transformation could be seen. Polymorphic modifications could have occurred through solid-solid transformation during the 24 hours allocated for setting the moulded tablets. Nevertheless, the existence of exothermic peaks could not completely be excluded as they may have been masked by the endothermic peaks of other components. The potential for such overlapping of the thermal profiles of just the saturated triglycerides contained in G50/13 is shown in Figure 2.2 in Section 1 as an example.

In addition, there is a possibility of these polymorphs forming mixed crystals or solid solution with each other. For example, the fatty acid moieties of the monoacid triglycerides in G50/13 are C_{12} to C_{18} and Table 2.1 in Section 1 lists the melting points and heat of fusion values for their major polymorphs. From the table, it could be seen that a particular type of polymorph of a triglyceride can have a melting point which is similar to another polymorphic type of the next triglyceride, which is conducive to solid solution formation (Sato and Garti, 1988). These mixed crystals could be stable enough to resist undergoing polymorphic changes during the heating scan of the DSC.

The proportions of the area under each peak was not equal indicating that the quantity, the crystallinity and/or the polymorphic state of the gelucire forms giving rise to those peaks, was/were not equal (Table 2.4). The heat of fusion (ΔH_f) value would be larger as the degree of crystallinity becomes higher and is also bigger for the more stable polymorphic forms compared to the less stable forms, as displayed by Table 2.1 for monoacid triglycerides. The heats of fusion for each peak quoted here were not the absolute values due to a certain degree of overlap of the peaks. The Solid Fat Contents (SFC) of the pure G50/13 and the drug dispersions were plotted which shows the proportion of unmelted matrix remaining at various temperatures. From Figure 2.5, it could be seen that there were three phases to the SFC profile of pure G50/13 and can be described as Low Melting Fraction (LMF) from 28°C to about 37°C, Middle Melting Fraction (MMF) from about 37°C to 46°C and High Melting Fraction (HMF) from about 46°C to 60°C. LMF, MMF and HMF incorporates Peak 1, Peak 2 and Peaks 3 and 4 respectively. The profile also exhibited

the dominance of the MMF over the other two fractions. As the average body temperature is 37°C, this profile may account for the controlled-release behaviour of G50/13 as only a small degree of softening occurs. The minimal quantity of the HMF suggests that it could be partly made up of the free fatty acids in G50/13 besides the high melting glycerides.

2.3.2 Paracetamol dispersions in G50/13

The peak temperatures for the paracetamol dispersions were essentially similar between the different loadings, with any differences being minor (Table 2.5 and Figure 2.4). The span of peak temperatures had broadened slightly for the paracetamol dispersions compared to pure G50/13 and the Peak 2 temperature had also decreased a little for all the loadings. Such an effect was also previously demonstrated by the addition of low concentrations of glutethimide to PEG 1500 which caused the endotherms to broaden and lower the peak temperatures (Ford, 1984). Even though the melting point of Peak 2 decreased on the addition of the drug, the melting points of Peaks 3 and 4 significantly increased instead. It had been shown before that in some cases, adding drugs to the carrier did not lower their melting points but had the opposite effect. The addition of indomethacin to triglyceride suppositories (containing prior additions of monoglycerides) caused higher melting temperatures to be obtained (De Muynck and Remon, 1992). It is feasible that Peaks 3 and 4 had a higher proportion of monoglycerides than the other two peaks as monoglycerides are known to have higher melting ranges that the other glycerides (Table 2.3 in Section 1). An interaction between the monoglycerides and paracetamol could have occurred, leading to the higher melting points of Peaks 3 and 4 for all the dispersions and higher heat of fusion values for the lower loadings.

Table 2.5: Means ± standard deviations of peak temperature values of paracetamol dispersions in G50/13 (°C).

	1st peak	*2nd peak*	*3rd peak*	*4th peak*
5%	36.2 ± 0.1	41.8 ± 0.2	51.1 ± 0.2	56.9 ± 0.1
10%	36.4 ± 0.1	42.5 ± 0.1	51.8 ± 0.1	57.0 ± 0.2
20%	36.8 ± 0.2	43.5 ± 0.3	50.4 ± 0.1	56.3 ± 0.2
30%	36.3 ± 0.2	42.8 ± 0.3	50.8 ± 0.1	57.0 ± 0.2

Table 2.6: Heat of fusion values of paracetamol dispersions in G50/13 (J/g).

	1st peak	*2nd peak*	*3rd peak*	*4th peak*	*Total*
5%	77.8 ± 1.3	52.8 ± 1.2	11.5 ± 0.5	2.4 ± 0.2	144.5 ± 2.3
10%	76.6 ± 3.5	38.3 ± 0.8	12.4 ± 0.3	2.3 ± 0.1	129.5 ± 4.5
20%	76.7 ± 0.9	30.9 ± 0.6	8.3 ± 0.3	1.4 ± 0.3	117.4 ± 2.0
30%	70.1 ± 1.5	27.6 ± 0.5	8.6 ± 0.2	1.8 ± 0.1	108.1 ± 2.0

The major change caused by the incorporation of the paracetamol was that Peak 1 has now the largest heat of fusion value (Table 2.6). ΔH_f of Peak 2 had decreased almost in proportion to the increase in Peak 1 and to a small extent, Peak 3 (Table 2.7). The SFC profile correspondingly showed an overall fall compared to pure G50/13 samples (Figure 2.5). Using the same classification of LMF, MMF and HMF as pure G50/13, it could be seen that the LMF has expanded substantially at the expense of MMF. The great increase in the LMF of the paracetamol dispersions suggests that the drug was stabilising the Peak 1 form of the gelucire. This form could partly consist of the less stable polymorphs of the gelucire components. Such retention at a metastable level could be the cause of the proportionate fall in the ΔH_f of the more stable Peak 2 leading to the reduction in MMF. The effect that the paracetamol has on the G50/13 structure may be chemical or physical, and it would be difficult to ascertain which from a DSC scan. The high volume of LMF and the drop in MMF would explain the softness of the moulded paracetamol dispersion tablets even after setting, and the difficulty encountered due to its stickiness when the tablets had to be comminuted down and placed in the DSC pans. Variation to the drug loading did not affect the solidity of the dispersions.

On the addition of 5% paracetamol, the total heat of fusion was quite similar to the value for the pure G50/13 even though the amount of gelucire present in this dispersion would be 5% less weight per weight (Tables 2.4 and 2.6). This could indicate that some of the drug had dissolved in the G50/13 during matrix preparation, that is throughout the melt-fusion process when all of the G50/13 was fully molten and had recrystallised within the gelucire structure upon cooling. The melting of the gelucire during scanning would also then result in the fusion of that amount of drug. If the difference between the total heat of fusion for 5% paracetamol dispersion and 95% pure G50/13 (Table 2.7) was taken to be

Table 2.7: Heats of fusion (ΔH_f) under each peak as percentages of the total heat of fusion of paracetamol dispersions in G50/13.

5% drug load	*1st peak*	*2nd peak*	*3rd peak*	*4th peak*	*Total*
% over measured total ΔH_f [1]	53.8	36.6	7.9	1.6	
difference in ΔH_f [2], (J/g)	41.9	-41.8	4.1	0.1	4.3
difference in proportions[3], (%)	110.5	-45.8	50.7	0.6	

[1] calculated as the percentage of ΔH_f of each peak over the total ΔH_f of the dispersion.

[2] calculated as measured ΔH_f for the dispersion - theoretical ΔH_f of pure G50/13. Theoretical values under each peak were calculated for the same amount of G50/13 in a 5% paracetamol dispersion (95%) from pure G50/13 data (Table 2.4), using Equation 2.2 but substituting the heat of solidification with heat of fusion.

[3] calculated as:

$$\frac{\text{\% over measured total } \Delta H_f \text{ - \% over theoretical total } \Delta H_f \text{ of pure G50/13}}{\text{\% over theoretical total } \Delta H_f \text{ of pure G50/13}} \times 100$$

10% drug load	*1st peak*	*2nd peak*	*3rd peak*	*4th peak*	*Total*
% over measured total ΔH_f	59.1	29.6	9.5	1.7	
difference in ΔH_f, (J/g)	42.6	-51.4	5.4	0.1	-3.3
difference in proportions, (%)	131.3	-56.2	81.2	6.1	

20% drug load	*1st peak*	*2nd peak*	*3rd peak*	*4th peak*	*Total*
% over measured total ΔH_f	65.3	26.4	7.1	1.2	
difference in ΔH_f, (J/g)	46.5	-48.8	2.1	-0.5	-0.7
difference in proportions, (%)	155.4	-60.9	34.3	-25.3	

30% drug load	*1st peak*	*2nd peak*	*3rd peak*	*4th peak*	*Total*
% over measured total ΔH_f	64.8	25.6	7.9	1.6	
difference in ΔH_f, (J/g)	43.7	-42.1	3.1	0.1	4.8
difference in proportions, (%)	153.6	-62.1	50.4	-0.8	

Figure 2.5: Solid Fat Content of paracetamol dispersions in G50/13 at different loadings of the drug

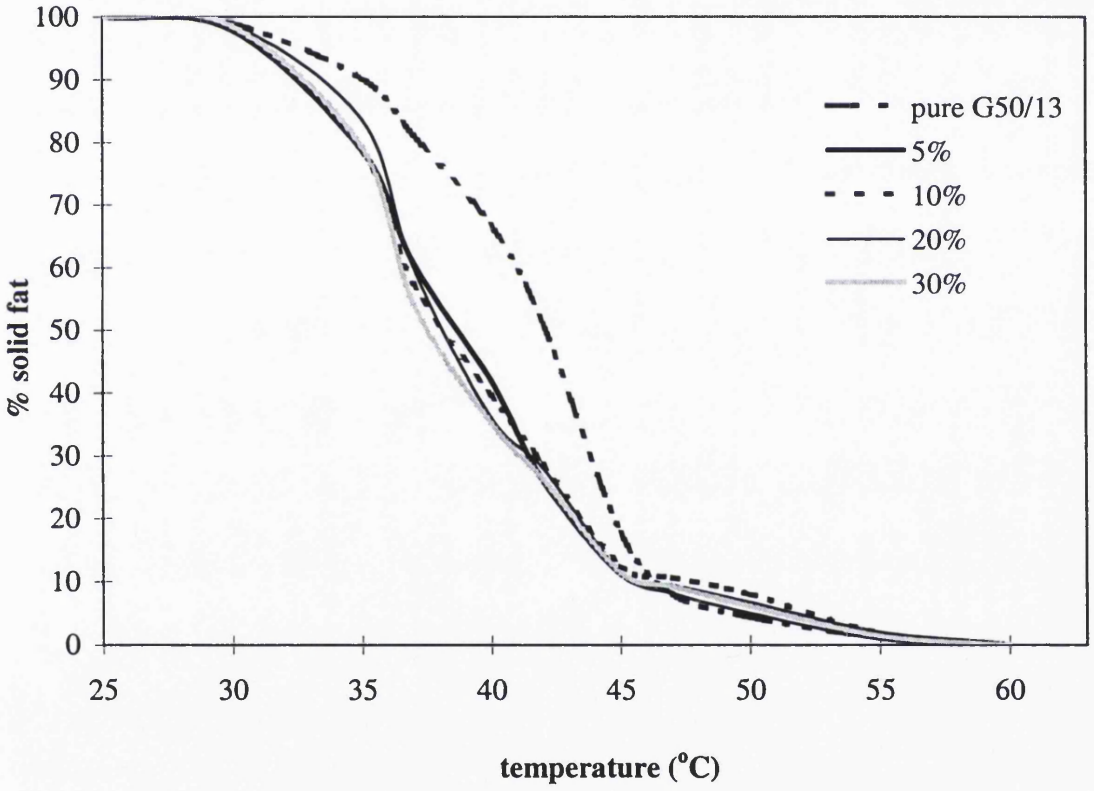

due to the dissolved drug and the amount calculated from pure paracetamol data (Table 2.8), then the solubility of paracetamol in the molten gelucire is 2.3%.

Table 2.8: Mean ± standard deviation of melting point (°C) and heat of fusion values (J/g) of paracetamol (heating rate: 2°C/min; the DSC thermal profile is given in Appendix 4).

	Melting temperature (°C)	Heat of fusion (J/g)
Paracetamol	169.6 ± 0.2	183.3 ± 0.8

This value for the solubility of paracetamol is an estimation because it was derived from the heat of fusion values of the carrier rather than the drug. A more common method of determining drug solubility in a carrier can be exemplified by Bodmeier et al (1990) who plotted the heat of fusion of propanolol and theophylline against their amount in a gelucire matrix and obtained their solubility from the intercept of the drug amount axis. This conventional method of heating until the excess drug melts and plotting the heats of fusion against drug loadings, so that the solubility could be determined from the intercept of the drug loading axis was not a practical technique to implement here because of poor reproducibility of the drug peak. The most likely cause of this was the gradual dissolution of the drug in the molten carrier.

This difficulty in observing a melting endotherm for the excess drug due to its dissolution in the molten carrier was also reported by Lloyd et al (1997a) who found that the endotherm for paracetamol which had been incorporated into PEG 4000 to be very broad and difficult to distinguish from the underlying baseline. The extrapolated onset of melting was lower than the normal melting point and the ΔH_f was also much lower than expected although that could be due to the problem in determining the start of the peak. Such difficulties were also encountered here with the G50/13 and may be due to the solubility of the paracetamol in the PEG component of the gelucire. The low scanning rate of 2°C/min used for the current study may have exacerbated this effect as was also shown by Lloyd et al (1997a) when lower scanning rates provided more time for the paracetamol to dissolve over a wide range of temperatures.

Looking at Equation 2.5 in Section 2.1.2.1, it was put forward that the melting of the

eutectic composition may be concealed by the melting of the excess carrier, if the carrier is a polymer or a similar substance that melts over a broad range of temperature. From this, it is possible that the higher than expected heat of fusion of the endotherm obtained from 5% paracetamol dispersion was partly due to the melting of a eutectic mixture within the G50/13 melting range. This eutectic mixture could have been formed with only some of the components of G50/13, resulting in the increase in the heat of fusion of Peak 1 due to the addition of the eutectic melting endotherm and the decrease in Peak 2 due to some of its components being taken up by the eutectic.

A eutectic composition was not found within the paracetamol loadings investigated here as there was an absence of a single, uncomplicated melting endotherm which was not due to the G50/13 nor the drug melting. In addition, the baseline drifts after the G50/13 melting endotherms caused by the melting of the paracetamol or its dissolution in the molten gelucire were consistently present which would only occur at the drug rich side of the eutectic composition (Ford, 1984). This indicated that if a eutectic composition existed between paracetamol and G50/13, it would be at the drug concentration of less than 5%.

At loadings higher than 5%, the thermal characteristics of the gelucire became more complex. The 10% dispersion had a deficit of about 2.5% of its heat of fusion compared to the theoretical value (Table 2.7). From the table, it could be seen that this difference was due to the more intense Peak 2 suppression. When a lesser amount of the more stable form or polymorph is made available, the total heat of fusion decreases accordingly. This could also indicate an increase in the amorphousness of the dispersion (Dordunoo et al, 1996). As the loading rose, this heat of fusion deficit diminished until 30% loading where there was a positive difference between the observed and theoretical total heat of fusion. This is because there was now more of the Peak 1 form to contribute to the total heat, possibly due to the augmentation of the metastable form to the eutectic melting.

2.3.3 Caffeine dispersions in G50/13

The peak temperatures and thermal profiles of the caffeine dispersions were similar to the pure G50/13 (Table 2.9 and Figure 2.6). Moreover, the SFC profiles indicate that the

solidity of the samples was not significantly altered by the incorporation of the caffeine with coinciding amounts of LMF, MMF and HMF between the drug dispersions and the pure G50/13 (Figure 2.7). Different loadings of the caffeine did not seem to have an effect on any of these profiles.

Table 2.9: Peak temperature values of caffeine dispersions in G50/13 (°C).

	1st peak	*2nd peak*	*3rd peak*	*4th peak*
5%	36.7 ± 0.2	43.5 ± 0.1	48.1 ± 0.5	54.6 ± 0.3
10%	37.0 ± 0.1	43.9 ± 0.1	48.4 ± 0.2	55.0 ± 0.1
20%	36.5 ± 0.1	44.2 ± 0.2	49.6 ± 0.3	56.5 ± 0.2
30%	36.8 ± 0.1	43.7 ± 0.1	48.1 ± 0.3	55.0 ± 0.2

Peak 1 had a higher heat of fusion value compared to the theoretical pure G50/13 value although to a much lesser extent than for the paracetamol dispersions (Tables 2.10 and 2.11). This implied that a eutectic melting could also be present within the caffeine dispersions melting endotherm. A slight decrease in the heat of fusion of Peak 2, again to a much lesser extent than the paracetamol dispersions, could be seen. There seemed to be a lack of the interaction that held most of the paracetamol dispersions in a metastable state in the caffeine samples.

Table 2.10: Heat of fusion values of caffeine dispersions in G50/13 (J/g).

	1st peak	*2nd peak*	*3rd peak*	*4th peak*	*Total*
5%	47.0 ± 5.7	90.6 ± 2.0	7.4 ± 0.5	2.3 ± 0.2	147.3 ± 8.0
10%	39.8 ± 0.5	89.9 ± 0.6	7.1 ± 0.1	2.2 ± 0.2	139.0 ± 0.7
20%	38.4 ± 2.1	85.0 ± 2.9	7.9 ± 0.1	2.5 ± 0.2	133.8 ± 4.4
30%	31.9 ± 0.7	70.2 ± 1.7	5.9 ± 0.2	1.6 ± 0.1	109.6 ± 2.2

The total heat of fusion values for all the dispersions were higher than that calculated for the corresponding contents of pure G50/13 (Table 2.11). If the excess heat of fusion was taken to be due to dissolved caffeine, then the amount of drug responsible for the increase was about 5-6%, with the exception of the 20% loading which showed an anomalously high

Figure 2.6: Thermal profiles of caffeine dispersions in G50/13 at different drug loadings

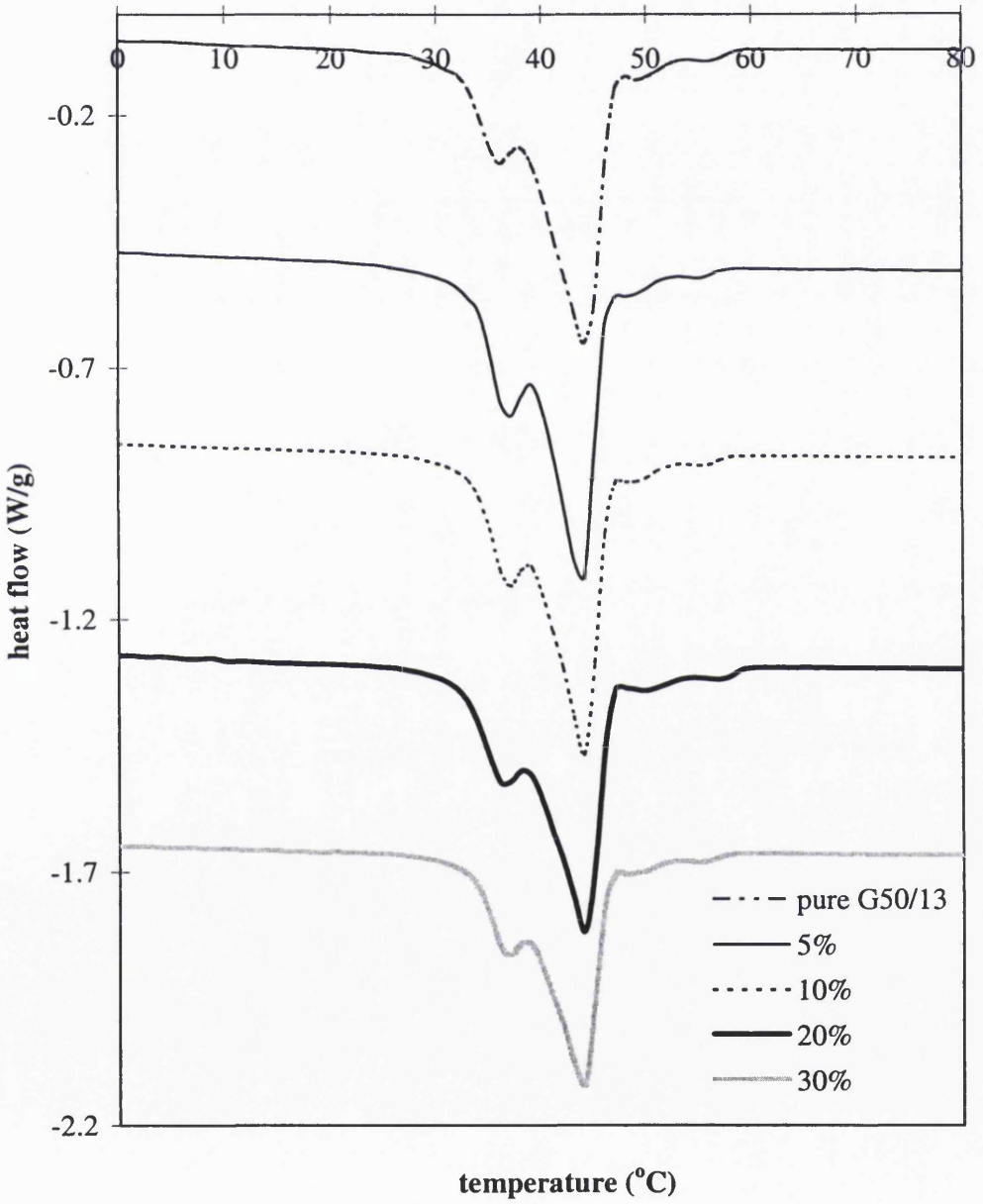

Figure 2.7: Solid Fat Content of caffeine dispersions in G50/13 at different drug loadings

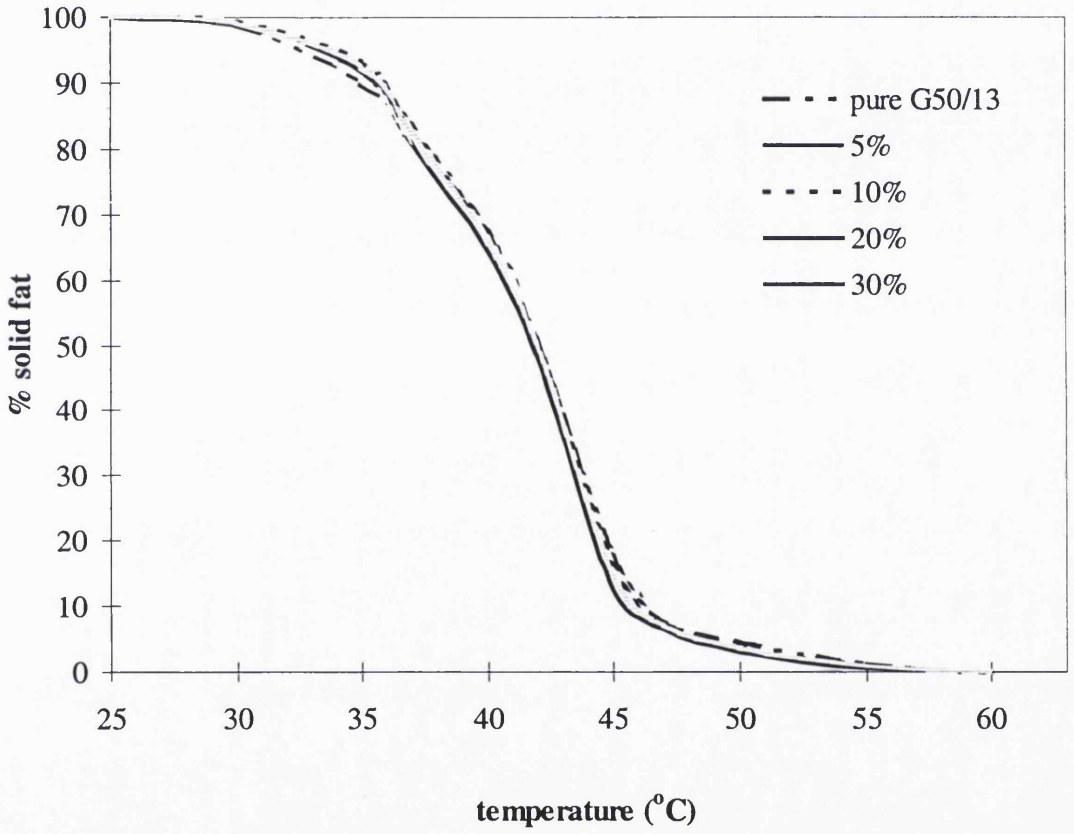

Table 2.11: Heats of fusion (ΔH_f) under each peak as percentages of the total heat of fusion for caffeine dispersions in G50/13.

5% drug load	*1st peak*	*2nd peak*	*3rd peak*	*4th peak*	*Total*
% over measured total ΔH_f	31.9	61.6	5.0	1.5	
difference in ΔH_f, (J/g)	11.1	-4.0	0.02	-0.05	7.1
difference in proportions, (%)	24.7	-8.8	-4.6	-6.7	

10% drug load	*1st peak*	*2nd peak*	*3rd peak*	*4th peak*	*Total*
% over measured total ΔH_f	28.6	64.7	5.1	1.6	
difference in ΔH_f, (J/g)	5.8	0.2	0.1	-0.01	6.2
difference in proportions, (%)	12.0	-4.2	-2.5	-4.8	

20% drug load	*1st peak*	*2nd peak*	*3rd peak*	*4th peak*	*Total*
% over measured total ΔH_f	28.7	63.5	5.9	1.9	
difference in ΔH_f, (J/g)	8.2	5.2	1.7	0.6	15.7
difference in proportions, (%)	12.2	-5.9	11.9	15.8	

30% drug load	*1st peak*	*2nd peak*	*3rd peak*	*4th peak*	*Total*
% over measured total ΔH_f	29.1	64.1	5.4	1.5	
difference in ΔH_f, (J/g)	5.5	0.5	0.4	-0.05	6.3
difference in proportions, (%)	13.7	-5.1	1.7	-8.6	

value. The true caffeine percentage is probably less than the above as it was difficult to accurately measure the heat of fusion of pure caffeine (Table 2.12) because caffeine undergoes vaporisation soon after melting and so, the heat of vaporisation overlaps the melting endotherm (Appendix 4). The heat of fusion of caffeine was taken from isolating the melting endotherm as far as possible from the rest of the endothermic processes. On the other hand, the higher heat of fusion for the caffeine dispersions could also indicate that the drug had merely increased the crystallinity of the G50/13 matrix.

Table 2.12: Mean ± standard deviation of melting point (°C) and heat of fusion values (J/g) of caffeine (heating rate: 2°C/min; the DSC thermal profile is given in Appendix 4).

	Melting temperature (°C)	Heat of fusion (J/g)
Caffeine	236.9 ± 0.2	124.7 ± 3.6

It was also difficult to quantify the amount of excess caffeine by its heat of fusion value in order to determine its solubility in G50/13 for the reason of its vaporising behaviour. In addition to that, the baseline of the DSC scan started to slope downwards at high temperatures, including at the melting temperatures of the drugs. This could be due to the deterioration of the G50/13 and therefore compounds the problem of obtaining an accurate and distinctive drug peak. Decomposition of samples during DSC heating had also been reported by Ford (1984) who detected an additional endotherm for PEG 20 000 melt dispersions with glutethimide and this decomposition was attributed to peroxides, which was thought to be a common by-product of PEG. Spurious peaks, peak broadenings and deviations from the baseline after a melting endotherm are other indications of decomposition (Ford and Timmins, 1989) as had been observed here for G50/13. This occurrence is not thought to cause adverse changes to the matrix stability because the drugs used in this study were incorporated into the molten carrier at a temperature (75°C) much lower than those of the drug melting points (169 and 237°C).

A similarity in the thermal profile of a mixture of a carrier and an incorporated drug with the thermal profile of the carrier alone was taken to indicate the absence of a drug-carrier interaction in an existing study (Serajuddin et al, 1988). At low loadings of α-pentyl-3-(2-quinolinylmethoxy) benzenemethanol in G44/14, the thermal profile was similar to the that

of pure G44/14 except for a slight increase in the broadness of the peak and a slight decrease in the endothermic temperature due to the dissolution of all the drug in the gelucire during the melting of the carrier. At higher loadings of the drug, a shoulder was seen on the higher temperature side of the melting endotherm of the dispersion, denoting the need for a temperature higher than the melting point of the carrier to melt the excess drug. However, the similarity of all the thermal profiles was taken to suggest that no interaction was occurring between the drug and the carrier, except for the dissolution process. In the current study, the thermal profiles of the caffeine dispersions were also very similar to its carrier G50/13, suggesting that no or very minor interaction had occurred between the two substances.

2.3.4 The effects of drug incorporation on the thermal structure of G50/13 matrices.

Overall, the total heat of fusion value was lower for the paracetamol dispersions than the caffeine dispersions. The thermal profile of G50/13 was greatly altered by paracetamol addition but to a much lesser extent by caffeine addition (Figure 2.8). A variation in the effects on the carrier induced by differing drugs had also been shown by Dordunoo et al (1996) when the addition of triamterene and temazepam both altered the DSC solidification profiles of PEGs but only the solidification temperatures of temazepam dispersions were affected by drug:carrier ratio. Additionally, the enthalpies of solidification for temazepam dispersions were also lower than triamterene with 10% of the former producing a lower than predicted enthalpy (by Equation 2.2) suggesting an increase in the amorphousness of the matrix dispersions. In the current study, 10% paracetamol dispersion produced a lower than expected ΔH_f but a higher value was obtained for the 10% caffeine dispersion (Tables 2.7 and 2.11). Hence, this suggests that the difference in crystal forms in the samples, possibly due to the interactions with G50/13 components, resulted in varying ΔH_f values.

The solid fat contents of both paracetamol and caffeine dispersions were not influenced by the amount of drug incorporated in the matrices (Figures 2.5 and 2.7). However, the SFC profiles of the paracetamol dispersions were greatly reduced compared to pure G50/13 whilst the incorporation of caffeine had a minimal effect (Figure 2.9). Paracetamol lowered the SFC of the matrix by increasing the LMF and closer examination of the thermal profile

Figure 2.8: Thermal profiles comparing pure G50/13, 10% paracetamol and 10% caffeine dispersions in G50/13

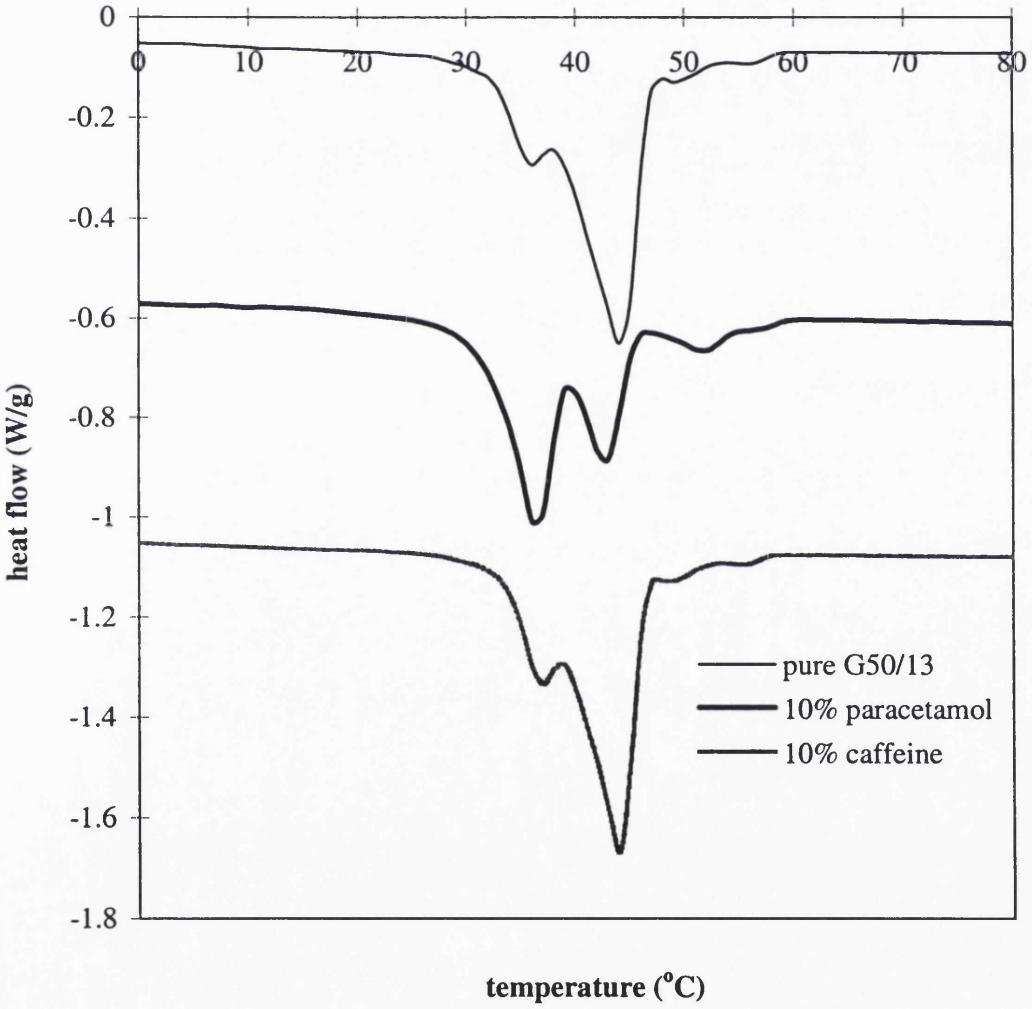

Figure 2.9: Solid fat content of pure G50/13 and 10% dispersions of paracetamol and caffeine in G50/13

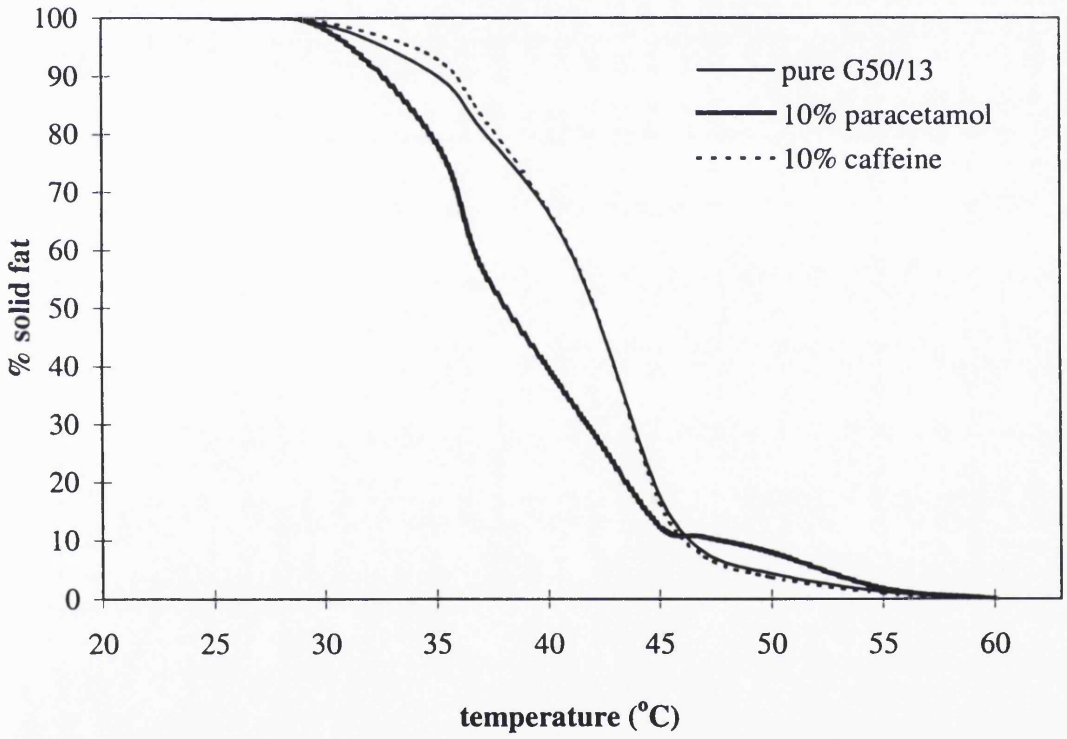

revealed that the melting of Peak 1 form for this drug dispersion overlapped the endotherm of Peak 2 for the pure G50/13, resulting in a smaller MMF for the dispersion (Figure 2.8). This difference between the solidity of the dispersions may have an implication on the in vivo release of the drugs from the matrices, with the samples containing a larger quantity of LMF giving a higher release rate due to softening of the carrier.

2.4 Conclusions

The thermal profile of G50/13 confirmed the heterogeneity of its components which could broadly be grouped into LMF, MMF and HMF. It could be postulated that the gelucire forms giving rise to each endothermic peak was composed of a variety of the gelucire components together with their different polymorphic forms even though their exact composition could not be elucidated except perhaps through complicated chemical extraction and analysis. From melting point and heat of fusion data of existing studies, it could be suggested that the lower melting peaks were composed of a bigger proportion of the less stable polymorphic forms and the higher peaks of the more stable forms. However, each peak was not thought to be exclusively due to a single polymorphic form as the polymorphs of the various components with similar melting ranges could form mixed crystals or solid solutions with one another. Components with more free hydroxyl groups could make up the higher melting fraction as shown by monoglyceride data, where even the metastable polymorphs of this glyceride had higher melting points than the stable forms of the triglycerides.

Since the glyceride component only constitute 20% G50/13, most of the thermal behaviour must rest on the PEG esters of fatty acids. This component probably also showed polymorphism and in addition, could form mixed crystals with other constituents, leading to what had been described previously as segregations of components which melting gave rise to the endothermic peaks (Sutananta et al, 1994b). The absence of exothermic peaks indicates that little or no structural rearrangements of these mixed crystals or solid solution due to melt transformation occurred during scanning. The importance of polymorphism on the thermal structure of G50/13 could be further clarified by performing ageing studies, especially at temperatures that may affect it.

The results of the paracetamol dispersions showed that the stabilisation of the lowest melting gelucire form was the most apparent outcome of the drug incorporation, with the corresponding increase in the LMF. This increase in the LMF occurred at the expense of the MMF, and led to the softness of the matrices. Paracetamol could have achieved this by preventing the rearrangements of aliphatic chains from the lower melting polymorphs to the more densely packed higher melting polymorphs, which could have occurred either by steric hindrance or chemical bonding.

The slight additional rise in the proportion of the Peak 1 form as the drug loading was increased suggests that the drug may be forming a eutectic with the gelucire components in the MMF which resulted in the lowering of ΔH_f of Peak 2. Therefore, the elevation in the LMF could be due to either the stabilisation of the less stable polymorphs or a eutectic formation but it could also be due to both factors. In addition, some of the drug could have been dissolved within the solid carrier but an accurate concentration of the dissolved drug was difficult to be ascertained by the DSC method due to its slow dissolution in the molten gelucire.

The thermal profile and the SFC profile of the G50/13 were not greatly affected by the incorporation of caffeine. This suggests that there was little or no interaction between the caffeine and G50/13 except for a possible eutectic formation as indicated by the slight rise in ΔH_f of Peak 1. An increase in the total heat of fusion values for all the caffeine dispersions exhibited a higher degree of crystallinity compared to pure G50/13 due to the dissolved drug within the matrix. These results show that different model drugs can affect the G50/13 matrices in dissimilar manner depending on their interactions with the various components and polymorphs of G50/13. Moreover, variation in the drug loadings did not significantly alter the thermal profiles of either drug dispersion indicating that the G50/13 matrices were more affected by the type of drug incorporated rather than their concentrations.

CHAPTER 3: MORPHOLOGICAL STUDIES USING DIFFERENTIAL INTERFERENCE CONTRAST (DIC) MICROSCOPY

3.1 Introduction

Microscopy has long been an invaluable technique in characterisation studies because it allows the visualisation of the material under investigation and is often used as a complementary tool to other methods of analysis. Magnification is not the only important element in this technique as the contrast of the image can also greatly influence the outcome of microscopical studies. Contrast gives the object visibility and distinguishes it from its background. This can be expressed by

$$Contrast = \frac{|I - I_B|}{I_B}$$

where $|I - I_B|$ is the absolute value of the difference between the luminous intensities of the object and its background.

Objects under microscopical study can have a degree of intrinsic contrast. However, the human eye/brain complex can only detect 2% and upwards of contrast (Bradbury and Evenett, 1996). When a light beam hits a specimen, there are a number of ways that they could interact, namely reflection, absorption, polarisation, refraction, diffraction and fluorescence. These interactions could in turn be manipulated to impart bigger contrasts. Refraction is the change in velocity of light when it crosses the boundary of media which have different refractive indices and this change may or may not be accompanied by a change in its direction (Bradbury, 1996). Refractive index, n, can be defined as the ratio of the speed of light in vacuum to its speed in that particular medium.

$$n = \frac{\text{velocity in vacuum}}{\text{velocity in medium}} = \frac{c}{v}$$

since $c = \lambda\nu$ and $v = \lambda_m\nu$, therefore

$$n = \frac{\text{wavelength in vacuum}}{\text{wavelength in medium}} = \frac{\lambda}{\lambda_m}$$

where λ is the wavelength of the light and ν is its frequency, which remains unchanged.

Figure 3.1: An illustration of *refraction* of a beam of light coming from a less dense medium to a denser medium.

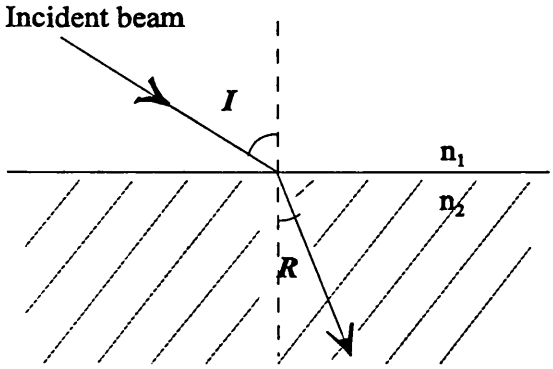

Snell's Law states that

$$\frac{\sin I}{\sin R} = \frac{n_2}{n_1}$$

where n_1 and n_2 are the refractive indices of the less and more dense media respectively.

The concept of refraction and refractive indices becomes beneficial when the object to be studied is transparent and cannot be stained to increase its contrast, as the phase of the transmitted light was discovered to be still altered by these transparent objects. The phase shift can be defined by the phase angle:

$$\varphi = \frac{2\pi}{\lambda} nz$$

where λ is the wavelength of the transmitted light, n is the refractive index of the object and z is its real thickness (nz is also the optical thickness of the object). In order to make this alteration detectable to the eye/brain complex or other detectors, it has to be transformed into light intensity changes. This vision has led to the design of phase contrast, interference and differential interference contrast microscopes.

3.1.1 Differential Interference Contrast (DIC) microscopy

Differential Interference Contrast microscopy evolved from transmitted-light interference microscopy which was used primarily to detect and measure phase differences in transparent samples (Dunn, 1998). Interference microscopy is called as such because

contrast in the sample is brought about by the interference after the recombination of the illuminating light beam which had been split into two and had been travelling along separately. Interference of these beams will give a measure of their optical path difference (OPD). DIC offers an advantage over simple polarised light microscopy in that it can still measure the OPD even in isotropic (non-birefringent) samples. OPD between two points is a measure of the distance that a light has to travel in a vacuum in order to be equivalent to the time taken for that light to travel between those two points in a particular medium. Ultimately, the OPD is the product of the physical path length of the light in the medium and the refractive index of that medium, after considering that refractive index is actually a measure of how much light is slowed down when travelling through that medium. Therefore, a transmitted-light interference microscope will measure the difference in the refractive indices of a sample that the two beams have passed through.

Robert Hooke, looking down his new invention, the compound microscope in 1665, extolled the 'fantastical colours' of interference fringes viewed on a piece of mica. However, it took a further 200 years before the first interference microscopes were available and even this was eventually superseded by the more popular phase contrast microscopes. Only when Nomarski developed the DIC microscope in 1955 did interference microcopy return to the forefront.

In the Nomarski technique, a plane polarised light beam from a polarizer is split into two by a Wollaston prism (Figure 3.2). A Wollaston prism is made up of calcite which is a birefringent material and two wedges of this material with their optic axes perpendicular to each other are cemented together. One of the beams, the specimen beam, travels through a particular area of the sample. The other beam, the reference beam, travels through an area which is very near to the first area. The separation distance between the two beams is smaller than the limit of resolution of the objective so that a single image is seen eventually. The OPD arising from the differences in the refractive indices of the two areas causes a phase shift between the specimen and the reference beams. A second Wollaston prism then brings the sheared beams back together. Due to the two beams being perpendicular to each other, a second polaroid, the analyser, is needed to cause the interference of the two beams in order to give an image. Here, the Normarski technique differs from classical interference

contrast techniques by utilising the local phase variation in the same sample, that is the reference beams travels through the area of the sample which is very close by to the area travelled by the analyser beams, rather than having one single reference beam travelling through an empty reference stage. Since the contrast arises from local phase differences, structures which are well defined with steep gradients in its optical thickness give better contrast with this technique rather than those with gentler slopes (Plášek and Reischig, 1998). On the other hand, the DIC is a very sensitive technique, which allows even an OPD of 2nm to be detected.

Figure 3.2: Diagrammatic representation of the DIC microscope and the shearing of the beams (based on Padawer, 1968).

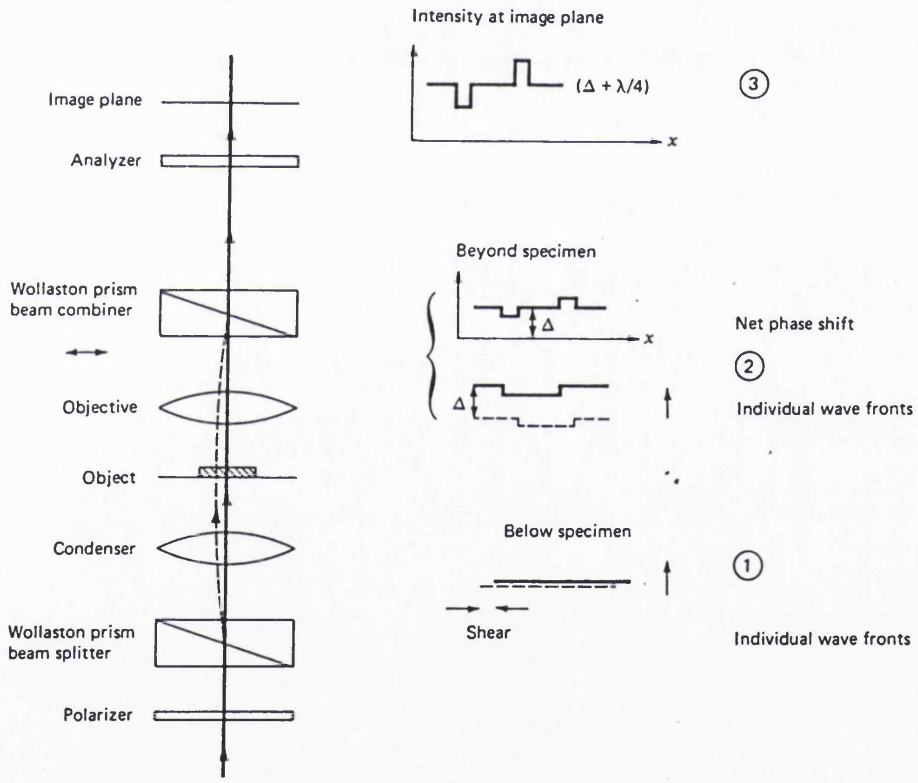

3.1.2 Köhler illumination

An illuminating system of a microscope has to provide a uniform and controllable area, as well as angle, of light. Köhler illumination is a technique of getting this uniform and controlled lighting in the plane of the sample. Correct illumination will cut out glare which can lead to image degradation and a reduction of resolution. This is because the

illumination of the area of view is controlled by the illuminating field diaphragm and the angle of the cone of light (which directly affects resolution) is controlled by the illuminating aperture diaphragm. To visualize the function of these diaphragms, it is first necessary to know that a microscope is made up of two sets of conjugate planes i) image forming set (also called field set) and ii) illuminating set (also called aperture set) (Figure 3.3).

Figure 3.3: Diagrammatic representation of the image forming and illuminating sets of conjugate planes. LC is the lamp collector lens, FI is the field-iris diaphragm, AI is the aperture-iris diaphragm and PIP is the primary image plane (from Bradbury, 1996).

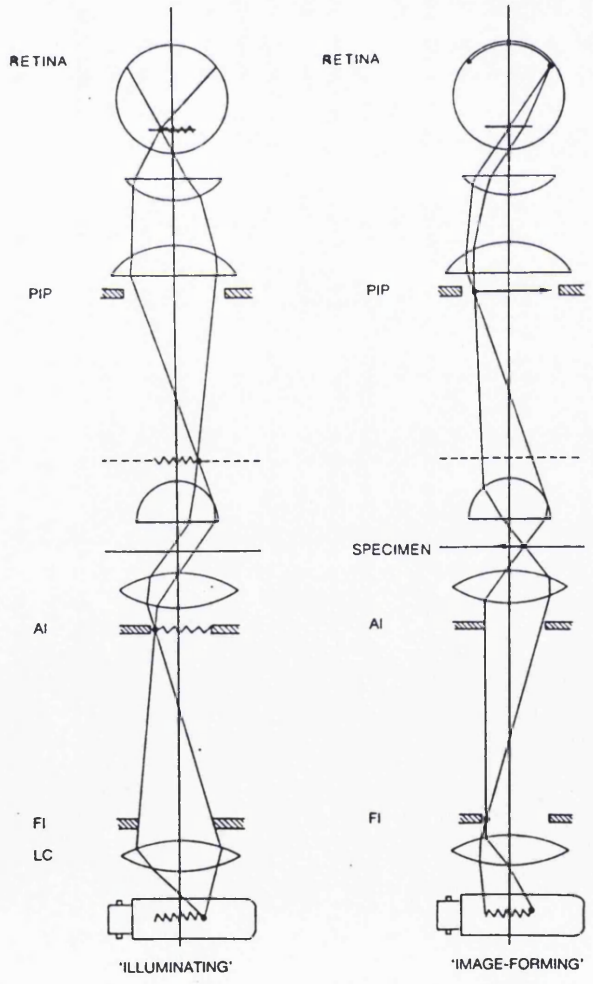

Source of illumination is usually the low-voltage, high-wattage tungsten-halogen bulb, with one long filament coiled closely to increase the magnitude of the light. The wavelengths of the light radiating from this type of source spans the spectrum, which makes it suitable for

colour photomicrography. Attempts to reduce the brightness of the light by lowering the voltage should be avoided as this leads to the light becoming more red. Neutral density filters should be used instead to cut the excess brightness. The lamp filament is arranged so that it is positioned near the focal point of the *collector lens*. These lenses act as a large and uniform secondary source of light, ideal for Köhler illumination. Additionally, the collector lens focuses the image of the filament onto where the diaphragm controlling the size of light to the condenser, called *aperture iris diaphragm*, is situated. This position is also the front focal plane of the condenser. The collector lens has to be sufficiently corrected so that this image of the filament is large enough to fully illuminate the above-mentioned condenser aperture, even at its maximal diameter. When the image of the filament is at this particular position, it is at the first part of the *illuminating* series of conjugate planes.

The second set of conjugate planes is called the *image forming* series. An iris diaphragm which is in front of the light source controls the size of the illumination leaving from here. This diaphragm, which is also called the *field diaphragm*, will get imaged by the condenser onto the specimen plane. The image of this diaphragm provides a way of checking the focus of the condenser; this image would be as sharp and in focus at an identical plane to the specimen. From here, the *image forming* series continues with the image of the diaphragm being formed on the primary image plane, which in turn becomes the 'object' for the eyepiece lens. The final image is formed on the retina of the eye.

Returning to the *illuminating* series, the second image of the filament is formed at the back focal plane of the objective. In between the front focal plane of the condenser and the back focal plane of the objective, the image of the filament is simultaneously providing an even source of illumination to the specimen plane. In this way, any dirt or imperfections on the filament are not focussed onto the specimen plane. The final image of this series is formed on the pupil of the eye, this position being called the Ramsden disc or the exit pupil, but this image is not focussed onto the retina and so, not 'seen'. The procedure for setting up the Köhler illumination will be outlined in the next section.

3.1.3 The characterisation of drugs and their carriers using microscopy

Hot stage microscopy (HSM) which is microscopy with a facility to heat or cool samples during observation has often been used with other thermal analysis methods such as Differential Scanning Calorimetry (DSC) to characterise lipids. Ginés et al (1995) observed that the DSC thermal profiles of cinnarizine and G53/10 melt dispersions showed a split endothermic peak due to the fusion of the drug during scanning. This was confirmed under HSM when the drug was seen to dissolve in the molten G53/10 up to a drug concentration of 40% w/w.

The construction of phase diagrams in order to find the eutectic composition was made possible by DSC and HSM for PEG 1500 and ibuprofen system (Shehab and Richards, 1996b), PEG 6000 and indomethacin fused system (Ford and Rubinstein, 1978) and HSM alone for lidocaine and prilocaine binary system (Brodin et al, 1984). HSM was also used to determine the effect of thermally cycling PEG 4000 with paracetamol (Lloyd et al, 1997b). Combining the data obtained from DSC and HSM allowed the interpretation of all the transitions observed on the thermal profile of PEG 6000 and by varying the thermal cycle together with the rate, the phenomenon of folded and extended chain melting was seen (Delahaye et al, 1997). This microscopy technique also showed that different cooling rates can affect the crystal structure of certain carriers such as Dynasan-114 (a myristic acid triglyceride) and this observation was supported by DSC data which showed that the thermal profiles of the samples recrystallised at various rates were dissimilar due to the formation of metastable polymorphs (Hawley et al, 1992).

3.2 Materials and Methods

3.2.1 Preparation of samples for Hot Stage Microscopy (HSM)

Using a microspatula, 2 mg of the comminuted pure G50/13 was placed on one end of the glass slide (Blue Star microslides, Chance Propper Ltd., 76x26mm, thickness 1.0/1.2mm) and a cover slip (borosilicate glass, BDH, 0.17mm, thickness no. 1 ½) was put on top. This amount was small enough to prevent melted carrier from running off the slides and kept the

sample under the cover slip. A smaller quantity of sample than 2mg was difficult to weigh out accurately to give the various loadings of drugs studied. The slide was positioned on the hot stage and all the heating or cooling rates used were 2°C/min.

The objective lens chosen for the HSM work was x10 because it allows a wider view of the sample and it has a sufficiently long working distance to permit the hot stage oven to be mounted onto the microscope stage. The images under the Olympus BH-2 microscope were captured by a Nikon F-601M fully automatic single lens reflex camera attached to an adaptor on the microscope (Olympus OM2-35mm camera system) for photomicrography, or captured by video camera and transmitted to a high resolution monochrome monitor attached to a printer (all by Sony). The samples were analysed at least three times. The magnification quoted in Section 3.3 was the result of capturing the image of a calibrated graticule and processing it in the same way as the Plates.

3.2.2 Analysis of drug loadings

For the physical mixes of the G50/13 and the drugs, paracetamol or caffeine (both from Avocado Research Chemicals Ltd., Lancs.) was accurately weighed to give the required loadings and placed together with the gelucire on the slide. The total weight for both components was between 2 and 3 mg which was still small enough to prevent the excess melt from running off the slide. The two components were gently mixed using a microspatula for 5 minutes to make the mixture homogenous. The solubilities of the drugs were investigated by mixing various proportions of the drugs to the gelucire.

The heating cycles were as follows: the samples were heated from ambient temperature (25±1°C) to 75°C, held there for 30 minutes, then cooled back down to 25°C and held there for another 30 minutes, finally being reheated until 75°C or the drug melting points in the case of G50/13 dispersions with paracetamol/caffeine. This heating protocol was chosen to mimic the protocol usually adopted in the formulation of dosage forms with gelucires. The initial heating was necessary to remove all thermal history from the lipid matrix. After cooling and allowing the mixture to equilibrate at ambient temperature, the sample was reheated in order to observe the structures formed during this process.

3.2.3 Setting up Köhler illumination

The procedure for setting up the Köhler illumination was as follows: A specimen with a known good contrast was placed on the specimen stage. The lowest objective lens was chosen (in this case, x10 objective lens), swung into place and the sample was focussed. The illuminating field diaphragm was closed until the edge of it could just be seen in the field of view. If this image was blurred, the condenser was focussed until it was at its sharpest. This hexagonal image of the diaphragm was then centralised with respect to the field of view by using the centring screws. The diaphragm was then opened until the outside edge of the hexagonal image was just out of view. The right eyepiece was removed in order to view the back focal plane of the objective. The illuminating aperture diaphragm was adjusted until the cone of light viewed on the back focal plane occupies 70-90% of the total visible area. A smaller cone of light could result in some of the resolution being lost and a bigger cone would result in glare and the reduction of the quality of the image. The eyepiece was returned, necessary filters put in place and the microscope was now ready for use. The whole procedure was repeated every time a new objective was used.

3.2.4 The Hot Stage

The hot stage apparatus used here was the Mettler FP52 and it is made up of a rectangular micro hot stage and an electronic control unit. It is almost identical to the first Mettler model, the FP2, as described by Kuhnert-Brandstätter (1971). The hot stage was heated by an electrical element on both sides of the micro oven. A platinum resistance thermometer, situated on the lower part of the oven near the observation aperture, detected the temperature. The sample to be observed had to be placed quite near one end of the microscope slide because of limited space within the oven itself. The slide was positioned with the sample coinciding with the observation aperture, and prevented from sliding out of position by a clip. A small cross-table controlled the movement of the slide but its range is limited. An appropriate heating rate was chosen (in this case, 2°C/min) and electronic control unit ensured the heating was linear. The range of the hot stage, without a sub-ambient cooling accessory is from room temperature to 300°C. An attached fan cools the oven down when performing a reverse ramp (i.e. cooling at a controlled rate) but this means

that a reliable cooling is only achieved with a slow rate. Continuous observation was facilitated by storage of temperatures within the unit. In combination with DIC, the onset of melting (t_{onset}) was taken to be the point when the birefringent colours change.

3.3 Results and Discussions

3.3.1 Pure G50/13

When pure G50/13 was first heated, the birefringent colours started to change approaching the onset of melting. Melting, once commenced, was gradual. After t_{onset} (41°C), two dominant structures could be seen floating in the melt (Plate1); a dense, compact and almost spherical form which had diameters of less than 100μm, together with a more diffuse, mesh-like and less defined shape form. As these structures continued to melt at about 48-50°C, the compact form gradually decreased in size and the mesh-like form increased its diffusiveness (Plate 2). Towards the end of the melting process (55°C onwards), when all other structures have melted, the mesh-like form was in a clearer view and it could now be observed that this form was clustered in a diffuse structure resembling sand dunes (Plate 3).

A precise melting point was difficult to be ascertained because the numerous components in gelucire gave a broad and gradual melting over a range of temperatures, as previously demonstrated by DSC (refer to Table 2.4 in Chapter 2). It was also difficult to determine the temperature when a particular structure dominated or melted. During melting, the ordered structures and the bonds within the crystals are gradually destroyed, resulting in the change in birefringence (Slayter and Slayter, 1992). However, the detection of this event was difficult as the unaided human eye cannot always distinguish the point of this colour change when it has been continually focussing on the sample for a period of time. Therefore, in addition to the birefringence change, the point at which liquid started to appear or when the solid structures began to lose their boundaries was also taken to be the onset temperature. The temperature at the end of the melting process (t_m) was easier to determine as it was taken to be the point when all the structures have melted and the birefringent colours diminished.

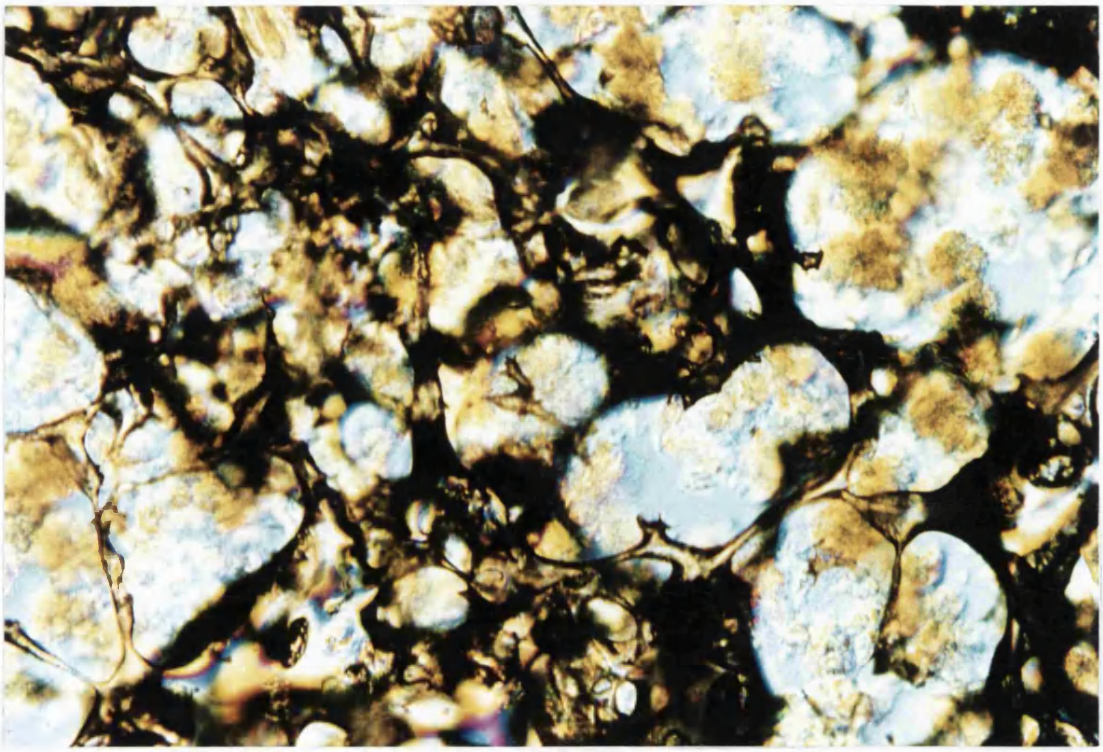

Plate 3.1: Pure G50/13 at 46.6°C during first heating **1:113**
(ratio represents actual length : length in plate, and will be the same for the rest of the plates in this chapter)

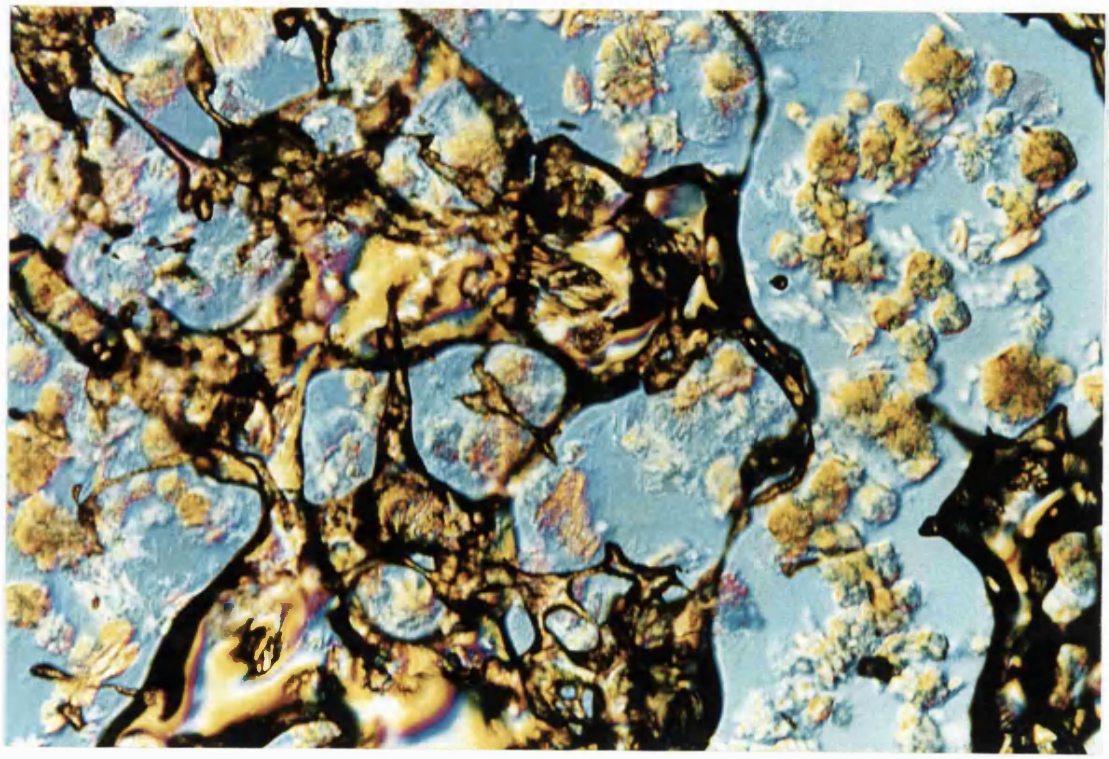

Plate 3.2: Pure G50/13 at 50°C during first heating

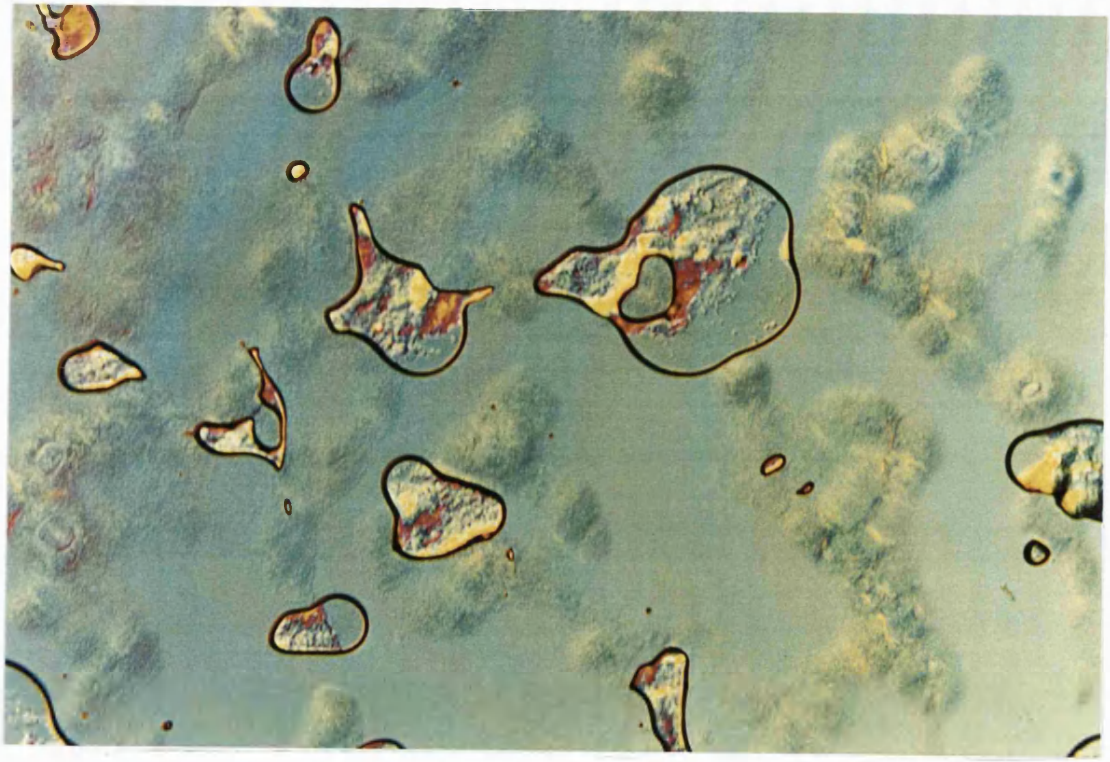

Plate 3.3: Pure G50/13 at 61°C during first heating

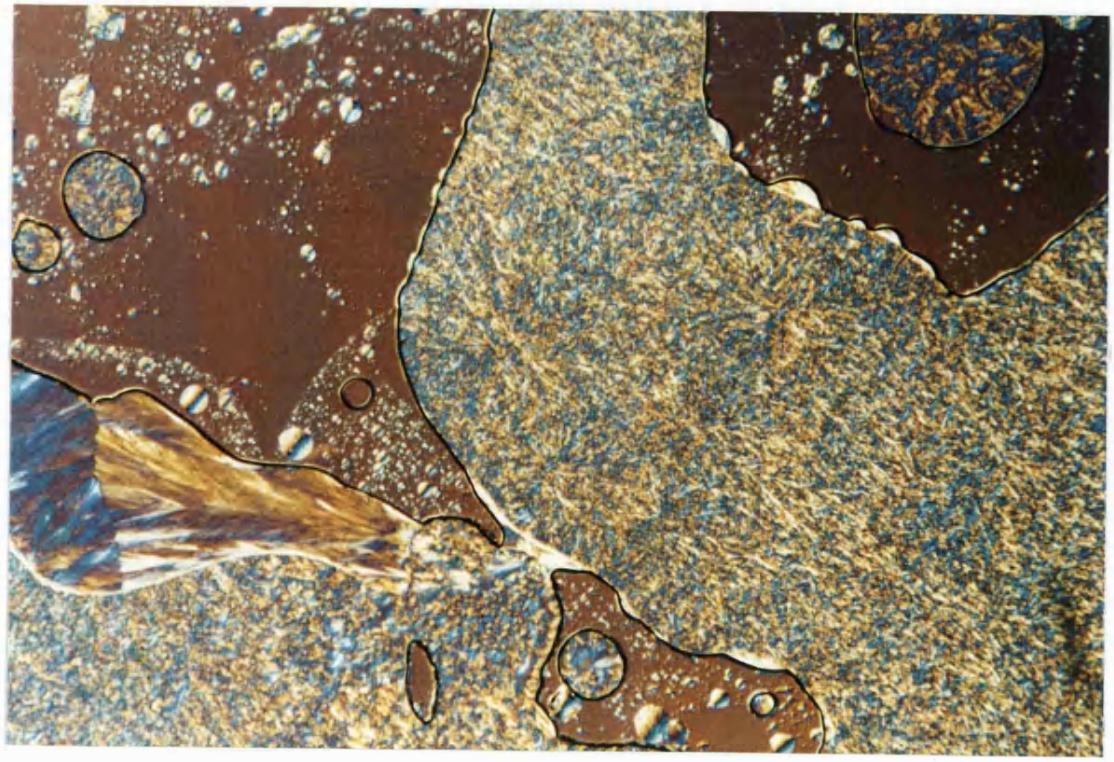

Plate 3.4: Pure G50/13 at 25°C after recrystallisation

The temperature at which the initial structures appeared during the cooling process ranged from 57.4 to 59.0°C. Feather-like spherulites developed later at about 47.5°C and spread in a finger-like pattern. This structure will be designated Form 3 in the reverse order of recrystallisation and is better represented in Plate 5 during the reheating process. Smaller, more compact spherulites resembling snowflakes (Form 2) surrounded and eventually enveloped the Form 3 structures. After a 30 minute hold at room temperature at the end of the cooling cycle, a structure which will be called Form 1 could be seen as streaks at some edges of the gelucire pool together with a denser population of the other crystals (Plate 4). Manning and Dimick (1985) also described such crystals appearing on the periphery of a cocoa butter melt during incubation at 26°C. This structure developed after other crystals of cocoa butter emerged which was similar to the crystallisation behaviour shown by Form 1 in the G50/13 system. Such pattern of recrystallisation is common in heterogenous lipids. Crystallisation of cocoa butter was divided into three stages; the induction phase, the primary crystallisation followed by the secondary crystallisation phase (Chaiseri and Dimick, 1995). However, such stages are not always so distinct especially in fast crystallising samples, when the secondary phase structures start to crystallise out before the primary phase is completed. Hence, the initial structures observed here were part of the induction phase, followed by the spreading of Form 3 during primary crystallisation and overlapped with the secondary crystallisation of Form 2.

During the reheating phase, Form 1 was the first to melt from about 40°C onwards (Plate 5). Then the round compact structures of Form 2 began to lose their shape finally followed by the melting of Form 3 (Plate 6). It was difficult at this point to distinguish the exact onset of melting for these small compact structures because the process was very gradual but it could be placed between 41.6 and 42.0°C. The larger Form 3 was observed to be diminishing from about 50°C onwards and most of the gelucire structures had melted by 57°C except for a few persistent structures which faded by 65°C. The melting of Forms 1, 2 and 3 correspond to the melting of LMF, MMF and HMF as previously described in Chapter 2. The temperatures quoted in the HSM studies are higher than those of Peak 1, Peak 2 and Peaks 3 and 4 on the DSC thermal profile because of the slight thermal lag caused by the layer of non-heat conducting gelucire and the aforementioned difficulty in detecting the exact melting point. Moreover, DSC is a technique that measures the overall

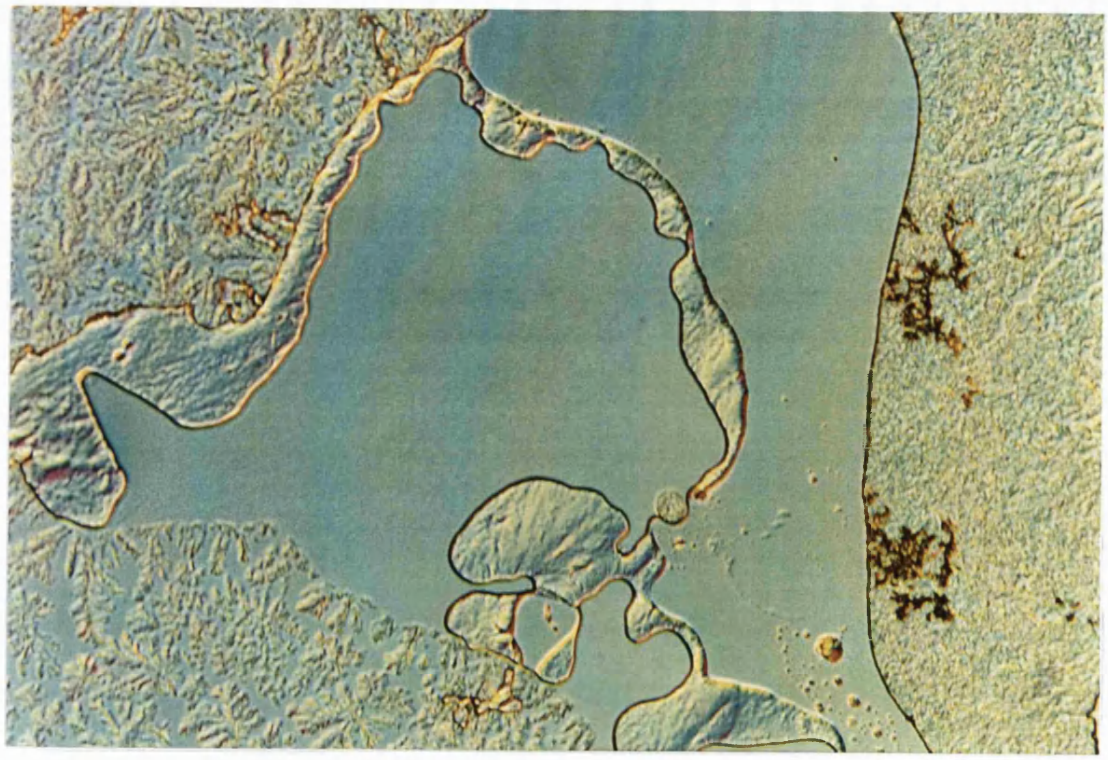

Plate 3.5: Pure G50/13 at 43.2°C during second heating

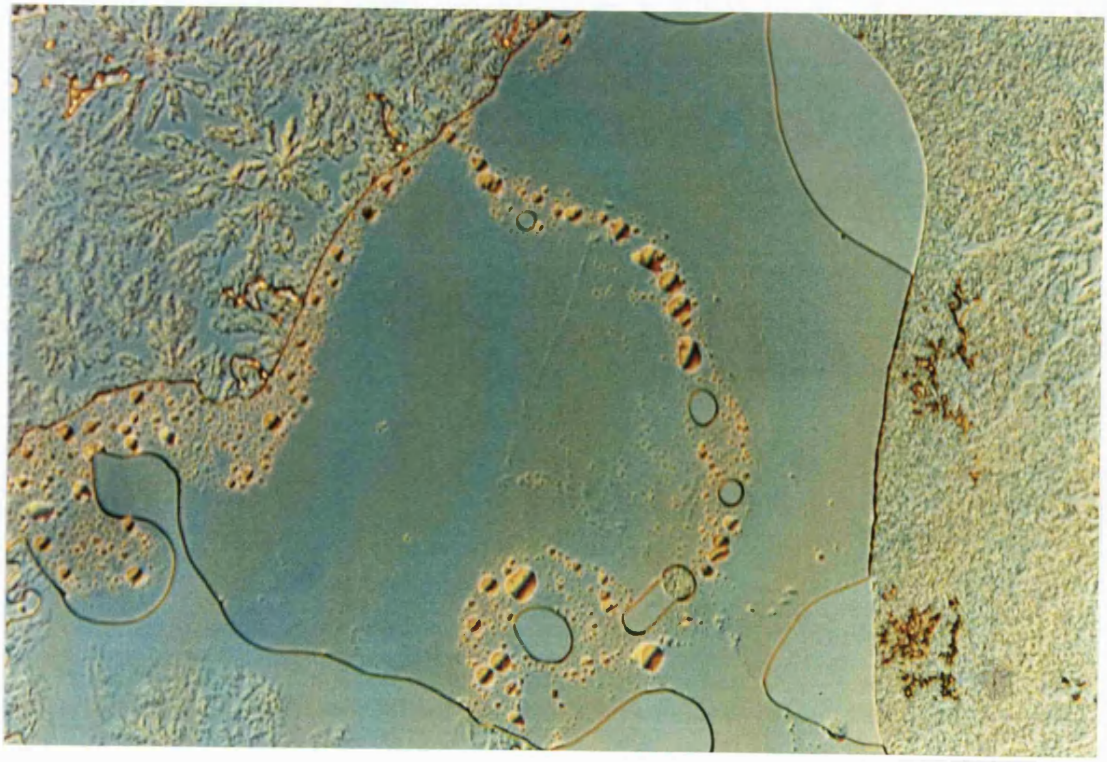

Plate 3.6: Pure G50/13 at 50°C during second heating

thermal changes in the bulk of the sample whereas HSM assesses the modifications within a smaller amount of crystals. Small differences between the melting temperatures found using HSM and DSC had previously been reported (Ford and Rubinstein, 1978; Shehab and Richards, 1996b, Delahaye et al, 1997)

It could be postulated that Form 1 has a higher proportion of the more polar components of the gelucire, such as PEG mono-esters or free PEGs. This is due to the translucent and non-spherulitic appearance of Form 1 combined with its particular melting range. PEG 1500 has the melting point of 42-45°C as previously determined by HSM (Ford, 1984). However, since free PEG 1500 cannot exist in G50/13 in a concentration higher than 7% (refer to Table 1.3 in Chapter 1) and the gelucire form under Peak 1 contributed to more than 25% of the total ΔH_f (refer to Table 2.4 in Chapter 2), the LMF must be constituted of other components besides PEGs. For example, the mixed crystals of α and β' polymorphic forms of trimyristin have a resemblance to Form 1 (deMan et al, 1985), and even though the total percentage of the myristic fatty acid in G50/13 is less that 5% (see Appendix 1) it could still form a part of Form 1.

In cocoa butter, small spherulites represent tightly packed molecules which exclude less polar impurities in its crystal lattice (Chaiseri and Dimick, 1995). Also in cocoa butter, this structure is thought to be induced when the butter exists in a purer state after most of the impurities had crystallised out in the primary phase. Therefore this suggests that the spherulitic Form 2 and Form 3 had higher concentrations of the lipid components. In addition, Forms 2 and 3 have similar morphology to the α and β' forms of tristearin which had been described as small and compact by deMan et al (1985) who subjected pure triglycerides to a similar heating and cooling protocol as this study followed by analysis using a thermal microscopy hot stage.

Peak 4 on the DSC thermal profile (Figure 2.4 in Chapter 2) could not be ascribed to any particular form but it had been put forward that nuclei or very small crystals in low concentration could remain undetected under the microscope (Loth and Bosché, 1996). However, the postulation made in the previous chapter that the HMF (which includes Form 3) is made up of monoglycerides and other high melting glycerides is supported by the fact

that recrystallisation as seen here occurred at a relatively high temperature. Fatty substances with a high hydroxyl value such as those with high contents of fatty acids, mono- and diglycerides were thought to be responsible for the formation of anisotropic structures at high temperatures (Loth and Bosché, 1996). Moreover, ultracentrifugation at elevated temperatures yielded sediments with higher concentrations of mono- and diglycerides. This fraction was thought to form solid phases with limited miscibility with other glycerides. Thus, the persistent structures seen at the end of the melting process of G50/13 could be confirmed as having a higher proportion of partial glycerides. This fractional crystallisation behaviour with various proportions of glycerides occurring at different stages has been shown by cocoa butter which is also a heterogenous fat (Chaiseri and Dimick, 1995).

3.3.2 Paracetamol dispersions in G50/13

On addition of paracetamol, the structures observed during the first heating of the physical mixes were similar to the ones for pure G50/13 sample during its first heating suggesting that the drug did not induce any morphological changes to the G50/13 structure prior to fusion (Plates 7 and 8). After holding the mixture at 75°C for 30 minutes, some of the paracetamol particles became smaller, indicating that the drug was partially solubilised in G50/13. However, even at 5% drug loading, the particles were still present after this 30 minute hold, showing that paracetamol solubility in G50/13 is lower than 5% at this fusion with carrier temperature. This supports the hypothesis made in Chapter 2 based on DSC data that the solubility of this drug in G50/13 was 2.3%.

During the cooling stage, recrystallisation occurred first in a few small gelucire pools without any drug in them, followed by the rest of the mixture. Impurities or foreign substances have always been shown to lower the solidification or melting point of the carrier (Lloyd et al, 1997b) and the G50/13:paracetamol mixture is no exception. Recrystallisation seemed to occur in layers (Plates 9 to 12). Form 3 emerged from about 49°C followed by Form 2 from 44°C which eventually engulfed the sample. A more compact form began to develop around where some of the paracetamol particles were (which shall be designated Form 2p, the letter p for paracetamol), although not all the drug particles acted as nuclei for this compact layer (Plates 11 and 15).

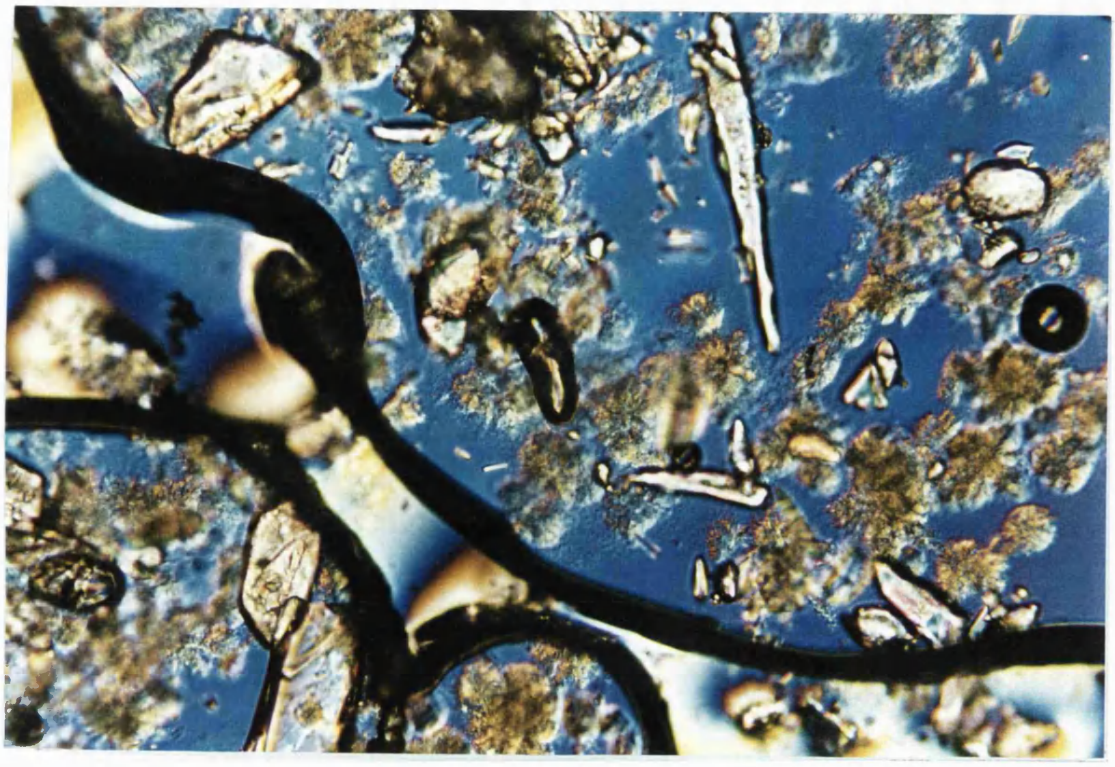

Plate 3.7: 5% paracetamol in G50/13 at 50°C during first heating

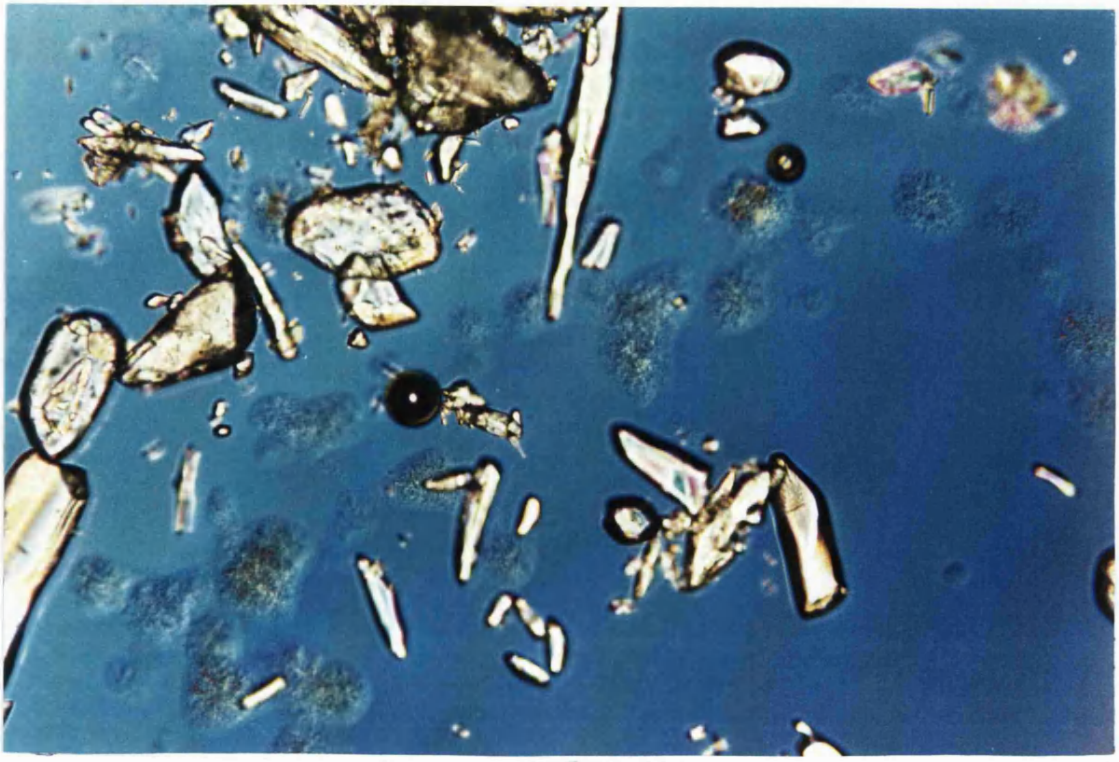

Plate 3.8: 5% paracetamol in G50/13 at 58.3°C during first heating

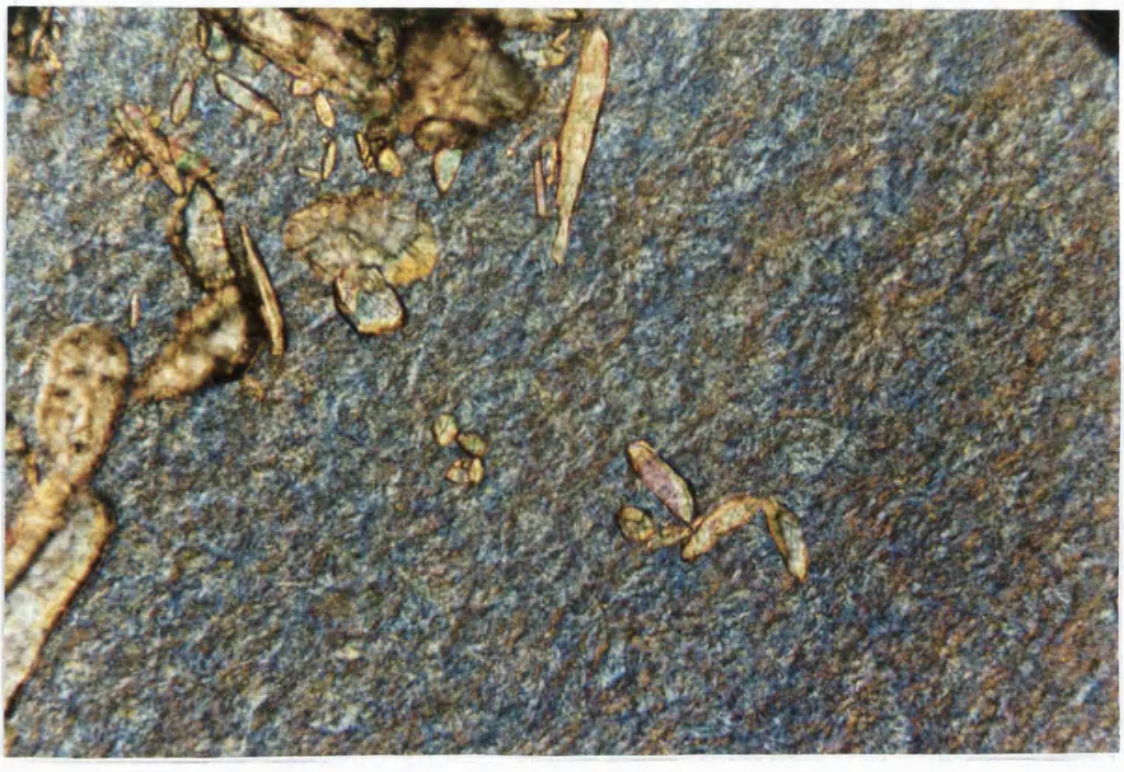

Plate 3.9: 5% paracetamol in G50/13 at 44.4°C during cooling

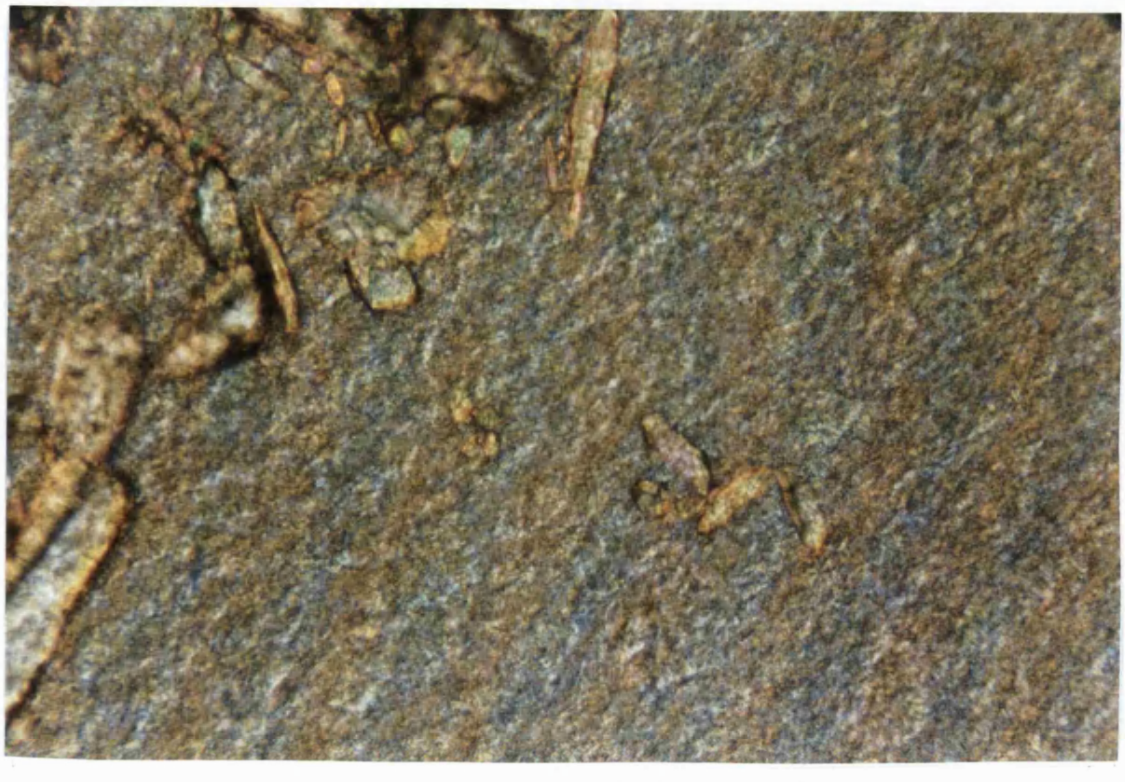

Plate 3.10: 5% paracetamol in G50/13 at 25°C during cooling

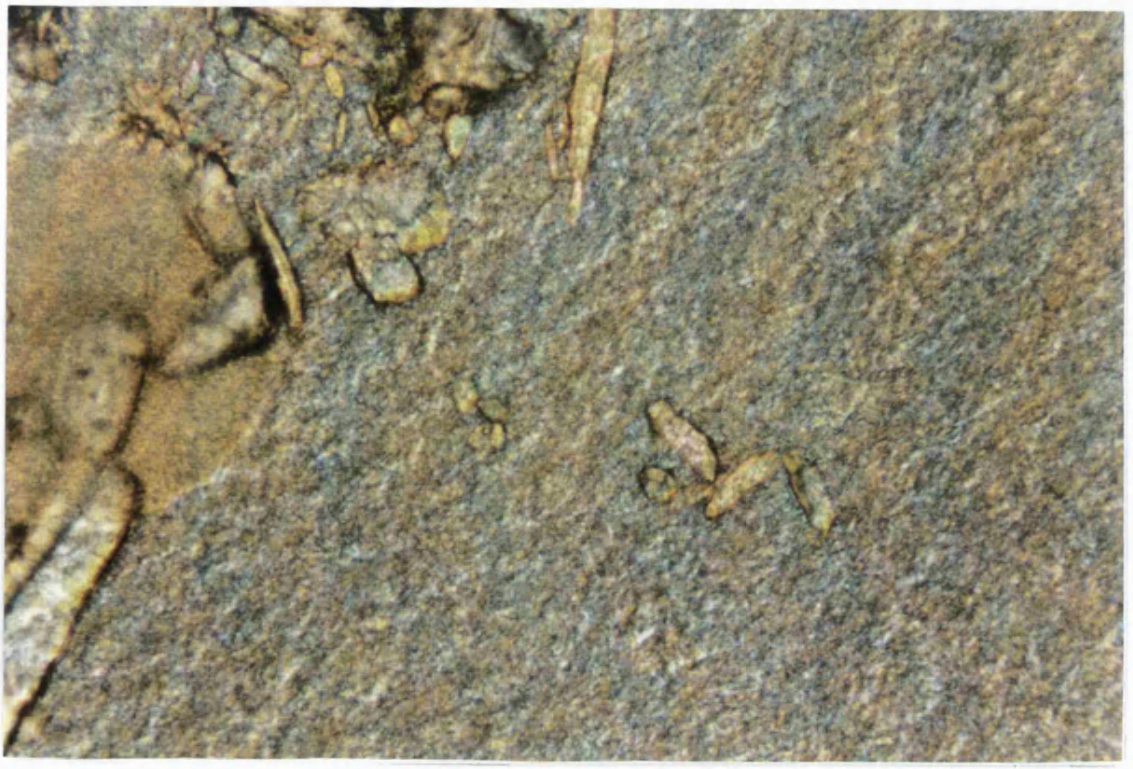

Plate 3.11: 5% paracetamol in G50/13 at 25°C after 10 minutes holding during cooling

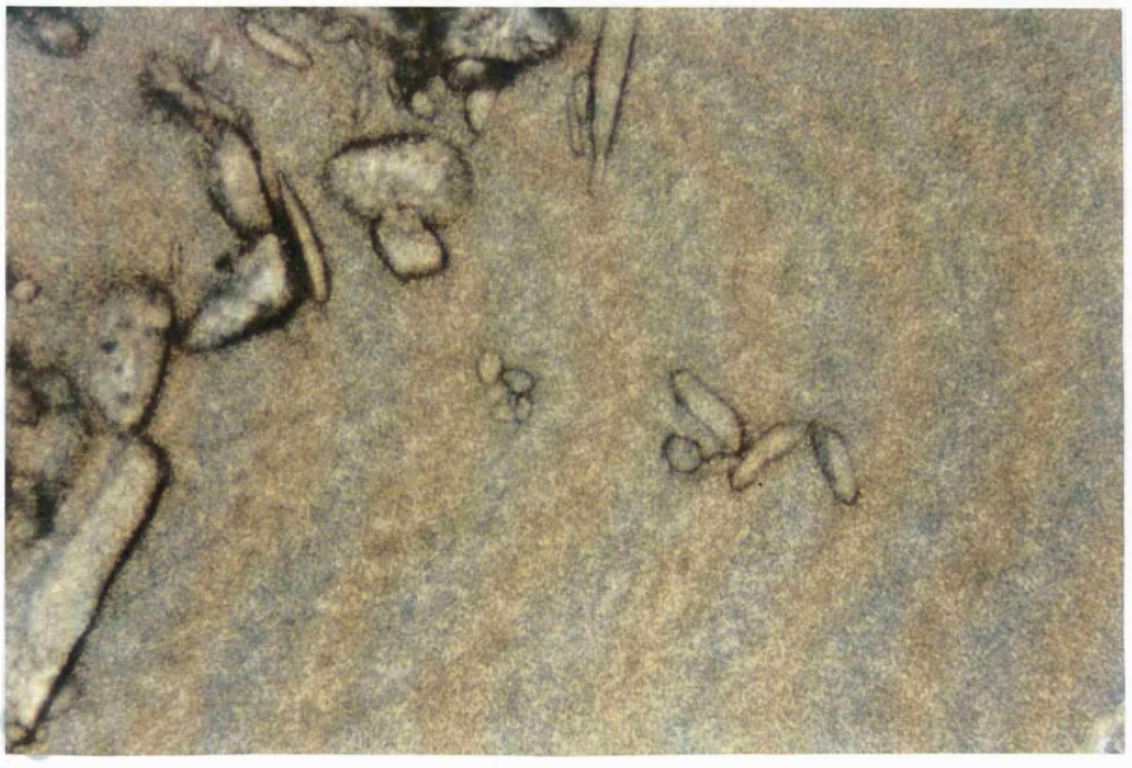

Plate 3.12: 5% paracetamol in G50/13 at 25°C after 30 minutes holding during cooling

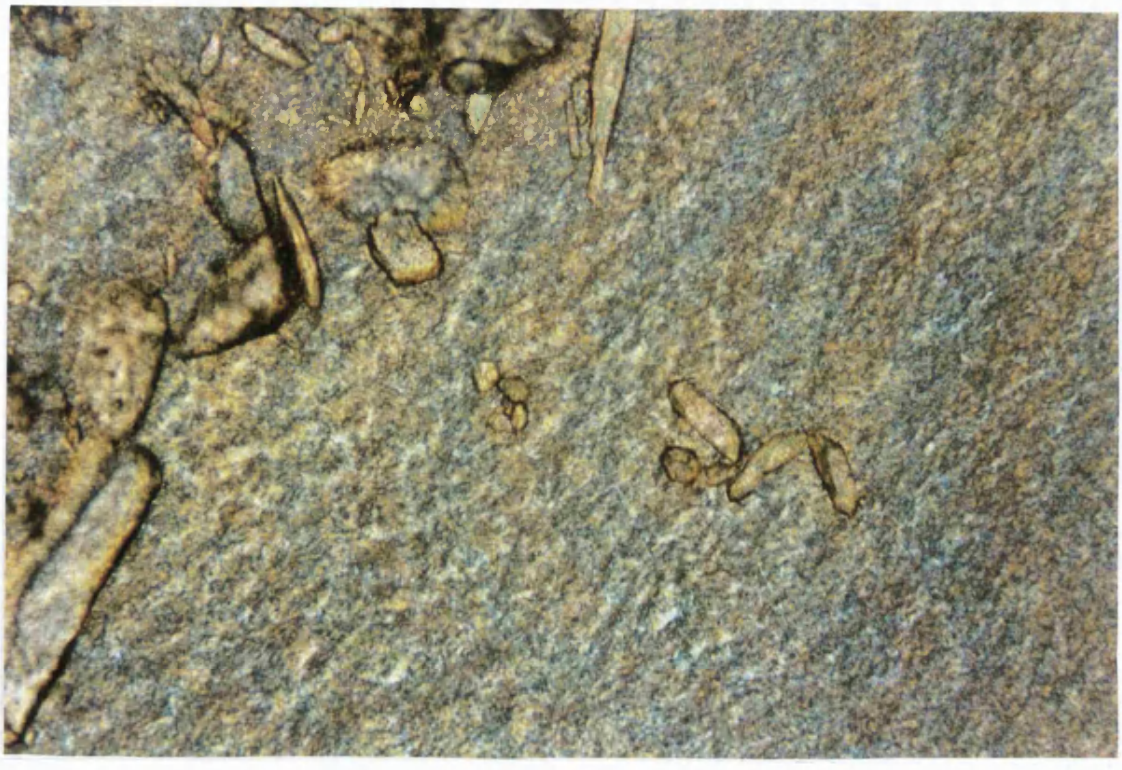

Plate 3.13: 5% paracetamol in G50/13 at 36°C during second heating

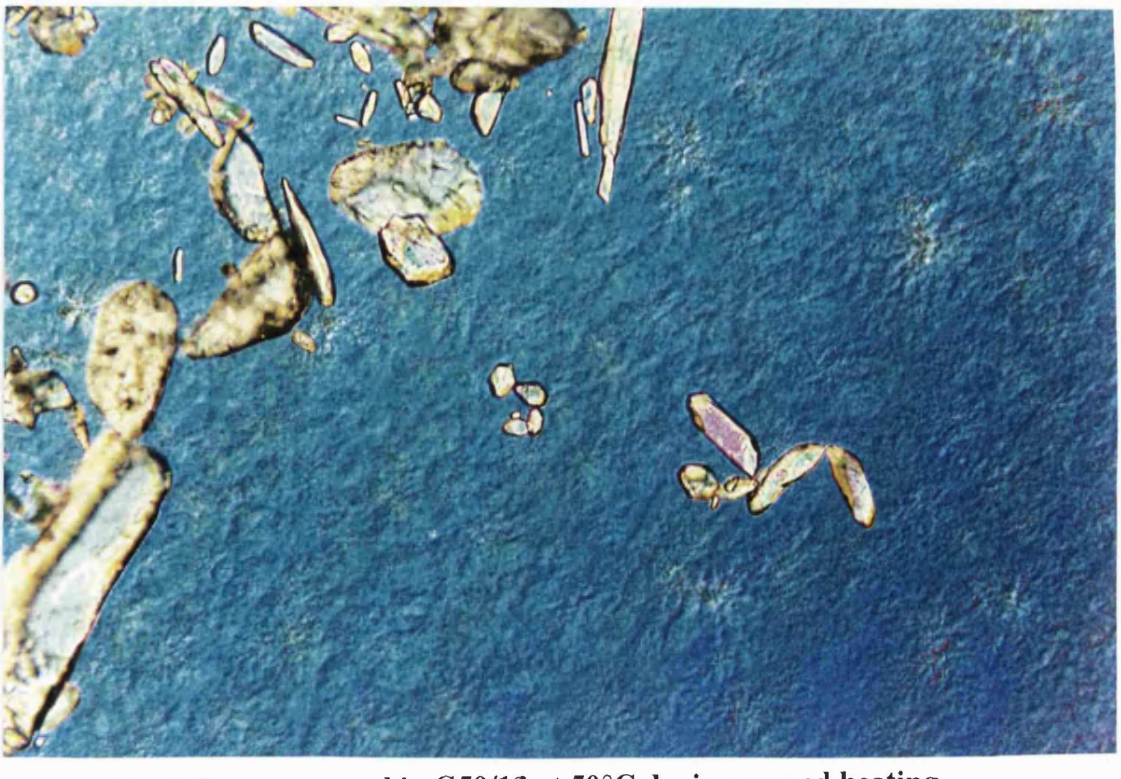

Plate 3.14: 5% paracetamol in G50/13 at 50°C during second heating

Plate 3.15: 10% paracetamol in G50/13 at 25°C during cooling

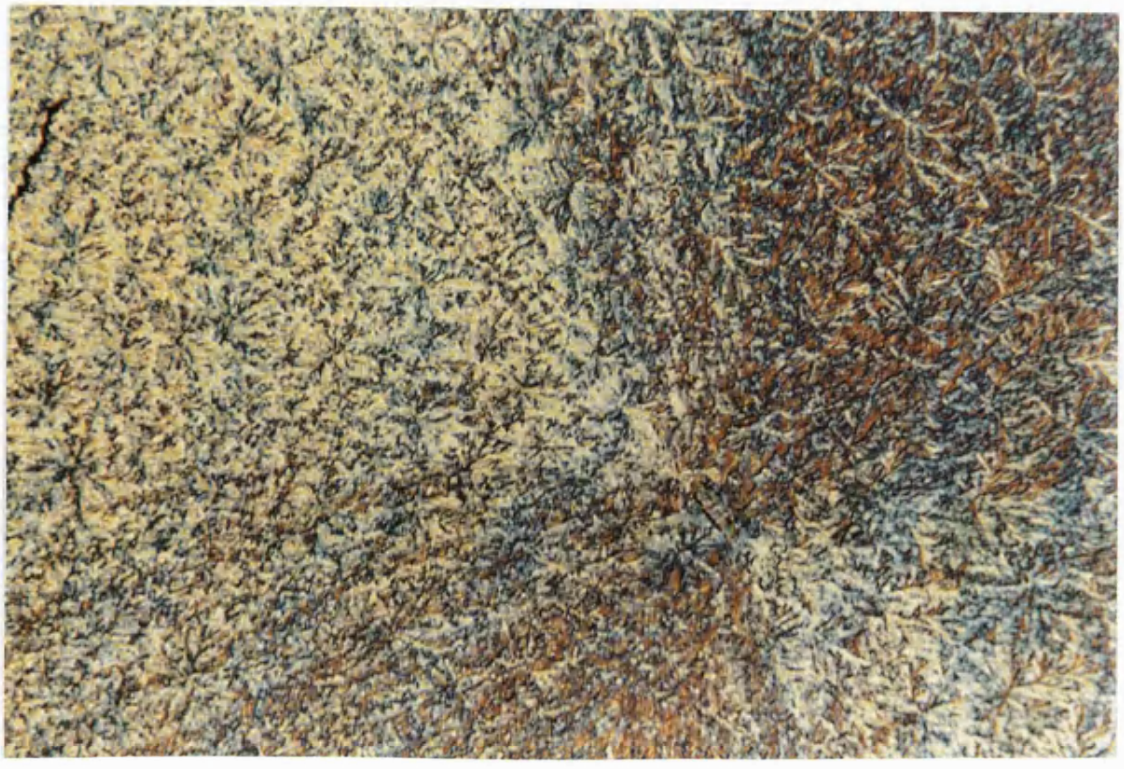

Plate 3.16: 10% paracetamol in G50/13 at 25°C after 30 minutes holding during cooling

Upon holding the sample at 25°C for 30 minutes, the compact structure developed in the vicinity of the paracetamol particles (Form 2p) had by now completely covered the mixture (Plates 12 and 16). On reheating, this layer melted away first (Plate 13), leaving the underlying structures which were larger and less compact to melt by gradually losing their shape, pattern and borders (Plate 14). Form 2p can be taken to represent the structure that contributed to the increase in the LMF of paracetamol dispersions as previously shown in Chapter 2. The change in birefringence together with the disappearance of the border to Form 2p alerted to this initial melting process from 33°C, followed by a more apparent melting from 42.5°C of the other forms. The relatively early melting and substantial proportion of Form 2p corresponded to the broadness and magnitude of Peak 1 in the DSC thermal profiles of these dispersions (Figure 2.4 in Chapter 2).

Further reheating caused the paracetamol particles to slowly dissolve in the molten G50/13 from about 90°C, confirming the same observation made in Chapter 2. This gradual dissolution led to the final melting point of the paracetamol to be lower than its usual (lower than 169.6°C quoted in Table 2.5 in Chapter 2) (Figure 3.4). The suggestion that undetectable paracetamol melting endotherm at low drug loadings was due to continuous dissolution in molten PEG 4000 was supported by also using HSM (Lloyd et al, 1997b). Beyond 20% loading of paracetamol, it became increasingly difficult to distinguish the structures during the heating and cooling cycles as the field of view was becoming more dominated by the drug particles. t_{onset} and t_m were approximated for the gelucire. Figure 3.4 can be regarded as a base for a phase diagram with the t_m of the gelucire as the solidus line and the final melting temperature of paracetamol as the liquidus line. In order to complete the diagram, lower loadings of the drug will have to be studied in order to find the eutectic composition, if any, or the solubility of the drug in the carrier.

3.3.3 Caffeine dispersions in G50/13

When caffeine was physically mixed with G50/13 and heated, the melting structures were similar to the pure G50/13 and paracetamol dispersions during the first heat. After holding the samples at 75°C for 30 minutes, some of the caffeine particles dissolved in the molten G50/13 (Plates 17 and 18). During cooling, needle-like projections started appearing from

Figure 3.4: Temperatures at which the changes occurred during the heating and cooling protocol of paracetamol dispersions in G50/13 (°C).

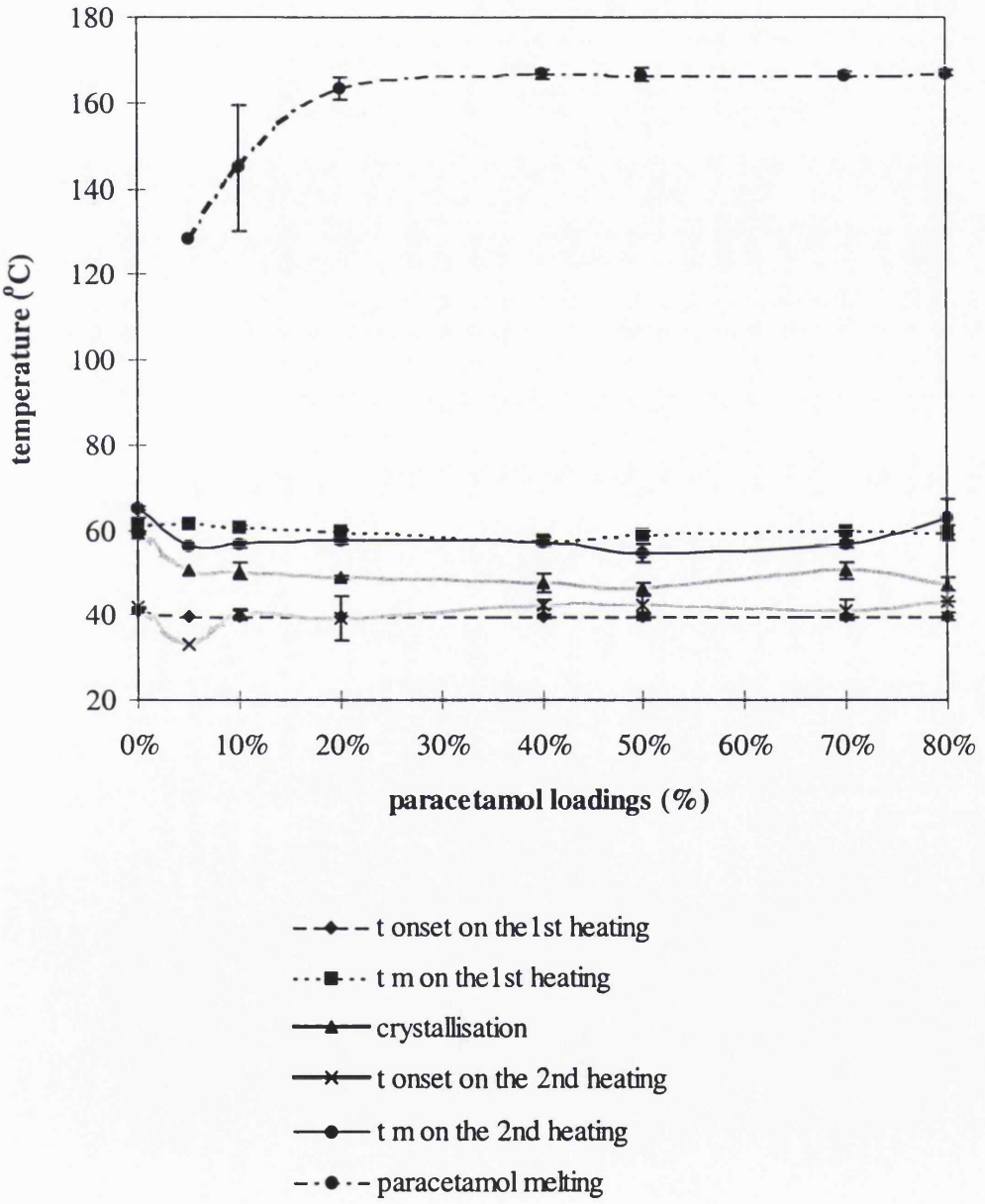

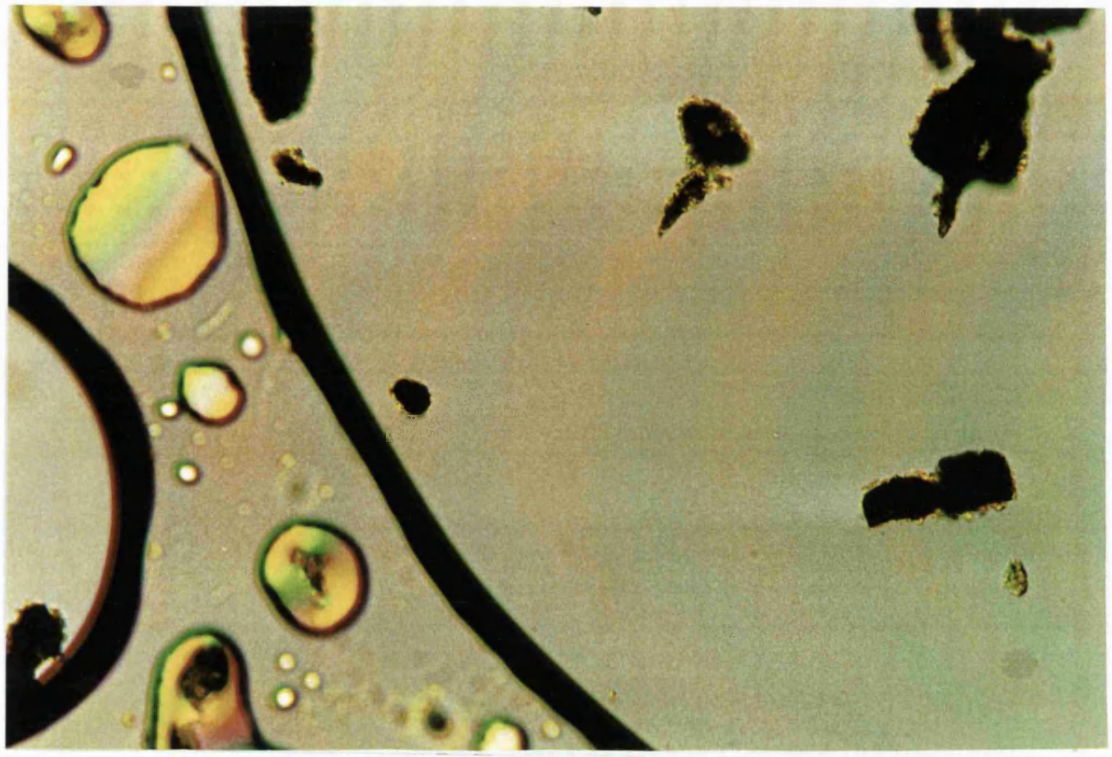

Plate 3.17: 5% caffeine in G50/13 at 75°C during first heating

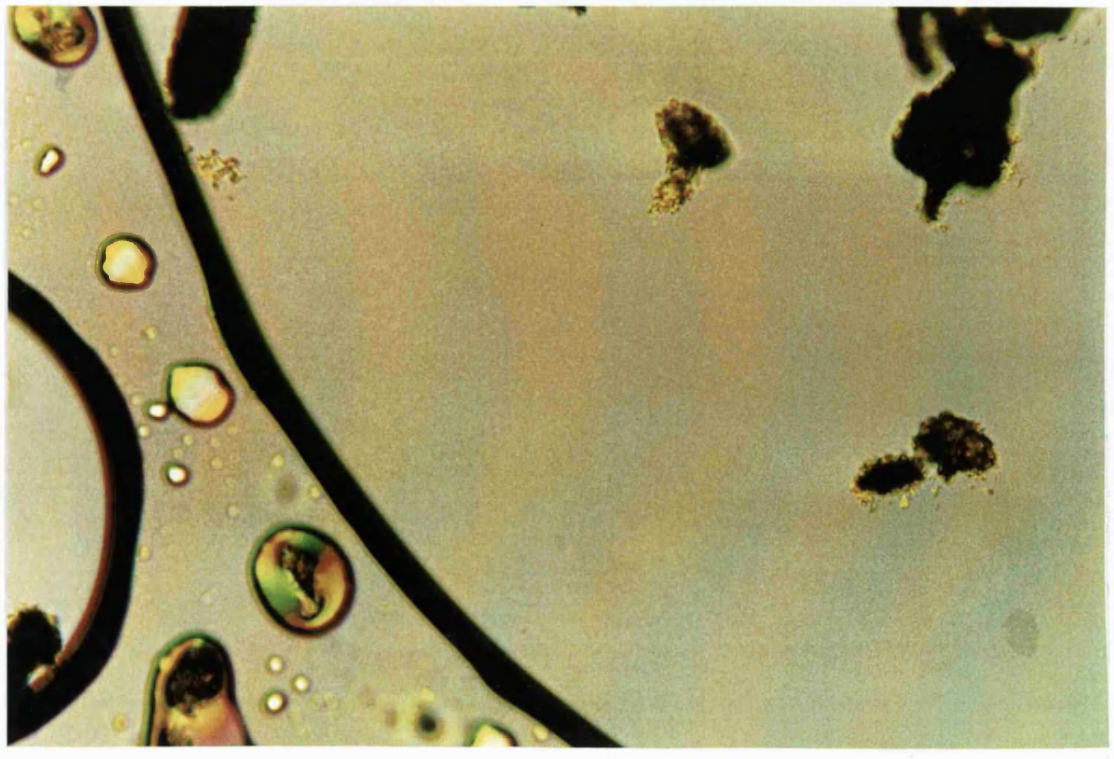

Plate 3.18: 5% caffeine in G50/13 at 75°C after 30 minutes holding

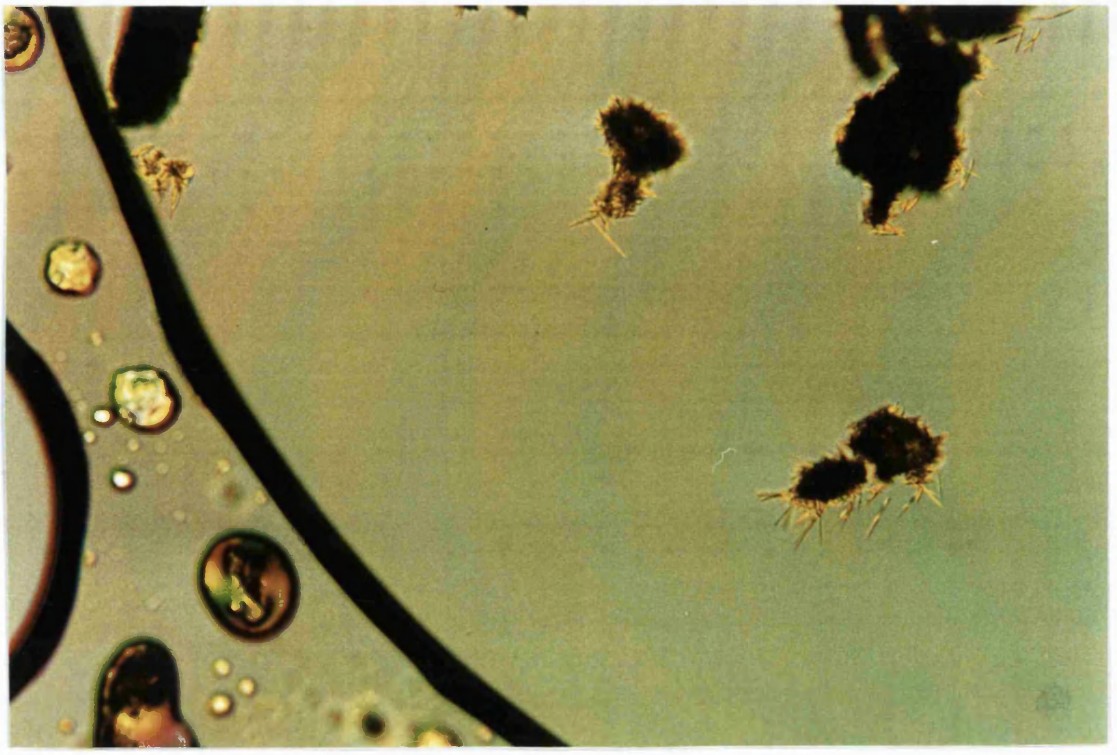

Plate 3.19: 5% caffeine in G50/13 at 50°C during cooling

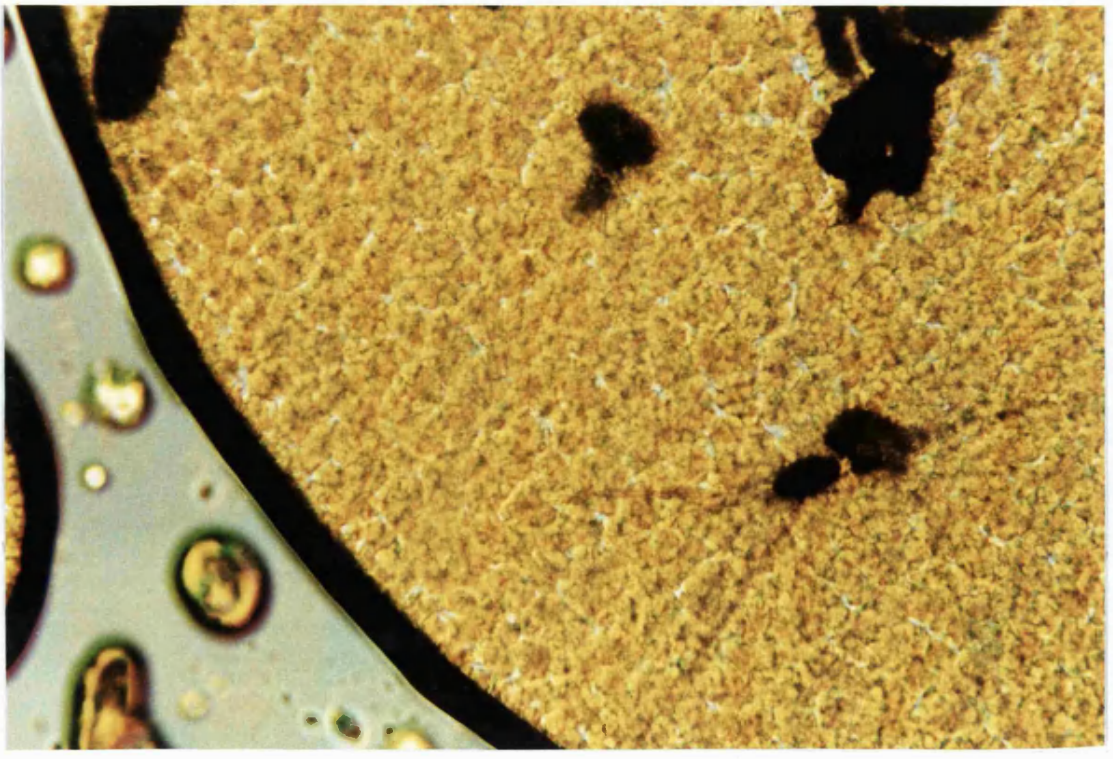

Plate 3.20: 5% caffeine in G50/13 at 25°C during cooling

about 50°C before any Form 2 or Form 3 surfaced (Plate 19). These `whiskers' projected outwards from existing caffeine particles, leading to the conclusion that they were the previously dissolved drug, now re-crystallising separately from the gelucire base. Manning and Dimick (1985) also described `needle' projections arising from `spiney' rosettes in cocoa butter but it is unlikely that the needle-like projections observed in the caffeine dispersions samples were due to the lipid matrix as no such projections were found in the pure G50/13 sample. As Forms 2 and 3 crystallised out from 46°C onwards and continued to develop, the caffeine further extended its projections into the G50/13 (Plate 20). Rod-shaped ibuprofen crystals and snowflake structures of Lutrol-F68 were reported to be growing at the same time but discretely during the cooling of the 40% w/w drug dispersion (Hawley et al, 1992). However, only one endotherm corresponding to the drug:carrier mixture was detected using the DSC and this is comparable to the caffeine:G50/13 system which showed similar thermal profiles to the pure carrier.

After holding the samples at 25°C for 30 minutes, the drug whiskers were engulfed by Form 2 crystals (Plate 21). On reheating, Forms 2 and 3 first started to melt from about 41°C and the drug projections then slowly dissolved in the molten gelucire (Plate 22). Further reheating caused the caffeine whiskers to completely dissolve by 85°C and the gradual particle dissolution resulted in the decrease of the usual melting point of the drug (lower than 236.9°C quoted in Table 2.12 in Chapter 2) (Figure 3.5). The melting of the drug whiskers during G50/13 fusion may have contributed to the higher than expected total ΔH_f as observed in Table 2.11 in Chapter 2. This effect had also been reported by Ginés et al (1995) who found that the dissolution of cinnarizine in G53/10 lowered the melting point of the excess drug and that the ΔH_f of the physical mixture with low drug loading was higher than anticipated due to the fusion of the drug in the molten gelucire.

3.3.4 The effect of drug incorporation on the morphology of G50/13

Paracetamol and caffeine displayed contrasting behaviour in G50/13. Solubilised paracetamol recrystallised out together with the gelucire in the form of a more compact structure (Form 2p). However, solubilised caffeine recrystallised separately and this was seen as the needle-like projections emanating from the drug particles as well as the discrete

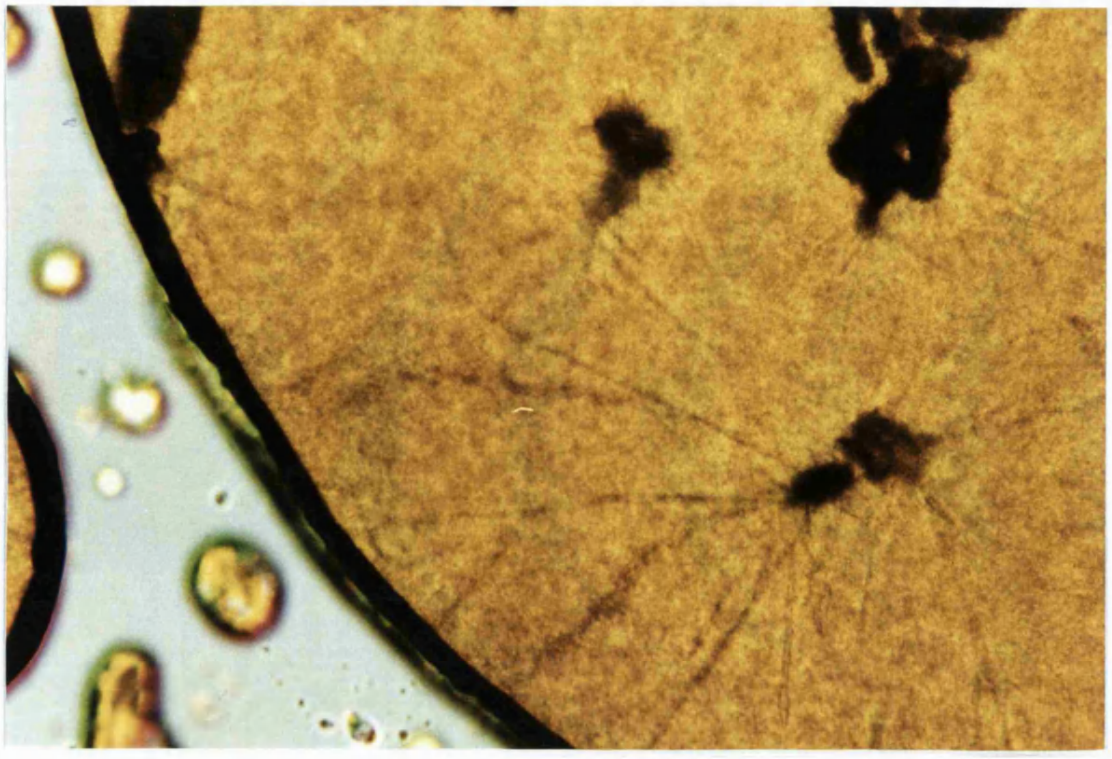

Plate 3.21: 5% caffeine in G50/13 at 25°C after 30 minutes holding during cooling

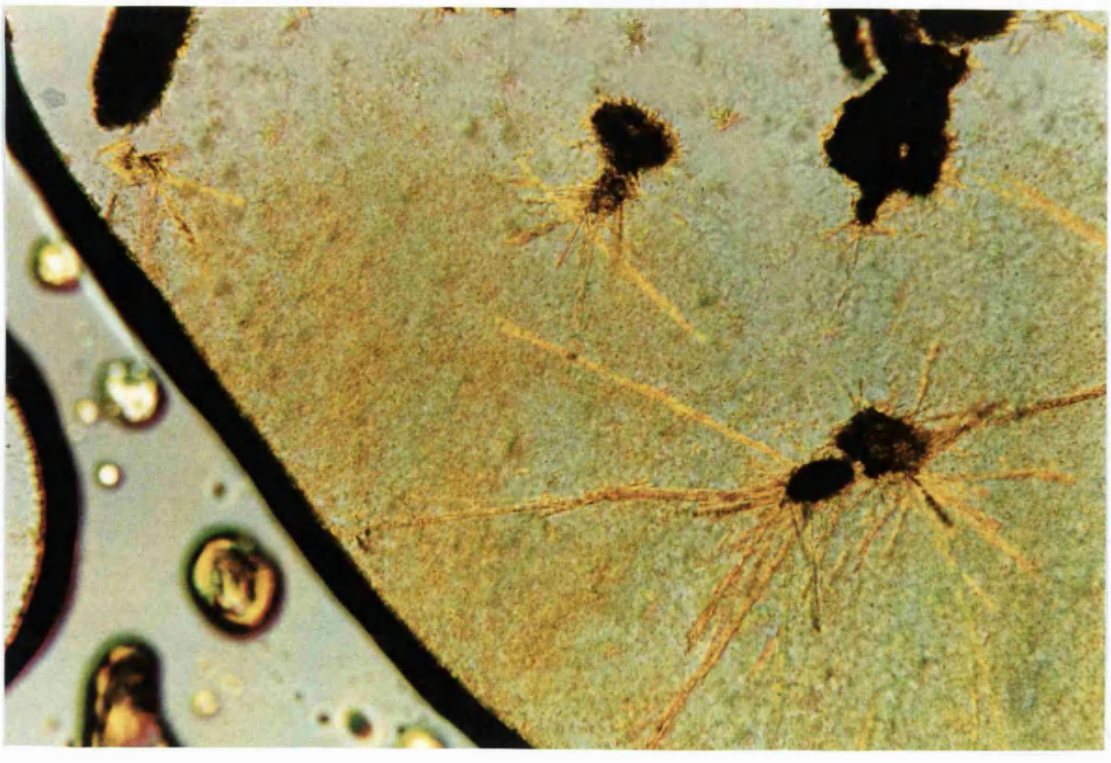

Plate 3.22: 5% caffeine in G50/13 at 50°C during second heating

Figure 3.5: Temperatures at which the changes occurred during the heating and cooling protocol of caffeine dispersions in G50/13 (°C).

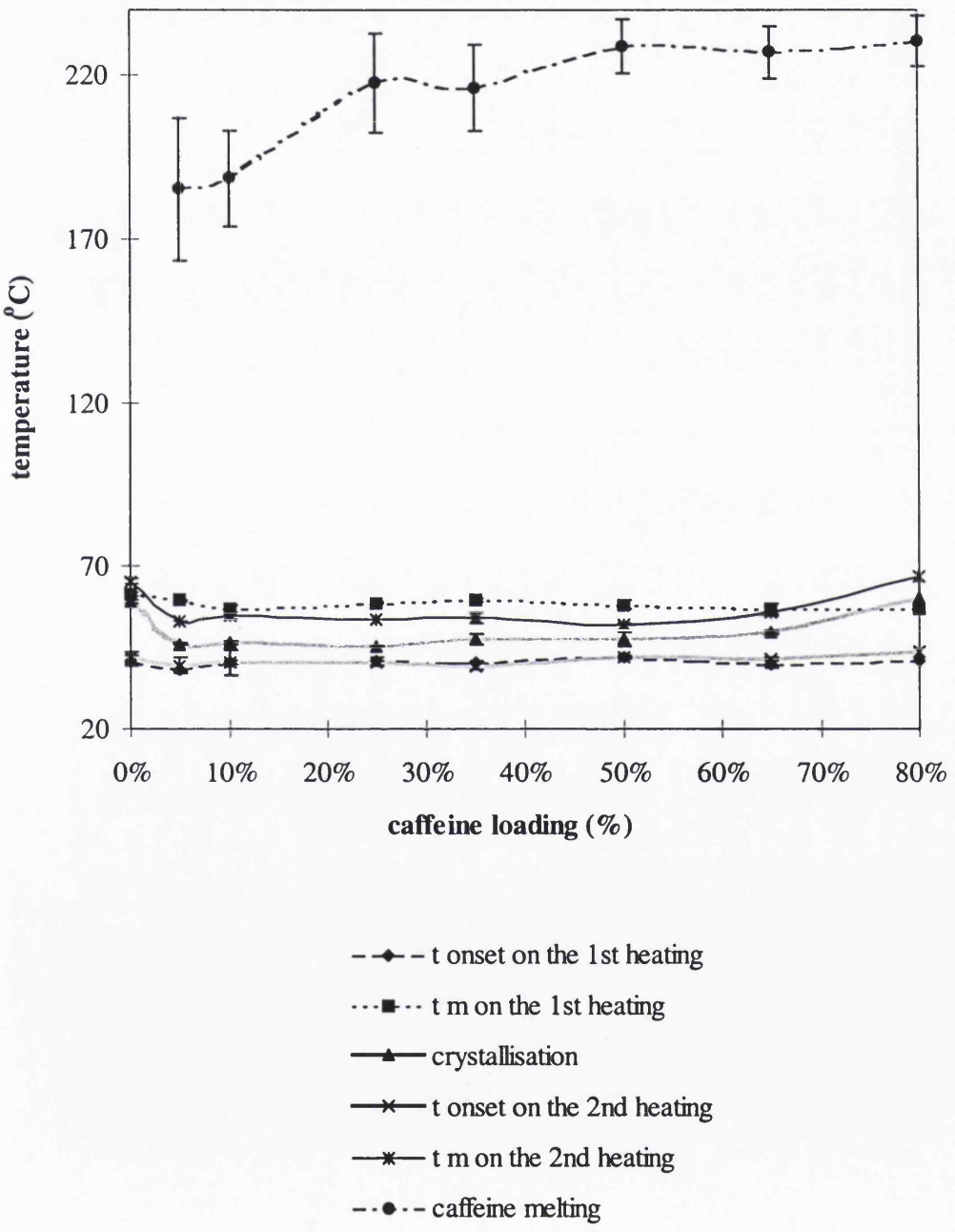

Plate 3.23: 10% paracetamol in G50/13 at 25°C after heating until all the drug melted and recrystallisation of this melt

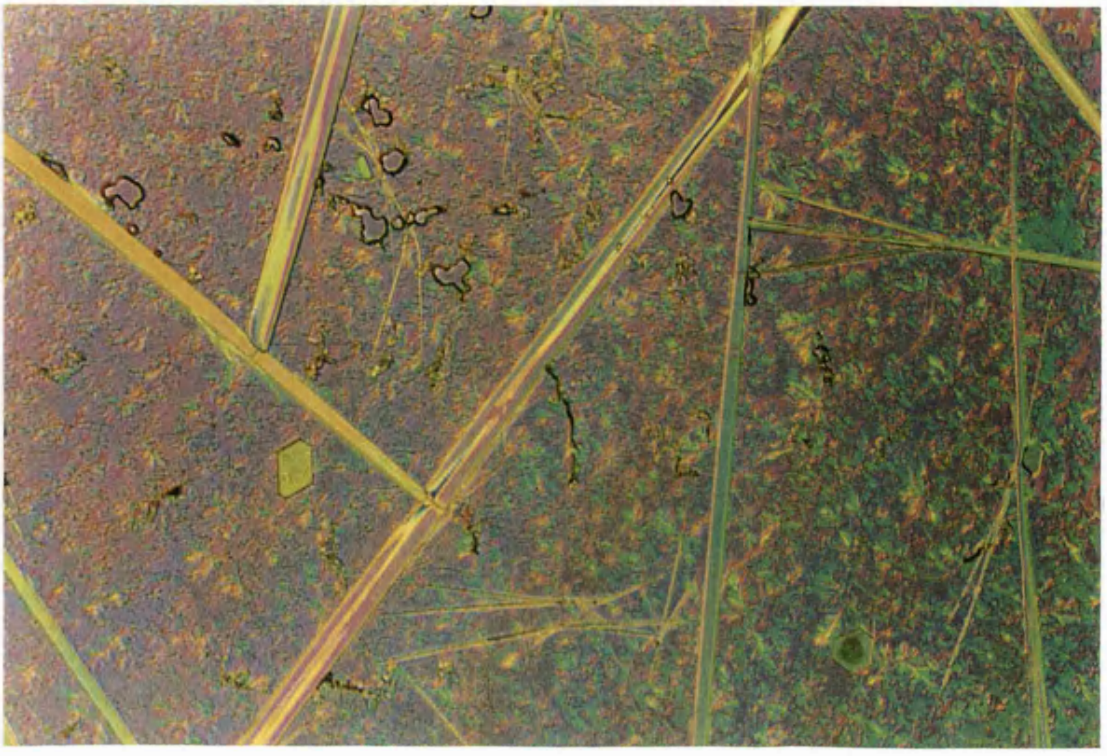

Plate 3.24: 10% caffeine in G50/13 at 25°C after heating until all the drug melted and recrystallisation of this melt

specks of drug crystals dispersed all over the cooled sample. These observations were confirmed by totally melting the paracetamol or caffeine particles in the G50/13 and seeing the result of the cooled mixture. It was found that there were no discrete paracetamol particles left and that the slide was covered by a compact, round structures whereas there were long blades of caffeine recrystallising out of the mixture (Plates 23 and 24 respectively).

The presence of paracetamol and caffeine particles after holding for 30 minutes at 75°C even at the low loading of 5% showed that the particles exist as a solid dispersion in the G50/13 matrix at this and higher concentrations. The effects of drug loadings on G50/13 structure were difficult to ascertain due to the drug particles obscuring the carrier crystals but at low loadings of 5% and 10%, no significant difference was observed except the availability of gelucire to solubilise the drugs. Therefore a small amount of solubilisation must occur at the higher loadings with the excess drug remaining as discrete particles in the solid dispersions, which was similarly exhibited by cinnarizine in G53/10 (Ginés et al, 1995).

The behaviour of the dispersions seen under microscopy reflects the results obtained from DSC studies in Chapter 2. The incorporation of paracetamol altered the G50/13 thermal profile by stabilising the form that gave rise to Peak 1 and subsequently decreasing the SFC. HSM demonstrated that the drug had indeed modified the gelucire structure by forming mixed crystals with some G50/13 components leading to the formation of Form 2p. The similarity between the thermal profiles of caffeine dispersions and pure G50/13 was taken to be showing the lack of interaction between the drug and carrier. HSM reiterated this by demonstrating that although there was some dissolution of caffeine in the carrier, the drug recrystallised out separately from the G50/13 without significantly affecting its structure.

3.4 Conclusions

The G50/13 is made up of different structures with different melting ranges which can be attributed to the numerous components within it. The microscopic technique did not show

upon heating, of one structure transforming into another in the melt. This is consistent with the absence of exothermic peaks on the DSC thermal profiles indicating the lack of melt-transformation during scanning. All the different forms existed from the beginning of heating suggesting that no solid-solid transformation occurred neither during this process and the melting of one form merely reveals more clearly the other underlying forms. The chemical composition of each form could not be established by using this technique alone; the melt would have to be incubated just below the melting range of each form, isolated and analysed using GLC or HPLC. Such procedures are time consuming and beyond the scope of this study. However, the melting behaviour suggests that the LMF contains a high proportion of PEGs and shorter chain triglycerides, the HMF has a higher concentration of the partial glycerides and the MMF is composed of the rest.

HSM has been shown to be an effective complementary technique to DSC. The various melting fractions observed on DSC thermal profiles corresponded to the different structures seen under microscopy. The higher melting forms tended to have larger crystals than the lower melting ones suggesting that the former have a higher proportion of more stable polymorphs. Incorporation of paracetamol had resulted in structural modification of G50/13 with a new form of mixed crystals emerging but the addition of caffeine did not lead to any such alterations. Dissolution studies would have to be performed in order to assess whether these structural differences would have an effect on the drug release behaviour.

CHAPTER 4: DISSOLUTION STUDIES ON THE RELEASE OF MODEL DRUGS AT DIFFERENT LOADINGS FROM G50/13 MATRICES

Previous chapters have revealed the physical structure of G50/13 after the heating and cooling protocol designed to imitate the manufacturing protocol of various dosage forms with this gelucire. Incorporating drugs into the gelucire base resulted in some modifications of the structure which to an extent depended on the solubility of the drug in the base. However, this information about the structure would be worthless without any performance studies. In this chapter, the moulded tablets of drug dispersions in G50/13 were investigated for their drug release behaviour.

4.1 Introduction

Even though many studies have been performed on the release of drugs from gelucires, the results obtained have occasionally been conflicting and may be heavily dependent on a particular set of conditions. This demonstrates the complexity of the system, so in order to maintain accuracy, the investigations quoted here are given in detail.

The enormous variety of formulations available means that there is also a variety of possible methods to evaluate the release of relevant drugs from these formulations. For block matrices such as tablets and capsules, the USP rotating basket apparatus is often the method of choice. For finer formulations such as oral spherical devices, pellets and granules, the paddle method is preferred. Similarly, the variety of ways that gelucires can be formulated into means that there are also a number of different ways to ascertain the release of drugs from these formulations. Several investigators in this field have adapted conventional dissolution testing in order to focus on a particular area of interest, for example, the mechanisms of release. For a more detailed information on the studies relating to the mechanisms of release, refer to Section 1 of Chapter 5.

4.1.1 The release behaviours of dosage forms

Gelucire has been made into many types of dosage forms due to its versatility of controlling the rate of drug release. In general terms, the more hydrophobic, the higher the melting point and the lower the HLB number gelucires tend to give a slower, more sustained release profile, whereas those gelucires of contrasting natures with the above mentioned are likely

to give rapid release profiles (Huet de Barochez et al, 1989; Brossard et al, 1991; Prapaitrakul et al, 1991; Ortigosa et al, 1991). Relationships between drug release and HLB values were sought; it was postulated that there existed an exponential or first order relationship between the cumulative amount of drug released and the HLB values (Baykara and Yuksel, 1991) and a log linear relationship between release rates and HLB values for certain drugs (Howard and Gould, 1987). The importance of HLB superseding the importance of the melting point was demonstrated by Prapaitrakul et al (1991) when the release rate of chlorpheniramine maleate was more affected by the change in the HLB values than the change in the melting points of the gelucires, and also by Doelker et al (1986) who found that gelucires with high HLB values gave a rapid drug release performance despite having high melting points as well.

Nevertheless, the melting point has such a great negative effect on release that increasing the melting point of the gelucire by 18°C will reduce the kinetics of dissolution by about 50% (Ortigosa et al, 1991). On the same note, low melting point gelucires give a fast drug release profile due to the facilitation of the dissolution and disintegration of the matrices (Doelker et al, 1986; Esquisabel et al, 1996). Altering the melting point factor of gelucires in order to obtain a particular release profile may be a more viable action than modification of their HLB values if the active ingredient to be incorporated is hydrophobic (Mouricout et al, 1990). These characteristics also affect the way that the drugs incorporated in them are released. Diffusion and erosion preceded by water absorption are thought to control drug release from the gelucires with HLB of about 14 (Bidah and Vergnaud, 1990) or HLB of 9 or higher (Kopcha et al, 1990) whereas diffusion was thought to govern the release from gelucires with HLB of about 1 (Bidah et al, 1992) or HLB of 7 or less (Kopcha et al, 1990). The higher HLB gelucires were thought to allow the uptake of water which then led to their swelling. Subsequently, erosion could occur more easily as the matrix now became more pliable and more susceptible to breakage (Kopcha et al, 1990).

Additionally, the way the drug is incorporated into the carrier will also affect the release. Amoxycillin granules containing various proportions of G64/02 showed no sustained release profile when prepared by evaporation method (Vila-Jato and Delgado-Charro, 1990) and similarly, tablets of quinidine gluconate with Precirol prepared by the wet granulation

method gave a faster release profile whilst tablets prepared by the hot fusion method gave slower and incomplete drug release (Saraiya and Bolton, 1990). However, when those two methods were also used to prepare PVP-nifedipine coprecipitate with G35/10, no difference could be seen in the results of the drug release (Vila-Jato et al, 1990).

4.1.2 Kinetics and mathematical modelling of release

Dissolution tests are amongst the most common type of studies performed by investigators and there is a great variety of the types of dosage forms tested for their release. The kinetics of the drug release from these dosage forms are also varied and often complex, and the mechanisms of release that are responsible for these kinetics are subjected to frequent debates. The mechanisms previously quoted for gelucires are diffusion (Aïnaoui and Vergnaud, 1998; Bidah et al, 1992), erosion (Bidah and Vergnaud, 1990,1991) and a combination of both (Laghoueg et al, 1989). The erosion process was thought to facilitate drug release so that the rate would be faster than for non-eroding matrices (Howard and Gould, 1987). When release was due to diffusion through the matrix, Higuchi (1963) found that it had a square-root of time profile:

$$M = Kt^{1/2} + C \qquad \text{....Equation 4.1}$$

where M is the amount of drug released, K is a diffusional term and C is a constant.

Kopcha et al (1990) developed a series of schemes based on the Higuchi studies (1963) to evaluate the mechanisms of release from various gelucires. Drugs will exist in a dissolved state within its matrix if the loading of the drug is below its solubility in the carrier. The dissolved drug will then diffuse to the interface and partition into the surrounding liquid. In this case:

$$Q = [\, D\,(2W_o - C_s)\,C_s t\,]^{1/2} \qquad \text{....Equation 4.2}$$

where Q is the amount of drug released per unit exposed surface area, D is the diffusion coefficient of the drug in matrix, W_o is the initial drug concentration, C_s is the drug solubility or saturation concentration of drug in the insoluble matrix and t is the time. As in most cases of formulation, $W_o \gg C_s$ and Equation 2 can be simplified to:

$$Q = (2W_o D C_s t)^{1/2} \qquad \text{....Equation 4.3}$$

However, when the drugs exist in a solid dispersed state and the diffusion occurs through water filled channels, formed by the dissolution of the drug particles on contact with the liquid medium instead of through the solid matrix, Equation 2 is modified to include a porosity and tortuosity term which takes into account the volume and length of these channels/pores:

$$Q = \left[\frac{D\varepsilon}{\tau}(2W_0 - \varepsilon C_s)C_s t\right]^{1/2} \qquad \text{....Equation 4.4}$$

where ϵ is the porosity of the matrix and τ is the tortuosity of the matrix. Again, if $W_0 \gg C_s$ so that the dissolution rate of the dispersed drug is the rate determining step:

$$Q = 2W_0(Dt/\pi)^{1/2} \qquad \text{....Equation 4.5}$$

From here, it could be seen that release is proportional to the amount of dispersed drug. The assumptions made for these equations are that pseudo-steady states together with sink conditions are maintained during release and a diffusional boundary layer is not present.

The solid dispersed drug could also be released through the swelling of the matrix instead. In this case, the process is described as a water front penetrating into the matrix and upon the matrix hydration, the drug within this hydrated area dissolves and diffuses out of the swollen region. If the drug has not completely dissolved within this hydrated region, diffusion then occurs from a saturated solution. The release from a single planar surface of the granular matrix can be given by:

$$\frac{M}{t^{1/2}} = S\left[D'C_s\left(\frac{2W_0}{V} - C_s\right)\right]^{1/2} \qquad \text{....Equation 4.6}$$

where S is the effective diffusional area, V is the effective volume of the hydrated matrix and D' is the apparent diffusion coefficient of the drug in the hydrated matrix which includes the tortuosity and porosity factors of the hydrated matrix. The assumption made here is that the surface to volume ratio remains relatively constant after the initial hydration period. Should the drug be completely dissolved within the hydrated region before diffusion, then Equation 4.6 is modified to:

$$\frac{M}{t^{1/2}} = 2W_0(S/V)(D'/\pi)^{1/2} \qquad \text{....Equation 4.7}$$

In all of these equations, the apparent diffusion coefficients, D or D′, are assumed to remain constant. Also, looking at Equations 4.2 to 4.4, if all other parameters could be assumed to be similar, the rate of release would depend on the solubility of the drug in the carrier when the drug is assumed to be dissolved in the carrier or when the drug loading is close to the solubility value.

Again, the mechanisms are also affected by the type of carrier. A gelucire which is lipidic, such as G50/02 was not thought to allow the surrounding dissolution liquid to diffuse through itself and so drug release occurred when the drug particles within the lipidic matrix dissolved on contact with the liquid (Aïnaoui and Vergnaud, 1998) or through the dissolution of an added hydrophilic excipient such as mannitol in Precirol (Parab et al, 1986). In addition, increasing the level of the lipidic G50/02 in a formulation elevated the predominance of diffusion as the release process (Kopcha et al, 1991). The dissolved drug then diffused out through the liquid within the matrix. In this instance, the progression of the liquid from the outside through the matrix and the diffusion of the dissolved drug through this liquid have to be regarded as controlling the release process. As a result, the kinetics adopting the principle of concentration dependent diffusivity with a finite coefficient of convective transfer was thought to be the more accurate approach to be applied to the in-vivo studies rather than the more established constant diffusivity with an infinite coefficient theory. When no swelling of the polymer was observed, it was thought that the liquid entered the matrix by replacing the dissolved drug and the increase in the diffusivity of the drug was related to the amount of water in the matrix in an exponential way (Aïnaoui et al, 1997).

The choice of the model drug to be incorporated into the matrix is important, as the release can be affected by the pH of the dissolution media. When the release from G50/13 was evaluated, it was found that in an acidic medium, the mechanisms of release were both diffusion and erosion but in a basic medium, only diffusion was observed (Kopcha et al, 1991). On a closer examination however, this was thought to be due to the pK_a of the drug, theophylline, being similar to the pH of the basic medium and that the diffusional release could be attributed to the pH partitioning effect. For the same reason, the release of indomethacin (pK_a = 4.5) from G46/07 or G33/01 was very slow in a pH 6.2 medium

because of its limited solubility in the medium (Vial-Bernasconi et al, 1995). However, whatever the mechanism(s) was/were, the release profiles of theophylline were similar indicating that overall release was not significantly affected by pH (Kopcha et al, 1991; Ortigosa et al, 1991) Amoxycillin had a low solubility and dissolution rate in media which were between pH 3 to pH 6 (Delgado-Charro and Vila-Jato, 1991). Additionally, it degraded in acidic environment so release was never completed. The antibiotic also has a limited absorption window in the intestinal area for the uptake of the drug. The release of amoxycillin from granules coated with G64/02 was found to be very fast in pH 1.2, slower at pH 7.5 and extremely slow at pH 4.5 (Delgado-Charro and Vila-Jato, 1992). In addition, the thickness of the G64/02 coating on the granules had the greatest impact on the rate of release in gastric juice, followed by intestinal juice and pH 4.5 medium respectively. Thus for amoxycillin, increasing the amount of coated gelucire to sustain drug release can actually result in lesser quantity of the drug being absorbed. The retardation of the drug release in the pH environment preceding the intestine meant that most of the drug will pass through the zone of absorption without being taken up.

With drugs that are freely soluble in water such as diltiazem hydrochloride, pH variation in the dissolution medium did not affect its release from its carriers (Kim and Fassihi, 1997). The pKa value of the drug also plays a part in determining the rate of release of the drug. Chlorpheniramine maleate, a basic drug which has a pKa of 9.16 would be 99% ionized in a medium of pH 1.2 compared to 97% in a medium of pH 7.5 (Prapaitakul et al, 1991). Therefore, the release was slower in pH 7.5 than pH 1.2 which could be due to the unionized drug having a greater affinity for the lipidic gelucire in comparison to the ionized drug. Clearly, it would be preferable to use a model drug which solubility is not affected by different pH dissolution media if the effect of pH on the actual carrier itself is desired. For instance, propanolol hydrochloride has a pKa of 9.4 and so would be fully ionized in both dissolution media of pH 1.2 or pH 7.4 (Bodmeier et al, 1990).

As mentioned before, the mechanisms of release are affected by the types of dosage forms involved. Gelucire has been formulated into dosage forms as simple as hard gelatin capsules (Doelker et al, 1983) to complex oral polymer-drug devices with a core and an erodible shell (Magron et al, 1987; Laghoueg et al, 1989). As for the latter, the mechanism

was similarly complex, involving diffusion of liquid through the shell and core, followed by the diffusion of drug out of the core and shell in this liquid and at the same time, erosion of the shell was occurring. Different types of dosage forms made from the same gelucires could give different release profiles. When monolithic capsules, granulate capsules and granulate tablets, all produced by melting-congealing (melt-fused) method, together with tablets obtained by direct compression were compared to one another, the release rates of proxyphylline was found to be vastly different even though the carriers used, Precirol WL 2155 (G64/02) and Compritol 888 (G70/02) were the same (Ratsimbazafy et al, 1997). Granulate capsules gave the fastest release followed by direct compression tablets, granulate tablets and monolithic capsules, in that order. The variation was attributed to the different methods of manufacture producing diverse dissolution surfaces. Granulate capsules had a high erosion contribution whilst the rest were predominantly diffusional with the weak erosion factor increasing with the dissolution surface.

Dissolution surfaces can also have an implication on the drug release in another way. When drug release is controlled by erosion, its rate is proportional to the area of the dosage form (Bidah and Vergnaud, 1990). On the assumption that erosion did not contribute to the release process, the kinetics of sodium salicylate release from G46/07 or G50/02 formulated as spherical beads can be described as diffusional, and an equation was derived to relate the kinetics to the bead radius and liquid/bead volume ratio (Bidah et al, 1992; Ainaoui et al, 1997). However, it is often misleading to take on the assumption that no erosion would occur as many gelucires do exhibit some erosional release. In addition, there are many models pertaining to the release of drugs from their matrix systems and dissolution testing can be modified to investigate a particular parameter of the models. Kopcha et al (1990) compared the dissolution profiles of gelucire disks with two different surface areas in order to study the surface area as a parameter. It was discovered that increasing the surface area resulted in the increase of the diffusion mechanism over erosion. This was true for the gelucires of various melting points and HLBs investigated, and also when theophylline or D&C yellow No. 10 marker was incorporated. Erosion was then deemed to be a minor component in the release of drugs from gelucires as erosion was expected to be greatly elevated when the surface area increased.

Following on from the above, when it was necessary to minimise erosion and disintegration in order to reduce potential surface area changes, the matrices were set in copper cups that allowed only a single surface to be exposed (Prapaitakul et al, 1991). A variation of this whereby the disks were obtained by slicing gelucire columns after being exposed to dissolution medium was performed by Dennis et al (1987). After drying these disks, percentage swelling was calculated and it was found that swelling and erosion played a role in the release of drug, in this case ketoprofen. The indication from these studies is that although similar matrix forms were utilised, the results obtained from the dissolution tests were open to a range of interpretation, depending on the particular focus of the investigators. When the disk method is used, the effect of dissolution medium entering into the bulk of the matrix through pores and/or intergranular spaces is minimised. However, for dosage forms such as tablets and capsules, this is a factor that must not be ignored. It is important to establish the mechanisms as accurately as possible if the matrices are intended for oral use. If the release from the matrices is erosion controlled, the in-vitro / in-vivo correlation could be poor because the formulations would be sensitive to hydrodynamic conditions (Howard and Gould, 1987; Dennis et al, 1988; Vial-Bernasconi et al, 1995). As this would lead to person to person variability, a diffusion controlled release is sometimes preferable to overcome this problem; erosion controlled formulations can then be reserved for drugs which have low solubility in water or the medium in which it needs to be released in. However, diffusional release is not without its own problems in that it is often affected by ambient conditions such as pH of the surrounding liquid and solubilities of the drug both in the medium and the carrier, as will be elaborated later.

In order to characterise the release of drugs from controlled release formulations, many mathematical models have been put forward. For such dosage forms, there may be more than just diffusion contributing to the mechanisms of release. The following equations quoted are revised versions of Equation 4.1 (Higuchi, 1963) which was associated primarily with diffusional release. One of them incorporated non-linear dissolution coefficients, k and n, and is expressed by:

$$\frac{M_t}{M_\infty} = kt^n \qquad \text{....Equation 4.8}$$

where M_t is the amount of drug released at time t and M_∞ is the total amount of drug

released from the dosage form (Peppas, 1985). The exponent n take the values $0.5 \leq n \leq 1$. When n is 0.5, the drug release is via diffusion and when it is 1, the release is zero-order, that is via swelling and erosion or dissolution of the polymer matrix. When the release can be related to cube root kinetics, n values have found to be about 0.7 to 0.9 (Trigger et al, 1988). Therefore, n gives an indication of the mechanics involved in the drug release. For a cylindrical formulation, n = 0.45 indicates a Fickian (diffusional) drug release, $0.45<n<0.89$ indicates an anomalous (non-Fickian) release and n = 0.89 indicates a Case II transport (swelling and erosion) kinetics (Ritger and Peppas, 1987). On the other hand, when t is 1, regardless of the value of n, the exponent k becomes the percentage of drug dissolved and so this exponent can be regarded as an indication of the actual drug dissolution rate (Delgado-Charro and Vila-Jato, 1991). k can also be regarded as the constant which takes into account the structural and geometric properties of the matrices. If the matrices are swellable and hydrophilic, and exhibit an initial burst effect of drug release, that is the release at the beginning of dissolution is very high followed by a more constant release rate, Equation 8 is modified to include a y-axis intercept, b (Colombo et al, 1995):

$$\frac{M_t}{M_\infty} = kt^n + b \qquad \text{....Equation 4.9}$$

In controlled-release formulations, especially those involving lipid matrices such as gelucires, Equation 8 may be too simplistic and does not give sufficient information regarding the release process. Beren and Hopfenberg (1978) modified this equation to give;

$$\frac{M_t}{M_\infty} = k_1 t + k_2 t^{1/2} \qquad \text{....Equation 4.10}$$

where k_1 is the coefficient which reflects the zero-order mechanism and k_2 reflects the diffusion mechanism. Therefore, the ratio of k_1 to k_2 will indicate the dominant mechanism. This equation gives a fairer representation of the release process as it takes into account the contributions of both mechanisms as it is so often the case with controlled- release formulations. The erosional coefficient, k_1 , can be described as:

$$k_1 = k'(cd) \qquad \text{....Equation 4.11}$$

where k' is the coefficient of mass transfer of the dissolved drug at the dissolution medium/swollen matrix interface and cd is the polymer volume fraction at the same

interface (Harland et al, 1988).

4.1.3 The effect of drug loading on the release profiles

Apart from the nature of the carrier, the concentration of the incorporated drug may also have an effect on the release profile. Increasing the drug loading increased the rate of release of chlorpheniramine maleate from gelucire matrices (Prapaitrakul et al, 1991), benzonatate from G50/13 (Doelker et al, 1986) and diltiazem from pectin:HPMC matrix (Kim and Fassihi, 1997). The kinetics of the diltiazem release varied with the concentration of the drug within the carriers, with the release of the low loading being mainly diffusional whilst the higher loadings showed both diffusional and swelling/erosion processes. Incorporation of sodium salicylate into the shell made of Eudragit surrounding a core of the same polymer revealed that the kinetics of release was influenced by the amount of drug in the shell (Ouriemchi et al, 1994). More was revealed when the rate of drug released was plotted against time; at the lower drug concentrations, there existed a minimum and a maximum in the rate of release.

In formulating quinidine gluconate with Precirol (glycerol palmitostearate) into tablets by hot fusion method or wet granulation method, it was found that as the Precirol content increased, the dissolution rate decreased; in other words, as the drug content increased, the dissolution rate increased as well (Saraiya and Bolton, 1990). Similarly, the release rate of theophylline from tablets containing only 5% Precirol was faster than those containing 7.5% and 10% Precirol. The release rates of the same drug in PEG 1500 : PVAc matrices increased with higher loadings of the drug and even the dissolution profiles varied with the loadings (Shehab and Richards, 1996a). However, when the drug incorporated into the hydrophilic carrier was hydrophobic, such as griseofulvin or oxazepam, increasing the drug loading resulted in a decrease in the dissolution rate (Sjökvist and Nyström, 1988; Westerberg and Nyström, 1993). This was due to the increase in the net drug particle size as the concentration became higher resulting in a decrease in the effective surface area, and for a hydrophobic, sparingly soluble drug such as griseofulvin, particle characteristics and dimensions play a very important role in its release.

In this study, the effects of different loadings of the two model drugs on their release from G50/13 matrices including possible variations to their release kinetics were investigated In addition, taking into account the similar solubilities in water of the two model drugs, any differences in their release profiles were elucidated. Previous investigations as had been reported in the preceding chapters were concerned with the structural composition and morphology of the matrices and their relationships to the release behaviour were assessed by performing the dissolution studies.

4.2 Materials and Methods

4.2.1 Fabrication of melt-fused tablets

It was decided that the model dosage form to be used was moulded tablet because this would be similar to the type of block matrix that gelucire would be used for, such as in hard gelatin capsules but without having to take into account the dissolution of the gelatin shell. Moulded tablets had first to be fabricated by the melt-fusion method. All the G50/13 used came from the same batch to ensure no batch to batch variability. The paracetamol and caffeine were used as received (Avocado, Lancs.) and sizes of the particles used were less than 100μm as determined by microscopy (refer to Appendix 4 for details). Determination of drug particle size ranges through microscopy before incorporation into gelucires was also performed by Kopcha et al (1990).

The gelucire was placed in a glass beaker and melted at 75°C in an oven (Townsend and Mercer, England) for 70 minutes. Gelucires are recommended to be melted down at 20°C above their nominal melting point by their manufacturer and the additional 5°C takes into account the slight fluctuations of temperature during the fabrication process.This quantity of time was necessary for all the gelucire to reach that temperature, melt and at the same time remove its thermal history. About 26g of G50/13 was used during each fabrication which would allow 12 tablets to be manufactured with some excess. Then the gelucire was taken out and placed on a magnetic hot plate stirrer (Corning Hot-Plate Stirrer PC-351) set to maintain the gelucire at 75°C. An accurately weighed sample of paracetamol or caffeine which would give 5, 10, 20 or 30% w/w of drug in the total mixture, was dispersed for 10

minutes in the molten gelucire. This length of time was found to be sufficient for all the lumps of drug to breakup under stirring, thus ensuring the homogeneity of the mixture. This method of drug incorporation into G50/13 using a magnetic hot-plate stirrer was also utilised by Huet de Barochez et al (1989). The mixture was returned to the oven for another 30 minutes to further ensure the removal of the gelucire thermal history. Then it was taken out and stirred for 30 seconds on the hot-plate in order to get a uniform dispersion, and poured into an aluminium mould. The mould was made from aluminium as it was found that copper moulds can cause the degradation of gelucire (Sutananta et al, 1994a). The mixture was allowed to set under ambient conditions for two hours before the excess matrix was cut away with a single-sided blade. The tablets were removed from the mould and now had the dimensions of 1.5 cm in diameter, 1 cm in height and 2g in weight. They were placed in a silica-gel desiccator for 12-24 hours to equilibrate.

4.2.2 Experimental protocol

USP II dissolution test employing the rotating basket method was adopted in this study and performed in a PharmaTest Type PTW S dissolution apparatus. Distilled water was used as dissolution medium and set to equilibrate at 37 ± 0.5°C. Six tablets were used for each run and the baskets were set to rotate at 100 times per minute. An automated dissolution system was not able to be used because the concentration of the drug released was too high for the range of the automated UV analyser and also the eroded gelucire made the solution too cloudy for simple UV analysis. Filtering through Pharmatest filters fitted at the ends of the sampling rods did not adequately remove the eroded gelucire. Therefore, at 30 minutes, 1, 2, 4, 6 and 8 hours, 1-2 ml of the dissolution media was removed from each flask through the Pharmatest filters and filtered again through 0.45μm cellulose nitrate membrane filters (Sartorius, Germany). The filters were previously found not to adsorb paracetamol nor caffeine. After appropriate dilution, the concentration of the drug in the clear solution was determined by reading the absorbance using a UV Spectrophotometer (Perkin-Elmer 554 UV-VIS).

The maximum peaks on the ultraviolet spectrum of the drugs in distilled water as determined on the UV spectrophotometer were 243nm for paracetamol and 273nm for

caffeine. Choosing the wavelength where the maximum peak is exhibited will minimise errors due to factors such as wavelength drift. Calibration curves were constructed for paracetamol and caffeine concentrations against the absorbances measured on the UV spectrophotometer used. The range of concentrations used gave absorbances up to 0.9, as it had been suggested that the intermediate range of absorbances, that is from 0.4 to 0.9, will provide the maximum accuracy to the readings (Harris, 1997). Absorbance which is too high will result in the difficulty in detecting the light passing through but on the other hand, it will be difficult to distinguish between the sample and reference cuvets if the absorbance is too low and the intensity of the light coming through is too high. There is a linear relationship between absorbance and drug concentration (r=0.999) up to 0.014mg/ml for paracetamol at the wavelength of 243nm, and 0.018mg/ml for caffeine at 273nm, both within the range of absorbance discussed above.

Through calibration curves, the concentrations of the saturated solutions of paracetamol and caffeine at 37°C in the distilled water used was found to be 21.6 mg/ml and 27.7 mg/ml respectively. This makes the solubility ratio of drug to water at 37°C to be 1:46 for paracetamol and 1:36 for caffeine as opposed to 1:70 and 1:60 respectively in water at 20°C (Clarke's Isolation of Drugs, 1990).

4.3 Results and Discussions

4.3.1 Paracetamol and caffeine releases from G50/13 matrices

Figure 4.1 showed that there were very small differences between the release profiles of the three drug loadings of paracetamol in G50/13. The slight increase in the release for 20% loading may be due to the disruption of the gelucire matrix by the drug particles. 30% loading gave an unexpected lower release but this could be due to the decrease in the quantity of gelucire available to solubilise the drug. There was also hardly any difference in the release profiles of the caffeine loadings as shown by Figure 4.2. The bigger standard deviations seen for the caffeine samples than the paracetamol samples indicate a bigger variation in their release. This lack of great changes in the release profiles due to drug loadings had also been shown before. The release profiles of the different loadings of

Figure 4.1 : Dissolution profiles of paracetamol loadings in G50/13

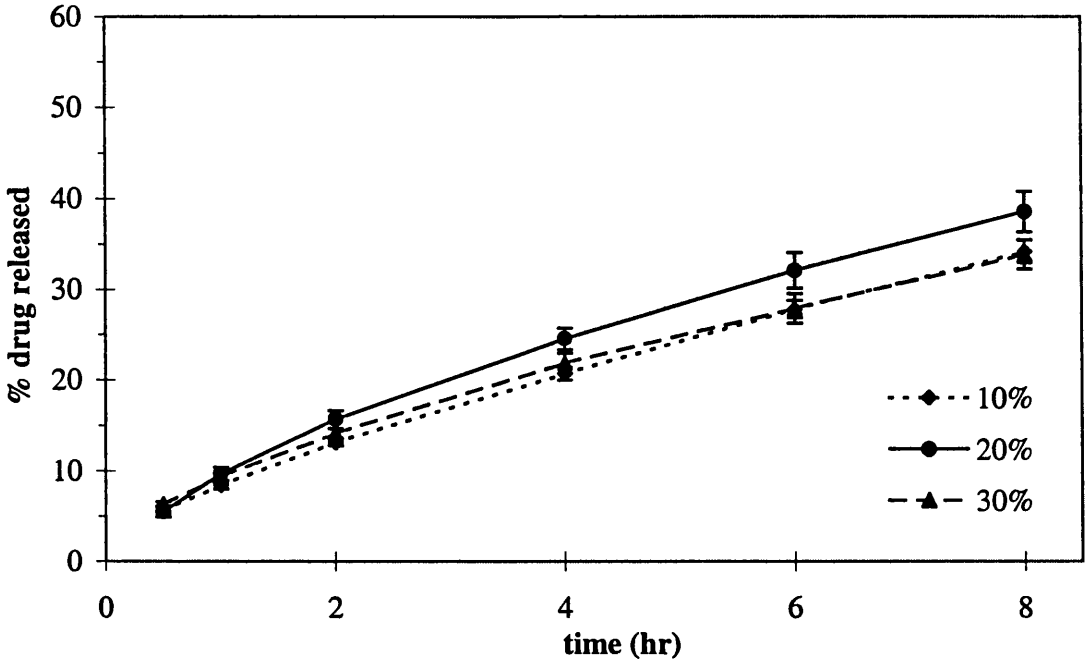

Figure 4.2: Dissolution profiles of caffeine loadings in G50/13

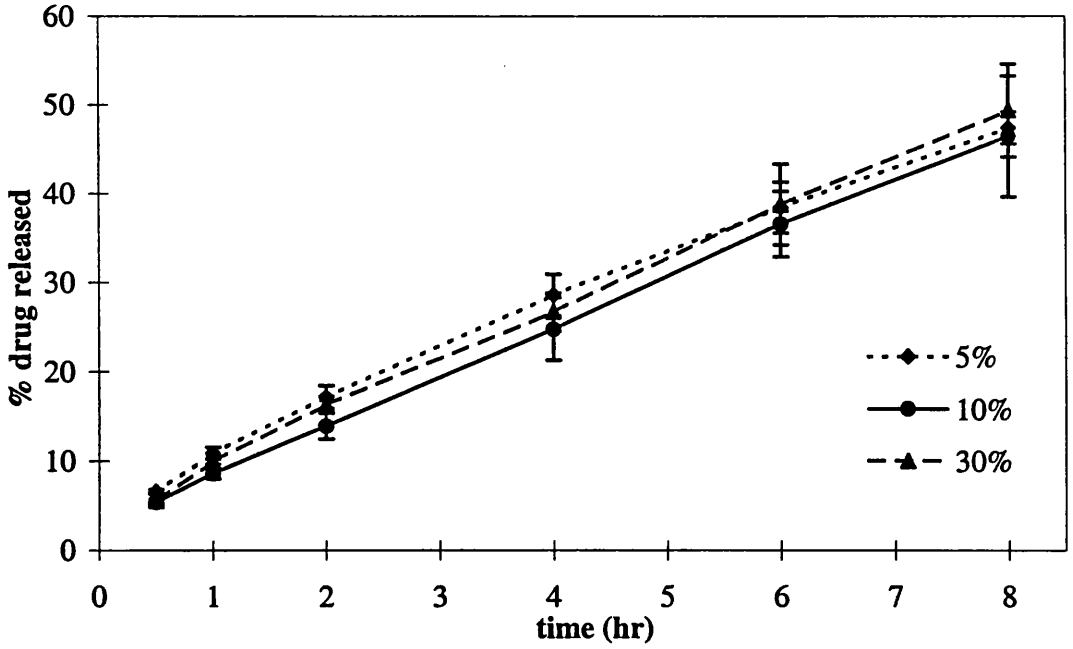

theophylline and also propanolol (10% to 60%) from matrices made up of G53/02 and G50/13 were found to overlap with one another (Bodmeier et al, 1990). Even though it was previously expected that the release would increase with the drug loading, this effect was more obvious for the compositions of matrices with decreasing levels of G50/13, that is as the HLB values became smaller. This indifference to drug loading was taken to indicate that the release was mainly a function of the matrix composition. Perhaps this was due to the more hydrophilic matrices (those with a higher proportion of G50/13 or pure G50/13 in the case of this study) already exhibiting erosion and dissolution of polymer and therefore, the small changes brought about by the different loadings would be masked.

Figures 4.3 and 4.4 were plotted from the amount of drug released between two time points over the time taken to liberate them, against time. The figures showed that apart from the initial burst of release, the rates were constant up to 8 hours of dissolution. This uniform release rate effect was seen for both drugs regardless of their loadings, which indicates that the matrices were able to give good sustained releases under those conditions.

4.3.1.1 Kinetics of paracetamol release

The kinetic equations were applied to the release profiles and the results were tabulated (Tables 4.1 to 4.3). The data were fitted to Equation 4.8 by using a power trendline curve fitting function which had the expression in the form of $y = kt^n$ ($r > 0.998$) and Equation 4.10 by a second-order polynomial fitting through the origin in the form of $y = k_1(t^{1/2})^2 + k_2(t^{1/2})$ of drug release plotted against $t^{1/2}$ curve($r > 0.998$) where t is the time. Fitting to Equation 4.1 was performed linearly against the $t^{1/2}$ curve ($r > 0.980$).

From Table 4.1, looking at the drug dispersions in G50/13, the values of n were between 0.5 and 1, indicating that both diffusion and swelling/dissolution/erosion contributed as mechanisms of drug release. In general, the release of paracetamol from the matrix relied more heavily on diffusion as the n value tended more towards 0.5 but erosion played a greater role in the release of caffeine (n values > 0.75). The n value for the release of another hydrophilic drug, salbutamol sulphate, from G50/13 was 0.68, thus also showing a non-Fickian transport mechanism (Esquisabel et al, 1996). During the process of

Figure 4.3 : Dissolution rates of paracetamol loadings in G50/13

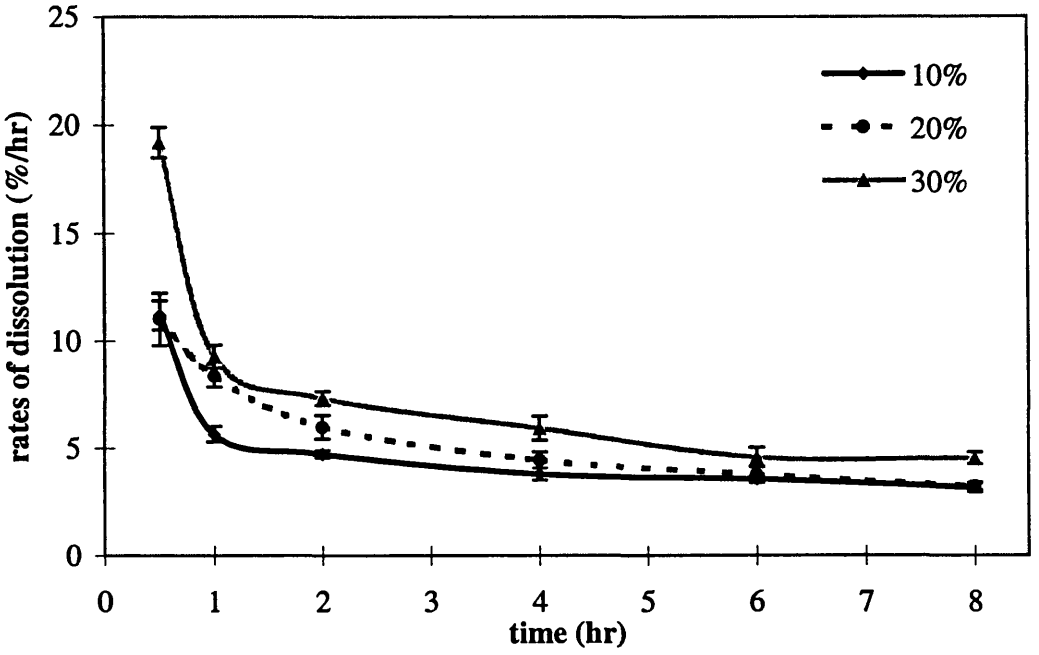

Figure 4.4 : Dissolution rates of caffeine loadings in G50/13

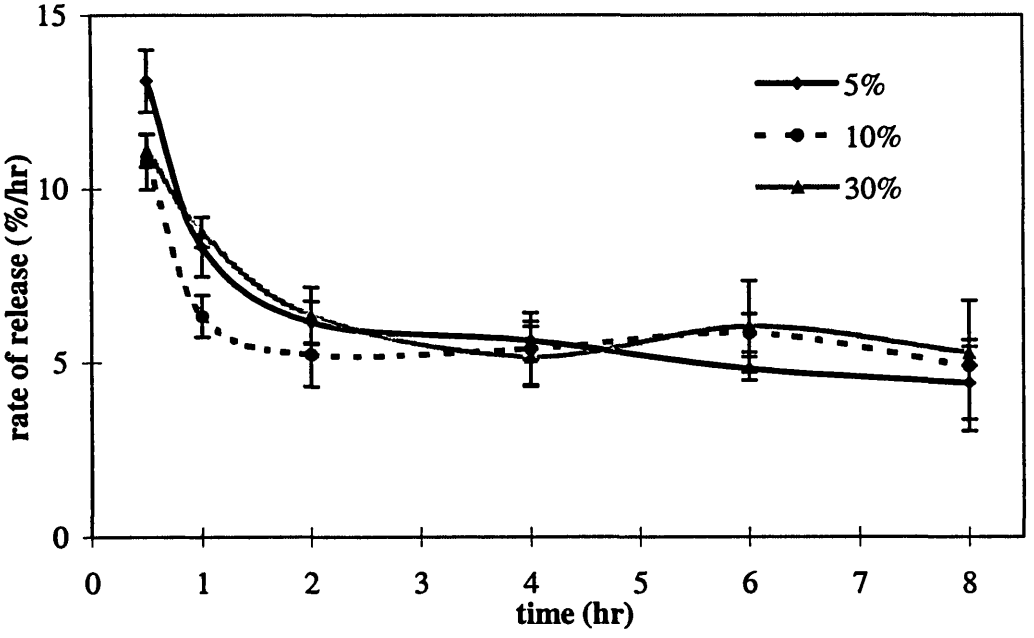

Table 4.1: Parameters calculated from the fitting of the dissolution data to the Equation 4.8 together with T50%, that is the time taken for 50% w/w of the paracetamol or caffeine to be released from the matrices.

Loading of drug (%)	Dissolution rate coefficient, k (%/hr)	Exponent n from Equation	Correlation coefficient, r^2	T50% (hour)
Paracetamol				
10	8.55 ± 0.43	0.65 ± 0.01	0.9988	13.32 ± 0.58
20	9.33 ± 0.80	0.69 ± 0.02	0.9980	11.97 ± 0.81
30	9.43 ± 0.37	0.61 ± 0.01	0.9996	14.21 ± 1.17
Caffeine				
5	10.72 ± 0.65	0.71 ± 0.01	0.9998	8.53 ± 0.56
10	9.20 ± 0.69	0.77 ± 0.03	0.9983	8.70 ± 1.40
30	9.60 ± 0.43	0.77 ± 0.03	0.9986	8.12 ± 1.09

Table 4.2: Parameters calculated from the fitting of the dissolution data to the Equation 4.10 together with the ratio of k_1 to k_2.

Loading of drug (%)	Exponent k_1 from Equation	Exponent k_2 from Equation	Correlation coefficient, r^2	k_1 / k_2
Paracetamol				
10	2.00 ± 0.05	6.42 ± 0.28	0.9999	0.31 ± 0.02
20	2.14 ± 0.05	7.75 ± 0.62	0.9978	0.28 ± 0.06
30	1.39 ± 0.14	8.02 ± 0.24	0.9998	0.17 ± 0.05
Caffeine				
5	3.29 ± 0.07	7.56 ± 1.08	0.9997	0.43 ± 0.08
10	4.03 ± 0.87	5.01 ± 0.23	0.9996	0.81 ± 0.21
30	4.34 ± 0.87	5.13 ± 0.52	0.9991	0.85 ± 0.26

Table 4.3: Parameters calculated from the fitting of the dissolution data to the Equation 4.1 .

Loading of drug (%)	Dissolution rate, k (%/hr$^{-1/2}$)	Correlation coefficient, r^2	t_{lag} (hr)
Paracetamol			
10	13.45 ± 0.42	0.9926	0.37 ± 0.01
20	15.54 ± 0.77	0.9988	0.38 ± 0.02
30	12.97 ± 0.75	0.9970	0.28 ± 0.01
Caffeine			
5	19.24 ± 0.98	0.9934	0.44 ± 0.01
10	19.16 ± 2.81	0.9847	0.53 ± 0.04
30	20.36 ± 2.54	0.9837	0.53 ± 0.05

dispersing the drugs in the molten G50/13, it was noticed that there was some difficulty with the caffeine. Even though the caffeine was thoroughly deaggregated before incorporation and dispersed carefully into the gelucire, some aggregation was observed within the molten carrier. These were carefully broken up to ensure a homogenous dispersion. This could be an indication that the coating of the individual drug particles by the gelucire was more effective for paracetamol than for caffeine. Such close contact between drug and carrier resulted in a lower porosity matrix (Saraiya and Bolton, 1990) and so, the more porous nature of the caffeine dispersions increased the contribution by erosion to the release kinetics.

There was no obvious trend in the n values as the drug loading was increased for the paracetamol dispersions and even though the n value was higher (0.65) for the lower drug loading (10%) and lower (0.61) for the higher drug loading (30%), this difference is small. However, the ratio of k_1 to k_2 exponents of Equation 4.10 of the two loadings as presented in Table 4.2, corresponded with the n values of Equation 4.8 in Table 4.1, in that the higher k_1/k_2 value for the 10% dispersion also indicated a higher contribution of erosion to its release from the matrix. Likewise, the lower ratio for the 30% showed that diffusion was more prominent. A possible explanation for this could be that there was more gelucire w/w of the matrix tablet in the 10% tablet, so when it came in contact with the water, it swelled and subsequently eroded. On the other hand, in the 30% w/w paracetamol dispersion, there was less gelucire for this process but more drug for the dissolution in contact with water and subsequently diffusion through the water filled pores of the paracetamol out of the matrix. This was also demonstrated in the release of quinidine gluconate, as its surface dissolution due to the high solubility of the drug in an acidic medium resulted in the formation of pores which in turn, allowed easier penetration by the dissolution medium (Saraiya and Bolton, 1990). Again, the relative closeness of the values and the anomaly of the 20% dispersion indicate that these factors may not be significant in conditions such as in vivo.

4.3.1.2 Kinetics of caffeine release

As presented in Tables 4.1 and 4.2, the k_1/k_2 value for the caffeine dispersions also agreed

with the n values and showed that erosion had a more prominent role here than in the paracetamol dispersions. However, unlike the paracetamol loadings, the erosion factor increased as the caffeine loading increased. This could be due to the caffeine particles dissolving and creating a more porous matrix from which erosion could occur more easily. At higher drug loadings, a considerably soluble drug will diffuse out and create more channels in the swollen matrix (Prapaitrakul et al, 1991; Kim and Fassihi, 1997). From Chapter 3, it was found that at 5% loading of caffeine in G50/13, the solubilised drug recrystallised separately as fine, needle-like network throughout the matrix. A higher k_2 factor for the 5% caffeine loading could be attributed to this fine drug crystals dissolving and diffusing out through the swollen gelucire.

This variation of the kinetic parameters with drug loading was also demonstrated by the release of diltiazem from pectin:HPMC matrices (Kim and Fassihi, 1997). At 5% loading, the n value of 0.65 and the low k_1/k_2 indicated a dominance of the diffusion mechanism. At 12% loading, the n value increased to 0.95 with k_1/k_2 value high indicating a switch to Case II transport kinetics (erosion/swelling/dissolution) but at even higher loadings of 20% and 24%, the values were in between those quoted for the other two lower loadings.

4.3.2 Comparison of the release behaviours of the model drugs from G50/13 matrices

Looking at the release of paracetamol dispersions compared to the caffeine dispersions, the release profile seemed to be higher for the caffeine containing samples, even after taking into account the slightly higher solubility of caffeine in water at 37°C (1.27x) than paracetamol, as shown by Figure 4.5 which compared the two drugs at the same loading. The difference in the solubilities of two model drugs (propanolol and theophylline, by a factor of almost 20) was reportedly not to significantly affect their release rates from matrices containing a proportion of G50/13, which indicated that the main parameter affecting the rates would be the carriers themselves (Bodmeier et al, 1990). Therefore, the elevated rates for the caffeine dispersions were possibly due to the higher coefficient of erosion as mentioned before. This higher rate for caffeine is not only seen in the mathematical fitting of the data in Table 4.3 but also in Figure 4.6 which compares the two drugs at the same loading. Additionally, there was a layer of opaque gel-like mass

Figure 4.5: Dissolution profiles of 10% paracetamol and caffeine in G50/13

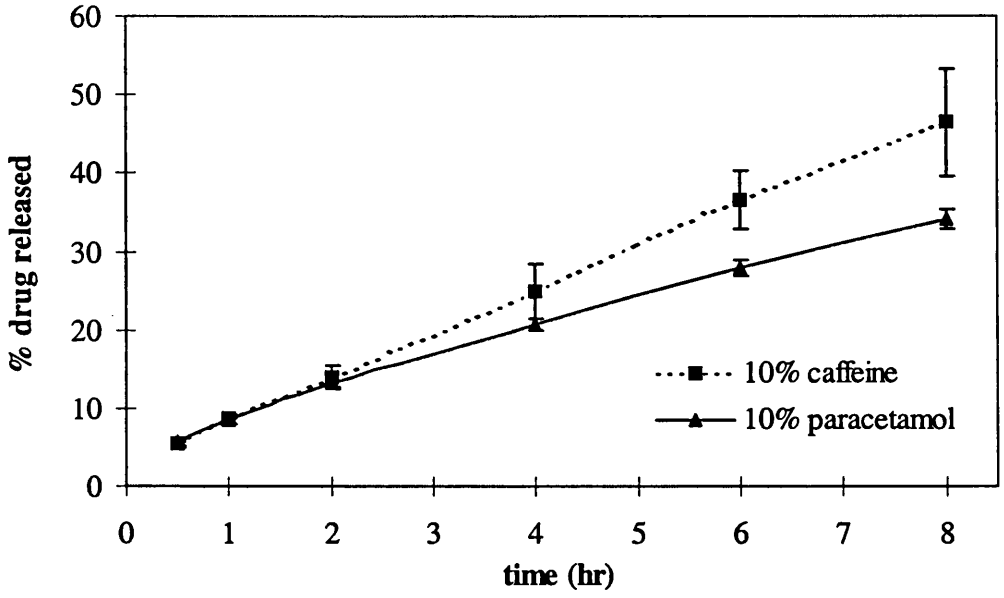

Figure 4.6: Rate of dissolution of 10% paracetamol and caffeine in G50/13

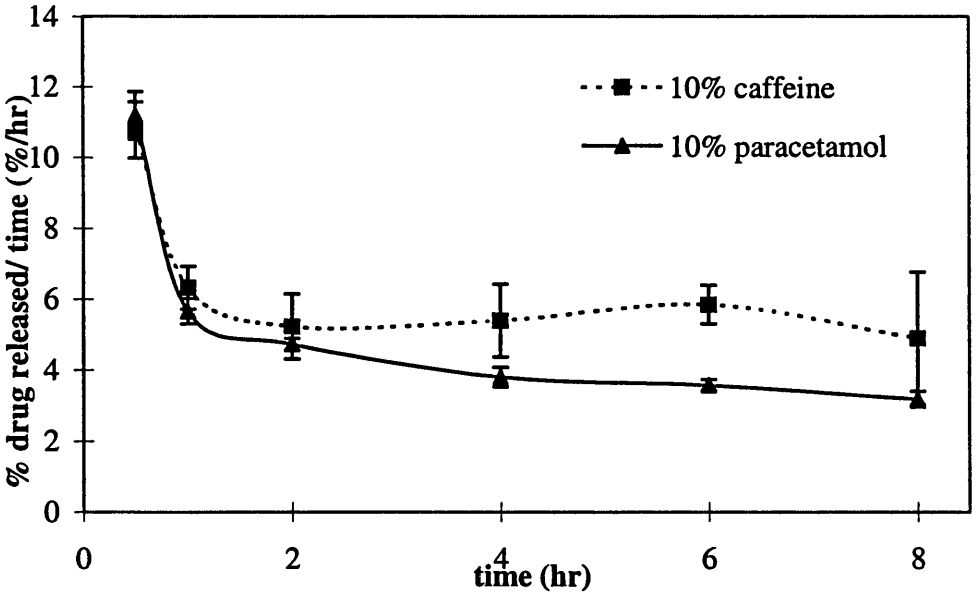

surrounding the paracetamol dispersion, which released the drug slowly by dissolution of the matrix and which may had been retarding the erosion. This was also reported by Parab et al (1986) who observed that the addition of mannitol to theophylline/HPMC/Precirol matrices caused a decrease in the drug release due to the formation of a gel mass and the retardation became more pronounced as the viscosity of this gel increased. The formation of such layers are due to the swelling of the carrier polymers on contact with liquid and these matrices did not show any erosion despite the swelling before the gel formation. Similarly, the release of benzonatate from G35/10 was retarded which was thought to be due to the formation of a hydrated layer around the matrix which impeded the disintegration of the mass (Doelker, 1986).

A matrix in this condition can be divided to several layers according to the degree of hydration (Ju et al, 1997): i) dry glassy core containing unhydrated polymer ii) swollen glassy layer containing some of the diffused liquid which in turn increased the mobility of the network and led to very strong chain entanglement iii) gel layer where there is proportionally less polymer due to increased swelling but the entanglements are still strong iv) diffusion layer where there is so little polymer that the entanglements become very weak and it is at the interface of this layer and the gel layer that polymer dissolution takes place, when the weakened entanglement can no longer hold the polymers together. Such dissolution at the water-gel interface where the polymer concentration is so low and water content is so high that the gel microstructure reached its maximum disentanglement was also demonstrated by pectin/HPMC-based matrix tablet containing diltiazem (Kim et al, 1997). The significance of this is that a relationship was found for hydrophilic polymers between diffusion coefficient of the polymer, D_p and both molecular weight, M, and concentration of polymer, C_p, whereby:

$$D_p = 7.24 \times 10^{-5} M^{-0.6} [1+700 (M/96000)^{0.7} C_p/8]^{-2}$$

It can be seen that the diffusion coefficient should change significantly within the diffusion layer. By taking into account that the molecular weight of G50/13 was the same in the paracetamol dispersion as in the caffeine dispersion, and that the diameter difference profiles of both samples showed that the paracetamol dispersion exhibited a higher degree

of swelling, the concentration of the gelucire at the diffusion layer was low, and thus the diffusion of the dissolved polymer was also low. This will have an impact on the drug release as the formation of water filled channels which will allow the dissolved drug to come out of the matrix or the progression of the matrix dissolution front will be slower.

The dissolution data from this study was also fitted to the Higuchi equation (Equation 4.1) and the results displayed in Table 4.3. Gelucire 50/13, in combination with other gelucires had been shown to cause the release of chlorpheniramine maleate in a linear manner to the square root of time, even though in this case, the erosion was deliberately reduced (Prapaitakul et al, 1991). It could be seen from Table 4.3 that the higher correlation coefficient values for the paracetamol dispersion than caffeine dispersion samples were indicative of the better fit to the Higuchi's model (Equation 4.1) for the former. The release rate constant for 20% loading was significantly higher than the other two. It could be a further evidence of the increase in the number of liquid filled channels created by the 20% loading, as was mentioned before. This increase in matrix permeability due to the formation of a continuous pore structure will also produce a release rate which was higher than that predicted by Equation 4.2 (Prapaitrakul et al, 1991). If erosion could be made to be excluded from the release kinetics, the resultant diffusional release could be predicted from Equations 4.4 and 4.5 for non-swellable matrices or even more accurate, from Equations 4.6 and 4.7 for swellable matrices, with each loading having its own ϵ and τ values which represent the porosity and tortuosity factors respectively. The high number of channels then leads to an increase of diffusion through pores and swelling/erosion through greater contact with the surrounding liquid.

The caffeine dispersion samples show a significantly higher rates of release compared to the paracetamol samples according to the k values (Table 4.3). This was confirmed by comparing the actual rates of release plotted against time, as shown in Figure 4.6. However, no significant difference in the rates could be established for the different drug loadings of caffeine and again, this was supported by the release rates profile, shown in Figure 4.4. The constant C in Equation 4.1 is indicative of physical parameters (Kopcha et al, 1990). If its value is small compared to K, it is taken as the experimental error or the error which occurred during curve fitting. If its value is a large positive number, the matrices are taken

to exhibit a burst release effect, as explained in Equation 4.9. If its value is a large negative number, as was found in this study, it is taken to indicate that there exists a lag time before the release from the matrices commences. Lag times, t_{lag}, were taken as where the linear regression lines intersect the x-axes. The longer lag times for 20% paracetamol dispersion, 10% and 30% caffeine could be indicative of the longer time necessary to establish the large number of liquid filled channel. For the 5% caffeine dispersion, the shorter lag time could be due to the fine network of recrystallised caffeine (as mentioned in Chapter 3) within the matrix dissolving on contact with dissolution medium far quicker than discrete drug particles. Even though the 10% paracetamol dispersion showed some recrystallisation within the matrix with the redispersion of the drug at almost molecular level (Chapter 3) and it could reasonably be expected to establish the dissolution especially though diffusion much quicker than the next loading up, the observed value was quite long. At this point, it could only be postulated that this lag was due to the modification of the physical structure of the matrix due to the dissolution of the paracetamol within it.

4.4 Conclusions

Even though there was a difference between the release of paracetamol compared to the release of caffeine from G50/13 matrices, varying the loadings of the respective drugs incorporated into the carrier did not significantly alter their profiles. Caffeine dispersions had higher release rates according to the dissolution profiles, the rates of dissolution and the dissolution rate coefficients obtained from fitting the data to mathematical models.

Incorporation of different drugs resulted in a difference in the kinetics of release. Dispersions of caffeine showed a higher contribution from erosion as mechanisms of release compared to the paracetamol dispersions, even though the diffusion mechanism was still dominant. The higher erosion factor could be due to the increase in the porosity of the matrices containing caffeine. On the other hand, diffusion was always high for the paracetamol dispersions possibly due to the way the partially solubilised drug recrystallised within the G50/13 matrix. In other words, the variation in the proportions of the contribution from the different mechanisms of release depended on the alteration of the carrier structure by the drugs incorporated.

CHAPTER 5: INVESTIGATIONS INTO THE MECHANISM OF DRUG RELEASE BY EROSION AND WATER UPTAKE STUDIES

5.1 Introduction

There have been many studies on the release of drugs from various lipid matrices, such as already discussed in the previous chapter. The investigators attributed the release of the drug to the erosion of the matrix and/or the diffusion of the drug through the matrix. Higuchi's (1961,1963) and Peppas's equations (1985,1986) were frequently used to fit the dissolution profiles of these dosage forms in order to ascertain the extent that each mechanism contributes to the drug release. However, since both mechanisms frequently play a role in the release of the drug, it is often difficult to know which is the dominant one.

5.1.1 Measuring the erosion and swelling of matrices

To overcome the problem mentioned above, each mechanism can be studied separately. For example, Dennis et al (1987), using Gelucire with the melting point of 50°C and HLB of 4.8, studied the release of ketoprofen powder incorporated into the gelucire matrix at various concentrations. Erosion was taken as the percentage capsule weight loss over time after subjecting them to dissolution process using the basket apparatus, and the swelling was taken as the percentage change over time in the diameter of wax columns immersed in liquid. It was found that even though the dissolution profile fitted the Higuchi equation, the main assumptions of this equation, that is, there is no loss of matrix occurring during the release and that a constant diffusion coefficient exists, had to be rejected. This was because increasing the loading of the ketoprofen decreased the swelling and the erosion of the matrix but according to Higuchi, the release rate should be independent of the drug concentration. It was also found that the decrease was coincidental with the concentration that surpassed the solubility of ketoprofen in the gelucire, that is, particulate dispersion should produce a lower release rate.

Kim and Fassihi (1997) also investigated the function of erosion as a release mechanism by physical measurements. Individual tablets consisting of diltiazem:gelatin granules in pectin:HPMC matrix were dried under vacuum until constant weight after being taken out from the dissolution flasks at selected time intervals. The dimensional changes to the tablets due to their hydration by deionised water at 37°C were also measured. The

hydrophilic matrix was found to gradually erode and subsequently dissolve at the end of the study. As the matrix swelled, the diffusional pathlength increased but this effect was counterbalanced by the dissolution of the polymers at the water-gel interface. Here, the disentanglement was so extensive due to the high concentration of water and low concentration of polymer that it dissolved away. Thus, the total release effect was linear. Such processes are illustrated in Figure 5.1.

Figure 5.1: Diagram illustrating the process that a hydrophilic matrix undergoes during dissolution (Kim and Fassihi, 1997). As water diffuses into the matrix, a phase transition to a rubbery state occurs when the threshold is exceeded (a→b). Drug is released by erosion or diffusion through the swollen matrix (b→c), which finally dissolves (d).

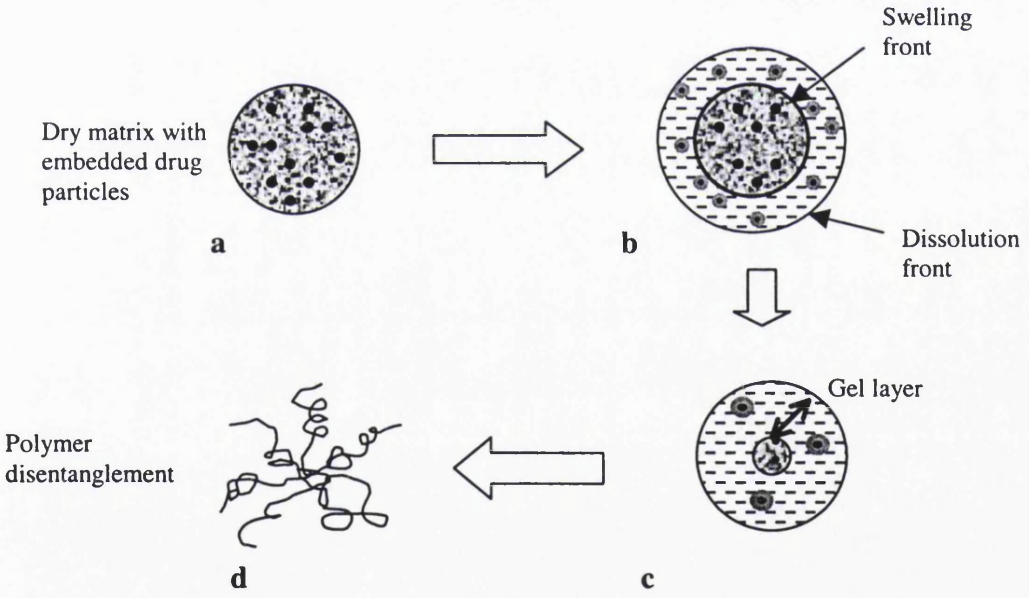

Colombo et al (1995) described the presence of several fronts when a matrix is put in a dissolution medium, namely a i) swelling front which represents the boundary between the dry polymer core and the rubbery gel state ii) diffusion front which separates the gel layer containing the undissolved drug from the layer containing dissolved drug and iii) erosion front which distinguishes the matrix from the dissolution medium. The observance of such fronts is likely to occur when a drug with a limited solubility in the

swollen polymer is dispersed in the system. The rates of processes such as water uptake, drug dissolution and erosion could then be calculated by measuring the movements of these fronts.

In addition to measuring the change in the dimensions, another method to determine the extent of matrix swelling was simply to measure the volume changes (Prapaitrakul et al, 1991). Gelucires were melted and allowed to congeal in a 10ml graduated cylinder. A specific volume of distilled water was then added to it, allowed to equilibrate for 24 hours and then the increase in the volume was read off.

5.1.2 The influence of the carrier composition on the mechanisms

Besides the drug that is dissolved in them, another factor that affects the mechanism of release is the composition of the matrix itself. Sutananta et al (1995) performed erosion and swelling studies on several gelucires with different melting points and HLB numbers. It was found that the more hydrophobic matrices such as those with only triglycerides and glycerides, released the drug at a very slow rate and at the same time, did not show signs of swelling nor erosion. The drug release fitted the model of diffusion-controlled release. This observation was also supported by a study on the release of proxyphylline from lipid matrices made of glyceryl tristearate and tribehenate (Ratsimbazafy et al, 1997) which found that the release from various dosage forms including monolithic capsules obtained by melt-congealing, was predominantly diffusional, with very little erosion and no swelling.

On the other hand, a base containing only PEG stearates such as Gelucire 55/18, exhibited swelling and erosion. The authors also found that a base such as G50/13 which is composed of both glycerides and PEG esters of fatty acids did not swell to the same extent as G55/18 (Sutananta et al, 1995). In that study, it was determined that the erosion was directly related to the water uptake and therefore, it was postulated that the erosion was caused by the inability of the matrix to support any more swelling due to spatial restriction, leading to disintegration at the matrix surface. G55/18 (which has a longer PEG backbone, molecular weight of 6000 as opposed to 1500 of G50/13) eroded when the gel layer which formed on the surface dissolved. Further studies on another

gelucire, namely G50/02 revealed that this matrix exhibited swelling and some erosion although it has a low HLB value similar to gelucires containing only glycerides, due to the presence of 20% PEG esters.

Dissolution studies in the previous chapter (Chapter 4) had revealed that the incorporation of different drugs into the G50/13 matrices had affected the way that these drugs were released. The mechanisms of drug release can be further elucidated by investigating the actual erosion and swelling behaviour of the gelucire matrix by physical measurements and the applicability of the mathematical modelling discussed in the dissolution chapter can be assessed.

4.2 Materials and Methods

5.2.1 Experimental protocol

The moulded tablets as fabricated for Chapter 4 were used for this study. The study was performed in the same dissolution apparatus as the previous chapter and the medium used was distilled water equilibrated at 37°C. A dissolution basket was put into an aluminium evaporating dish, weighed (weight DB) and marked with a dissolution flask number. Six tablets were weighed (weight X) and their diameters measured (diameter A). After putting the tablets in the baskets, a dissolution process was started. At 30 minutes, 1 hour, 2, 4, 6 and 8 hours, a basket was taken out. Excess water on the basket was removed with a tissue paper, placed on its corresponding evaporating dish and the stopwatch started. After allowing it to stand at room temperature for exactly 3 minutes, the tablet with the basket and dish was weighed immediately (weight Y). The tablet was then taken out of the basket and put on the platform of a travelling microscope (Griffin and George Ltd., Great Britain). The diameters of the tablets were measured to 0.001 cm (diameter C). The travelling microscope was used instead of a micrometer because there was a tendency to deform the soft and wet gelucire tablet when measuring with the latter. The tablets were then put in an oven and dried over 24 hours at 75°C until a constant weight was achieved (weight Z). Three repeats of the studies were performed.

5.2.2 Measurements of matrix erosion, water uptake and diameter difference

The matrix erosion was calculated as:

$$\text{matrix erosion} = \frac{[X - (Z - DB)]}{X} \times 100$$

....Equation 5.1

The water uptake by the tablets was calculated as:

$$\text{water uptake} = \frac{(Y - Z)}{Z - DB} \times 100$$

....Equation 5.2

The diameter difference of the tablets was simply:

$$\text{diameter difference} = \frac{(C - A)}{A} \times 100$$

....Equation 5.3

5.3 Results and Discussions

5.3.1 Erosion characteristics of pure G50/13 and its drug dispersions

Figure 5.2 showed that pure 50/13 eroded over time and its erosion profile over 8 hours seemed to follow a bimodal pattern. However, on closer inspection this pattern could be attributed to the result at 6 hours, which showed an exceptionally high erosion. Since the profile showed that the rate of erosion was constant until after 4 hours where there was a noted increase before reverting back to the lower rate at 6 hours, the erosion profile could be better described as linear. Incorporating paracetamol into the matrix caused it to erode at a more constant rate, resulting in a smoother erosion profile but the total erosion was less than for pure G50/13. Increasing the loading of paracetamol caused a slight decrease in the erosion but this was not a significant change.

There were slightly higher rates of erosions for the caffeine dispersions in G50/13 than for the pure G50/13 but this was only significant for the 30% caffeine loading, as shown

Figure 5.2: Erosion profiles of pure G50/13 and paracetamol dispersions in G50/13 at different drug loadings

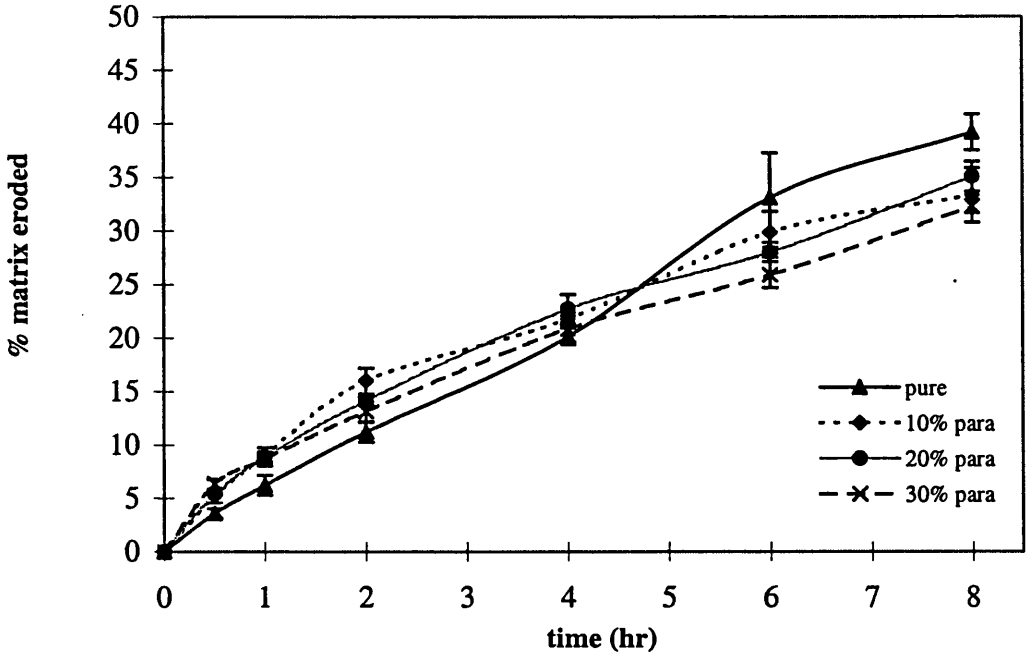

Figure 5.3: Erosion profiles of pure G50/13 and caffeine dispersions in G50/13 at different drug loadings

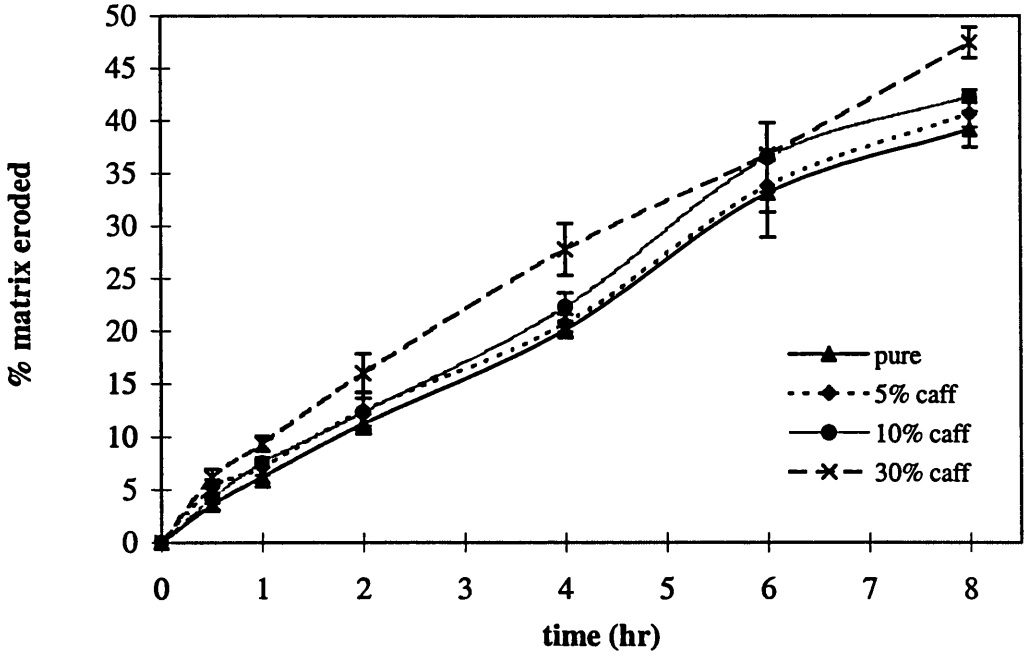

by Figure 5.3. The erosion profiles of the caffeine loadings followed a similar pattern to the pure G50/13, except at 30% loading where the erosion was higher and more consistent. This suggests that at lower caffeine loadings, the erosion behaviour was governed by the G50/13. At 30% loading, the leaching of the drug caused an even more porous matrix to be left behind due to the higher proportion of the caffeine. This resulted in a higher erosion rate due to the reduced cohesion of the carrier (Doelker et al, 1986).

5.3.2 Water uptake characteristics

At the beginning of the study, there was a high rate of water uptake as the water penetrated through the outer layer of the dry matrix and was retained within it, as shown by Figure 5.4. The matrices became increasingly swollen and as the limit was reached, erosion commenced. From then on, the rate of water uptake became lower as the rate of water penetration through the deeper layers of the matrix was countered by the rate at which the water saturated outer layer was being eroded. The water uptake increased over time as the increasingly smaller tablet provided increasingly bigger surface area over volume ratio allowing more contact with the water. For the pure G50/13 tablets, the water uptake profile again showed a slight bimodal pattern. The rate of uptake was constant until after 4 hours when the rate started to decrease. This was consistent with the increase in the erosion rate at the same time, indicating that the heavily saturated layer built up to this point was being removed from the matrix core. Hydration of the G50/13 matrices followed by its erosion had previously been reported (Bodmeier et al, 1990; Sutananta et al, 1995).

Figure 5.4 indicated that increasing the loading of paracetamol decreased the water uptake as compared to pure G50/13. This could be expected as there was less gelucire to imbibe the water. However, at 10% loading, the tablet could take up as much water as the pure G50/13 tablets. This suggests that perhaps the mixed crystal structure of the matrix with the solubilised paracetamol had a greater tendency to uptake water. With all the paracetamol dispersions, the uptake profile was constant after the initial high rate during the first ½ hour.

Figure 5.4: Water uptake profiles of pure G50/14 and paracetamol dispersions in G50/13 at different drug loadings

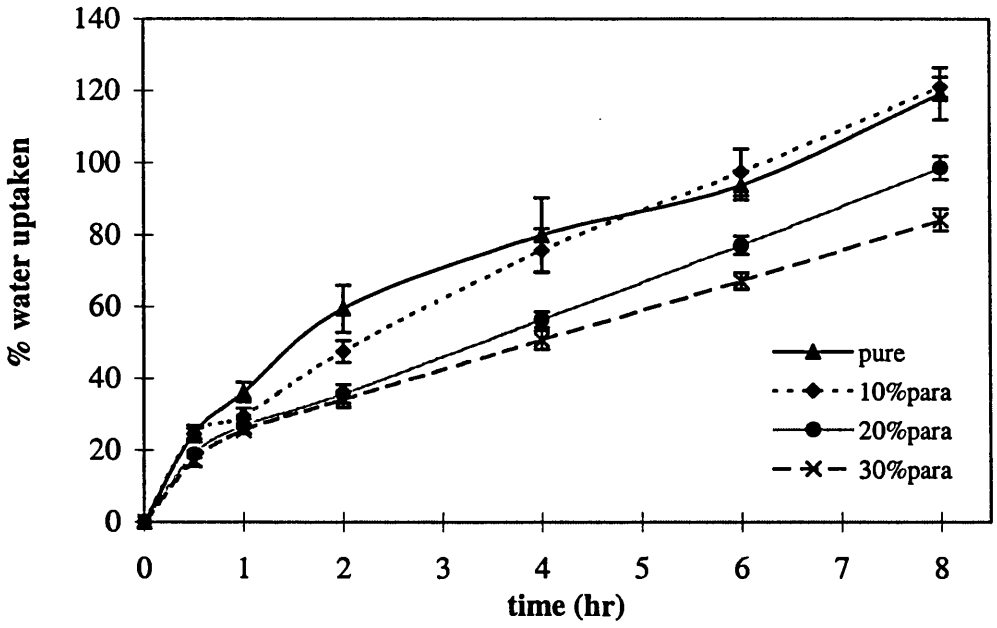

Figure 5.5: Water uptake profiles of pure G50/13 and caffeine dispersions in G50/13 at different drug loadings

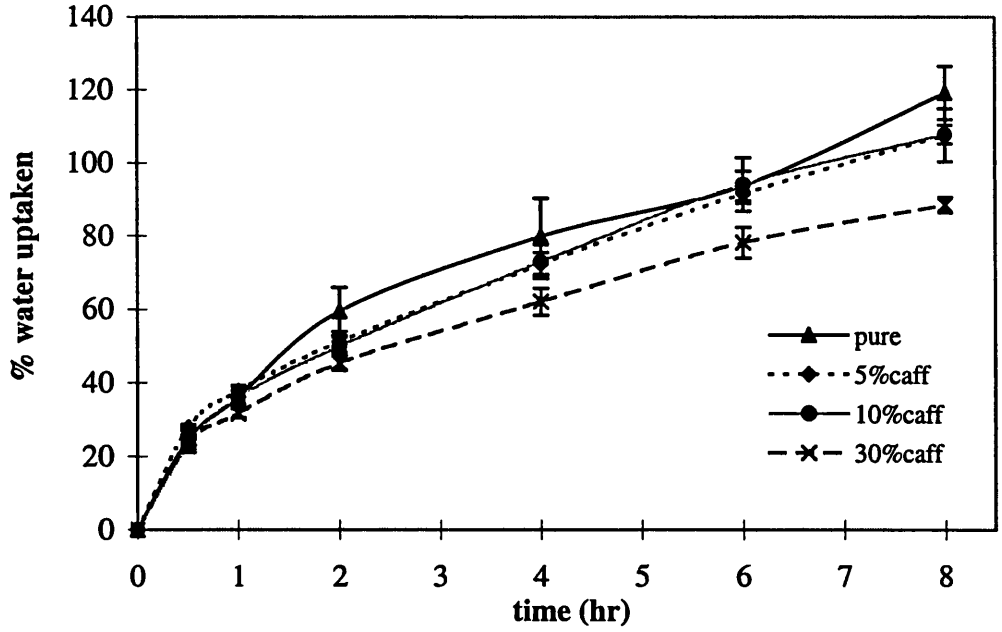

Increasing the caffeine loading also decreased the water uptake and even a loading as low as 5% showed this effect, as presented by Figure 5.5. The water uptake at low drug loadings was slightly lower than the pure G50/13 but the rate of all the loadings was also constant.

5.3.3 The relationship between erosion, water uptake and diameter differences

Figure 5.6 showed that the diameter of the pure G50/13 increased as the tablet took up the water from its surrounding and swelled, and the rate of increase was very high initially but became almost plateau after 2 hours. This was because the erosion process commenced and removed the outer layer almost as fast as it swelled (surface erosion). After 4 hours, the diameter decreased (but still bigger than the original tablet) which was consistent with the increase in erosion, brought on by the saturation of the outer layer with water until it can longer support the weight. The removal of the swollen layer front can also be attributed to the dissolution of G50/13 due to the disentanglement of the long molecular chains. This was also shown by a previous study on pectin:HPMC matrices which are hydrophilic carriers (Kim and Fassihi, 1997). The matrices demonstrated high water uptake and swelling, leading to volume changes and subsequently reaching its maximum after 2 hours, after which the changes decreased. Since intensive erosion only started occurring after this point, it was concluded that during the initial stages, the matrices could accommodate the swelling without a high degree of chain disentanglement, erosion nor polymer dissolution.

For the 10% paracetamol dispersion, the initial diameter increase was lower than for pure G50/13 tablets, as displayed by Figure 5.6. Looking at its water uptake profile, there was less water uptake than the pure G50/13 in the beginning, so there was less swelling (Figure 5.4). As erosion was slightly higher than the pure tablets at this stage, this indicates that it did not need to swell as much as the pure G50/13 tablets in order for surface erosion to occur. However, as the diameter increase for the 10% paracetamol was constant and as the erosion profile was also increasing, these suggested that swelling continued in its role as the more dominant mechanism. Whereas the pure G50/13 took up water, swelled and reached its limit very quickly, the paracetamol dispersions had a more uniformed profile, with the uptake and swelling being more

Figure 5.6: Diameter difference profiles of pure G50/13 and paracetamol dispersions in G50/13 at different drug loadings

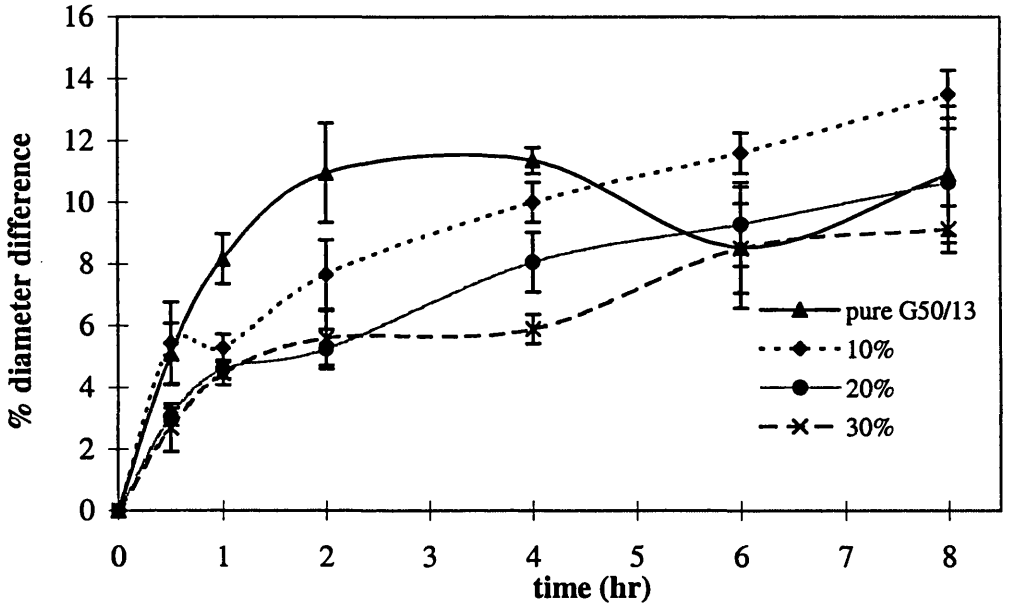

Figure 5.7: Diameter difference profiles of pure G50/13 and caffeine dispersions in G50/13 at different loadings of the drug

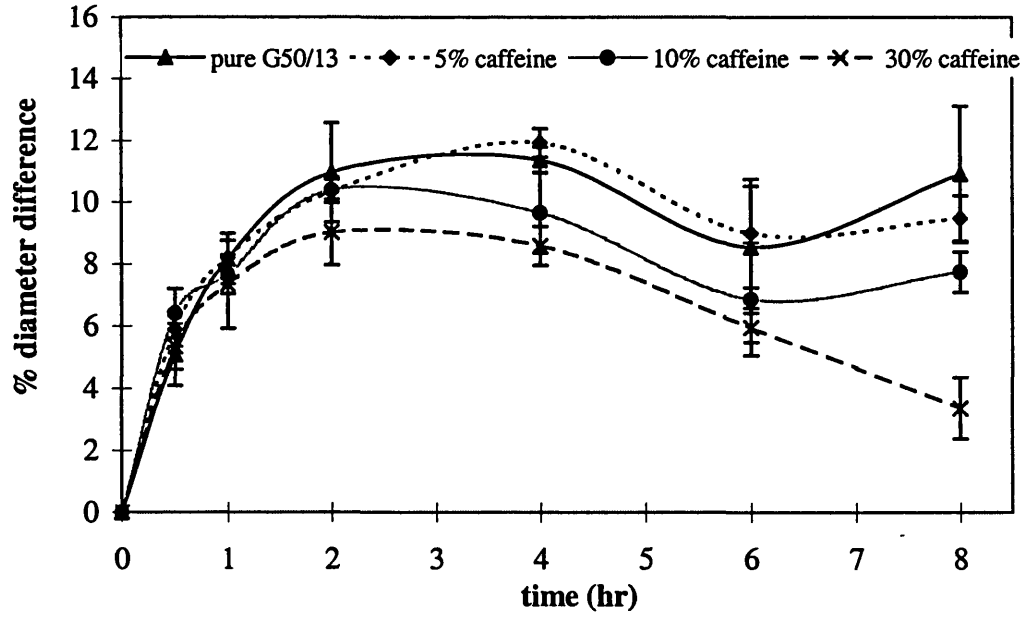

gradual, with also the 10% dispersion having the biggest capacity for swelling. This was similar to the observation made by Dennis et al (1987) that the lowest concentrations of ketoprofen in G50/4.8 led to the greatest water penetration, swelling and surface erosion. Increasing the concentration lessened these processes especially when the solubility of the ketoprofen in the gelucire was exceeded and the dispersion was in particulate form.

As exhibited in Figure 5.7, the caffeine dispersions in G50/13 had similar diameter difference profiles to the pure G50/13 tablets and this is consistent with the observations that the erosion and water uptake profiles were also similar to the pure G50/13 tablets (Figures 5.3 and 5.5). The highest drug loading (30%) tablets after the initial high swelling rate and its subsequent decrease, did not seem to recover its swelling capability, as shown by the low diameter difference value at 8 hours. Since the erosion rate did not increase notably and the rate of water uptake only decreased slightly, this could indicate that the porous structure (as mentioned in section 5.3.1) did not allow much swelling to occur as the water occupied the pores, rather than hydrating the molecular chains. Increasing the loading of caffeine increased the total erosion, in contrast to the findings of Dennis et al (1987), but consistent with the observations made during an investigation into the mechanisms of drug release from gelucire bases by Sutananta et al (1995). The authors found that at higher drug loadings of theophylline in G55/18 (20 or 30% compared to 2%), there was an increase in erosion. In addition, the release of the drug from G50/13, which was thought to be governed predominantly be erosion, also increased as the theophylline loading increased. Dennis (1988) who attributed the release of ketoprofen from G50/13 to erosion further supports this hypothesis. In that study, it was found that between 0 to 60% of the release, the rate was nearly zero-order but this was not applicable further on as the gradual reduction of the dosage form area due to the surface erosion dominated process resulted in the lowering of the release rate. Further evidence was found when decreasing the basket rotation speed gave a slower but more reproducible drug release. This increase in erosion could be due to the weakening of the matrix due to the drug particles disrupting the bonds between the molecules of the gelucire base.

Comparing the diameter difference profiles of paracetamol to caffeine dispersion in G50/13 at the same drug loading of 10%, it is apparent that the paracetamol sample has a greater ability to swell, as presented by Figure 5.10. It could be postulated that incorporation of this drug into the gelucire matrix had caused a modification in the matrix structure so that it allowed greater relaxation of the long PEG ester chains. This seems to be a more likely explanation than the modification causing the matrix to be able to take up more water as the water uptake profiles of the paracetamol and caffeine dispersions were similar. Studies performed using the hot-stage microscopy technique (Chapter 3) showed that the paracetamol was partly soluble in the gelucire matrix when the base was molten and on cooling, the dissolved drug recrystallised within the gelucire, in a form of mixed crystals or at least very finely dispersed crystals. On the other hand, any dissolved caffeine recrystallised out separately and was still present as a solid dispersion. It is likely therefore, that this incorporation of the paracetamol at a molecular level can affect the structure and behaviour of the gelucire base. It could be suggested that after the initial burst of swelling, the water imbibed gradually dissolved this very fine drug, slowly relaxed the gelucire chains which surrounded it and got incorporated within this structure. Therefore, the swelling was more gradual and sustained. Moreover, a thick, opaque gel-layer was seen on the surface of the paracetamol sample whilst a thinner and less gel-like layer surrounded the pure G50/13 and caffeine dispersion samples. Looking at the smoother erosion profile of 10% paracetamol dispersion, it is possible that erosion occurred through the dissolution of this gel-layer rather than the mass disintegration at the surface of the 10% caffeine sample.

5.3.4 The relationship between the erosion studies and dissolution studies

The studies in this chapter were performed in order to study the mechanisms of drug release from G50/13 and to compare them to the results obtained by mathematical modelling. In Chapter 4, it was found that overall, erosion was more prominent for caffeine dispersions than paracetamol dispersions. Additionally, erosion was higher for the low loading of paracetamol but the opposite was true for the caffeine dispersions. Looking at the diameter difference profiles of paracetamol dispersions (Figure 5.6), it could be seen that the 10% loading had swelled much more that the other loadings.

Figure 5.8: Erosion profiles of pure G50/13 compared to 10% paracetamol and caffeine dispersions in G50/13

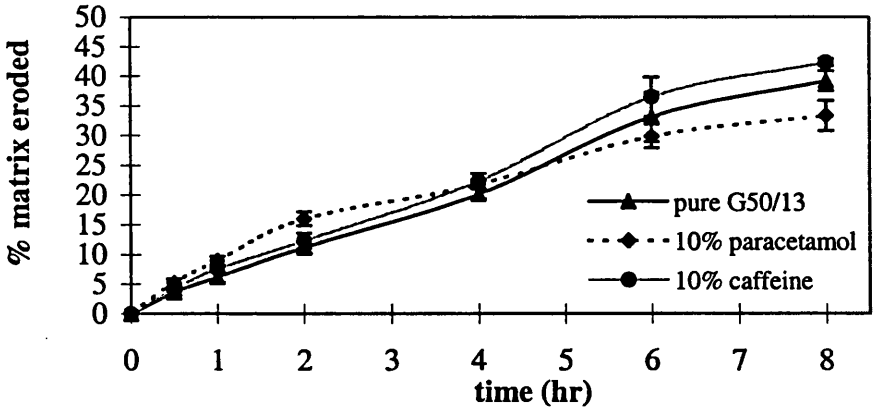

Figure 5.9: Water uptake profiles of pure G50/13 compared to 10% paracetamol and caffeine dispersions in G50/13

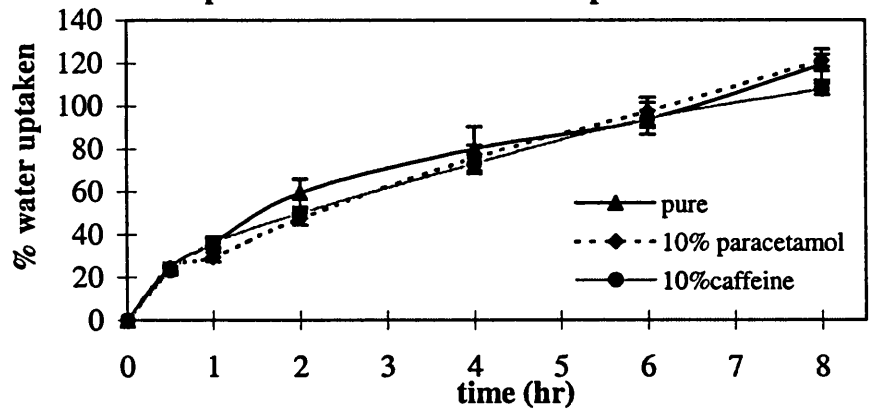

Figure 5.10: Diameter difference of pure G50/13 compared to 10% paracetamol and caffeine dispersions in G50/13

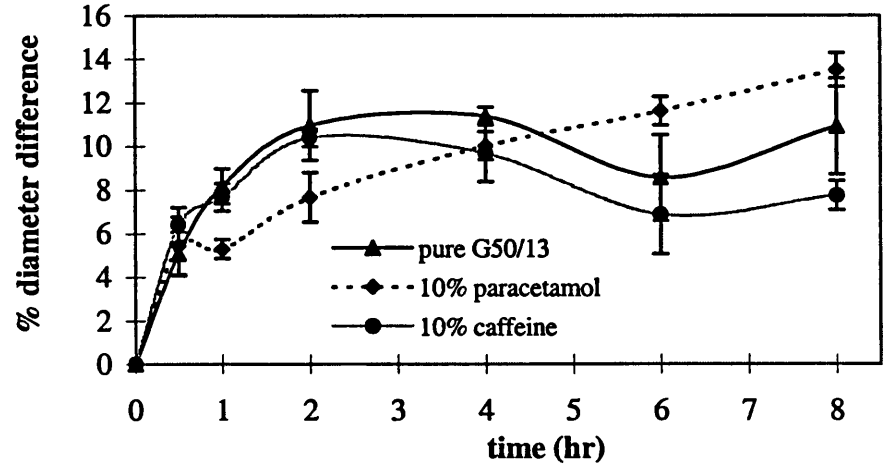

According to Bidah et al (1992), the increased swelling of a matrix, in their case, Sumikagel, moves the kinetics away from diffusion towards erosion. In the same way here, the increased swelling of the low loading paracetamol dispersion raised its erosion factor. To a small extent, the erosion profiles of the paracetamol loadings (Figure 5.2) confirmed this with a slightly higher profile for the low loading.

The processes of swelling, erosion and drug release are intrinsically related to each other for G50/13 matrices. Swelling of the matrix leads to its erosion after a certain threshold and this will increase the drug release. When these two processes become synchronised, the rate of drug release can become almost constant (Colombo et al, 1995), as shown by Figures 4.3 and 4.4 in the previous chapter. Prevention of such processes from occurring has an effect on drug release as demonstrated by (Prapaitakul et al, 1991). The release rate of chlorpheniramine maleate was not significantly different regardless of it being dispersed in a G50/13 matrix or a G33/01 matrix even though the volume expansion of G50/13 on addition of water was twice that for G33/01, when the succeeding processes of erosion and disintegration were suppressed. As mentioned in Chapter 4, the drug release seemed to be indifferent to the effect of drug loading. It is possible that the increasing porosity of the matrices which would have been the result of higher drug loadings was compensated by retardation of chain relaxation by undissolved drug. The presence of drug at high concentrations near the swelling front prevents the macromolecular relaxations that mostly occur in this region (Colombo et al, 1995).

Such correlation of the erosion/water uptake/diameter difference studies to dissolution studies is useful in determining the kinetics of drug release, not just for the overall profile but also at particular periods of release. While mathematical fitting of the drug release indicated a high level of erosion for the caffeine dispersion (Chapter 4), the erosion profiles of the lower drug loadings show that at the beginning of the release process, the erosion was lower than for the paracetamol dispersions (Figures 5.3 and 5.2). Since the drug release for the caffeine dispersion was consistently higher than the paracetamol dispersion, it could be suggested that the diffusion mechanism contributed heavily to the caffeine release at low loadings at the start of the release process. Hydrophilic matrices with water soluble drugs such as diltiazem:gelatin granules in

pectin:HPMC had been shown to change release kinetics as dissolution progressed (Kim and Fassihi, 1997). Comparing the release of diltiazem to the erosion pattern of the matrices, it was found that the high release initially was predominantly diffusion controlled but as time progressed, it was subsequently dominated by erosion. In Chapter 4, the paracetamol dispersions had a better fit to the square root kinetics than the caffeine dispersions. In this chapter, it could be seen from the diameter difference and erosion profiles (Figures 5.9 and 5.10) that by the end of the study, the paracetamol samples had swelled more but eroded less than the caffeine samples. These profiles gave more support to the notion of a more diffusional release for paracetamol. Furthermore, the failure of matrices to conform to the zero-order release profile with the subsequent inclination towards square root kinetics is the result of the recession of the matrix boundary at which dissolution happens, from the surface releasing the drug (Fassihi, 1987). The increasing pathlength which the dissolved drug has to travel or in other words, the increasing tortuosity, leads to a decreasing release rate.

An investigation to study the kinetics of drug release of sodium salicylate from spherical oral devices made from G46/07 found that the rate of erosion and thus, the rate of drug release were proportional to the area of the device (Bidah et al, 1990). However, it did not take into account the swelling factor as the actual fitting of the data was performed against the weight of the device to the power two-thirds and by mathematical manipulation this was related to the area. The present study clearly shows that rate of drug release (Chapter 4) did not follow the same profile as the diameter difference which can be related to the area (Figures 5.6 and 5.7). Therefore such a simple relationship between the release and area could not be applied here.

5.4 Conclusions

The erosion profile of pure G50/13 was not constant throughout the duration of the study. Erosion was preceded by water uptake and the subsequent swelling due to this water ingress. The swelling process occurred quite vigorously for the pure carrier so that its limit was achieved at a relatively short time which then led to the shedding of the water saturated layer. Incorporation of different drugs gave dissimilar erosion profiles with the paracetamol dispersions giving a smoother, more constant process

whilst the caffeine dispersions gave a similar fluctuating profile as the pure G50/13. The overall erosion for the paracetamol dispersions was also less compared to the pure G50/13 but the caffeine dispersions gave a contradictory result.

The type of drug incorporated also affected the swelling ability of the matrices. Paracetamol dispersion samples were able to swell to a greater extent than the other samples without great erosional process occurring at the same time. This was thought to be due to the modification of the gelucire structure by the partial solubilisation of paracetamol within it (Chapter 3). Caffeine dispersions gave a more porous matrix and hence, eroded to a greater extent as swelling occurred. The lower Solid Fat Content at 37°C of the paracetamol dispersion samples (Chapter 2) may contribute to the lower erosion and higher diffusion factors of the release. A softer matrix may not be able to erode as effectively as a more solid one as more water is able to be accommodated within the soft structure so that greater swelling occurred.

The erosion and swelling profiles gave good correlation to the kinetics of release obtained from fitting dissolution data to mathematical models (Chapter 4). The caffeine dispersion samples gave a higher erosional process according to the models and this was confirmed by its erosion profiles. Likewise, the small decrease in erosion as the paracetamol loading was increased and the elevation of the same process for the higher caffeine loadings were also reflected by the mathematical fittings especially by Equation 10 (see Chapter 4). Therefore, it could be concluded that fitting dissolution data to this equation would give an indication of the mechanisms responsible for the release of drugs from G50/13 matrices.

CHAPTER 6: INVESTIGATIONS INTO THE EFFECTS OF AGEING G50/13 MATRICES USING DSC

The behaviour of formulations after storage at certain conditions may be dissimilar to that when they are newly manufactured. This change may be related to structural modifications within the matrices and it would be useful if such modifications can be detected so that the performance of the aged formulations can be anticipated to a certain extent. It would additionally be beneficial if the effects of other determinants such as temperature of storage and incorporation of drugs could be elucidated.

6.1 Introduction

Characterisation of ageing effects of solid dispersions is another analysis that can be effectively performed by DSC and many investigators have exploited this fact. Chiou and Niazi (1971) scanned the eutectic composition of sulphathiazole-urea immediately after the preparation of the dispersion and after the storage under ambient conditions. An exotherm indicating crystallisation was detected in the freshly prepared but not the stored dispersion. However, the melting endotherm was present in both fresh and stored samples. When one hour old and aged chlorpropamide-urea dispersions were scanned using DSC, it was found that the aged samples which were stored at either 60°C for 96 hours or at ambient temperature for four weeks did not show any endotherms which corresponded to the solidus line of a phase-diagram (Ford and Rubinstein, 1977a). Additionally, the peaks which corresponded to the liquidus line were 2-3°C higher for the aged samples. This was thought to be due to an increase in the crystal size as the ageing process continued and the presence of trapped air in the sample due to the contraction of the melt upon cooling (Ford and Rubinstein, 1977b).

The incorporation of drugs into the carriers may or may not have a bearing on the ageing behaviour and again the changes can be detected by DSC. Storing triglyceride suppositories over a 260 day period resulted in the increase in the melting temperature, with the most rapid rise occurring over the first 55 days. Addition of indomethacin to the suppositories did not seem to greatly affect this increase (De Muynck and Remon, 1992). Bodmeier et al (1990) investigated the characteristics of propanolol and theophylline dispersions in a carrier mixture containing Gelucire 50/13 and the solubilities of the drugs in the fatty base were determined. This was important due to the fact that if the amount of drug dissolved

in the matrix during manufacture exceeded its solubility, the drug might crystallise out during storage and affect its stability. The length of time and the temperature during melt-fusion and the subsequent holding time will be more crucial for the soluble or partially soluble drug.

In formulations where the excipients involved are not only the main carriers but also other ingredients added to optimise the release, it is important to check their interactions as storage of active drugs mixed with these excipients can sometimes lead to the drug being adversely affected. The interactions found initially within the newly manufactured formulations may not coincide with those found after a certain period of storage. Even though initial DSC scans of freshly prepared mixtures showed that a drug, at 10% loading, was incompatible only with mannitol and magnesium stearate, further scans after storage of 1 month at 50°C and 75% relative humidity revealed that the drug no longer degraded with those excipients, but with stearic acid, calcium sulphate dihydrate and avicel (Giron, 1986).

6.1.1 Mechanisms of change upon ageing

Holding fats at a certain temperature and time had been shown to increase the proportion of crystalline structure in them. Yap et al (1989b) characterised palm oil and hydrogenated palm oil and listed amongst others the following findings:

Sample	Dropping point (°C)	Solids at 20°C (%)	Total ΔH of crystallisation (J/g)	$\frac{\Delta H \text{ isothermal}}{\Delta H \text{ total}}$ (%)*
palm oil	38.5	16	20.2	59
hydrogenated palm oil	54.9	85	108.2	0

* determined from an isothermal holding at 20°C for 30 minutes.

It is clear from the results that holding the palm oil under those conditions had increased its crystalline structure. Chemical processes such as hydrogenation can increase the solidity of the fat and that isothermal holding at that temperature and length of time would not

further increase its crystallinity. G50/13 is made from hydrogenated palm oil although 80% of it is esterified with PEG. It would be of interest to note in this study whether holding the gelucire at this temperature would increase its crystallinity.

Besides the increasing crystallinity of the fatty base upon storage, changes to the matrix characteristics are also due to polymorphic transformations during the ageing process. It had been previously shown that the storage of triglyceride suppositories resulted in an increase in the melting range, heat of fusion (Liversidge et al, 1981) and X-ray diffraction intensity of the stable form (Yoshino et al, 1981). This was brought about by the conversion of the less stable triglyceride polymorphs of the components such as α and β' to the more stable form, β. Storage temperatures were also crucial with higher temperatures being able to cause the conversion to occur more quickly due to the implications on the kinetics. In addition, the rate of this conversion decreased with increasing chain lengths, thought to be associated with the steric hindrance of the long hydrocarbon chains. A change to a higher melting polymorphic form when stored at an elevated temperature was also exhibited by indomethacin suppositories made from a fatty base, Witepsol (Yoshida et al, 1991). The suppositories had an increase in their melting point, 37.3°C as opposed to 34.9°C, when stored at 25-30°C instead of 4°C. The authors had previously shown through X-ray diffraction analysis that the unstable crystal form in the base had changed to a more stable form after storage at a high temperature.

Mechanisms of ageing were found to be influenced by factors such as preparation conditions and gelucire compositions. For example, storing a gelucire composed of only triglycerides, G43/01 being one of them, prepared by flash cooling it in liquid nitrogen resulted in a stable, equilibrium form being obtained after only 14 days whilst the slow cooled variant of the same sample acquired the stable form after 280 days (Sutananta et al, 1994b). Even when the gelucires were still made up of only glycerides but have a slightly more varied composition such as G54/02 which in addition to the triglycerides, also contains mono-and diglycerides, the ageing effects can already be different. An equilibrium structure could not be reached even after 280 days for either the fast or the slow cooled samples of G54/02 and this was thought to be due to the segregation of the low and the high melting components into different microscopic areas within the base. To reiterate this point,

G55/18 which is composed of only PEG esters of fatty acids was not greatly affected by the preparation conditions nor the storage time.

Segregation of components can be presented in many forms. In palm stearine, the triglycerides can be divided into the low melting (such as PLP and POO) and the high melting fractions (such as POS and PES) (Busfield and Proschogo, 1990). DSC scans showed endothermic peaks corresponding to such fractions. After the process of hydrogenation, much of the lower melting fraction was transformed to the higher melting fraction as shown by the proportional increase in the higher temperature range melting. Additionally, melting before the hydrogenation occurred in two stages but after the process occurred at only one stage. This was thought to be due to the facilitation of the formation of mixed crystals between transformed triglycerides and existing high melting triglycerides. Formation of these mixed crystals may have a bearing on the ageing effects. Closely mixed glycerides or solid solutions of glyceride polymorphs could separate out as distinct regions after a period of storage at a particular temperature (Timms, 1980).

Precipitation of the fatty base after storage is another variation of component segregation. Thermal analysis had been used to reveal that the total melting point of fatty suppositories increased after storage and this phenomenon was caused by the components which melted at different temperatures separating from the suppository base, enhanced by storing the samples above room temperature. This was probably due to the higher kinetic energy acquired by the molecules as was also demonstrated by the disordered layered structure of triglyceride suppositories transforming into the ordered crystalline structure when held at a higher temperature (Laine et al, 1988). Movements of the molecules into their positions in a crystal lattice or any other orientation are facilitated by this kinetic energy.

6.1.2 Solid Fat Content (SFC) in the ageing process

Investigations into the effect that storage has on SFC had mostly centred on triglyceride suppositories as the formulation. This is because a change in the solidity of the dosage form would be more critical in suppositories as the release of drug in the body depends on the melting of the fat in the body. An increase in the solidity of the suppositories may lower the

bioavailability of the drug dispersed in them (Eckert et al, 1982a,b). The Solid Fat Index (SFI) which is the SFC beyond 37°C in this case, increased for the triglyceride suppositories during storage at 30°C for up to 4 weeks (Saito et al, 1994). The magnitude of this effect relied on the composition of the matrix with the base which contained some hexaglycerol pentastearate showing a smaller increase than the base with only triglycerides in it. The process thought to be responsible for this consequence was the polymorphic transformation of the glycerides to a more stable form and this transformation was completed within 2 weeks of storage, indicated by the lack of change in the SFI beyond this time. DSC thermal profiles of the matrices confirmed the polymorphic transformation, demonstrated by the splitting of the main endothermic peak into two peaks after storage. This hardening effect, reflected in the rise of melting times, could be accelerated by storing the fatty suppositories at temperatures which are very close to the bases melting ranges (Thoma and Serno, 1982).

In another study, an increase in the SFI in the range of body temperatures was also found upon the ageing of suppositories (Coben and Lordi, 1980). Instead of polymorphic transformations, the modifications were associated with amorphous to crystalline transitions and this process was found to be dependent on the storage temperature. Nevertheless, polymorphic modification is still the factor frequently stated as the main reason for the changes. The low melting fraction (LMF), the middle melting fraction (MMF) and the high melting fraction (HMF) of milk fat had the melting ranges of >15°C, 35-40°C and >50°C respectively (Timms, 1980). The different polymorphs within each melting fraction of LMF, MMF and HMF were found to have undergone conversion during storage resulting in higher heats of fusion being obtained. Some of the evolved polymorphs were very stable and did not alter further. The calculation of the SFC would be useful in this current study in order to see whether ageing would alter the proportions of the different melting fractions which would have a bearing on the solidity of the matrices.

6.2 Materials and Methods

The manufacture of the moulded tablets used as the source of samples in this study has been previously described in Chapter 4. After equilibrating the freshly prepared tablets over

silica gel for 24 hours, the tablets were stored in sealed silica gel desiccators either in a temperature controlled room held at 20°C or in an incubator oven held at 37°C. Holding the glyceridic formulations at an elevated temperature to accelerate the ageing had been performed in other studies (Moës and Jaminet, 1976; Coben and Lordi, 1980). At the time intervals of 7, 30, 90 and 180 days after the beginning of storage, some of the tablets were taken out to be analysed. The tablets were first equilibrated over silica gel for 24 hours to achieve ambient temperature and then comminuted down as described in Section 2 of Chapter 2. The samples were then placed in the DSC pans, sealed and scanned at 2°C/min. The scans for each pure G50/13 or its 10% drug dispersions were performed five times, with all the repeats completed within 20 hours so that the time interval and the conditions affecting the sample of the first scan were not significantly different to those affecting the sample of the last scan.

6.3 Results and Discussions

6.3.1 Pure G50/13

Overall, there was little change in the temperatures of Peaks 1 to 4 after ageing the pure G50/13 at 20°C (Figure 6.1, in addition, all the tabulated data for this chapter can be found in Appendix 6). There was a slight increase in the temperatures of Peak 1 and Peak 3 after 180 days ageing which could indicate a movement towards a more stable form. It is still possible, even when the highest melting polymorph is achieved, for the final melting point of this stable form to be increased upon storage (Liversidge et al,1981). The elevation in the total heat of fusion after 180 days ageing showed an increase in the crystallinity of the matrix and/or an increase in the proportion of the more stable polymorphic forms of the glycerides and fatty acids.

Peaks 1, 3 and 4 showed a significant increase in their heats of fusion values after ageing. This probably indicates that the crystallinity of the gelucire forms that gave rise to those peaks was increasing. It could be surmised that the amount of each polymorphic form within those peaks was also growing. This is because the elevation in the heat of fusion values of Peaks 1, 3 and 4 seemed to have occurred at the expense of Peak 2. Storage at

Figure 6.1: Thermal profiles of pure G50/13 after ageing at 20°C

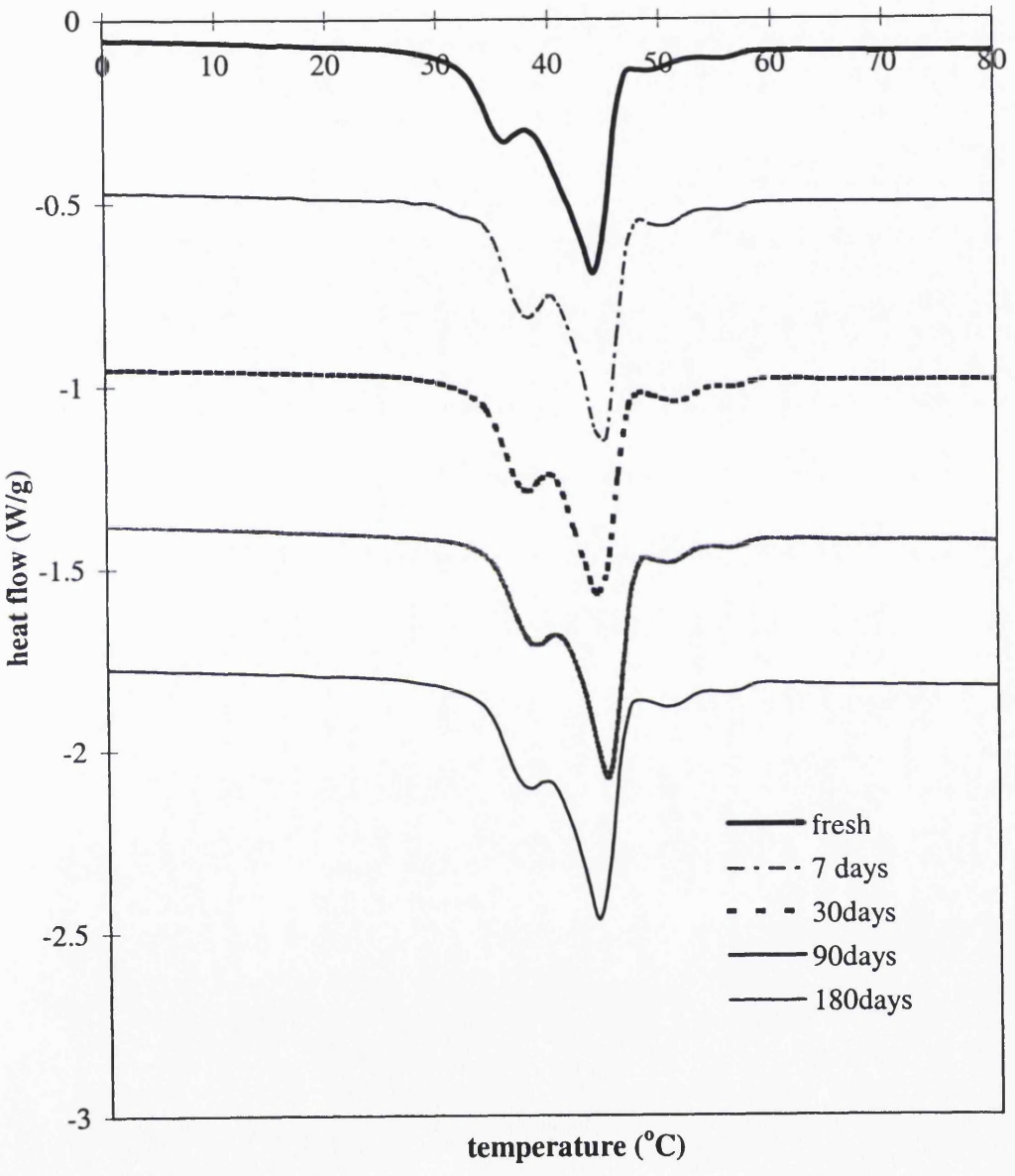

N.B. Endothermic heat flow for all the Figures is in the downwards direction.

The thermal profiles are vertically offset for clarity.

20°C could have stabilised the polymorphic forms of Peak 1 but accelerated the transformation of certain Peaks 3 and 4 polymorphic forms from Peak 2 forms. The contradictory effects of storage on the polymorphic forms of various peaks could possibly be due to the difference in the gelucire components that constitute each peak. Certain polymorphic forms which are not the most stable form of a particular glyceride can be very unchanging under certain conditions, such as that shown by the β'-2 in the HMF of milk fat which remained unaltered after storage at 40°C for 31 days even though the other polymorphic forms of the rest of the fractions were transformed (Timms, 1980). Polymorphic forms which make up Peak 1 were regarded as metastable as they had the lowest melting range but at 20°C, could be very stable and were not tending towards Peak 2. Another explanation for this effect of the reduction in Peak 2 heat of fusion value is that some of the components making up the gelucire form that gave rise to that peak had segregated out and are now contributing to the composition of the other peaks, possibly by forming solid solutions with them. The increase in the crystallinity of the gelucire forms that gave rise to Peaks 1, 3 and 4 could be an exclusive process that was not related to polymorphic changes, as had previously been shown for substances containing mixtures of glycerides (Yoshino et al, 1984). Therefore the increase in the heats of fusion was a total effect of polymorphic transformation and elevation in crystallinity.

Storing the pure G50/13 samples at 37°C showed a drastic change in its thermal profile whereby Peak 1 corresponding to the freshly prepared sample had now fused with the next peak so that a peak temperature could only be observed as that for Peak 2 (Figure 6.2). Binary mixtures of triglycerides including tripalmitin and tristearin also demonstrated a reduction in the number of transitions on the thermal profiles upon ageing with an eventual melting point emerging (Liversidge et al, 1981). The elevation of temperatures for the other peaks after 30 days at 37°C suggests that the gelucire forms were becoming increasingly stable. The fusion of lower melting form to Peak 2 could mean that the polymorphic forms of Peak 1 had transformed to the higher melting, more stable forms of Peak 2. This transformation could be of the melt type because the temperature of storage coincides with the melting point of Peak 1. Holding the sample at or near the melting temperature of a less stable polymorph will transform it to a more stable form and this is a concept capitalised by the tempering process.

Figure 6.2: Thermal profiles of pure G50/13 after ageing at 37°C

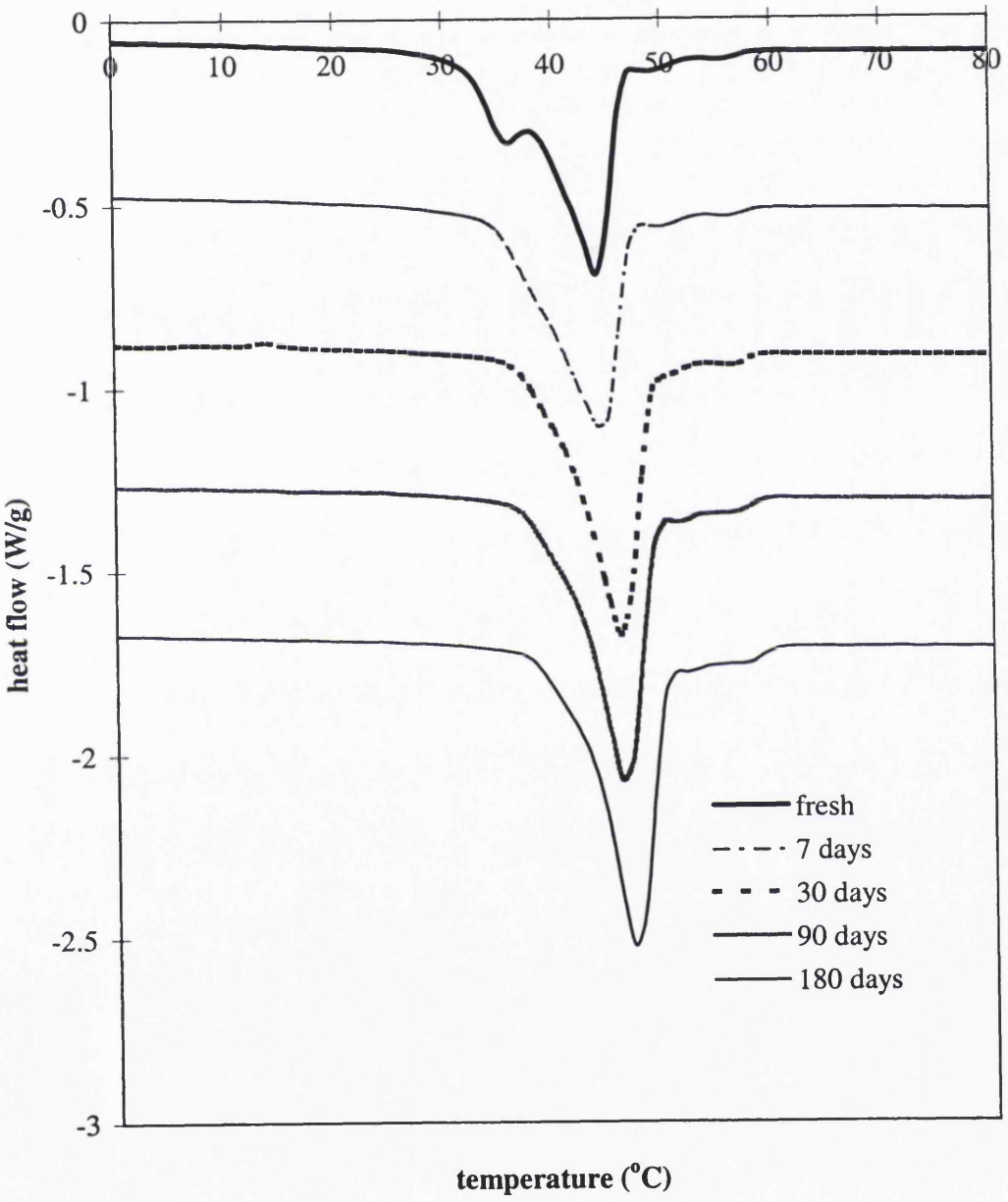

Tempering had been reported to greatly affect the rate of phase change, crystal size and especially the rate of polymorphic transformation (Timms, 1984). The heat of fusion value for the merged form became increasingly higher over time compared to the combined heat of fusion values of Peaks 1 and 2 of the freshly prepared samples. Also, the percentage increases in the total heat of fusion values for samples aged at 37°C were higher than those aged at 20°C. In addition to the increase in crystallinity, the higher values for 37°C stored samples were likely due to the bigger amount of the more stable polymorphic forms as these forms have the higher heat of fusion values. A conversion to glycerides stable forms was obtained after storage at more elevated temperatures (Yoshino et al, 1984).

The storage of fatty suppositories also demonstrated similar small shifts in the position of the peak temperatures upon ageing of up to 6 months at room temperature, regardless of the initial peak positions (Coben and Lordi, 1980). In addition, there was sharpening of the peak and an increase in peak height throughout the duration of the storage. Storing the samples at temperatures just below their melting ranges were also found to have accelerated the reaching of their equilibrium crystalline state.

Liversidge et al (1981) attributed the increase in the melting points of triglyceride suppositories upon ageing to the polymorphic transformation of metastable forms to stable forms. The most significant change to the melting profile when stored at room temperature occurred within the first day, followed by slower increases on the successive days until a final maximum value was achieved. Elevating the temperature of storage minimized the time taken to achieve this final value due to the energy supplied to the molecules aiding their orientation into the stable polymorphic forms. When this storage temperature exceeded the melting point of the base, it was not able to stabilize itself in its most stable form in the time allocated until analysis so that the base would have a very low melting point when resolidified. It was important therefore, for the current study to put aside enough time (24 hours) from the time the samples were taken out from their storage environs to the time of their analysis, in order to allow the samples to equilibrate at room temperature.

The thermal profiles of the pure G50/13 after being aged at 37°C were similar to the thermal profile of non-heat treated sample of G50/13, that is the sample in the condition

received from the manufacturer without first subjecting it to the heating and cooling protocol (Figure 6.3). Figure 6.3 was obtained from a comminuted whole batch of G50/13 and is different from Figure 2.3 which was obtained from different positions within a batch. The peak temperatures of the untreated G50/13 were close to those of the aged samples and a total heat of fusion value similar to the untreated sample was achieved by the samples stored at 37°C by 30 days of ageing. This gave an indication that pure G50/13 aged at 37°C was relatively stable.

Figure 6.3: Thermal profile of untreated G50/13

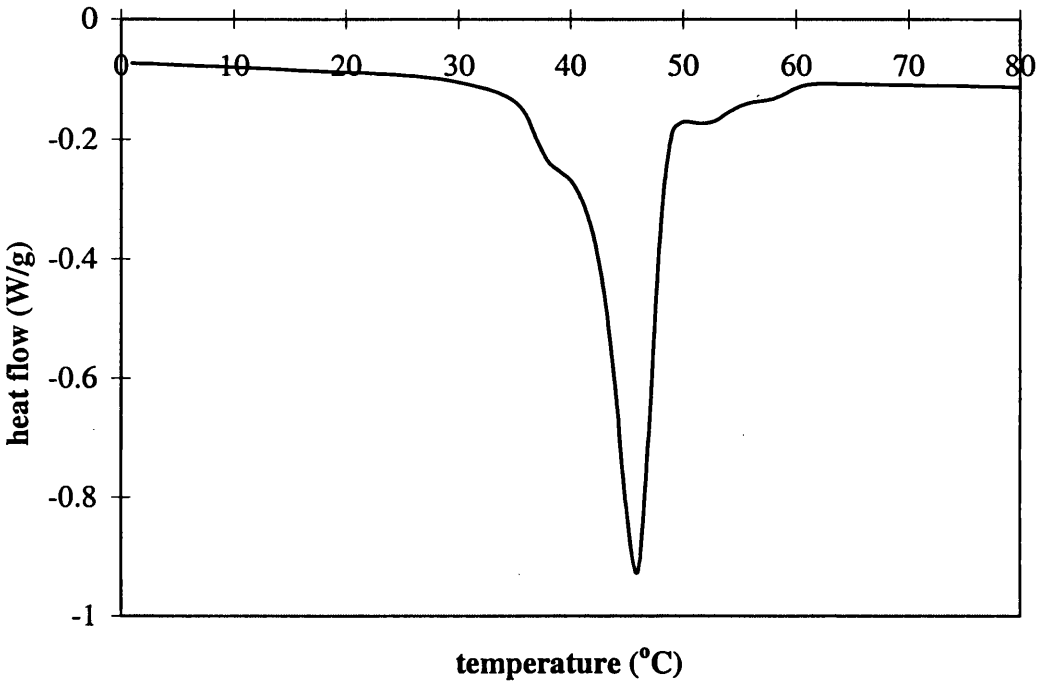

The transition to more stable forms of fat matrices was shown to be accelerated at higher temperatures of storage (Yoshino et al, 1981). Furthermore, ageing at 37°C offered an advantage over untreated G50/13 in that the unstable form that gave rise to Peak 1 was no longer present in the former samples. This could ensure that no great changes in polymorphic forms or stable/unstable forms would occur further after storage at long periods of time. Even though Peak 1 was not as distinctive in untreated G50/13 samples as heat treated ones, a clear shoulder on the lower temperature side of the main peak suggested that there still existed less stable forms which could be susceptible to modifications in the untreated samples. Therefore, even though storage at 37°C can be referred to as an accelerated ageing condition, the outcome after 180 days was not totally coincidental with the untreated sample but this minor difference may be beneficial to the matrices.

Work performed by Sutananta et al (1994b) postulated that the numerous endothermic peaks on a G50/13 thermal profile were due to the segregated gelucire components. The number of peaks evolved was also dependent on the cooling rate used when setting the base with fast cooling (in liquid nitrogen) producing more peaks than slow cooling (10°C/hour). On storing the samples at room temperature, the thermal profiles changed even after only two weeks with new peaks emerging and the existing peaks becoming more distinct. After 280 days, the thermal profiles for both of the samples were still non-equivalent considered to be caused by the components being far too segregated to be recombined into an equilibrium structure. However, this current study showed that tempering the G50/13 at a temperature just at the first peak resulted in the structure that resembled more closely to the equilibrium structure (represented by the untreated G50/13) to be achieved more quickly. Changes as a result of tempering usually suggest that polymorphic transformation is involved. Moreover, bases which contain mixed glycerides and other constituents tended to be crystallised in a metastable form.

There was probably less of the α form of the triglycerides crystals than the β' form in this metastable crystal mixture as the gelucire is composed of previously hydrogenated oils. Hydrogenation increased the ordering of molecules and so, facilitated the crystallisation of the β' form over the less ordered α as demonstrated by the DSC scans when the lower melting peak of palm stearine was gradually replaced to an extent by a slightly higher melting peak as the hydrogenation times increased (Busfield and Proschogo,1990). On tempering at 37°C, sufficient energy was probably supplied in order for the transformation to the more stable β forms of the glycerides to occur. In a study with G43/01 which contained only triglycerides, the investigators concluded that in order for a stable form to be obtained, a tempering temperature that was approximately 9°C below the desired peak needed to be used (Sutananta et al, 1994b). However, on closer examination, this suggested temperature also happened to be in the vicinity of the first endothermic peak, with the desired stable peak being the second endotherm. Therefore, for the most stable form to develop upon ageing, it would be necessary to hold the gelucires for a certain time period at a temperature which is close to the first endothermic peak of the thermal profile, not just below the largest and presumed most stable peak. Achieving a desired form by tempering is not restricted to the carrier only but also to the drugs. Holding gepirone hydrochloride at

a temperature just below the first endotherm of its thermal profile transformed it to a higher melting, more stable form and holding at this temperature for a longer period finally transformed even this form to the most stable form (Behme et al, 1985).

6.3.2 10% paracetamol dispersion in G50/13

No major changes could be seen in terms of the peak temperatures for most of the duration of the ageing. Only after 180 days storage at 20°C it could be distinguished that Peaks 1 and 2 had slight elevations of temperatures and heat of fusion values whilst Peak 3 had small declines, giving rise to the observation that the peaks were moving towards the centre of the thermal profile after a long period of ageing (Figure 6.4). The slight decline for Peak 3 could signal the exclusion of certain high melting components from the gelucire forms that gave rise to this peak after 180 days. The total heat of fusion after various periods of ageing fluctuated but this value after 180 days was significantly higher (tested with Student's two-sample t-test at 0.05 significance level) than the freshly prepared sample, which like the pure G50/13, suggests an increase in the crystallinity of the sample.

Storing at 37°C changed the thermal profile significantly and also caused certain peaks to split further (Figure 6.5). After 7 days ageing, a higher melting form emerged to give a subpeak to Peak 1. It could be postulated that storage at this temperature had caused the transformation of many components within Peak 1 to their higher melting polymorphs and this change was big enough to not only push the temperature of Peak 1 to be higher but also to produce another form of this dispersion. The Peak 4 form could have developed a mixed crystals aggregate with the Peak 3 form since it had now been reduced to a shoulder of Peak 3. After 30 days ageing, the subpeak to Peak 1 seemed to have merged with Peak 2 and in addition, there now emerged a higher melting subpeak to Peak 2 which was then reduced to a shoulder after 180 days. Peak 1 became progressively less prominent until it fused with Peak 2 after 180 days.

The classification of subpeaks is only arbitrary as subpeak 1 and Peak 2 of 7 days aged sample could be Peak 2 and subpeak 2 of 30 days aged samples respectively. They were labelled according to the main peak which the subpeak temperatures were closest to. The

Figure 6.4: Thermal profiles of 10% paracetamol dispersions in G50/13 after ageing at 20°C

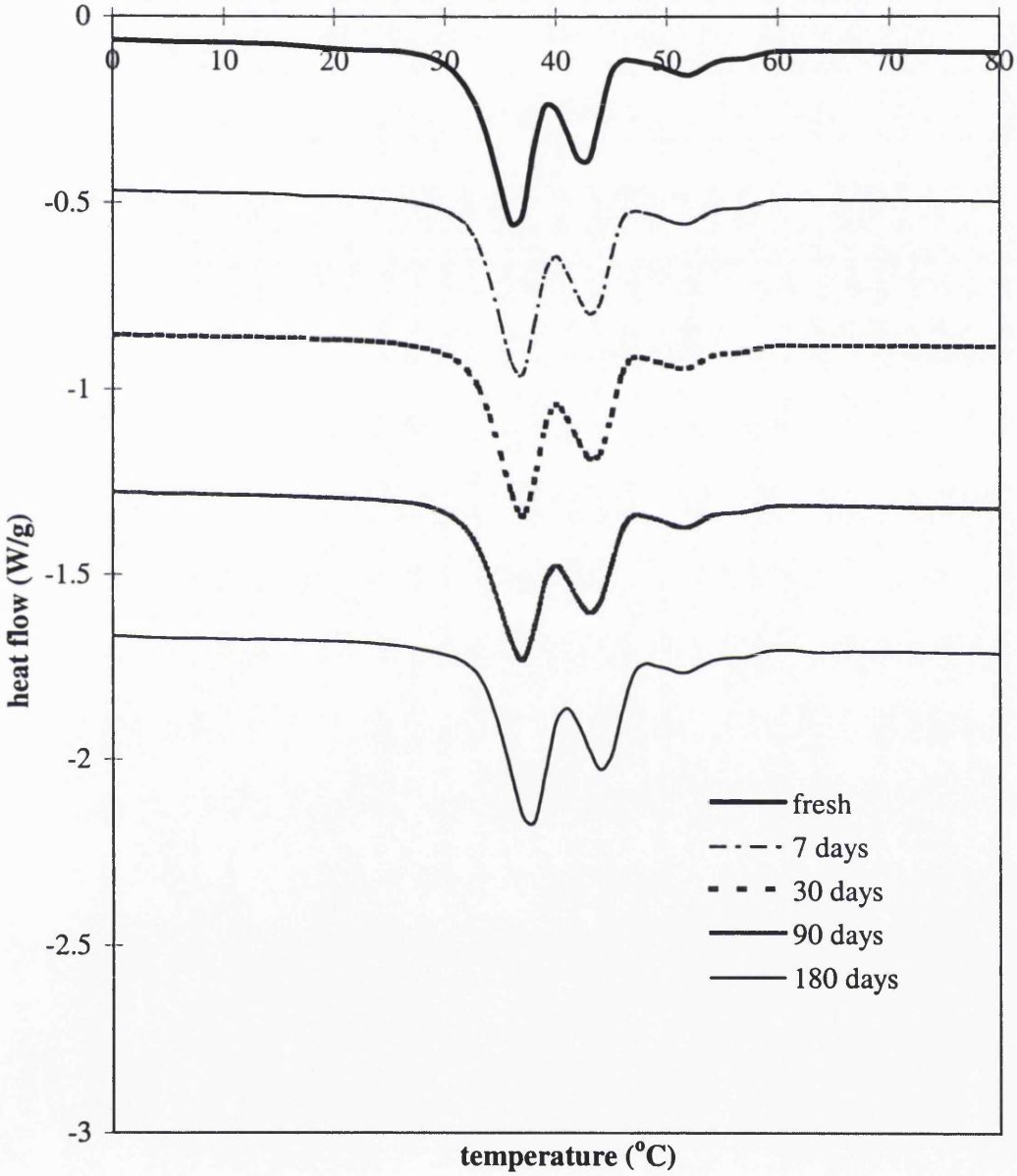

Figure 6.5: Thermal profile of 10% paracetamol dispersions in G50/13 after ageing at 37°C

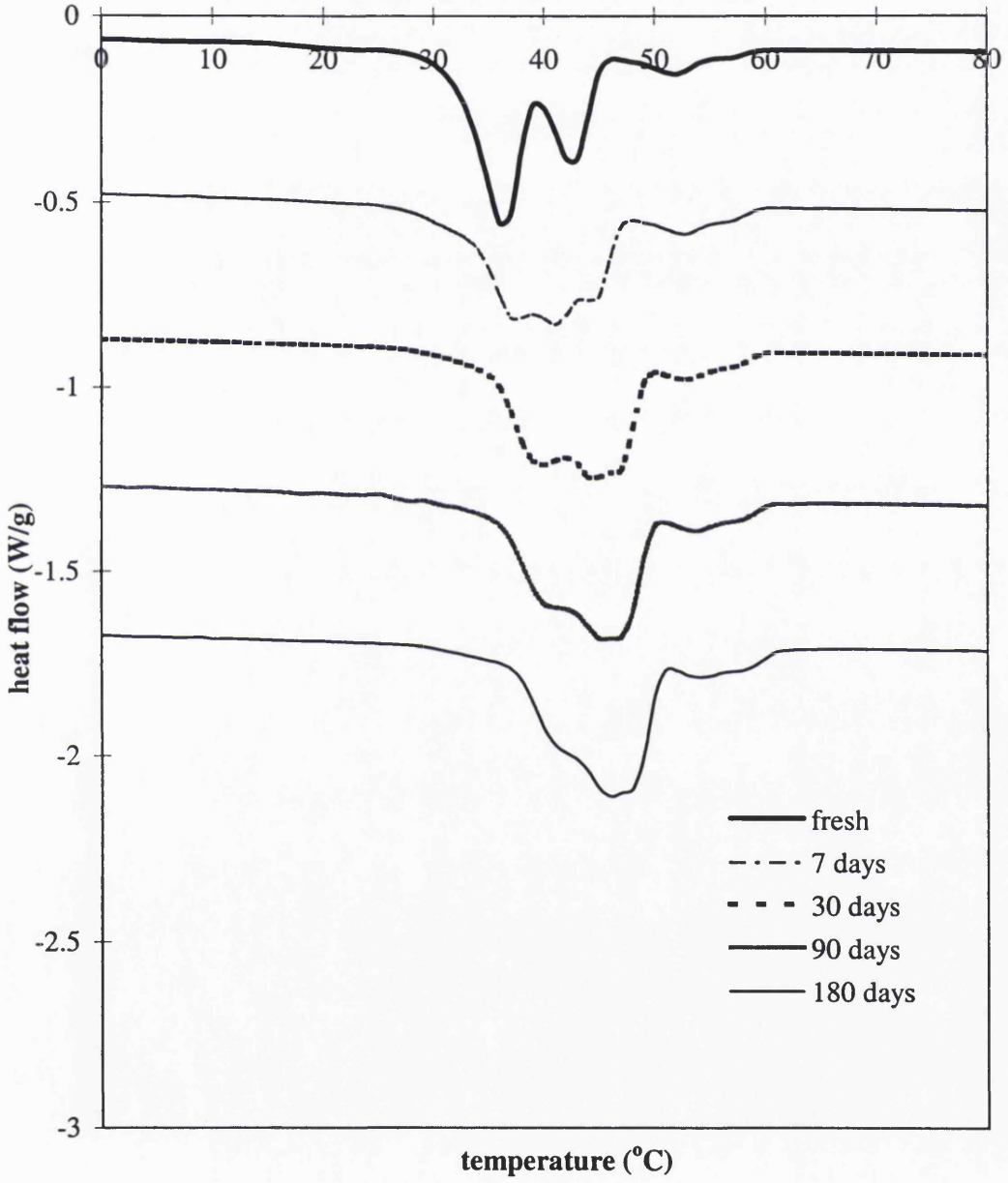

formation of subpeaks was due to the storage temperature being 37°C because this occurrence was not observed for samples stored at 20°C. The increase in the total heat of fusion values to be higher than 20°C stored samples reflected the gain in crystallinity and the transformation to more stable forms. This transformation to higher stability forms was further evidenced by the movement of the subpeak towards the higher temperature ranges. The thermal profile of milk fat showed that the melting peak of the high melting fraction was very wide and thought to be partly due to this fraction crystallising out together with some lower melting glycerides in a semi-stable mixture (Timms, 1980). When the fat was tempered, the solid solutions were able to isolate out into their equilibrium compositions and proportions at this temperature. In G50/13, the metastable forms seen on the addition of paracetamol were eventually transformed closer to an equilibrium composition after storage at 37°C.

This modification to the higher melting, more stable forms occurred more gradually for the 10% paracetamol dispersion samples than for the pure G50/13. Peak 1 fused with Peak 2 after only 7 days ageing at 37°C for the pure G50/13 sample but Peak 1 of the paracetamol dispersion sample decreased in amount slowly while at the same time giving rise to new, higher melting subpeaks. It could be stated that the presence of paracetamol caused a resistance to the transformation to more stable forms, even after a tempering process. It had been reported that during transformation, the glycerol group structure of glycerides remain unaltered but the lateral arrangements of the hydrocarbon chains in the dimeric units become dissimilar (Timms, 1984). Thus, it could be possible that the paracetamol molecules were disrupting these lateral arrangements of the hydrocarbon chains.

6.3.3 10% caffeine dispersion in G50/13

A small increase in the peak temperatures and the total heat of fusion values after being aged at 20°C indicated the gradual transformation to more stable forms as with previous samples (Figure 6.6). The rate at which the fusion value for Peak 1 was depreciating with the concurrent increase in the value of Peak 2 was higher than for the pure G50/13 samples. By 180 days ageing, Peak 1 of the caffeine dispersion samples had already been reduced to a shoulder on the main Peak 2, giving a profile which is similar to the untreated G50/13.

Figure 6.6: Thermal profiles of 10% caffeine dispersions in G50/13 after ageing at 20°C

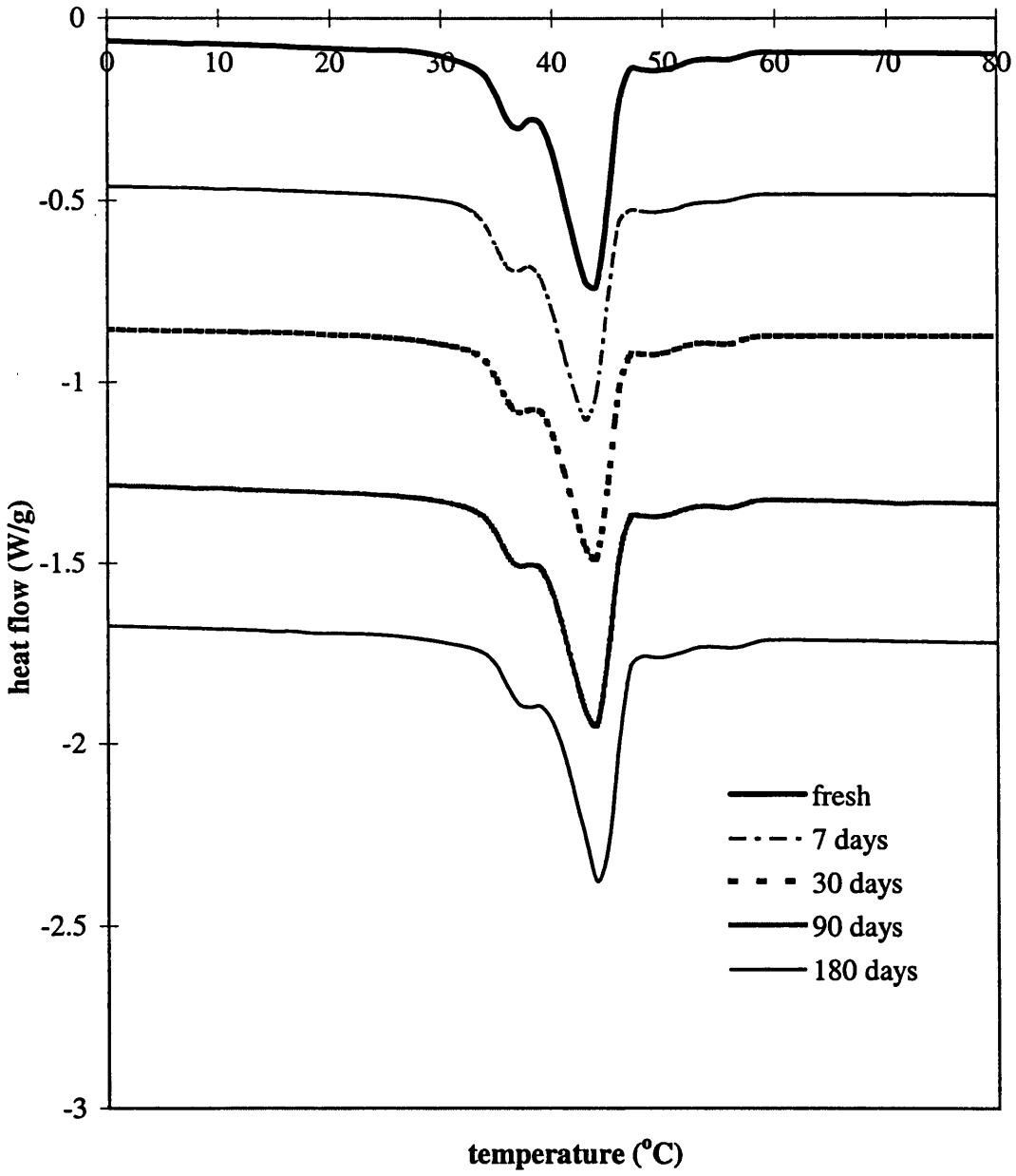

Storage at 37°C also caused an increase in the peak temperatures but to a bigger extent than storage at 20°C. An elevation in the melting ranges of drug incorporated fatty suppositories upon storage at a higher temperature than ambient had been demonstrated by de Blaey and Rutten-Kingma (1976). The rearrangement of components within the gelucire forms that gave rise to Peaks 3 and 4 could have lead to the formation of solid solutions within the structures, thus no longer presented as separate peaks but as a common, expanded endotherm after 180 days (Figure 6.7). As expected, the total heat of fusion values increased after ageing for the same reasons postulated for pure G50/13 and 10% paracetamol dispersion samples. A decrease in Peak 1 heat of fusion value together with an increase for the Peak 2 value was a similar event to the sample aged at 20°C, but at a slower rate than pure G50/13.

Overall, caffeine dispersions in G50/13 seemed to be the least affected samples after ageing, either at 20°C or at 37°C. Caffeine seemed to resist the transformation of the metastable forms to the more stable ones when held at 37°C more successfully than paracetamol as even after 180 days ageing, Peak 1 was still present and not fused to the bigger Peak 2. A possible explanation could be that the temperature of Peak 1 of the freshly prepared 10% caffeine dispersion sample was the highest amongst all the freshly prepared samples and closest to the storage temperature of 37°C, so that there was less Peak 1 melt to transform than the other samples. Transformation had to proceed through a limited melt-transformation process and the slower solid-solid transformation.

6.3.4 Solid Fat Content (SFC)

As previously stated in Chapter 2, there are three phases to the SFC profile of pure G50/13 and can be described as Low Melting Fraction (LMF) from 28°C to about 37°C, Middle Melting Fraction (MMF) from about 37°C to 46°C and High Melting Fraction (HMF) from about 46°C to 60°C. It was observed that pure G50/13 samples which were aged at 20°C had a lower quantity of LMF but a higher quantity of HMF than freshly prepared samples (Figure 6.8). The quantity of MMF was similar amongst the samples and since this fraction represented the majority of the matrix, it suggested that storage at this temperature did not alter the melting behaviour to a great extent. At any given temperature, the amount of solid

Figure 6.7: Thermal profiles of 10% caffeine dispersions in G50/13 after ageing at 37°C

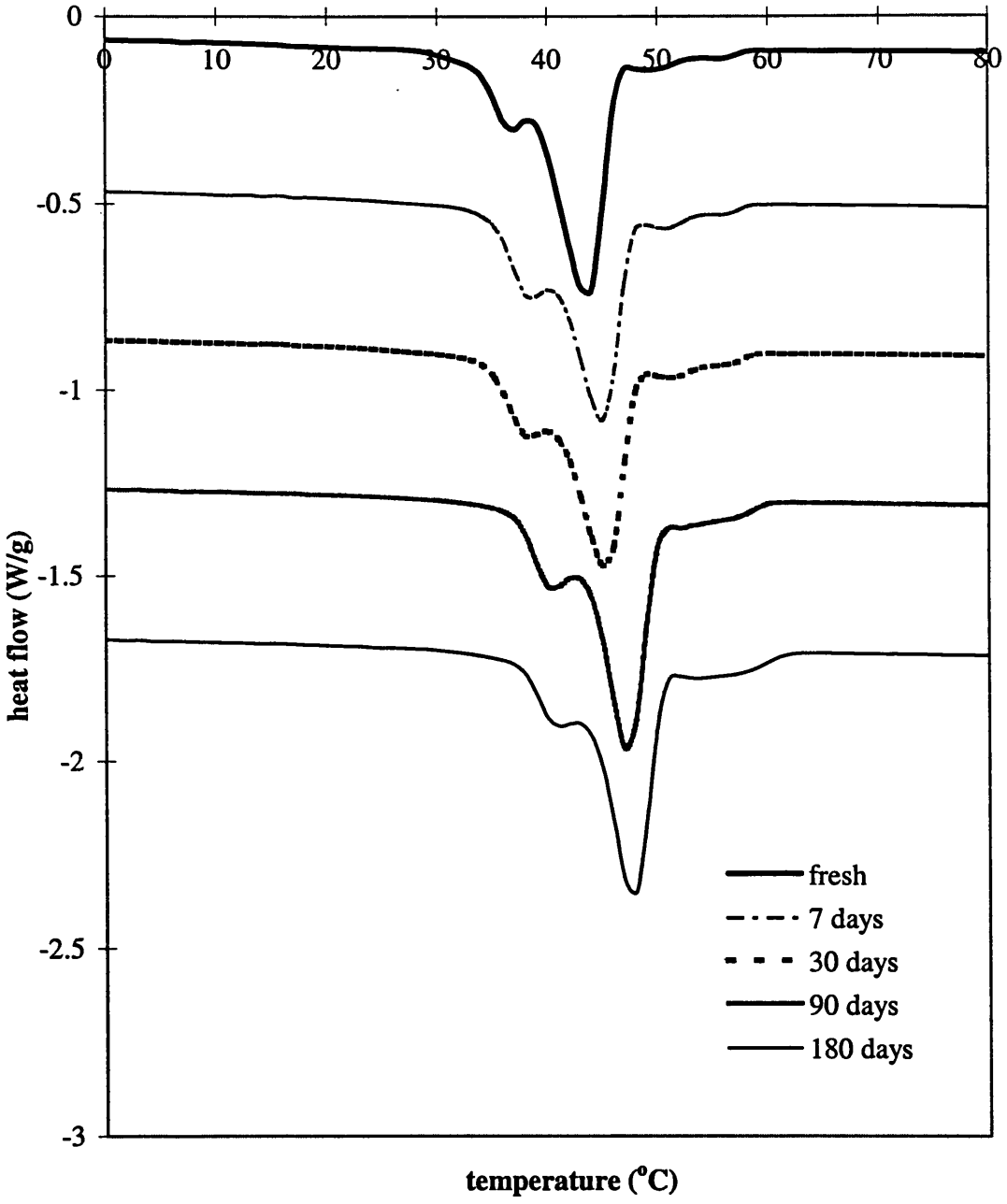

Figure 6.8: Solid Fat Content of pure G50/13 after ageing at 20°C

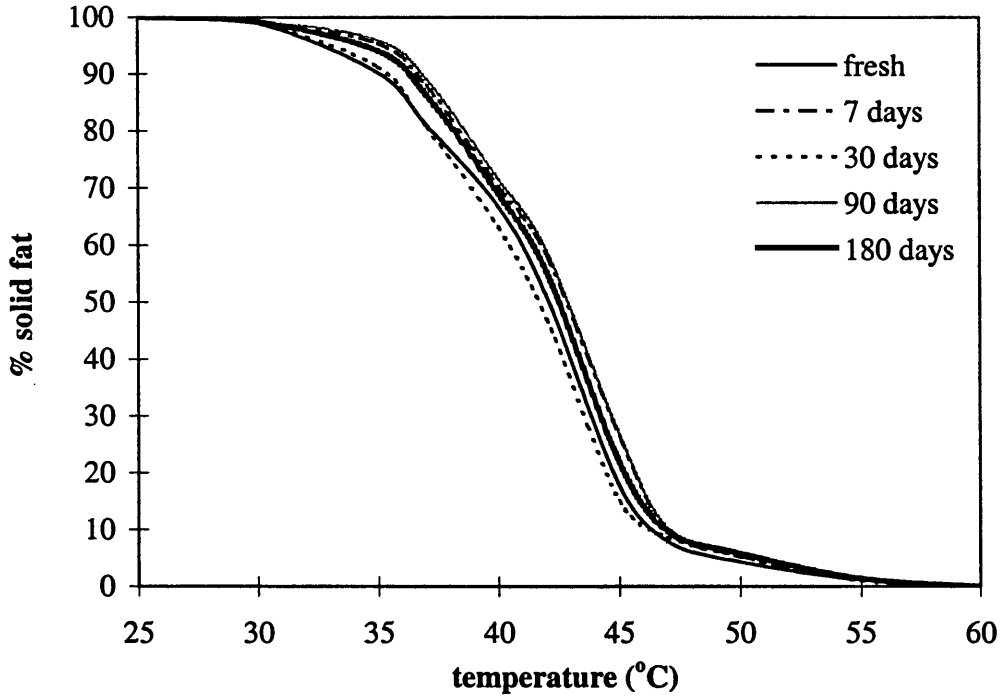

Figure 6.9: Solid Fat Content of pure G50/13 after ageing at 37°C

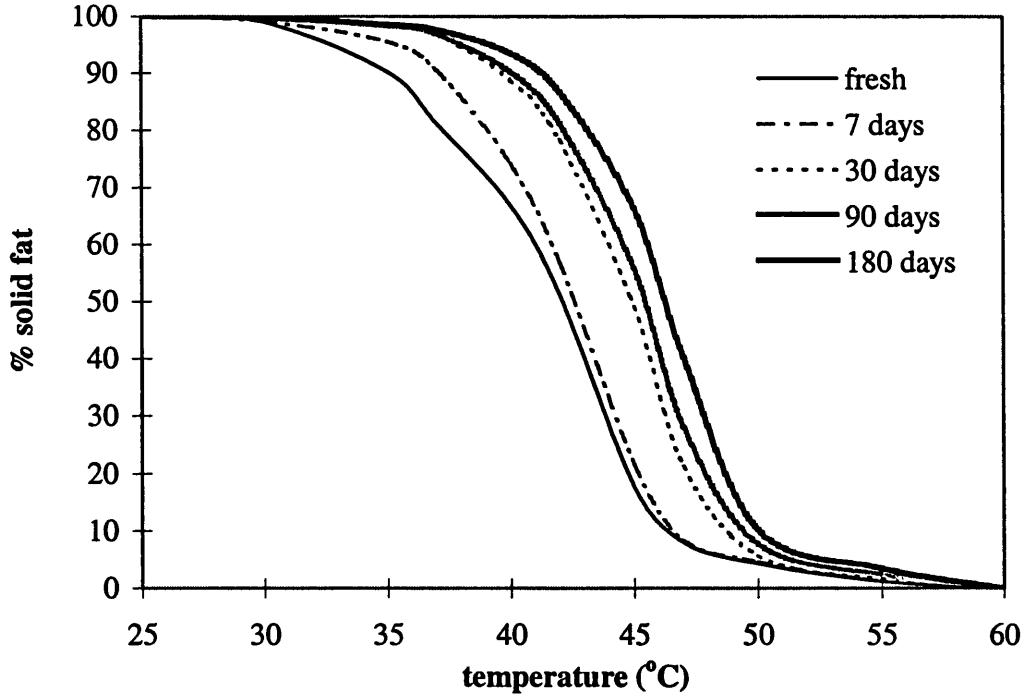

fat was slightly higher for the aged samples than for the freshly prepared samples (with the exception of samples aged for 30 days between 36.5°C and 46.5°C). Ageing at 37°C decreased the LMF and increased the HMF vastly, with the percentage of the matrix remaining as solid at any particular temperature being elevated with the period of ageing (Figure 6.9). This suggests that ageing at this temperature increased the hardness of the matrix.

For the 10% paracetamol dispersion in G50/13, ageing at 20°C only significantly changed the SFC profile after 180 days where the fall in the amount of LMF was compensated by the slightly higher MMF, but the HMF was still similar (Figure 6.10). Ageing at 37°C greatly decreased the LMF and increased the HMF to the extent that the MMF was reduced in quantity as a result (Figure 6.10). This more apparent change was due to the low solid content of the freshly prepared sample which resulted in the crystals being more prone to polymorphic changes (deMan and deMan, 1994). The proportion of the matrix that remained solid over the temperature range was very high for the aged samples and the biggest rate of increase occurred within the first 30 days of storage. The increase in the SFC was evident even by manual handling of the sampling, whereby freshly prepared paracetamol dispersions were difficult to comminute down for the DSC due to their softness and stickiness but the problem was overcome after ageing.

An alternative to the SFC value as an indication of solidity and hardness or the total heat of fusion value as an indication of crystallinity is the liquefaction time of formulations at a particular temperature. This method was often utilised in glyceridic formulations in the form of suppositories whereby the amount of time taken for the dosage form to liquefy and therefore processes which can influence this are crucial to the drug release profile. In suppositories made from a mixture of mono-, di- and triglycerides and also in bases made from partially polyoxyethylenating those glycerides, the liquefaction time at 37°C was found to increase upon storage at a higher temperature (Moës and Jaminet, 1976). For the paracetamol dispersions of these bases, the liquefaction time of the freshly manufactured suppositories was lower than the pure bases, probably due to the drug acting as an impurity and lowering the melting point. However, upon storage, the time increased until it superceded that of the pure bases which had been aged under the same conditions. Such rise

Figure 6.10: Solid Fat Content of 10% paracetamol dispersions in G50/13 after ageing at 20°C

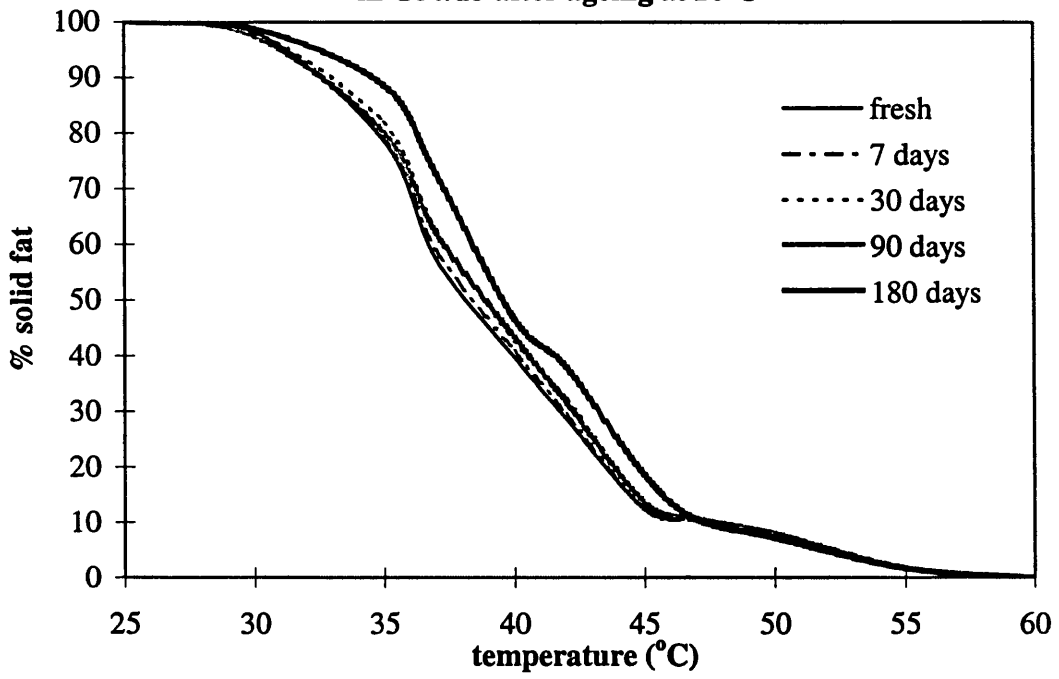

Figure 6.11: Solid Fat Content of 10% paracetamol dispersions in G50/13 after ageing at 37°C

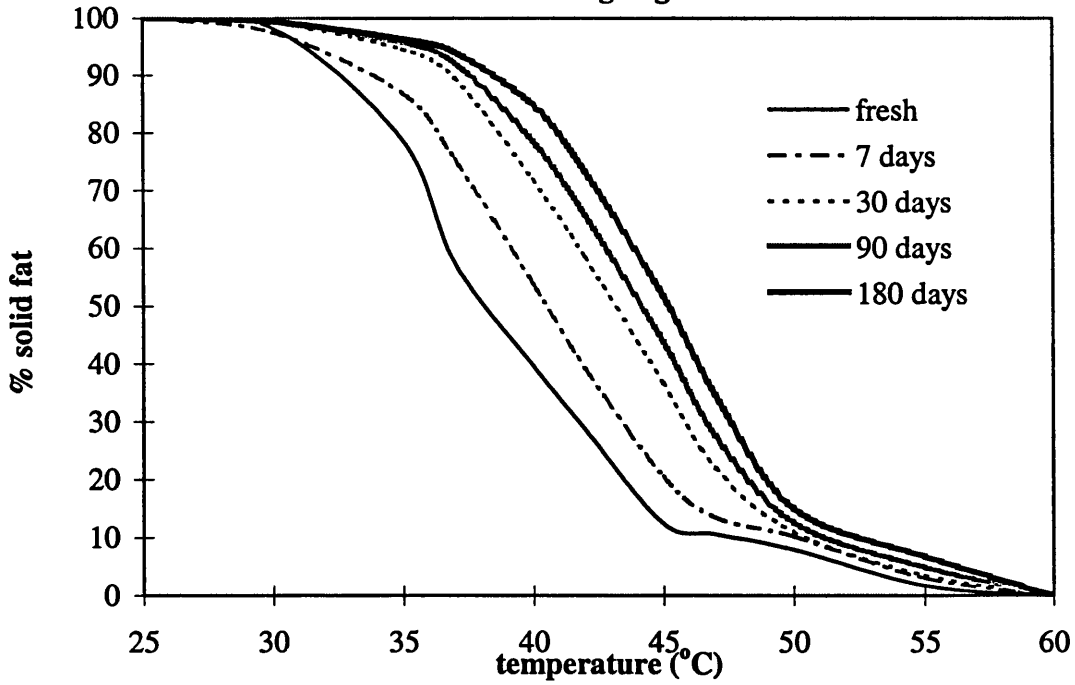

in the time was thought to be due to polymorphism, especially in the light of other studies.

In this current study, the total heat of fusion values for pure G50/13 and its paracetamol dispersions were raised during ageing especially after storage at the higher temperature of 37°C. When the values were calculated for the amount of the pure G50/13 corresponding to that in the 10% paracetamol dispersion (90%), they were similar or only a little higher than the values of the paracetamol dispersion. Figures 6.9 and 6.11 also showed that if the SFC at 37°C of the pure G50/13 and its paracetamol dispersions, both previously stored at 37°C, were compared the values for the paracetamol dispersions were lower. Presumably, if the liquefaction time was measured, the paracetamol dispersions would have shown shorter time than the pure G50/13 samples. This indicates that the dispersions of the same drug in different carriers even though similar in composition, would not necessarily give identical results and this is more apparent when the samples are subjected to accelerated ageing conditions.

The SFC profiles of the 10% caffeine dispersion samples aged at 20°C were similar in HMF and LMF content, with the SFC being slightly higher for the aged samples within the MMF range for the longer stored matrices (Figure 6.12). Storing the samples at 37°C changed the profiles extensively with all three factions being affected (Figure 6.13). Aged samples showed less LMF and MMF but a lot more HMF than freshly prepared samples. The effect could be seen even during the early stages of the ageing process followed by another big change after 90 days ageing.

The freshly prepared samples of paracetamol or caffeine dispersions in G50/13 in this study might not have recrystallised completely even after 24 hours equilibrating over silica gel. This could partly be due to the cooling rate of the molten mixture as it was poured into the aluminium mould. The mixture was cooled down from 75°C to the ambient temperature (25±1.5°C) and solidification occurred rapidly which was beneficial to the formation of the matrix as it could set before the drugs could possibly sediment but on the other hand, resulted in a lower solid content than if it had been slow cooled. All of the samples demonstrated that the solidity of the matrix can be vastly and quickly increased by storing them at 37°C. This will have a bearing on the physical state of the actual samples which

Figure 6.12: Solid Fat Content of 10% caffeine dispersions in G50/13 after ageing at 20°C

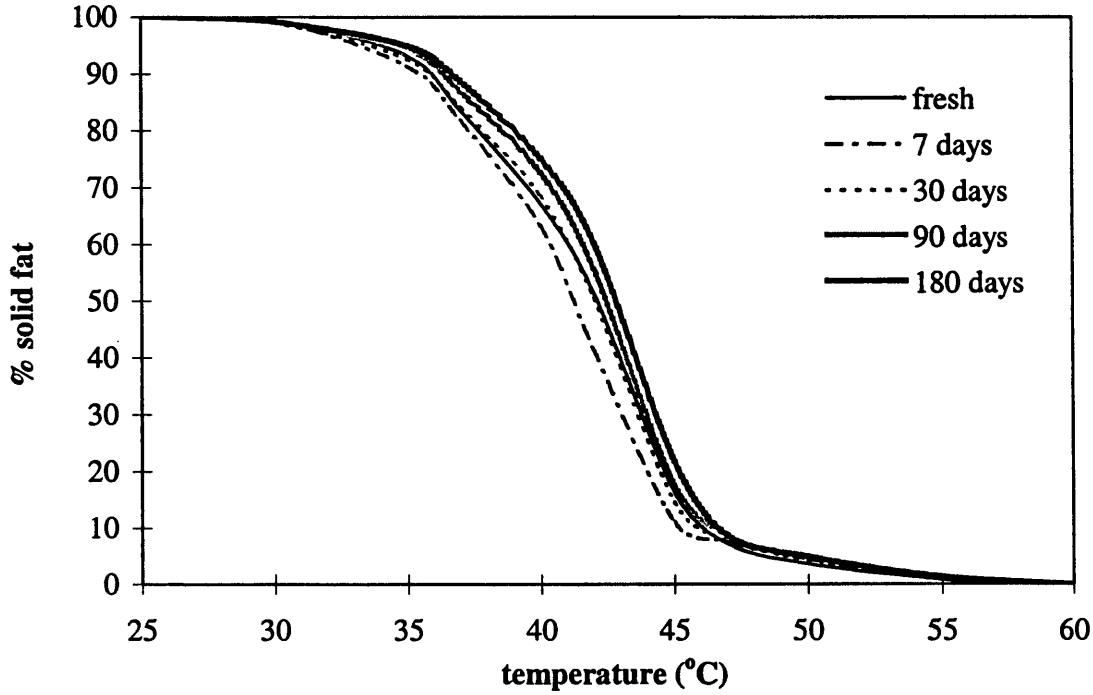

Figure 6.13: Solid Fat Content of 10% caffeine dispersions in G50/13 after ageing at 37°C

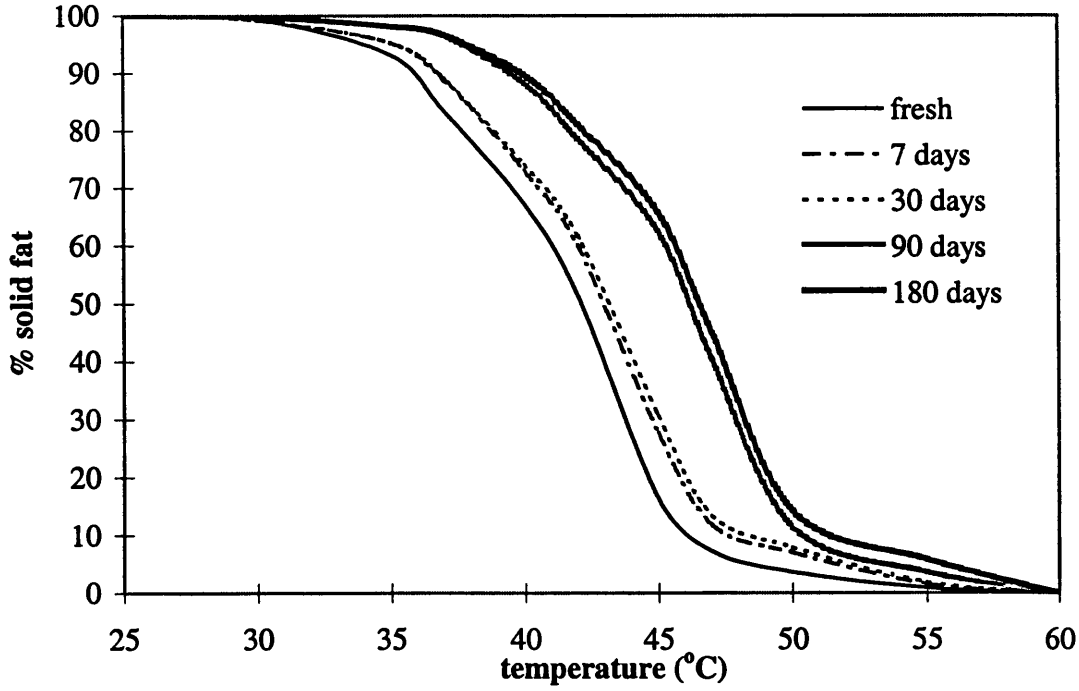

may affect other factors such as their disintegration, dissolution and digestability in vivo.

6.4 Conclusions

In general, ageing the samples increased their crystallinity and polymorphic stability. The extent at which these occur depend on the temperature of storage and the incorporated drugs. The rise in the crystallinity was revealed by the increase in the total heat of fusion values and this rise was more apparent for the samples stored at 37°C. Storage at this higher temperature provided kinetic energy to the gelucire molecules so that their long hydrocarbon chains can arrange themselves into the crystalline structure more quickly and easily. The rise in polymorphic stability, that is the transformation of the less stable forms of the gelucire components to the more stable forms was evidenced by the shift of the peak temperatures towards the higher ranges. More importantly, the transformation could be seen as the changes to the heat of fusion proportions under each peak. Again, these changes were more considerable for the samples stored at 37°C with the reduction or disappearance of the area under the lower melting peaks and the simultaneous gains of the higher melting peaks.

The modifications brought about by ageing had the greatest impact on the10% paracetamol dispersion in G50/13 because of the increase in the solidity and hardness after storage at 37°C. Polymorphic changes could be seen to occur in stages as shown by the emergence of the subpeaks. Previous stabilisation of the lowest melting peak by the incorporation of paracetamol was gradually eroded away by the inclination of the gelucire to transform to higher melting forms especially when supplied with kinetic energy. Incorporation of caffeine into G50/13 did not have a great effect on the freshly prepared samples. However, after storage it was found that although the crystallinity was increasing as was for the other samples, the caffeine sample displayed the least amount of polymorphic transformation. Incorporation of caffeine also stabilised the lowest melting form but this fact was not apparent until the samples stored at 37°C was analysed and it was found that the form (Peak 1) was still present even after 180 days. The stabilisation of this form by paracetamol was more obvious due to the extent of this phenomena but caffeine stabilisation of this form,

even though small, was more uniform throughout the ageing process.

The SFC profiles can give an indication of the solidity of the matrices and the changes to it upon ageing, therefore highlighting potential benefits or problem that could arise after storage. A decrease could mean that tablets formulated with G50/13 could stick to each other or have a change in dosage forms dimensions when the forms knock against each other in a container. On the other hand, an increase in the solidness could lead to drastic changes to the dissolution profiles and so the SFC could provide some information on which matrices would be suitable for a particular release requirement.

CHAPTER 7: MORPHOLOGICAL INVESTIGATIONS INTO THE EFFECTS OF AGEING G50/13 MATRICES

Part I: Polarising and Differential Interference Contrast Microscopy

As with the studies on the effects of drug loadings on G50/13 matrices, microscopy studies were performed here in order to look at the gelucire structure and its dispersions. In the previous chapter, the structure was assessed by using the thermal analysis technique of Differential Scanning Calorimetry. Another thermal analysis technique, Hot Stage Microscopy, was also included here and thus any morphological changes that can be related to the variations in the thermal profiles of the last chapter can be determined.

7.1 Introduction

Microscopy techniques have long been invaluable in elucidating the structure of compounds. It is sometimes useful to be able to visualise the difference in the structures to observe the changes, if any, to the compound due to storage and ageing, especially in materials with fatty acids and glycerides in them which frequently have shown to change their characteristics with time. However, this technique has to be used in conjunction with other techniques, such as DSC or X-ray crystallography due to its limitations (Chapman, 1962). In addition, a change in the crystal structure after ageing does not necessarily correlate to a change in the polymorphic form because the same glyceride polymorph can manifest itself in different crystal forms.

7.1.1 The use of microscopy techniques in ageing studies

Microscopy can be used to detect the state of a system after ageing for a certain time. Polarizing microscopy (see below) revealed that no crystallisation of α-pentyl-3-(2-quinolinylmethoxy) benzenemethanol occurred in PEG 1000, PEG 1450, PEG 8000 and G44/14 after storing them for one month at room temperature when the concentration of the drug was 100mg per capsule (Serajuddin et al, 1988). Raising the concentration of the drug to 125mg per capsule or higher however, resulted in crystals of the drug being observed in the matrix, even after storage of less than seven days, and the number of crystals increased with the initial drug loading. This led to the conclusion that at loadings of 100mg or less per capsule, the drug formed solid solutions with the carriers and at higher

concentrations, exhibited the solid dispersion systems.

Ageing of PEG 6000 showed that there were structural changes occurring to the crystallised melt for up to 30 days of storage (Ford and Rubinstein, 1979). Increased details of the spherulites which crystallised initially and deepening of radial striations were observed. These changes were thought to be due to the molecular orientation of the PEG molecules. Incorporation of indomethacin into this PEG led to dark aggregates which projected into the spherulites being formed. On ageing, these dark aggregates developed further, together with the radial striations of the PEG spherulites until the generation of a fine structure within the spherulites which signalled the formation of the final stable structure. Elevating the amount of indomethacin added to the polymer correspondingly increased the time taken for the stable form to develope due to the decrease in the rate of crystallisation. This increase in crystallinity was then associated with the decrease in the dissolution rate of the drug upon ageing.

7.1.2 Polarised light microscopy

In polarisation microscopy, a transmitted light microscope is fitted with two polaroids, the polariser and the analyser. The polariser is placed in the illuminating light path and the analyser in the imaging light path. The polariser allows light of only one plane to go through (for example, E-W) and the analyser is arranged so that it allows light of a perpendicular plane to go through (N-S); they are said to be *crossed* relative to each other. Contrast arises from this dark background if an anisotropic sample is placed between them which alters the plane of light so that some can go through the analyser.

Anisotropy arises when the electronic configurations of the atoms and molecules in a medium have preferred orientations. When light hits the medium, the configurations can absorb quanta or delay it. This delay give rise to a change in the refractive index. The extent of the interactions depends on the direction of the polarised light relative to the electronic orientations of the medium. Following from that, when the interactions result in the variation of the refractive index, the medium is said to be *birefringent.*

In a birefringent material, the light is split into two components vibrating at 90° to each other. The speed (and therefore the refractive index) of these waves of light then become different. This will result in an optical path difference (OPD) between the waves of light by the time they leave the material (refer to Section1, Chapter 3 for OPD). Here, the OPD can also be defined as;

$$OPD = (\text{birefringence, } n_1\text{-}n_2) \times (\text{thickness, } t)$$

Depending on the OPD, the light emerging from the material is planar, ellipsoid or circular. When this light hits the analyser, waves which are totally planar and are of the E-W orientation are completely extinguished. Waves which are planar but are of N-S orientation are completely transmitted and waves in between the two orientations are partially transmitted depending on the magnitude of their N-S components. These phase differences give rise to contrast.

Polarized light microscopy is mostly used in determining the melting point of a substance. It is ideal for monitoring the endpoint of a melting process because the field goes completely dark when the last traces of the crystal are melted. However, it is not suitable in observing the onset of a melting process nor the sublimation process that may occur during the heating (Kuhnert-Brandstätter, 1971). It is also not suitable for materials that can transform from an optically anisotropic crystal to an isotropic one because the temperature of this transformation may be mistaken for the melting point. For example, tris-(hydroxymethyl)-aminomethane undergoes an enantiotropic transformation at 135°C but its melting point is at 171°C, so the lost of birefringence at the lower temperature could erroneously be thought as the melting temperature. Sometimes, it is more useful to not completely cross the polarizer and the analyser, so that the contrast comes from the interference colours instead and borders of the melt could be seen to distinguish it from enantiotropic transformation.

The principles of Differential Interference Contrast (DIC) Microscopy had previously been described in Section 1 of Chapter 3.

7.2 Materials and Methods

7.2.1 Preparation of samples

Pure G50/13 samples were prepared by melting the untreated G50/13 for 70 minutes at 75°C in an oven, as detailed in Chapter 4 for the preparation of moulded tablets. At the same time, glass microscopic slides and cover slips (as described in Chapter 3) were placed in the same oven to allow them to equilibrate at that temperature. The gelucire was taken out and stirred over a magnetic hot-plate stirrer for 10 minutes so that the same preparation conditions would be applied to the samples of pure G50/13 and also its drug dispersions. Some of this molten gelucire was drawn up a glass pipette which was also equilibrated at 75°C and a couple of drops were placed on the slides so that a thin film of the sample was obtained when the cover slips were positioned over the drops without excess gelucire running off the slides. The slides remained in the oven for another 30 minutes before being removed to be cooled to room temperature. The samples were then arranged in flat containers with silica gel in them and the containers were sealed to prevent moisture going into them. Storage of these samples was again at 20°C and 37°C. At certain time intervals, the containers were taken out and equilibrated at room temperature for 24 hours before the samples in them were analysed.

For the drug dispersion samples, 10% paracetamol or 10% caffeine was incorporated during the 10 minute stirring on the hot-plate stirrer. The drops containing the drugs had to be placed carefully on the slides because the molten carrier tended to accumulate around the drug particles so that very thin films were difficult to obtain for the drug dispersion samples.

7.2.2 Microscopic analysis of samples

Analyses of the samples were performed using a microscope fitted with Differential Interference Contrast (DIC) prisms (see Chapter 3) or polarisers for polarising microscopy. The samples were placed on a hot-stage and the heating rate used was 2°C/min. Changes to the structures after ageing and during heating were noted and photomicrographs of these

were taken. The samples produced here were different from the samples in Chapter 3 in the way that the former was prepared by putting the molten sample on the slides and setting it at ambient conditions for 24 hours, in the same way as the moulded tablets were made and the resultant layer of the matrix was more compact, whereas the latter samples were prepared by heating and cooling them on the hot-stage itself and analysed in a short time after recrystallisation.

7.3 Results and Discussions

7.3.1 Pure G50/13

One of the more prominent structures to be seen under DIC on the freshly prepared pure G50/13 was the dark blue short streaks, which looked like splatters of raindrops on a hard surface. Interspersed were also light coloured streaks together with darker shapeless forms (Plate 7.1). At about 34°C onwards, the lighter coloured forms began to melt, revealing the darker background of the slides. Then from 42°C onwards, the raindrop structures started to fade and undergo a phase change which could be observed as the colour became darker and lost their blue hue. At 46°C, the heterogenous structures seen at the start of the heating process had disappeared and a more uniform structure was exposed. This could be seen as the multicoloured field of view was replaced by a monotone structure which reflected the lost of structures that gave rise to the difference in the phases on the sample resulting in the variation in colours under DIC microscopy. By 48°C, the only structure left that could be seen was very faint which persisted to about 54°C. The temperatures at which these changes occurred could be correlated to the peak temperatures seen on the DSC thermal profile of the same sample (Appendix 6). With this technique, the start of the melting of Peak 1 (36.0°C on the DSC thermal profile) could be observed from 34°C onwards because the melting endotherm was broad. Subsequent phase changes could also be related to the DSC thermal profiles such as the endothermic peaks at 44.0°C and 48.7°C. However, the change correlating to the final endothermic peak on the DSC thermal profile at 55.7°C could not be seen on the HSM samples. This could be due to the gelucire form which gave rise to this peak being in a very small quantity.

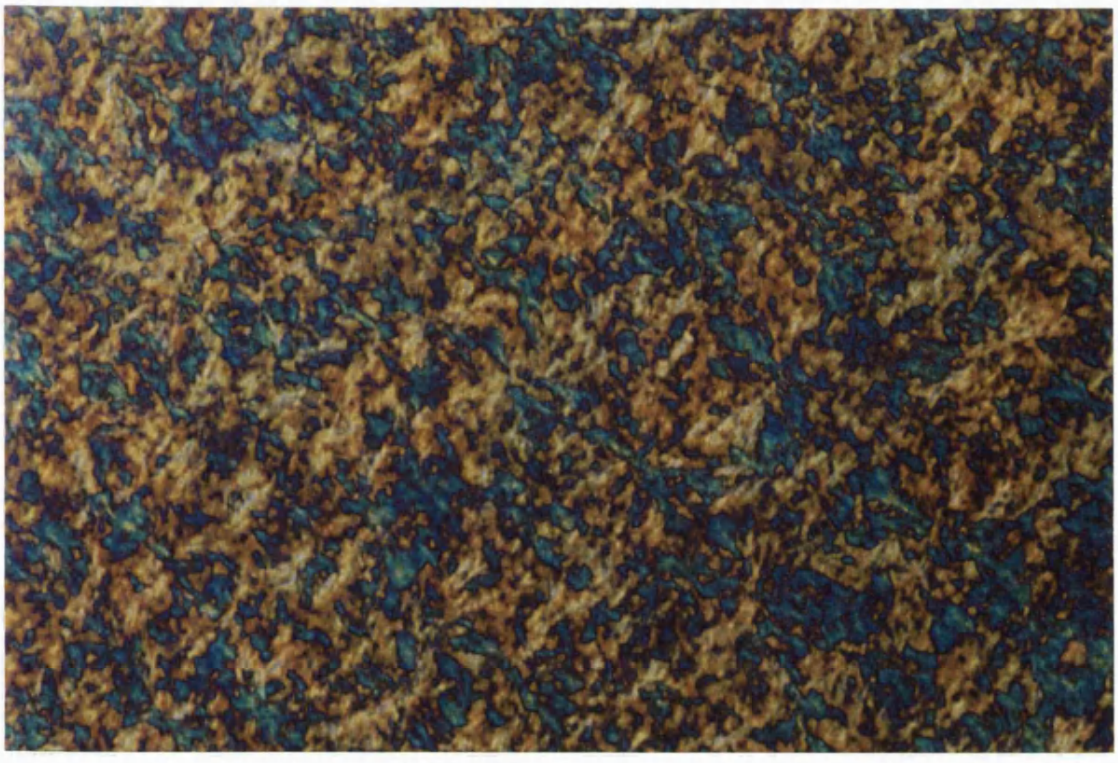

Plate 7.1: Freshly prepared pure G50/13 under DIC **1:440**

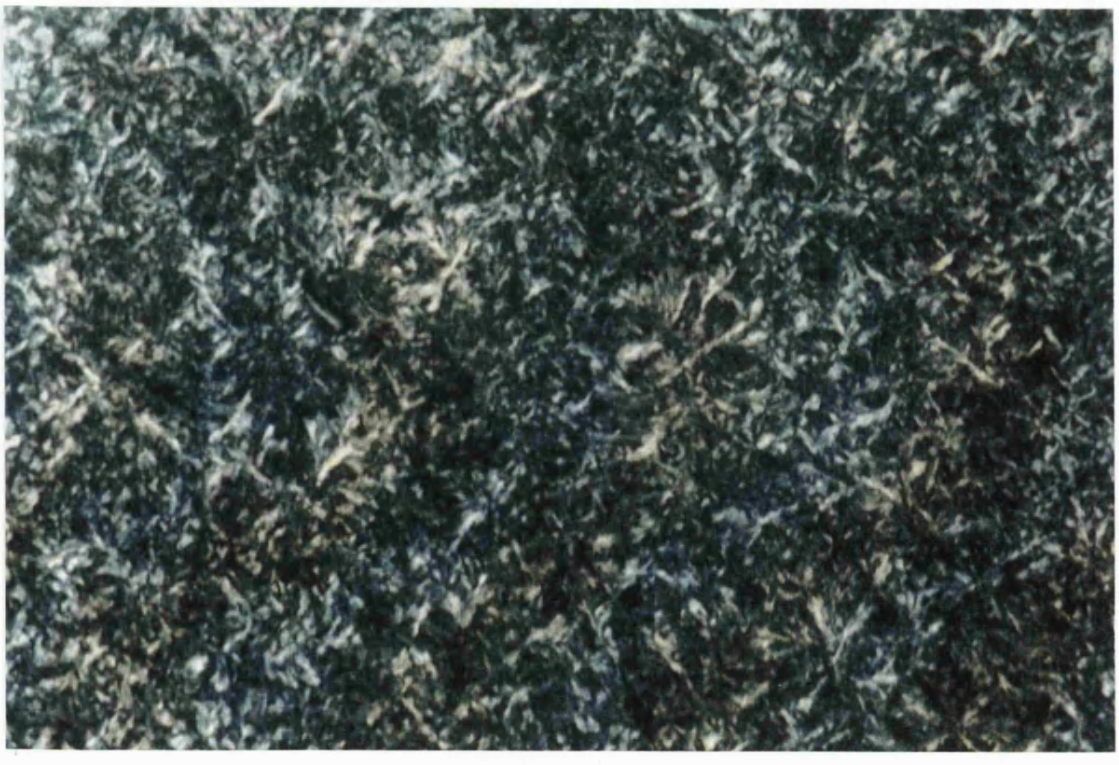

Plate 7.2: Freshly prepared pure G50/13 under crossed-polars **1:440**

Under polarising microscopy, it could be observed that the blue raindrop structure and the light-coloured streaks on the sample under DIC, were seen here as white structures against a black background which meant that those structures were crystalline and able to rotate the plane-polarised light (Plate 7.2). The light coloured streaks could be seen under crossed-polars as feathery. The raindrop structures could be mixed crystals composed of mainly β polymorphs as this structure resembled the β crystals of palm oil margarine which under polarising microscopy were observed to be like agglomerates of needle-like structure (deMan and deMan, 1994). It was more difficult to detect the onset of melting (t_{onset}) or the phase changes using polarising microscopy than DIC because changes under crossed-polars can only be seen as graduations in shades of grey or the fading of the white crystalline structures. Initial phase change was determined to be at 39°C and by 46°C, most of the white crystalline structures had disappeared leaving some persistent white streaks. These then faded between 48°C and 49°C, indicating that also under polarising microscopy, the structure that gave rise to the final peak of the DSC thermal profile at 55.7°C could not be ascertained.

Storage at 20°C after 7 and 90 days did not seem to alter the structures compared to the freshly prepared samples (Plates 7.3 and 7.4). The initial melting started to become discernible at 36°C which was slightly higher than the fresh sample but this correlated with the small increase in the Peak 1 temperature according to the DSC thermal profiles of the samples aged for the same number of days (Appendix 6). The processes of the phase changes followed a similar pattern to the freshly prepared samples with the melting of the lighter coloured structures followed by the blue raindrop streaks which underwent intensive melting at 44°C until a faint structure was left which persisted until 54°C. Under crossed-polars, the shape of the gelucire structure giving rise to Peak 2 was more pronounced when the Peak 1 structure melted. The Peak 2 structure was seen to be shaped like snow flakes and when this melted away, structure which looked like feathers was revealed (Plates 7.5 to 7.7).

Ageing at 37°C had increased the raindrop structures (emerged as the blue structures) (Plates 7.8 to 7.10). The onset of melting occurred at around 42°C which was later than the fresh or aged at 20°C samples and the change was rapid once it commenced. DSC thermal

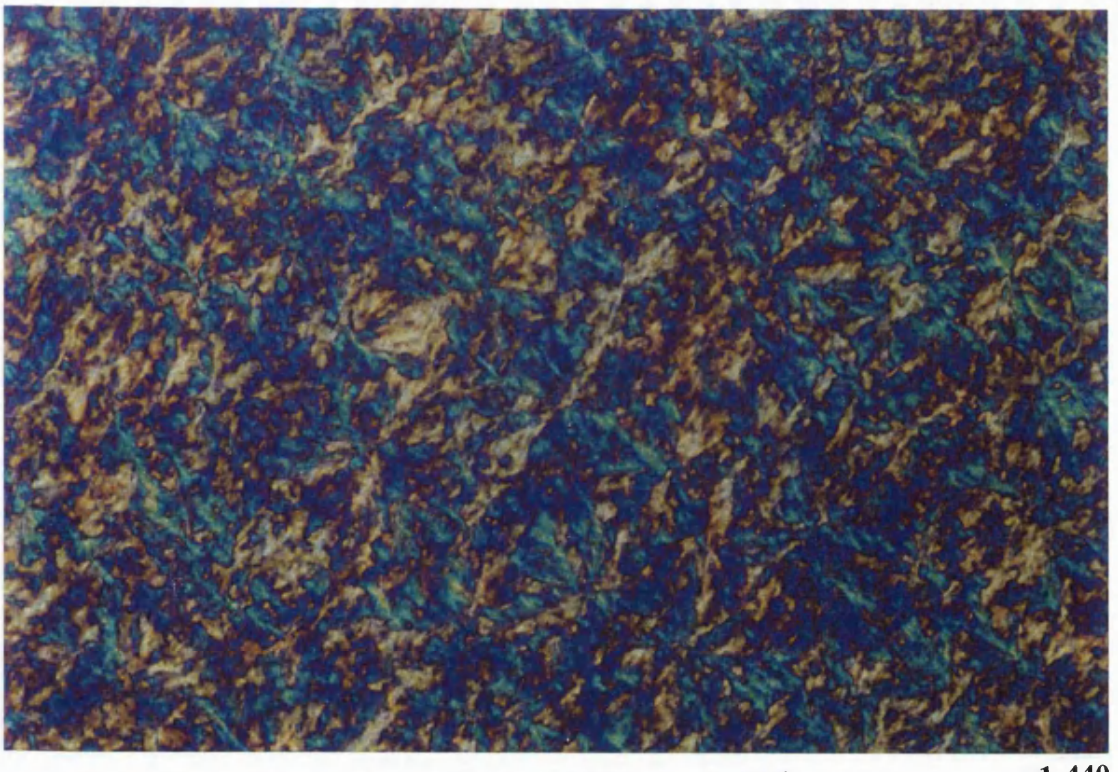

Plate 7.3: Pure G50/13 aged for 7 days at 20°C under DIC **1:440**

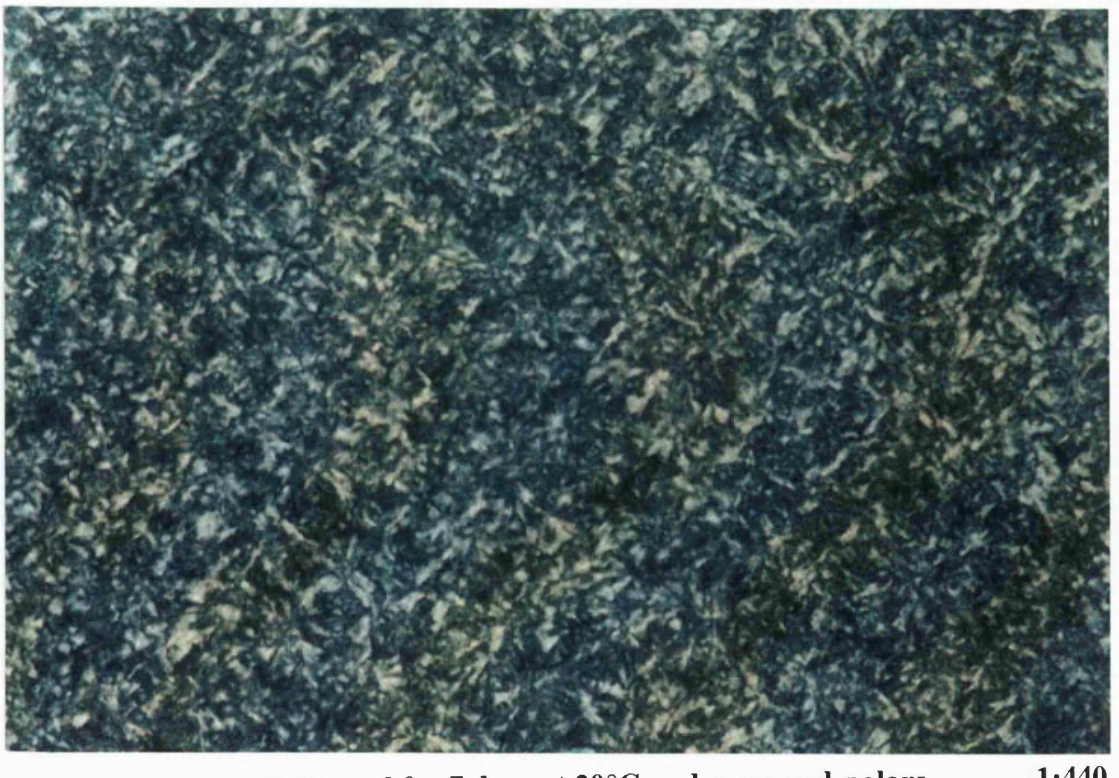

Plate 7.4: Pure G50/13 aged for 7 days at 20°C under crossed-polars **1:440**

Plate 7.5: Pure G50/13 aged for 7 days at 20°C under crossed-polars **1:110**

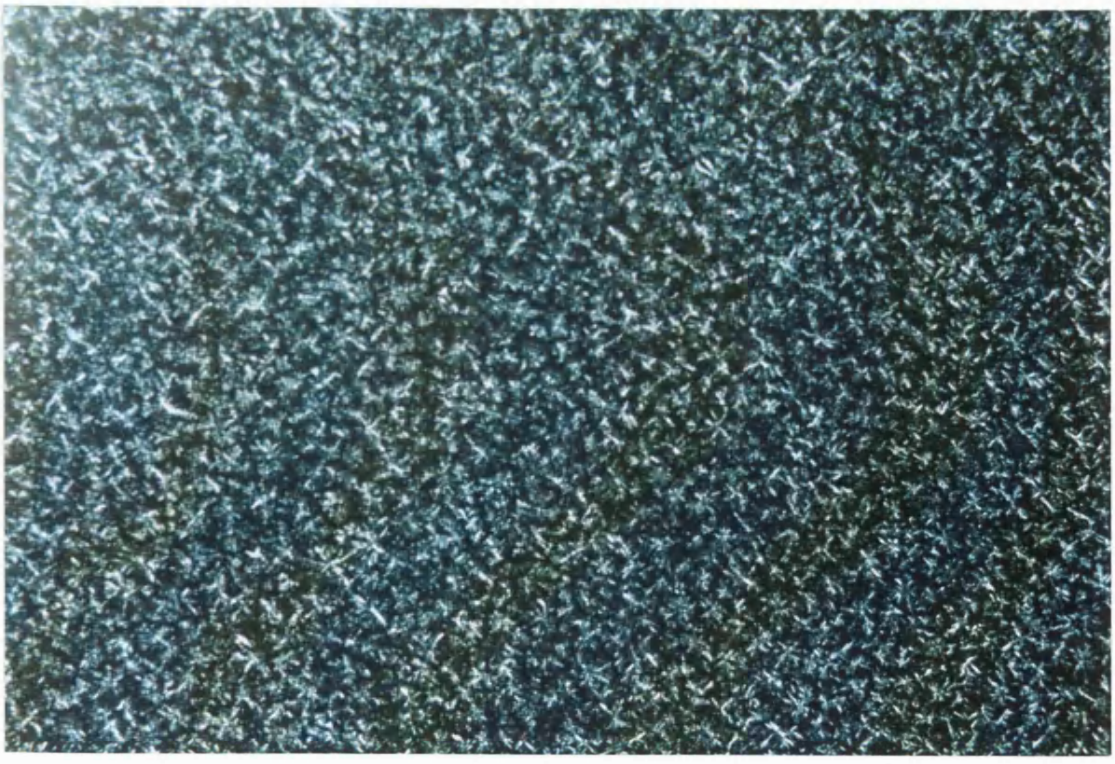

Plate 7.6: Pure G50/13 aged for 7 days at 20°C under crossed-polars at 44°C **1:110**

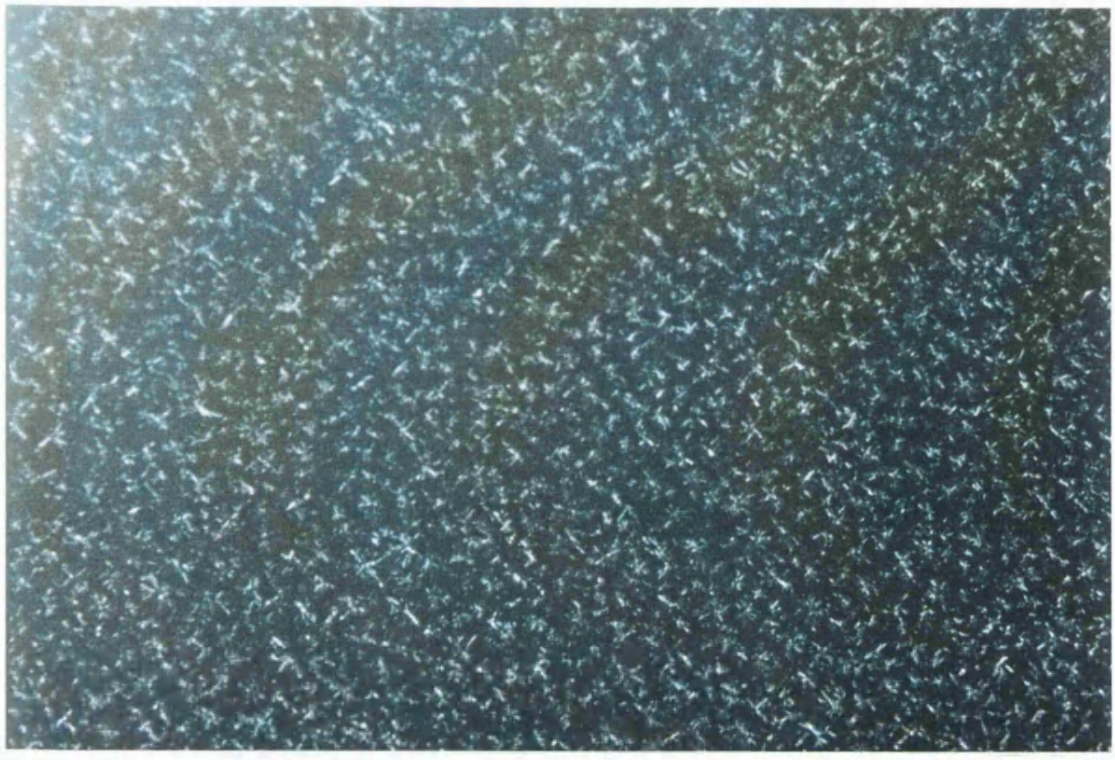

Plate 7.7: Pure G50/13 aged for 7 days at 20°C under crossed-polars at 46°C **1:110**

Plate 7.8: Pure G50/13 aged for 7 days at 37°C under crossed-polars **1:110**

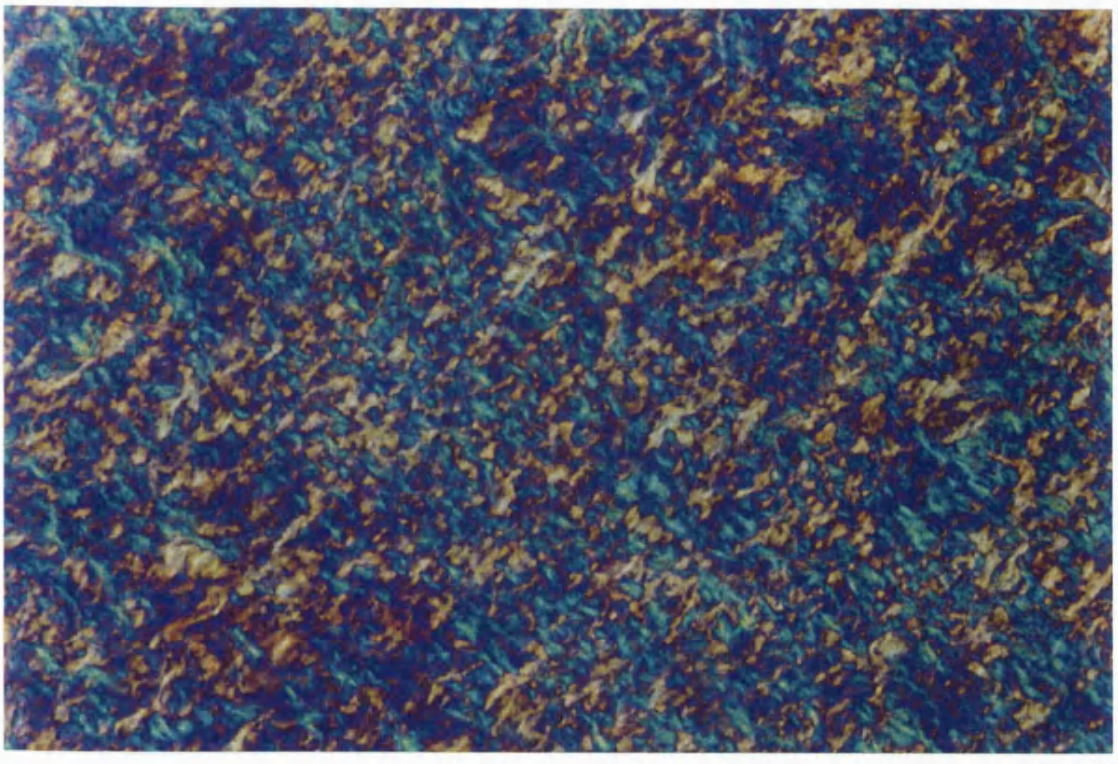

Plate 7.9: Pure G50/13 aged for 7 days at 37°C under DIC **1:440**

Plate 7.10: Pure G50/13 aged for 7 days at 37°C under crossed-polars **1:440**

profile revealed that Peak 1 had merged with Peak 2 with a larger combined heat of fusion value and this was the reason for the later onset and the more prominent melting. In addition, the small β' crystals of palm oil margarine had been reported to transform to the larger β crystals with an increase in the melting point of about 2-3°C (deMan and deMan, 1994). By 48°C, the only structure that could be seen was the feather-like, which were all gone by 54°C. Polarising microscopy also showed the pronounced melting from 42°C onwards with the melting of the snow flake structures followed by the feather structures. There were more gelucire crystals still left at 44°C for the samples aged at 37°C than the freshly prepared or aged at 20°C samples. This confirmed the transformation of the lower melting temperature structure to the higher one upon ageing at this temperature, which on the DSC profile was represented by Peak 2. However, as with the freshly prepared samples, polarising microscopy showed a lower temperature (49.7°C) for the complete disappearance of the structures compared to the DIC technique (54.4°C).

7.3.2 10% paracetamol in G50/13

No obvious change in the structures could be seen for this sample compared to the pure G50/13 except for their proportions in relation to each other with larger areas of the light coloured structures could be discerned in the paracetamol dispersion sample (Plates 7.11 and 7.12). On heating, it was discovered that the initial phase change where the light-coloured structures slowly became superceded by a darker background colour occurred at a slightly lower temperature (about 33°C) than the pure G50/13 sample. It happened even though the temperatures of Peak 1 on both DSC thermal profiles of the pure G50/13 sample and the paracetamol dispersion sample were similar (36.0°C and 36.4°C respectively) because the heat of fusion values indicated that the form that gave rise to Peak 1 was 126% larger for the paracetamol dispersion sample than the pure G50/13 sample. Therefore, any change in this form including melting would be apparent more quickly for the paracetamol samples than the pure samples.

By 35°C, the melting was proceeding at a higher rate and at 44°C and onwards, the raindrops structure was no longer present. At 54°C, a faint mesh-like structure could still be seen floating on the molten gelucire and this faded by 56.5°C. A higher final melting

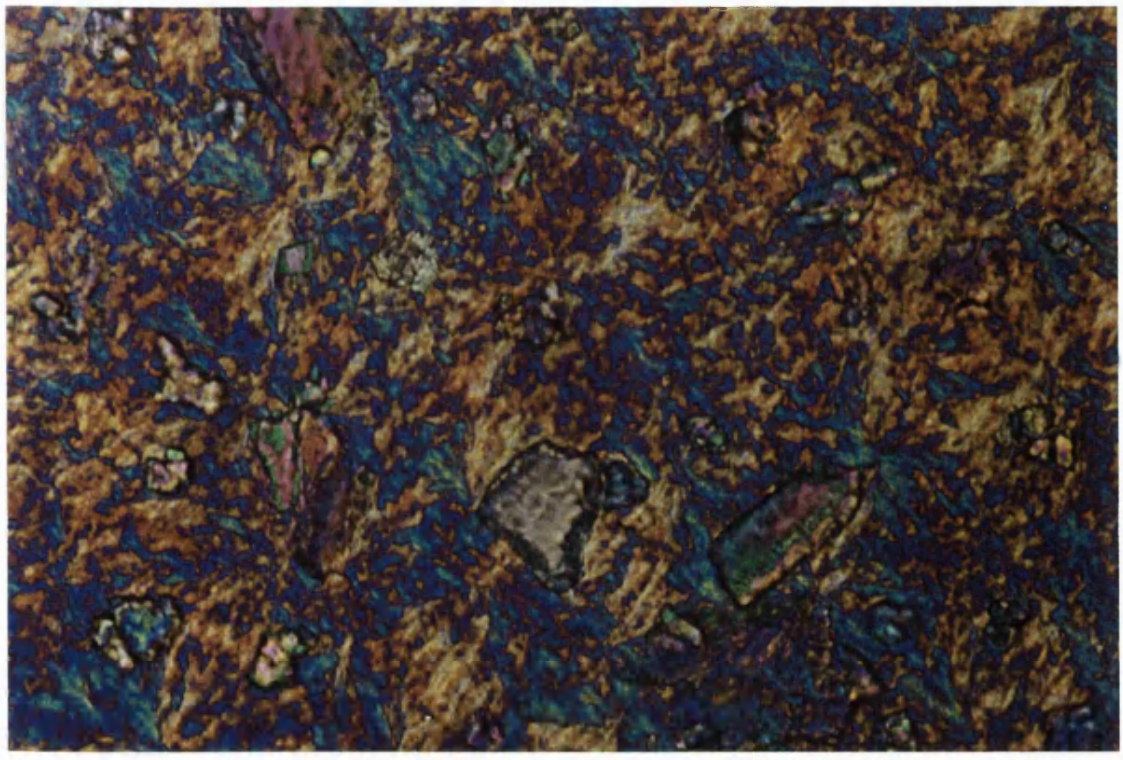

Plate 7.11: Freshly prepared 10% paracetamol in G50/13 under DIC 1:440

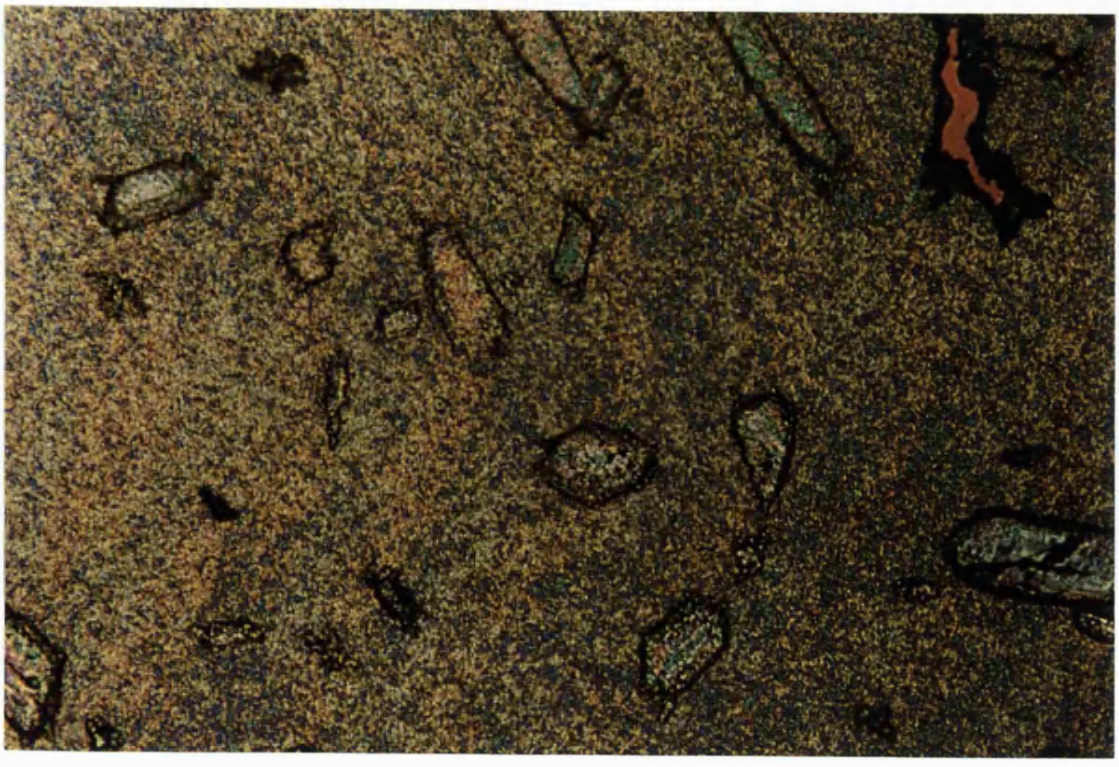

Plate 7.12: Freshly prepared 10% paracetamol in G50/13 under DIC 1:110

temperature for this dispersion could be explained by noting the Peak 3 temperature of the paracetamol DSC thermal profile which was higher than the pure G50/13 sample by 3°C. Nevertheless, similar to the pure sample, the Peak 4 form which had an endotherm at 57°C on the paracetamol dispersion DSC thermal profile could not be observed here. From about 90°C onwards, the paracetamol particles could be seen dissolving in the molten carrier and the final melting temperature of the drug was between 130.7°C and 147.3°C, which was much lower than the melting point of the drug on its own of 169-171°C. The use of polarising microscopy confirmed the results obtained by DIC. This time, the initial melting was easier to be observed because as was mentioned, the proportion of the matrix melting at the lower temperature was much higher than for pure G50/13. The only difference observed between the DIC and polarising microscopy results was that no more gelucire crystals could be observed under crossed-polars from 50°C onwards whereas structures could still be seen until 56.5°C under the DIC.

Ageing at 20°C demonstrated that the phase changes did not differ greatly from the freshly prepared samples, with the initial melting being observed at 34°C and an increase in the rate at 42°C. However, Plate 7.13 and 7.14 indicated that there were more morphological changes that occurred when the samples were stored at 37°C. The beginning of the melting process was difficult to observe in the samples aged at 37°C, possibly due to the smaller amount of the lowest melting form compared to the freshly prepared sample, as indicated by DSC. It became more obvious that melting was occurring from 39°C onwards when polarising microscopy disclosed that there was less crystals from this temperature onwards and the remaining crystals were of the bigger and more definite shaped variety. There was another prominent decrease in the amount of crystals observed after 45°C which was due to the melting completion of the form associated with Peak 2 of the DSC thermal profile and structures could still be seen until 56°C under DIC microscopy. For the samples aged for longer (90 days), the structure of the crystals seemed bigger than the rest with a change in phase being observed as early as at 34°C. As the melting progressed, structure which looked like long fern leaves was gradually revealed especially from 42°C onwards and which eventually melted at 58°C (Plate 7.15). This structure could probably be associated with Peak 2 of the 90 days aged at 37°C DSC thermal profile which evolved partly from the transformation of a lower melting form and which could still be seen until 58°C (even

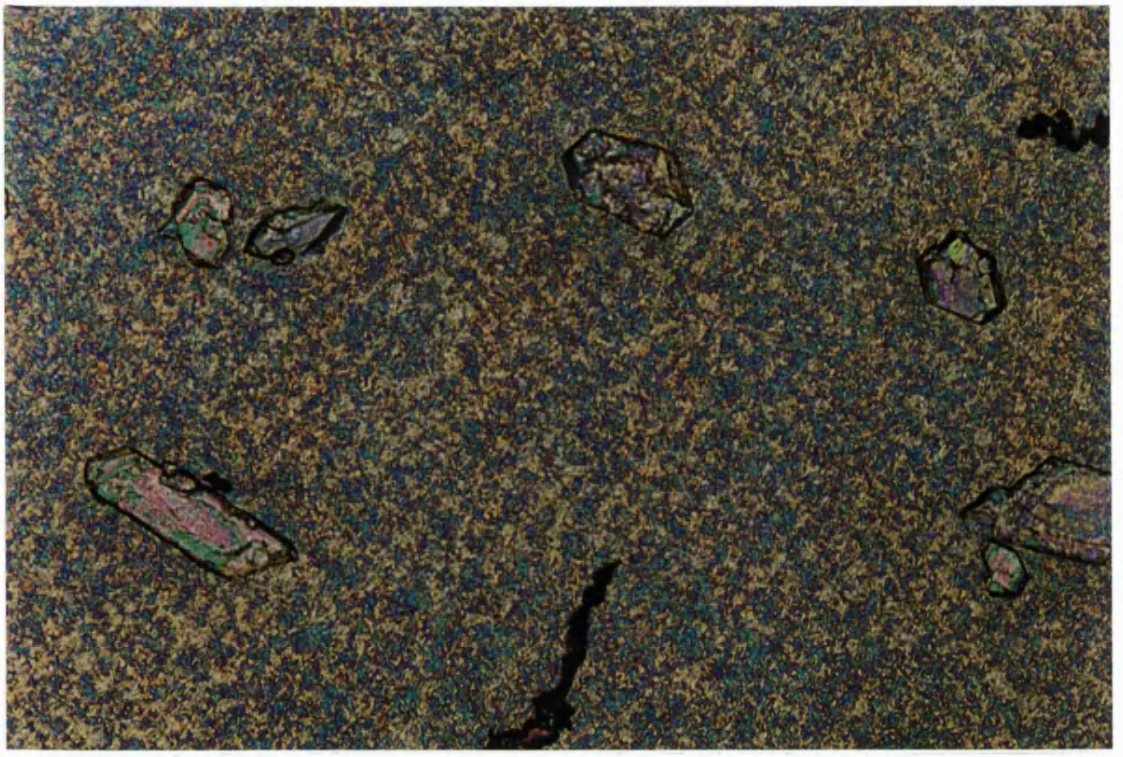

Plate 7.13: 10% paracetamol in G50/13 aged for 7 days at 37°C under DIC 1:110

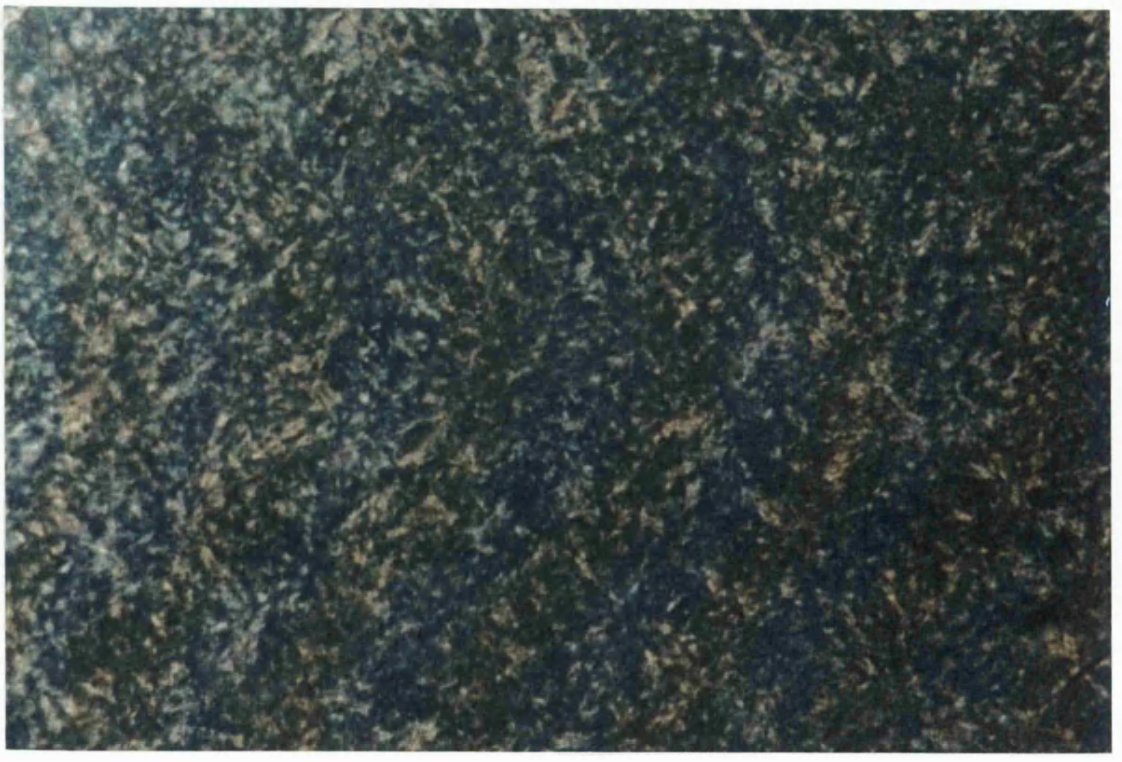

Plate 7.14: 10% paracetamol in G50/13 aged for 7 days at 37°C under crossed-polars 1:440

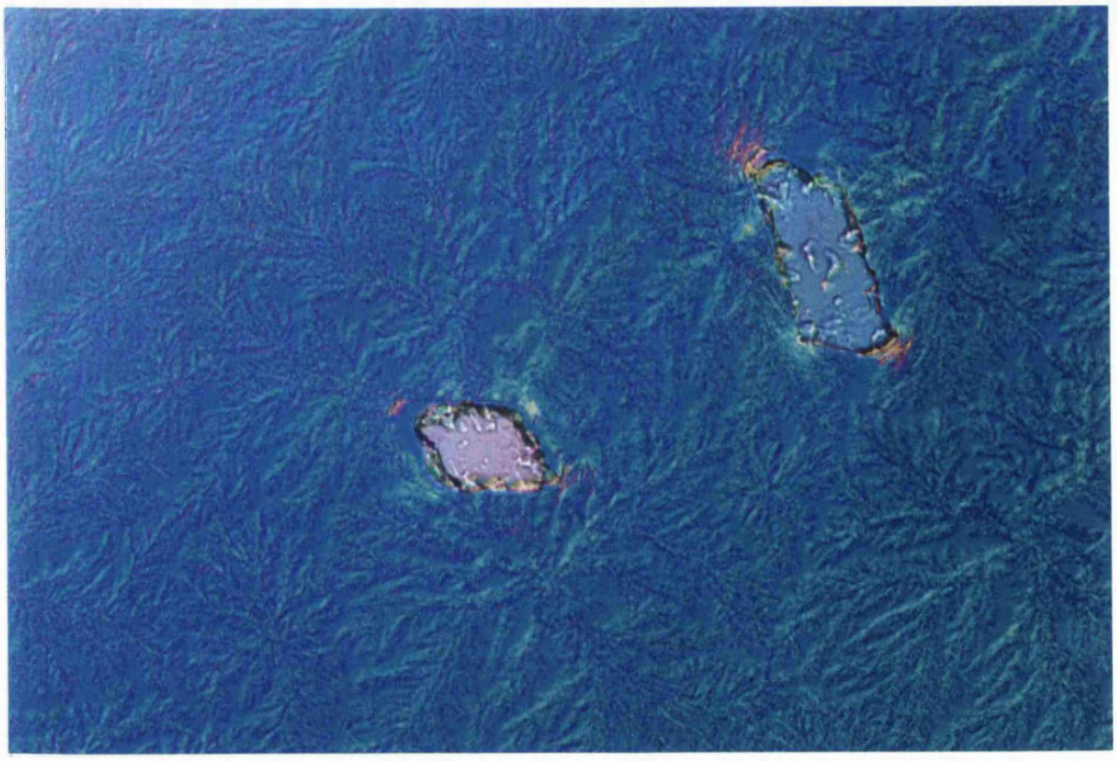

Plate 7.15: 10% paracetamol in G50/13 aged for 90 days at 37°C under DIC at 46°C **1:110**

Plate 7.16: Freshly prepared 10% caffeine in G50/13 under DIC **1:440**

though superimposed by the form of Peak 3) because of its higher stability. The paracetamol particles were completely melted between 132.5°C and 147.5°C.

6.3.3 10% caffeine in G50/13

The samples for the 10% caffeine dispersion in G50/13 were thicker than the other samples and this made the structure of the crystals less defined under microscopy at room temperature, as demonstrated by Plate 7.16. This was due to the tendency of the drug particles to aggregate which resulted in more of the G50/13 being pulled towards the particles when molten and so when set, there was more matrix between the slide and the cover slip. The first phase transition due to melting observed for 10% caffeine dispersion sample was at about 34°C. The melting seemed to occur in layers; after the top layer had faded, the underlying layer almost all diminished by 44°C. This then revealed the drug particles in the form of needles dispersed all over the matrix which became even clearer with the melting of the background gelucire structure from 48°C. The needle-like particles of caffeine could have been formed during the preparation of the sample where part of the drug was solubilised in the molten carrier. The drug then crystallised out upon setting the sample and the random dispersion of the needles could have been due to the stirring of the mixture during the incorporation of the caffeine. The origin of these fine particles was confirmed when heating the sample to 75°C showed that the entire recrystallised drug dissolved in the molten carrier. The rest of the caffeine particles were found to have melted between 208°C and 215°C, well below the melting ranges of caffeine on its own which was 234-239°C.

Polarising microscopy as expected, could not detect the initial melting clearly. Moreover, the thickness of the sample made any changes under the crossed-polars less apparent. However, as with the DIC, the drug needles could be seen clearly from 44°C, corresponding to the melting of Peak 2 (43.9°C) on the DSC thermal profile and even more so from 48°C onwards, corresponding to the melting of Peak 3 (48.4°C).

The phase changes occurred at about the same temperatures for the samples aged at 20°C with the melting from 34°C onwards revealing the fine needles of caffeine embedded in the

remaining matrix. By 44°C, most of the Peak 2 form had finished melting as indicated by another phase change under DIC (Plates 7.17 and 7.18). The melting of each form was suggested by the increased visibility of the fine drug crystals in the needle-shape which could be clearly seen under polarising microscopy. This technique of microscopy also showed that after ageing at 37°C, the morphology was still obscured by the thickness of the sample, as exemplified by Plate 7.19, but at 45°C, a lot of the gelucire structures had melted thus revealing the caffeine needles (Plate 7.20). Ageing for longer (90 days) at this temperature showed under polarising microscopy that a phase change had already occurred at 42°C which was the melting of the lowest temperature form. At 46°C, another phase change started to occur and this corresponded to the melting of the form with the greatest heat of fusion value, Peak 2, and the structure that remained was small and round which persisted until 58°C. This structure was also seen for the pure G50/13 sample aged under the same conditions. Also from this temperature onwards, the fine caffeine needles could no longer be seen and could be assumed to have dissolved in the molten carrier. This demonstrated that increasing the period of ageing at 20°C did not affect the structures to a great extent but doing the same at 37°C lead to an elevation in the melting ranges.

7.4 Conclusions

Microscopy techniques confirmed the postulation made under Chapter 2 that the different gelucire forms which gave rise to the various endotherms on the thermal profiles were present from the beginning of the process. In other words, no transformation from one form to another occurred during the actual heating programme of the DSC nor the HSM. The morphology of the higher temperature form was revealed rather than developed as the lower temperature form melted and this was correct for the fresh as well as the aged samples.

The presence of crystals at the lower temperature range as observed by polarising microscopy confirmed that the lower melting peak was not composed of amorphous structures. Ageing the pure G50/13 samples at 20°C only led to melting temperature being slightly higher and the outline of the structures observed for the fresh samples being more intensified, reflecting the slightly higher stability and crystallinity of the aged structures. The dominance of the higher melting form at the expense of the lower form was reflected

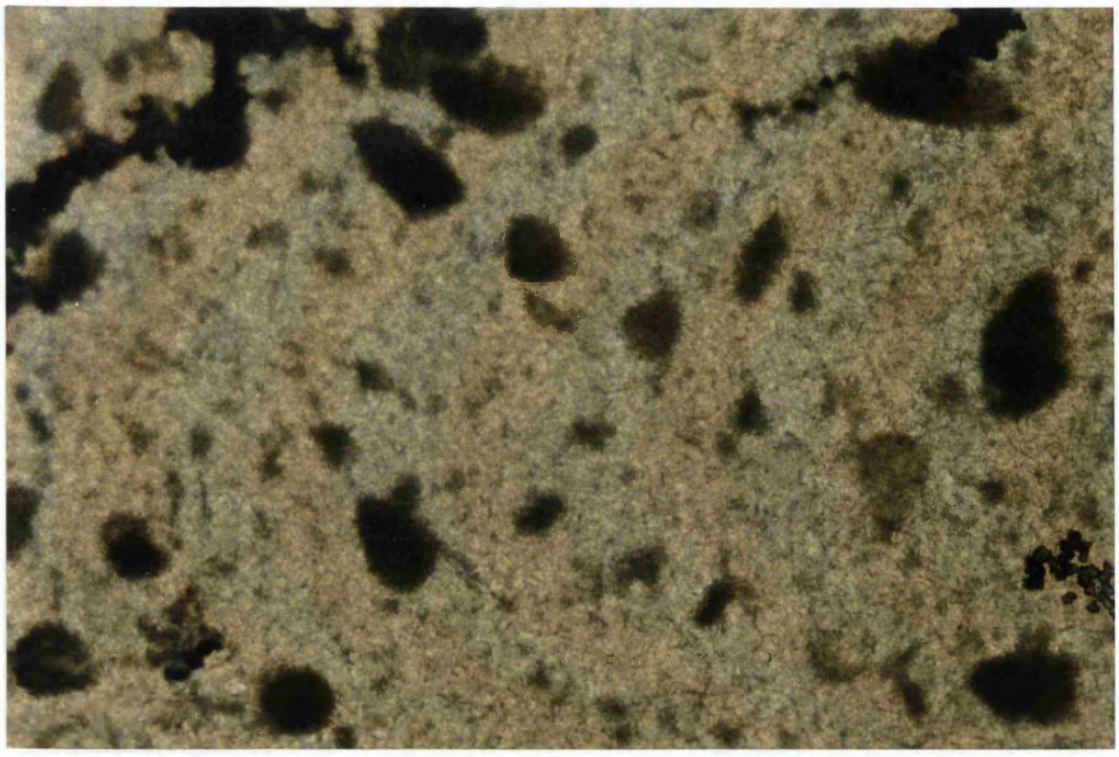

Plate 7.17: 10% caffeine in G50/13 aged for 7 days at 20°C under DIC 1:110

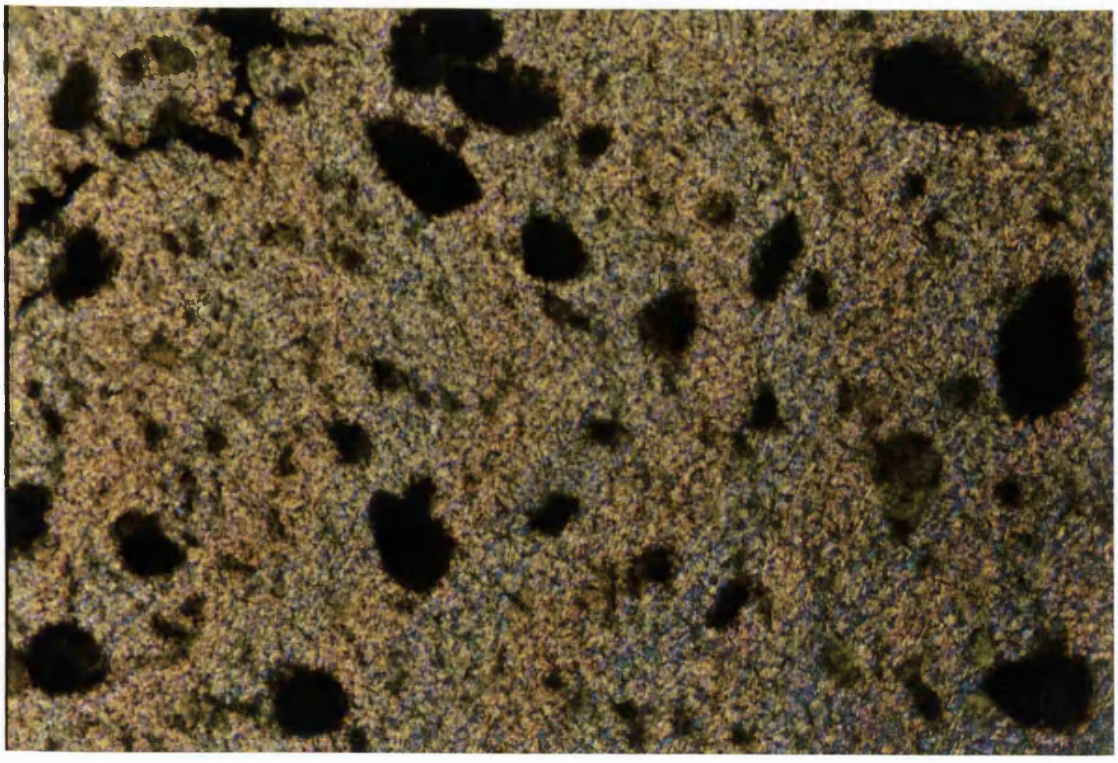

Plate 7.18: 10% caffeine in G50/13 aged for 7 days at 20°C under DIC at 44°C 1:110

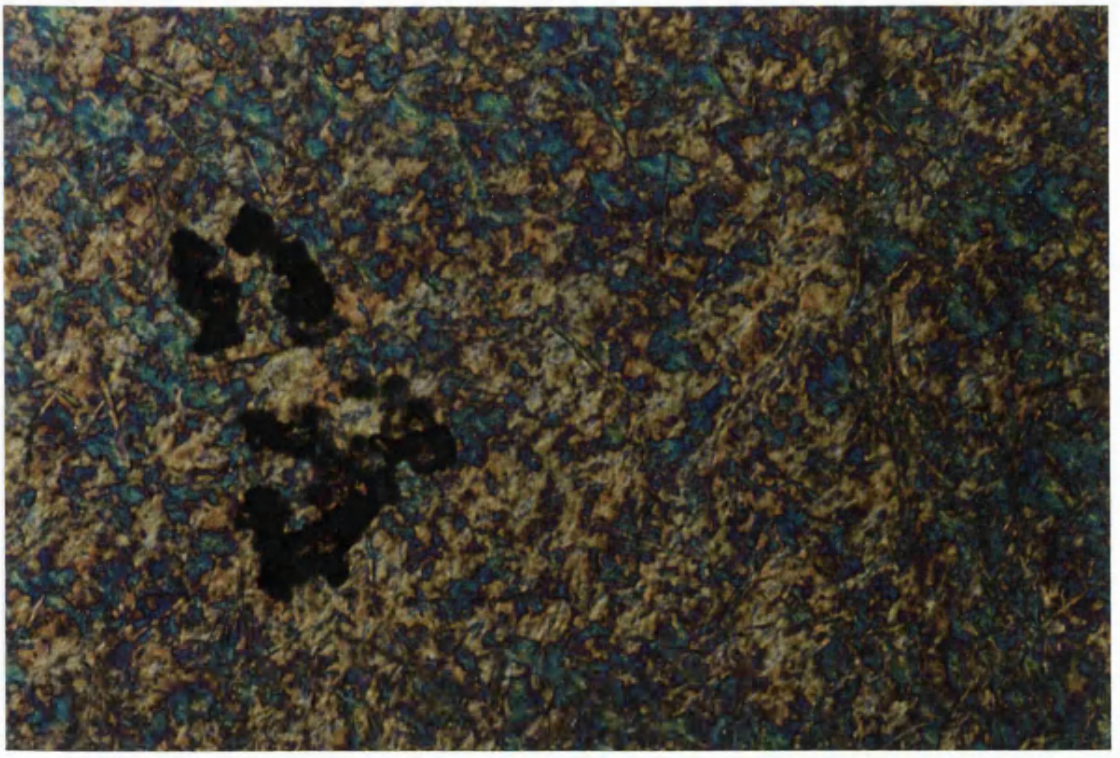

Plate 7.19: 10% caffeine in G50/13 aged for 7 days at 37°C under DIC 1:440

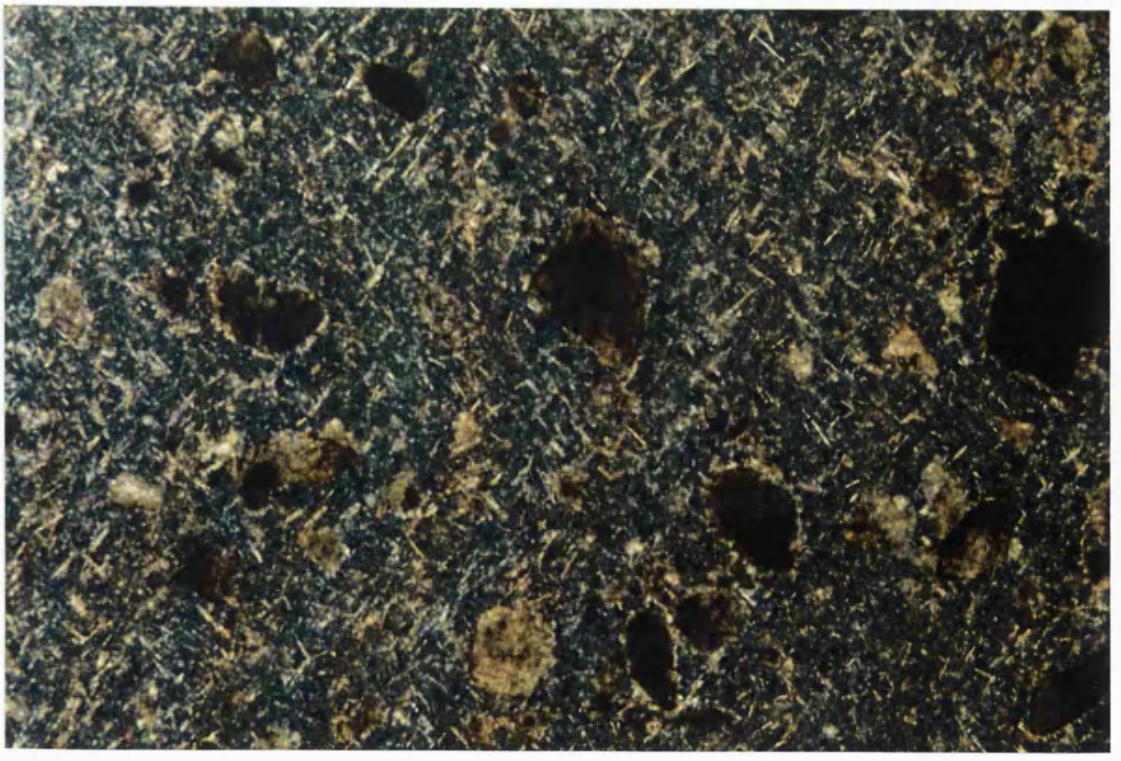

Plate 7.20: 10% caffeine in G50/13 aged for 7 days at 37°C under DIC at 45°C 1:110

by the late onset and the more extensive melting of the main gelucire structure after storage at 37°C. However, even though Peak 1 had merged with Peak 2 as seen for the DSC thermal profile, the structures observed under microscopy for this sample indicated that the form that was in the lower melting peak was still present here. Therefore, this suggests that the LMF was also made up of other constituents besides the metastable forms of MMF or HMF components. Polarising microscopy revealed an increase in crystallinity after ageing.

The bigger magnitude of melting at the beginning of the heating process suggested that the proportion of the lower melting form for the paracetamol dispersion sample was larger than the pure G50/13 sample. After storage at 37°C, the proportion of this form decreased but an increase was seen for the higher melting form represented by a bigger crystalline structure and which higher stability led to the persistence of this form even at higher temperatures. The thickness of the layers on the microscope slides of the caffeine dispersion samples meant that the structures could be discerned less distinctly. However, the proportions of the forms melted at certain temperatures were similar to the pure G50/13 samples.

The changes observed under microscopy reflected the changes seen on the DSC thermal profiles for the fresh and the aged samples. The lower melting form had a more diffused morphology whilst the higher melting forms gave a more distinct structure with bigger crystals indicating the latter were made up of more stable forms. Ageing resulted in a bigger proportion of the larger crystals developing, confirming DSC findings that storage, especially at 37°C allowed the transformation to more stable polymorphic forms.

Part II : Scanning Electron Microscopy (SEM)

The morphology of the gelucire samples was not restricted to being investigated by polarizing or DIC microscopy. For a more topographical image of the structures especially on the surfaces of the matrices, SEM was employed.

7.5 Introduction

7.5.1 The Principles of Scanning Electron Microscopy

In SEM, the specimen can be regarded as the origin of many radiation emissions. Each emission from every point on the specimen can impart information about the structure and composition of the material. In simple terms, in SEM, the radiation from the electron gun acting as the source is focussed into a probe (Figure 7.1). The probe is in the form of a beam of energetic electrons and directed by the scanning deflection coils, it then rasters, i.e. moves in x-y direction line by line across the specimen. The coils, situated near the objective lens, are electromagnetic and are subjected to electric signals to control the scanning. The resolving power in this microscope is limited by the size of the focussed probe. Therefore, the condenser here acts similar to the objective lens in a light microscope because the objective lens determines the resolving power there (Slayter and Slayter, 1992). The whole set-up is under vacuum to allow the flow of electrons. The resultant radiation leaves the specimen as an output signal which is then collected by the input transducer, usually a scintillation device which discharges a stream of visible photons when hit by an electron. From the transducer, the signal enters the amplifier situated outside the high-vacuum region and subsequently the signal can be applied to an oscilloscope in order to form an image on the TV screen or applied to a computer for data processing (Skoog et al, 1998).

One of the advantages of using this technique is that any mode of radiation from the probed specimen can be chosen. In other words, a specific portion of the radiation emitted from the sample can be picked out. The most common is the secondary electrons mode. This further enhances the image contrast which since having a greater depth of field, can be observed

more readily by the viewer than a transmission image. Additionally, the contrast can also be adjusted electronically. In this form of microscopy, there is no need to make the specimen as thin as possible to impart transparency. With most SEM instruments, the resolution is around 10nm, with an optimum of 3nm. Its magnifications can be from 1,000 (which is the highest in light microscopy) to 20,000 times the original image.

Figure 7.1: Organisation of the column of a SEM (Lee, 1993).

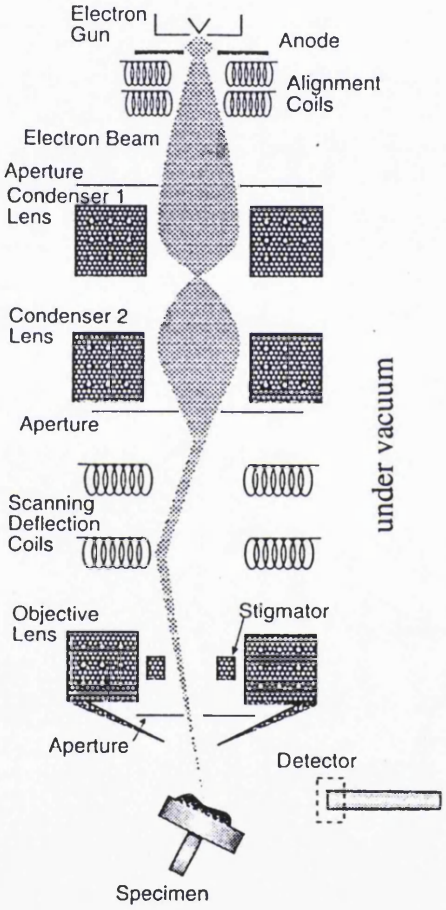

The specimen is usually coated with about 10nm layer of metal coating (gold or palladium, sometimes platinum), applied by a sputter coater at low vacuum. This is done because heavy metal improves the specific contrast of the image by enhancing the electron reflection and by providing a homogenous source of secondary electrons. Resolution is improved when the re-emitted electrons only originate from the secondary electron source rather than from collisions further down the specimen. Furthermore, the metal coating also protects the specimen from mass loss due to beam damage, provides a layer of high thermal

conductivity and thus minimising the overheating of the specimen, and also stream off excess surface charge in order to minimise charging artifacts on the image (Slayter and Slayter, 1992).

7.5.2 Characterisation of lipid formulations and their polymorphic forms with SEM

SEM had been used to characterise the surface of formulations such as wax microparticles (Bodmeier et al, 1992) whereby the porosity of the Gelucire 64/02 microparticles was attributed to its partial hydrophilicity, causing a fraction to dissolve in the aqueous medium it was made in. To obtain the optimum formulation parameters to make lipid micropellets by spray drying and spray congealing, the surface microstructure of the end-products was examined with SEM (Eldem et al, 1991a). It was found that even though some carriers had the same dominant triglyceride in them, the other minor glyceridic components were different and this difference may lead to different surface structures and crystallization properties on the pellets.

More importantly in terms of this study, SEM is also used to characterise the polymorphic forms of lipids, for example when the lipidic dosage forms are made through different methods. Spray drying and spray congealing lipid micropellets made from glycerol behenate and glycerol tristearate have shown that both processes result in the crystallisation of the unstable form which transforms into the stable form on storage at high temperatures (Eldem et al, 1991b). Together with DSC, the crystalline and compositional properties of cocoa butter crystals were elucidated (Manning et al, 1985). Holding the crystallization process at various temperatures caused different crystal structures to appear under SEM. These differences were confirmed with DSC which showed a different population of polymorphs for each of them. Similarly, SEM had been able to reveal the various patterns of polymorphs of several monoacid triglycerides and hydrogenated canola oil which thermal properties were already determined by DSC (deMan et al, 1985).

Besides DSC, SEM has also been used in conjunction with X-ray crystallography in order to determine the crystalline state of the formulation. Storing the solid dispersions of tolbutamide with urea at 25°C for five months revealed crystal growth under SEM.

However, the X-ray pattern of this aged dispersion was indistinguishable from the fresh dispersion which showed no drug peaks at all, hence indicating that the crystalline growth observed under SEM was due to the carrier, urea.

The objective of this current study is to determine whether the crystal structure of the matrix would be altered by the ageing process. By using this method, the morphology of the matrix can be observed on the actual melt-fused tablets that were used for the other analyses and the feasibility of SEM as a complementary technique can be assessed.

7.6 Materials and Methods

The melt-fused moulded tablets were prepared in the same manner as described in Chapter 4 previously. Two tablets were used for the scanning of each type of sample. One tablet was scanned with the upperside (the side where excess matrix had to be removed from by a sharp blade during manufacture) upwards and the other tablet with the underside (the side which comes in contact with the mould) upwards. The tablets were kept in a silica gel desiccator at 0% RH at 20°C and 37°C. Freshly made samples (made and stored in a silica gel desiccator within 24 hours of scanning) and samples stored under conditions stated above for 7, 30, 90 and 180 days were scanned. The stored samples were allowed to equilibrate to room temperature under silica gel for 24 hours before scanning. The samples were then attached to the SEM stub using DAG carbon cement (Leit-C) and placed in Emitech K550 Sputter Coater for 3 minutes at 30mA using a gold target to achieve the coating. The samples were viewed and photographed under Phillips XL20 Scanning Electron Microscope.

7.7 Results and Discussions

In contrast to the other chapters, the results here will be discussed under the headings of each storage condition rather than the type of sample, that is pure G50/13, 10% paracetamol or caffeine in G50/13. This is because the observations indicated that the more substantial changes were brought about by the ageing and the temperature of storage.

7.7.1 Freshly prepared samples

Microcracks were seen on the surfaces of the freshly made pure G50/13 and 10% caffeine samples as exemplified in Plate 7.21 for the latter, with more being observed on the surfaces of the caffeine samples. These microcracks could have been due to the contraction of the matrix as it set and recrystallised, as the solid gelucire occupied less volume than the more mobile molecules of the melt (Small, 1986). The various gelucire forms that gave rise to the peaks on the DSC thermal profiles (see Section 3 of Chapter 6) could have different degrees of contraction thus resulting in splits in the matrix. The extent of the contraction of fats can also depend on the type of polymorph, for example the α, β' and β forms of cocoa butter have the contractions of 0.060, 0.080 and 0.097 ml/g respectively (Seguine, 1991). Patches of rough-surfaced irregular structures were seen at some of the junctions of the microcracks in both samples. The patches were slightly smaller in size (in the region of 350 by 150μm^2), on the caffeine samples than the pure samples. The limitations of the SEM mean that we cannot be sure whether the structures emerged from between the cracks or are just imperfections of the surface at the area of weakness surrounding the microcrack junctions.

Plate 7.22 revealed that the 10% paracetamol dispersion sample had patches of dark areas with no defined shape which could be due to a softer matrix. Being under vacuum and coated, some regions then appeared darker. The nature of this sample under SEM confirmed the findings of Chapter 2 which showed that the incorporation of paracetamol resulted in a bigger proportion of the lower melting form of the matrix being stabilised, which endotherm was under the designated Peak 1.

7.7.2 Storage at 20°C

After 7 days of storage, the microcracks deteriorated and this extended to the development of crags for the caffeine samples (Plate 7.23). The undersides of the moulded tablets (which came in contact with the aluminium mould and which surface was not scraped by the blade) also had microcracks similar to the uppersides. The surfaces of the 10% paracetamol dispersion sample still had dark patches, as revealed by Plate 7.24. Again, this showed that

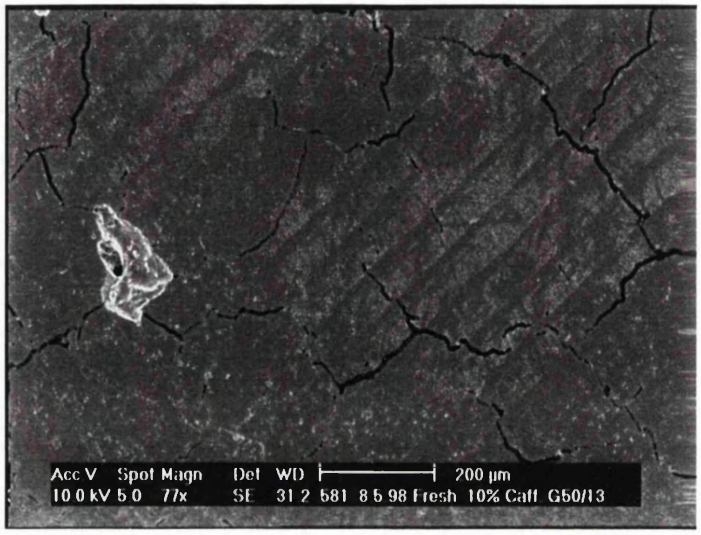

Plate 7.21: Freshly prepared 10% caffeine in G50/13

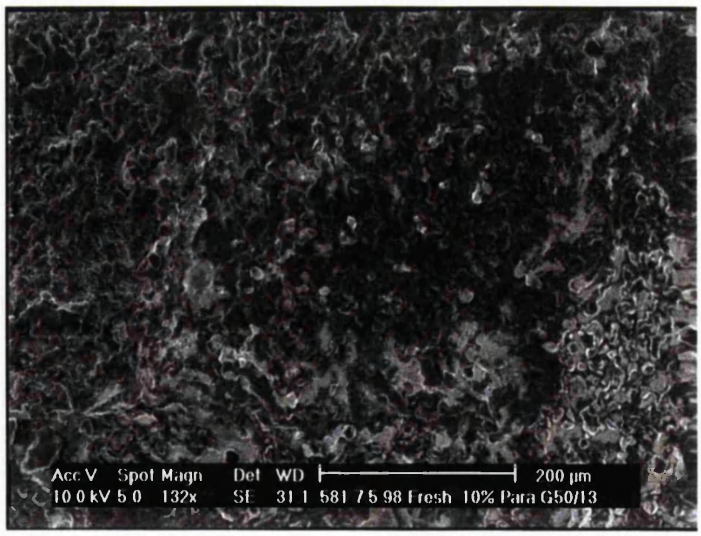

Plate 7.22: Freshly prepared 10% paracetamol in G50/13

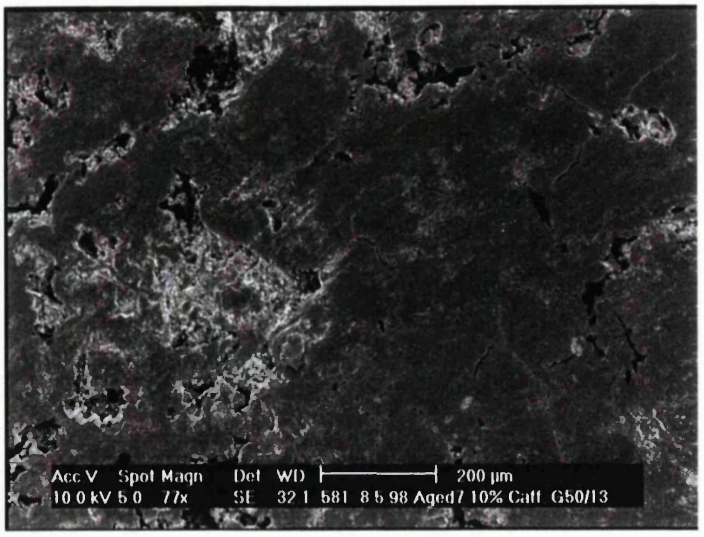

Plate 7.23: 10% caffeine in G50/13 aged for 7 days at 20°C

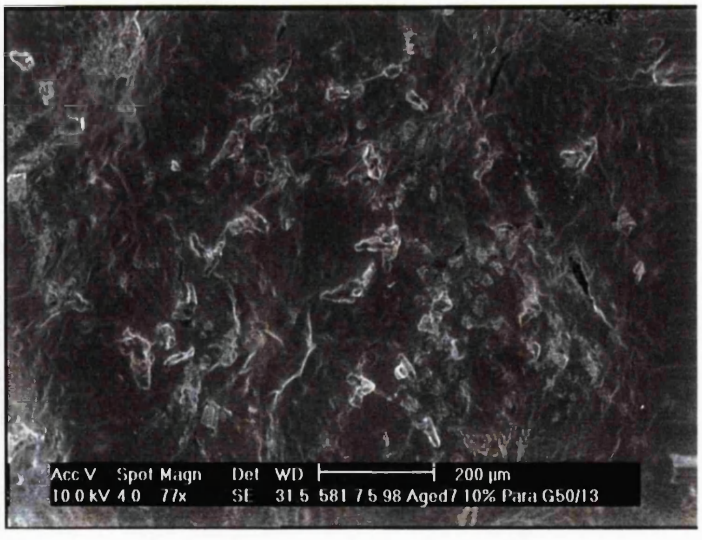

Plate 7.24: 10% paracetamol in G50/13 aged for 7 days at 20°C

the lowest melting form was the biggest proportion of the matrix.

The microcracks on the surfaces can no longer be observed after 30 days of storage, perhaps due to the roughness of the surface. Structures which resembled scales were seen in abundance (Plate 7.25). Interestingly, in the crags on the surfaces of the caffeine dispersion samples, thin needle-like structures could be seen jutting out with some looking more string-like. These needle-like structures were of variable lengths with widths of about 2μm (Plate 7.26). Plate 7.27 showed that the 10% paracetamol sample no longer had dark patches and its surface had become rougher than the pure sample with rocky structures approximately from 8 by 4 μm^2 to about ten times that size being observed. These structures could be formed from the crystallisation of the previously soft and oily matrix. It could also be due to the gelucire being sucked out by the vacuum as previously seen in the paracetamol samples stored for a shorter period of time. However, this is unlikely as it would have been more feasible for the softer fresh and 7 days stored samples to show this rocky surface due to the greater ease of being sucked out than the 30 day stored sample. Moreover, Figure 6.4 in Chapter 6 showed that the proportion of the Peak 1 form had decreased in contrast with the Peak 2 form indicating that the rocky structures may be the transformed gelucire.

After 90 days storage, structures that looked to be possibly the beginning of scales-like and leaf-like structures were emerging from the surface of the pure G50/13 and caffeine dispersion samples, as demonstrated for the former (Plate 7.28). All the samples still showed some dark regions and the paracetamol dispersion sample showed spherical structures which could be the soft gelucire being sucked out. Plate 7.29 shows that the surface of the pure G50/13 aged for 180 days was similar to the 90 days aged sample except scalier and this also applied to the 10% caffeine dispersion sample. The 10% paracetamol sample still showed the soft spherical structures. Overall, even though all the samples showed less dark patches than the 90 day samples indicating an increase in crystallisation of the matrix forms, the persistence of these regions suggests that the lowest melting form was still in a sufficiently large proportion to cause this characteristic.

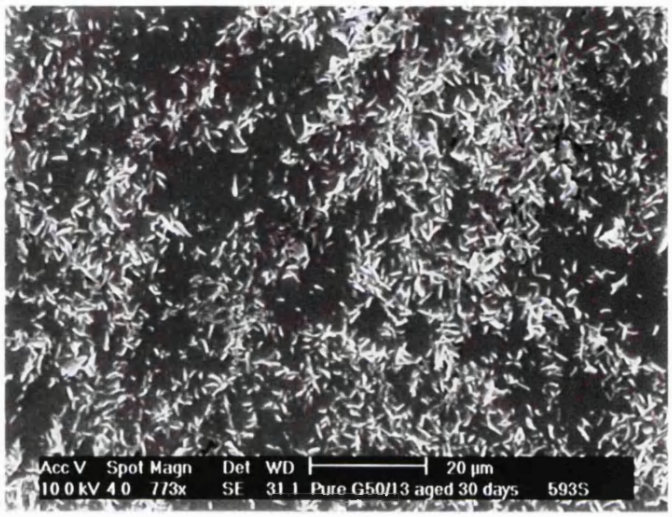

Plate 7.25: Pure G50/13 aged for 30 days at 20°C

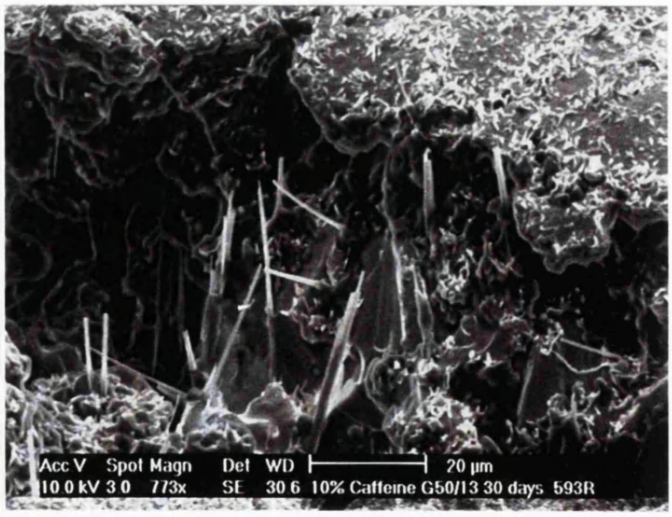

Plate 7.26: 10% caffeine in G50/13 aged for 30 days at 20°C

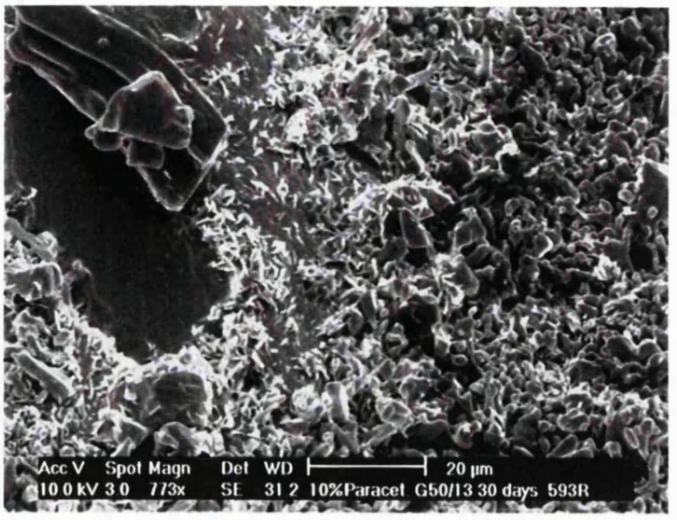

Plate 7.27: 10% paracetamol in G50/13 aged for 30 days at 20°C

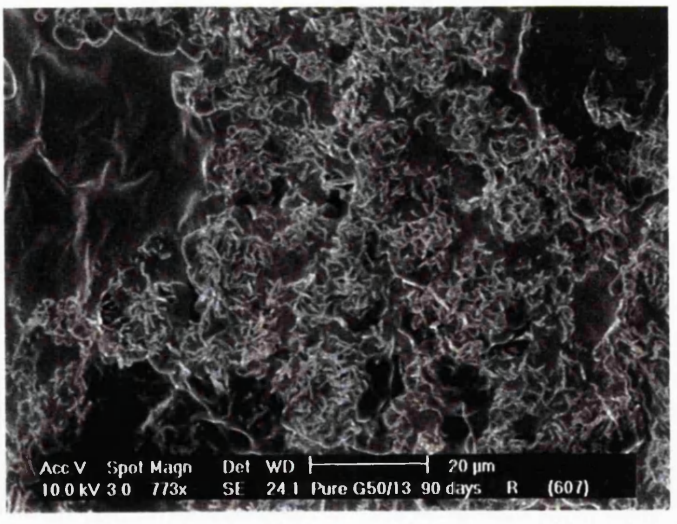

Plate 7.28: Pure G50/13 aged for 90 days at 20°C

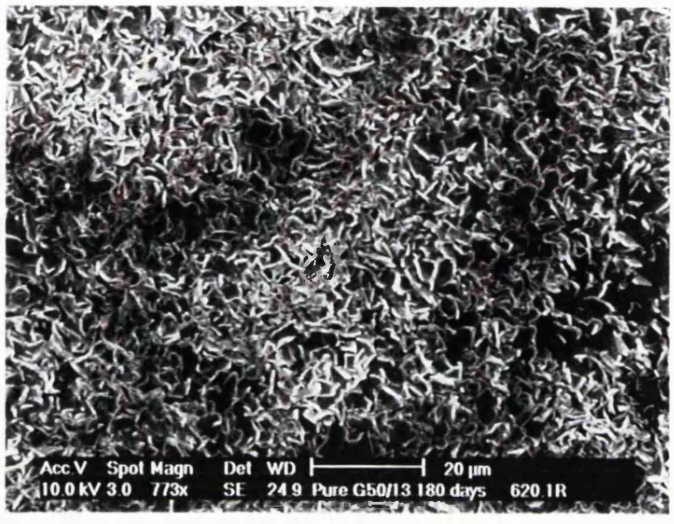

Plate 7.29: Pure G50/13 aged for 180 days at 20°C

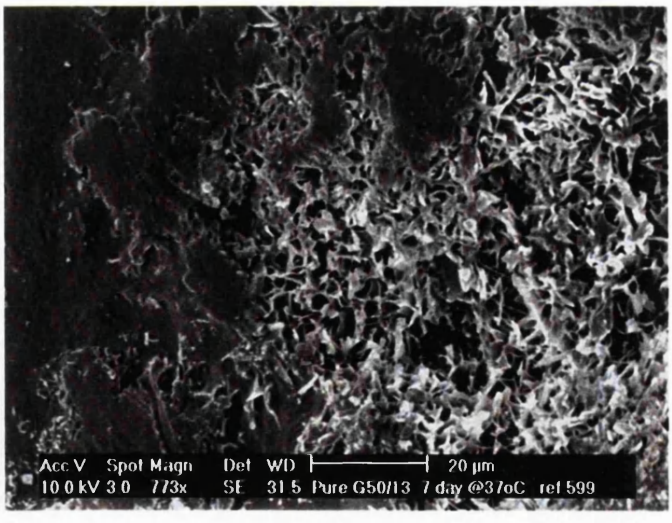

Plate 7.30: Pure G50/13 aged for 7 days at 37°C

7.7.3 Storage at 37°C

Microcracks which were seen previously on the surfaces of the pure and caffeine dispersion samples stored at 20°C after 7 days were not visible here. During storage at this higher temperature, the more mobile gelucire molecules could have occupied the spaces where previously there had been cracks. Contraction of the matrix is greatly minimised when the fatty base had undergone a tempering process and a stable glyceride modification was obtained (Müller et al, 1989). The surfaces of both samples were rougher and scalier than their respective samples stored at the same number of days at 20°C as exemplified by the pure G50/13 sample (Plate 7.30), and there were no significant differences between the pure and the caffeine samples. However, the surface morphology was vastly different for the 10% paracetamol dispersion sample. There was no longer any dark patches or softness to the sample, as was when stored at 20°C. A very `leafy' layer, as can be seen in Plate 7.31, had pushed through the smoother top surface. The leafy structure was the largest gelucire structure to be seen under SEM and each `leaf' measured about 15μm by 7μm long. The occurrence of this structure coincided with the transformation of the Peak 1 form to the subpeak 1 and Peak 2 forms (refer to Figure 6.5 in Chapter 6). This suggests that the lower melting form which had previously contributed to the soft nature of the matrix had converted to higher, more stable forms with correspondingly larger crystal sizes.

The scaly structure of both the pure G50/13 and the 10% caffeine dispersion samples had become more prominent and compact by 30 days storage as exemplified by Plate 7.32 for the pure sample. The scaly structure of the caffeine samples gave string-like projectiles from their tips, which are finer than the needle-like projections from the sample stored at 20°C (Plate 7.33). The width of the string is about 0.25μm and can be as long as 7μm. From the DSC data in Appendix 3, it could be seen that greater changes occurred in the Peak 3 and Peak 4 forms for the caffeine dispersion sample when stored at 37°C. At this stage, it could be postulated that these projections were due to these respective forms. From Plate 7.34, it could be seen that the structure for the 10% paracetamol became more compact with a slight change in its morphology compared to the 7 days aged sample. Such change is reflected in the appearance of the subpeak 2 form (Figure 6.5, Chapter 6) which resulted from the transformation of the lower melting forms.

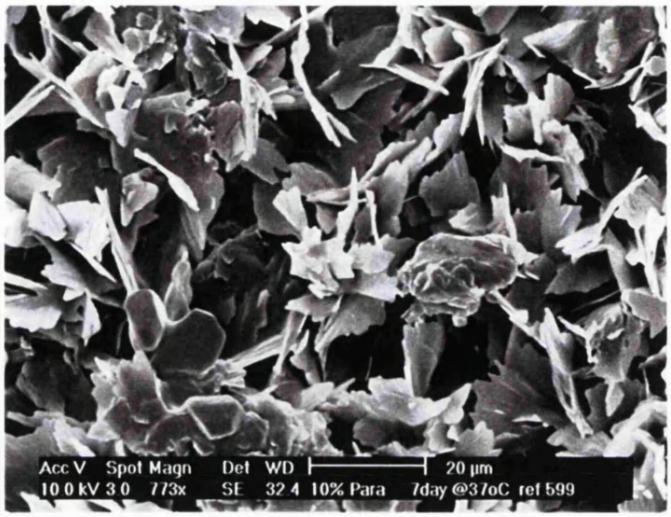

Plate 7.31: 10% paracetamol in G50/13 aged for 7 days at 37°C

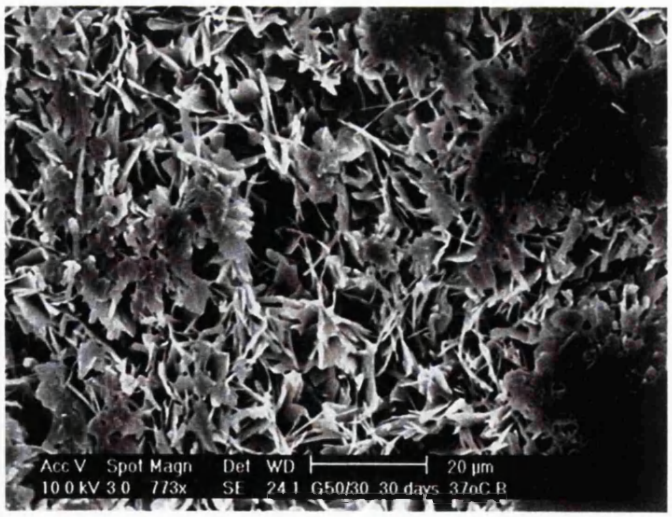

Plate 7.32: Pure G50/13 aged for 30 days at 37°C

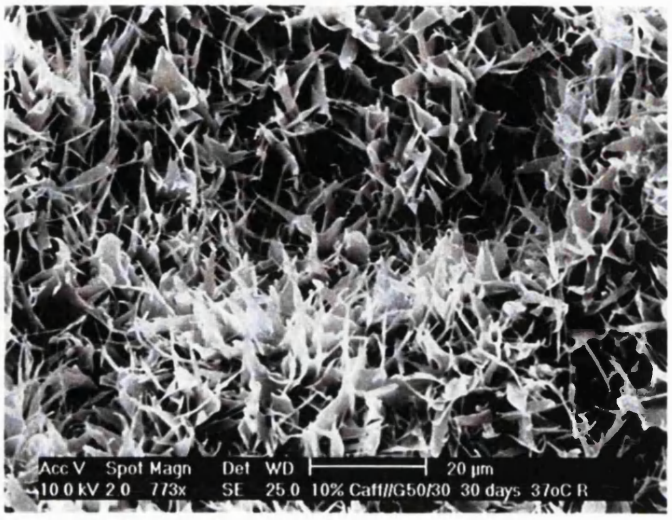

Plate 7.33: 10% caffeine in G50/13 aged for 30 days at 37°C

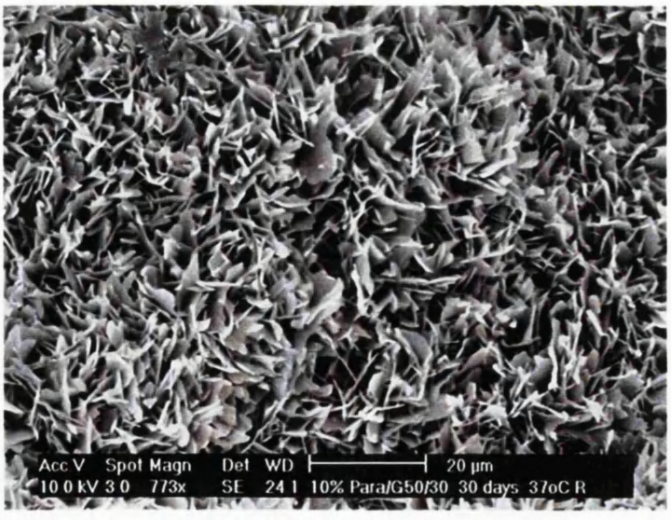

Plate 7.34: 10% paracetamol in G50/13 aged for 30 days at 37°C

Samples stored up to 90 days showed a more dense scaly and leafy layer. The sizes of these structures were quite similar for all the samples. The stringy projectiles could no longer be seen on the upperside of the caffeine dispersion samples but now were present at both undersides of the pure and caffeine moulded tablets, as shown in Plate 7.35 for the pure sample. The strings on the leaf structures of the caffeine samples seemed thicker (about 65μm) and longer (about 12μm) than those after 30 days storage. Peak 3 with its greater heat of fusion due to the incorporation of Peak 4, as shown in Figure 6.7 in Chapter 6, could be responsible for this modified caffeine structure.

There was almost no difference between the samples aged 90 and 180 days at 37°C for the pure G50/13 and 10% caffeine dispersion samples except for a very slight increase in the scaly structure size as shown by Plate 7.36 for the pure sample. The stringy structures were also no longer present on all the samples. Smooth patches which were still present in the 90 days samples were absent from the 180 days samples which also did not show any dark patches. The uppersides were similar in appearance to the undersides of the tablets for each of the sample. The paracetamol dispersion sample did not vary from the other samples stored at different times. These observations indicate that the system had been stabilised and that the morphology will no longer change in a significant manner with increasing number of storage days.

The surfaces of the samples generally became rougher as the storage period became more extended. This was due to the increasing crystallinity of the samples and the crystals were forced to develop out of the surface because of the spatial availability. As the number of days of storage increased, bigger crystals developed and pushed through the smoother upper layer of the tablet (Plate 7.29). In the confectionery industry, such roughness can be detected by the naked eye on chocolate or cocoa butter products. A score system was devised whereby the degree of glossiness or dullness of the surfaces determines the acceptability of the product (Laustsen, 1991; Samsudin and Rahim, 1996). The imperfections on the surfaces of the samples could have also contributed to the roughness whereby the unevenness of the surface due to the scraping of excess fat during preparation of the moulded tablets with a blade might have provided a base from which the crystals could develop from. Areas where the blade came into contact with the gelucire and pressure

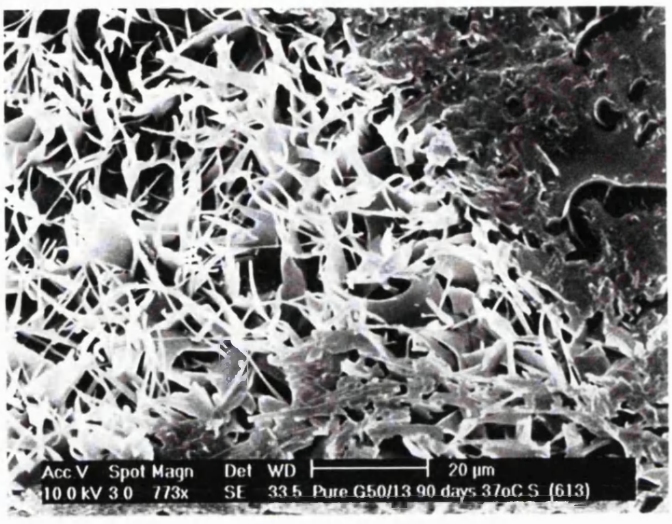

Plate 7.35: Pure G50/13 aged for 90 days at 37°C

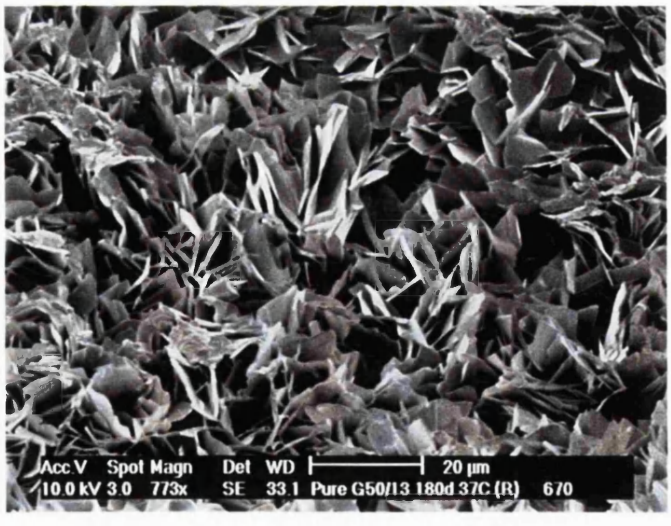

Plate 7.36: Pure G50/13 aged for 180 days at 37°C

was applied may have become the smooth patches still found on the samples even after many days of storage. The pressure may have compressed the growing crystals and changed the form to a type that resisted morphological modifications. Added to that, the rate of cooling would have been faster on the surfaces as they were exposed to the ambient air and the aluminium mould, resulting in a different form of crystals to develop from within the tablet. Heathcock (1993) elaborated on the plate-like crystals of cocoa butter that were able to pack flat against a mould transforming into elongated crystals frequently of more than 1μm.

The increase in crystal sizes upon ageing suggests that the more stable form of gelucire had larger crystals. This is consistent with the observations of Eldem et al (1991) who found that spray-congealing lipid micropellets of various types and composition produced unstable polymorphic structures due to their rapid crystallisation from melts which resulted in smooth surfaces. This development from smooth to rough surfaces was also indicated by Sato (1988) who described the crystal of the α form as very thin, measuring less than a few micrometers and the β form as large crystals with sizes between 20 and 100μm which often develop in clumps. The needle-like projections seen on the caffeine dispersion sample at 30 days ageing at 20°C (Plate 7.26) could be the β′ form of a lipid component as Sato (1988) described this form as having the morphology of long needles, of less than 5μm. The appearance of these needle-like projections on the caffeine dispersions samples before any projections could be seen on pure G50/13 samples could indicate that the structure was not due to the fatty base after all. The needles could be the drug crystallising out separately from the rest of the gelucire as had been shown previously under DIC and polarised microscopy, especially as the projections were seen within the crags and not on the surfaces.

The development of larger crystals upon the ageing of fat systems under certain conditions can be described as the 'blooming' effect (Hachiya et al, 1990; Flack and Krog, 1990) which was attributed to the rapid formation of the β phase (Lutton and Fehl, 1970). This effect is frequently stated in investigations which are concerned with the food industry such as dairy and confectionery. In chocolates, blooming was thought to be due to the transformation of the β-2 cocoa butter polymorphic form to the more stable β-1 form.

However, Laustsen (1991) showed that blooming could also be caused by other fats, even when they are mixed with cocoa butter. Lauric acid hard butter was mixed with different quantities of cocoa butter and the blooming effect was assessed. This study proved through gas-liquid chromatography that although the tendency to bloom increased with the concentration of the cocoa butter incorporated, the actual fats in the bloomed areas contain higher concentrations of lauric acids (C_{12}) than the initial fat phase. Thus the investigators postulated that the bloom was caused by the migration of the triglycerides, mainly trilaurin, to the surface of the compound rather than the migration of the cocoa butter as had been frequently thought. One of the explanations put forward for the increase in bloom when the cocoa butter concentration was increased was that more liquid fat was created by the eutectic effect caused by the incompatibility of the cocoa and lauric hard butters. This liquid fat could then migrate to the surfaces and recrystallise to form the bloom. In the current study, the small quantity of free fatty acids in G50/13 could also contribute to the migration of liquid fat to the surfaces.

However, this is not the only mechanism by which bloom can appear as the nature of bloom is a function of the fat system used (Laustsen, 1991). When domestic hard butters of the non-lauric type were mixed with cocoa butter, blooming was observed but the composition of the bloom was almost identical to the initial fat phase, in contrast to the lauric acid hard butter which bloom was more concentrated in that particular fatty acid. It was then thought that the blooming process here occurred due to crystal modification rather than the migration of the triglycerides as in lauric:cocoa butter mixture. Other explanations for blooming include the efflorescence or the incipient crystallisation of dissolved ingredients (Senior, 1974). This blooming is different from the more common fat blooming in that here, it is caused by the migration of components incorporated into the base which have melting ranges close to the storage temperature.

The greatest change however, was caused by storing the samples at 37°C (Plates 7.30 onwards). The blooming effect was more readily seen on cocoa:lauric fat butter stored at 37°C (Laustsen, 1991). Blooming had been reported as frequent occurrence for fats stored at temperatures near their melting range (Senior, 1974). When spray-dried micropellets containing GTS-33 (a mixture of 65% tristearin and 35% tripalmitin) were stored at

different temperatures, their initial unstable polymorphic forms were altered (Eldem et al, 1991). Storing them at -18°C and 4°C did not cause major changes to occur in that the unstable α form was still the dominant structure, which then melted upon heating and recrystallised as the stable β form. Keeping them at 25°C, however, resulted in the mixture of both α and β forms being present from the onset. Finally, only the stable form was found in the micropellets stored at 37°C indicating that all the unstable form transformed into this form when stored at this temperature.

Soft lipid products are more susceptible to bloom (Cebula et al, 1991) and this is because the low melting fats will be able to migrate to the surface more readily (Urbanski, 1991). This may be reason that the paracetamol samples which were soft and lacking a defined structure at the beginning of storage at 20°C (Plate 7.24), already had stable, large crystals at only 7 days storing at 37°C (Plate 7.31). The `strings' at the end of crystals on pure G50/13 or caffeine dispersion samples could be a segregated component of the matrix being pushed out (Plates 7.33 and 7.35). In cocoa butter, crystal protrusions were ascribed to Form III and Form VI polymorphs (Hicklin et al, 1985). Okada (1970) reported the growth of 'whiskers' in hardened palm kernel oil and hardened coconut oil, both of which contain lauric oil, when the fats were aged for 20 days at 5°C. The whiskers looked flat and those which developed from hardened palm kernel oil turned about halfway through the growth. Closer observation of these whiskers showed that there was a step-like pattern which developed in a particular direction. However, no whiskers could be seen after other storage conditions nor on other hardened oils. After ageing the G50/13 and its dispersions for 180 days, these `strings' can no longer be seen, perhaps they had become detached from the rest of the crystals or that the bases of the crystals had built up to the tip of the `strings' like the step-like pattern shown by Okada (1970).

Incorporating different drugs led to different morphology of the surfaces. Samples with 10% paracetamol dispersed in the G50/13 were very soft but those with 10% caffeine dispersed in them were more solid and similar in morphology to pure G50/13 samples. Eldem et al (1991) found that the incorporation of estradiol cypionate resulted in an adverse crystalline structure of lipid micropellets and it was thought that this drug acted as a destabilizing agent which disrupted the crystal packing and molecular arrangements of the

glyceride crystals. Paracetamol could have had the same disruptive influence on the G50/13 crystals, leading to lower stability crystals.

7.8 Conclusions

SEM was thought to be a feasible complementary technique in the characterisation of G50/13 structure. Ageing resulted in observable differences in the crystals of the matrices which confirmed the outcome of the DSC and DIC studies which also showed the influence of storage on the structure. It was also easier to distinguish the differences between the crystals using the SEM compared to polarising or DIC microscopy because of the three-dimensional image that was projected.

Storage increased the crystallinity of the structure, seen as the increasing roughness of the tablet surfaces. The developing crystals pushed through the surfaces from within the matrices when space became limited. Increasing the number of days storage at 20°C mainly led to more of these crystals developing whereas the same procedure at 37°C not only elevated the crystallinity but also showed some polymorphic transformation had occurred. Incorporation of different drugs also affected the structure of the matrices with paracetamol causing the lower melting form of gelucire to be stabilised. Ageing then affected this drug dispersion the greatest by increasing its crystallinity and transforming it to the more stable structure, seen as the compact and large crystals present on these matrices.

Part III : The effects of incorporating sorbitan monostearate into G50/13

7.9 Introduction

In Chapter 6, it was demonstrated that storing the G50/13 matrices at 37°C gave an accelerated ageing effect with the final structure produced being very stable. This is similar to a tempering process whereby a particular fat polymorph which is required is induced into formation by holding the initial fat at a certain temperature, with the exception that many of these processes were performed in order to maintain the fat at a less stable polymorphic form. However, this stable form produced by storage at 37°C had also resulted in large crystals pushing through the surfaces of the matrices, as observed under SEM (Chapter 7, Part II). Such large crystals alter the surface characteristics and may cause a disruption of the matrices.

The incorporation of additives such as surfactants can affect lipids although their influence on the polymorphic forms is different in fatty acids compared to triglycerides. In fatty acids, additives can act as modifiers of crystal structure during crystallisation and as retarders of polymorphic transformation in solution (Aronhime et al, 1990). The effectiveness of emulsifiers at this role depends on their molecular structure that is the balance between the ideal size of the hydrophilic moiety and the linear structure of the aliphatic chain, rather than their HLB number. In triglycerides, surfactants are thought to affect the mobility of the fat molecules and therefore the kinetics of phase transformation but not the arrangements of the molecules in crystal packing which is related to its thermodynamics. The influence of the emulsifiers on glycerides can shed light on the polymorphic transformation process, such as when the hydrophilic part of the emulsifier had more effect on the α to β transformation of trilaurin than the hydrophobic part, leading to the conclusion that the transformation was related to the glycerol moiety of the triglyceride.

Cocoa butter can exist in a number of polymorphic forms and the transformations of Form I to V was thought to be melt mediated whilst Form V to VI was thought to be solid mediated. Garti et al (1986) found that Form V could be prevented from transforming to

Form VI by adding sorbitan esters or mixtures with ethoxylated sorbitan esters. After ageing, the melting endotherm had split indicating that some of the V form had changed to VI and that the addition of sorbitan tristearate retarded this process.

7.10 Materials and Methods

10% w/w of sorbitan monostearate (SMS) (Sigma Pharmaceuticals, UK) was added to molten G50/13 in the same way that the model drugs were incorporated (see Chapter 4). SMS was chosen because it is a solid surfactant; solid surfactants had been shown before to retard polymorphic transformations whilst liquid surfactants had been shown to enhance transformations. A preliminary DSC study also showed that SMS has a melting point which would allow it to melt during the heat-fusion protocol used for G50/13 (Table 7.1). Furthermore, it has a small enough hydrophilic head to present structural compatibility with the lipid component (Aronhime et al, 1988). SMS is an amphiphilic molecule with a long saturated hydrocarbon chain which will allow it to crystallise together with the lipid component and the hydrophilic head will facilitate this by crystallising with the PEG component.

Table 7.1: Peak temperature and heat of fusion value for pure SMS.

peak temperature (°C)	53.4 ± 0.1
heat of fusion (J/g)	94.6 ± 0.2

7.11 Results and Discussions

Table 7.2: Peak temperature and heat of fusion values for 10% sorbitan monostearate (SMS) in G50/13 after ageing for 7 days at 37°C.

	1st peak	*2nd peak*	*3rd peak*	*4th peak*	*Total*
peak temperature, (°C)		44.2 ± 0.1	49.1 ± 0.2		
heat of fusion, (J/g)		137.1 ± 5.5	7.8 ± 0.9		147.5 ± 2.8

Comparing the results obtained from the DSC scans for the 10% sorbitan monostearate in G50/13 stored for 7 days at 37°C (Table 7.2) with those from pure G50/13 stored under the same conditions (Appendix 3), it could be seen that the temperatures for the remaining peaks for the matrix containing the SMS were similar to Peaks 2 and 3 of the pure G50/13 sample. This similarity indicated that the addition of the SMS had not affected the gelucire form that melted at those values. However, Figure 7.3 showed that the peak which melted at the higher temperature was broader than Peak 3 of the pure G50/13 (Figure 6.1). Such broadening suggested that the gelucire form of Peak 4 of the pure G50/13 could have either formed a solid solution with Peak 3 or that Peak 4 was a result of a polymorphic transformation from some of the Peak 3 structure and that the addition of SMS had suppressed this transformation.

Under SEM, pure G50/13 matrices had previously shown scaly and stringy structure as a result of a blooming effect when aged for 90 days at 37°C (Part II, Plate 35). After 10% SMS was added, the resultant matrix did not show the scaliness on either of its surfaces (Plate 7.37 and 7.38). The relative smoothness of the matrix indicated that the incorporation of SMS into G50/13 had prevented the blooming effect by suppressing the emergence of the bigger sized crystals. It was first thought that this effect acted on the form that gave the biggest peak on the DSC thermal profile by reducing its crystallinity but it was found that the proportion of the heat of fusion of this peak over the total heat of fusion was similar to the pure G50/13 sample. The most apparent difference between the thermal profiles of the pure G50/13 samples and those which incorporated the SMS was the suppression of the highest melting form (Peak 4 of the pure G50/13 profile). This then suggested that the blooming effect was mainly due to this form. The blooming phenomenon had been observed in substances containing fat before especially in chocolate products and had been defined as the migration to the surfaces of the chocolate of a molten fat or fractions of the mixed triglyceride of which the cocoa butter is composed and their subsequent solidification, resulting in a progressive loss of gloss (DuRoss and Knightly, 1965). Crystals were thought to be liquefied by the released heat of fusion as one polymorphic form transformed to a more stable one and creep to the surface by capillary action. It is possible therefore, polymorphic transformations that occurred during the storage gave out enough heat of fusion that a segregated fraction of G50/13 which most likely gave rise to

Figure 7.2: Thermal profile of 10% SMS in G50/13 after ageing for 7 days at 37°C

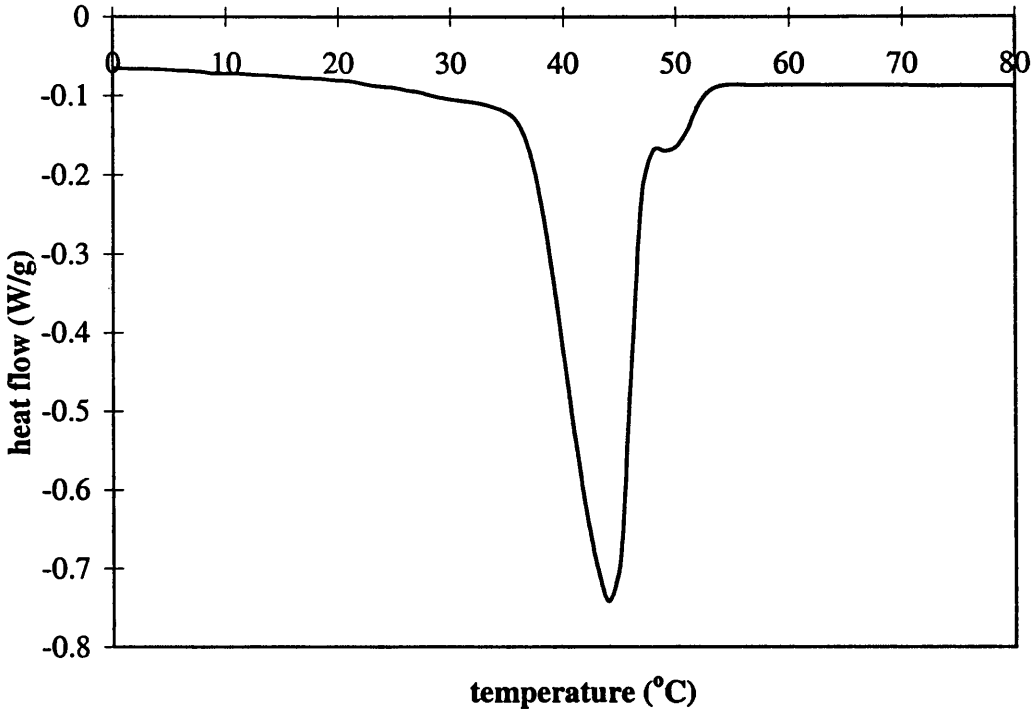

Figure 7.3: Thermal profile of pure sorbitan monostearate (SMS)

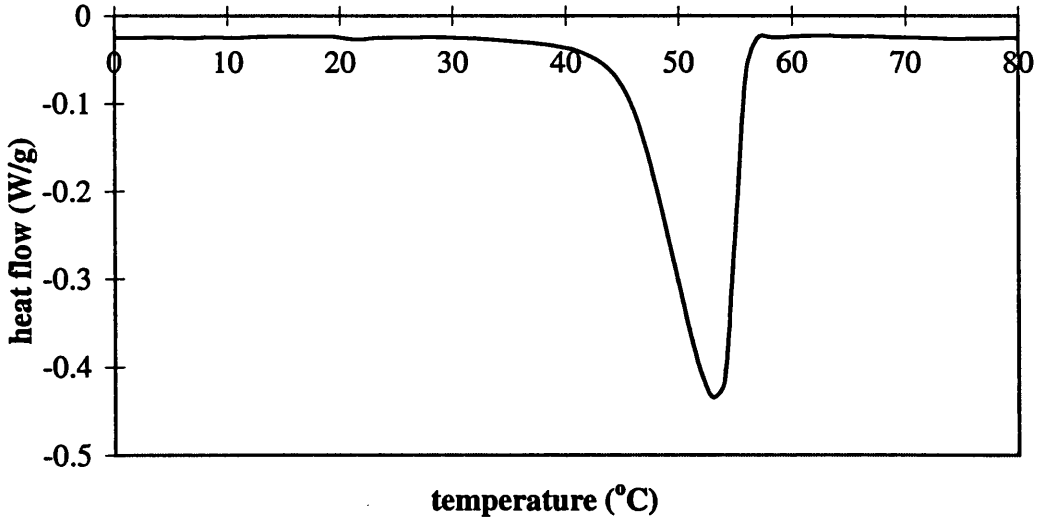

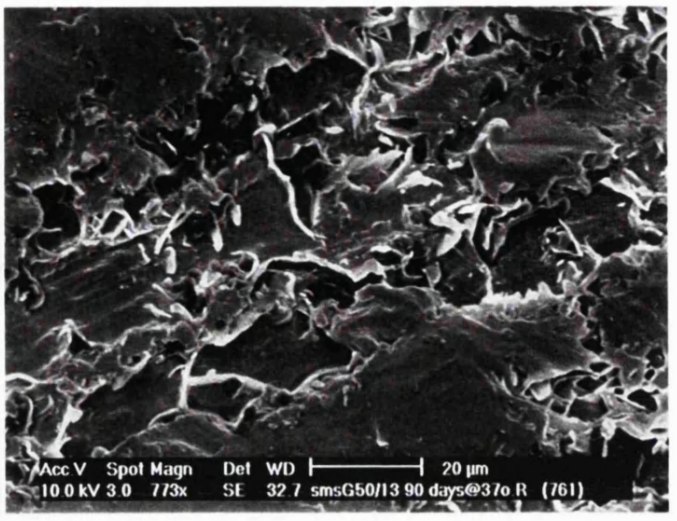

Plate 7.37: 10% SMS in G50/13 aged for 90 days at 37°C (upperside)

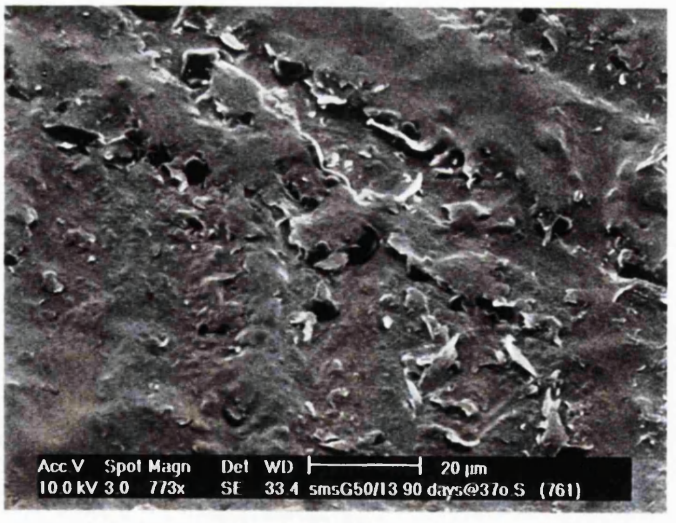

Plate 7.38: 10% SMS in G50/13 aged for 90 days at 37°C (underside)

Peak 4 of the thermal profile had diffused to the outer layer of the matrices. Referring to Appendix 3, the form of G50/13 which gave rise to Peak 4 increased in its heat of fusion value with time, corresponding to the rise in the total heat of fusion.

The rise in the heat of fusion value of this form over time was greater when stored at 37°C than at 20°C which was mirrored by the more intense blooming on the pure G50/13 matrix surfaces over time as seen under SEM when aged at 37°C as opposed to 20°C. This indicated that the migrated G50/13 fraction solidified and increased its crystallinity upon storage which manifested as the large, scaly structures. The presence of sorbitan monostearate prevented the segregated fraction from creeping to the matrix surfaces during polymorphic transformations (DuRoss and Knightly, 1965). It was thought that the surfactant was able to do this by forming a strong monolayer due to the presence of many hydroxyl groups in it. In other studies using surfactants in fats, the addition of solid sorbitan esters was found to retard the transformation of the V to VI polymorphic form of cocoa butter (Aronhime et al, 1990). The delay was thought to be due to the formation of hydrogen bonds between the hydroxyl groups of the surfactant and the carbonyl groups of the triglycerides. Such effect is possible only if the emulsifier has a good structural affinity with the fat; those which are not may actually have an opposite effect, that is to enhance the transformation instead.

The presence of Peak 4 form in samples without the SMS could be due to the solid-solid polymorphic transformation from the Peak 3 form because Peak 4 diminished when the emulsifier was added and sorbitan esters had been shown to hinder the solid-solid transformation (Aronhime et al, 1990). Thus, the negligible effect of the SMS on the proportion of the Peak 2 form indicated that most of the Peak 1 form to Peak 2 form transformation that occurred during the storage at 37°C was of the melt transformation type. Furthermore, the effectiveness of the emulsifier as a transformation retarding tool seemed to decrease the closer the holding temperature was to the melting temperature of the less stable polymorph, for example Peak 1 form. Guth et al (1989) found that at temperatures which were close to the α-form (of SOS) melting, the transformation of this form to the next more stable form, γ, was rapid and the retarding effect of SMS was small. After a longer period of ageing, this effect became even lesser and almost all the α-form was

allowed to transform to the γ form.

The impact of the blooming phenomenon would be the greatest in dosage forms which have a layer of coated gelucire on them. These include oral spheres (Magron et al, 1987; Laghoueg et al, 1989) and coated granulates (Delgado-Charro et al, 1991, 1992). Coated fatty materials had been known to be more susceptible to this effect than solid slabs (Urbanski, 1991). Changes to the crystal structure on these coatings could lead to a decline in the integrity of the layer and the breakdown of gelucire function such as the loss of the sustained-release profile of their dosage forms.

7.12 Conclusions

The main cause of the blooming phenomenon in pure G50/13 was postulated to be due to the form that gave rise to Peak 4 in the HMF. Addition of the SMS suppressed this peak and at the same time resulted in smoother surfaces on the matrices which indicated that no recrystallisation into the stable larger crystals occurred. However, it is also possible that SMS prevented the movement of the LMF components to the surface and the transformation to the more stable crystals occurred within the matrix. Incorporation of SMS could therefore inhibit the development of bloom and avert the potential breakdown in the integrity of G50/13 layer. However, many more studies could be performed in the future to elucidate the mechanism by which SMS exerts its influence on G50/13. Ageing G50/13 matrices containing SMS over various periods of time and analysing them with DSC could determine the effectiveness of the retarding effect and the influence of the surfactant on the structure with time. In addition, the influence of SMS on G50/13 at different temperatures could also be investigated which may shed light on the possibility of the behaviour being a kinetic effect.

CHAPTER 8: THE EFFECTS OF AGEING ON THE TENSILE STRENGTH OF G50/13 MATRICES

8.1 Introduction

The hardness and tensile strength of formulations are factors which had not been frequently assessed by investigators who were looking into the effects of aging on dosage forms. An exception to this is the investigation into the influence of aging on several gelucires including G50/13 (Sutananta et al, 1994b). The cooling rates used during solidification had an effect on the tensile strength of the gelucire bases although the actual outcome still depended on the gelucire composition (Sutananta et al, 1994a). In addition, upon storage, the gelucires with high glyceride contents or those containing only PEG esters such as G55/18 gave increased values of tensile strength whilst those with more mixed compositions of glycerides and PEG esters such as G50/13 demonstrated a decrease in the values instead. This led to the postulation that there was a correlation between the chemical structure and alterations to the tensile strength, and that the decrease seen for the more mixed composition gelucires was due to the redistribution of the individual components relative to each other rather than due to the combination of changes in the tensile strength of each component. Nevertheless, the change in the mechanical properties of materials related to gelucire components such as PEGs may still provide some information on the ageing effects. For example, pure PEG 1540 did not exhibit significant changes to its tensile strength when stored at 5°C for 2 to 120 hours (Kellaway and Marriot, 1975).

8.1.1 The effects of ageing on the tensile strength of lipids

Many investigations on the influence of ageing on the strength and hardness of formulations have been centred on triglyceride suppositories. These qualities were assessed by measuring the load that the base can withstand before collapsing, so that potential alterations to drug release and breakages can be avoided (Senior, 1974; Fontan et al, 1991). Triglyceride based suppositories were found to harden upon storage and this was thought to be solely due to the change from partially amorphous layered structures to crystallised form, without any occurrence of polymorphic transformation (Coben and Lordi, 1980; Laine et al, 1988). Hosny et al (1990) reported that the hardness of triglyceride based suppositories (Novata BD and Witepsol H15) formulated with ampicillin was raised after storage of 8 months. These tests which utilised the Erweka breaking strength tester also

found that drug incorporation had a variable effect on suppository hardness but ageing increased this attribute regardless of drug incorporation. The changes to the suppositories were also postulated to be due to the transformation of the less stable fat polymorph to a more stable form (Liversidge et al, 1981; Pryce-Jones et al, 1989). The breaking hardness of several fatty suppositories was tested after 1 week and 3 months storage, and it was discovered that this value was higher for the majority of the bases except for Witepsol H15 which hardly altered (Regdon et al, 1994).

Hardening of formulations can also be a result of the precipitation of a dispersed component with time (Chiou and Riegelman, 1971). However, a gradual reduction in the hardness could occur if the samples were held at a certain temperature for a too long period of time and this is called overaging. Changes at a macroscopic level may also involve a change at a mechanical level such as that found in G43/01 when the formulation which showed large spherulites under HSM was also the one which showed the lowest tensile strength value (Sutananta et al, 1994b). This was thought to be due to the size of the molecular aggregates causing a reduction in the polymer toughness and making it brittle. However, this occurrence was not seen for the other gelucire bases analysed. Correlations between the mechanical hardness of a fatty material with the peak area of a particular DSC endotherm had also been established (Lipp and Anklam, 1998).

8.1.2 The relationship between tensile strength and drug release behaviour

It would be advantageous if an association could always be determined between the hardness or tensile strength of formulations and the drug release profiles after an ageing process. As mentioned before, a decrease in the tensile strength values was obtained for the pure G50/13 matrix upon storage at room temperature (Sutananta et al, 1994b). The investigators also went on to discover that the release profile of theophylline from this base became elevated after ageing (Sutananta et al, 1995). A linear relationship between the release time of prednisolone and the breaking load of the PEG 4000 suppositories was also found (Kellaway and Marriot, 1975). In addition, there was a corresponding increase in the disintegration time of several fatty suppositories with their elevated breaking hardness after storage for several months (Regdon et al, 1994).

Nevertheless, this relationship is not always attained as was discovered for indomethacin-PEG 6000 tablets prepared from melt dispersion granules (Ford and Rubinstein, 1980). When the disintegration time for the tablets decreased significantly upon aging, it was attributed to the increase in their hardness which led to an improvement in the efficiency of the system. However, this feature was not followed by a rise in the dissolution rate. This gain in hardness with age was thought to be due to recrystallisation of the melt and this effect was sensitive to the storage temperature with great changes occurring when the tablets were stored at 25°C and 35°C but smaller increases for those stored at 45°C. Tablets made up of low-substituted hydroxypropylcellulose show contrasting results with some high tensile strength tablets showing low release and disintegration rates whilst other high strength tablets ageing high release profiles (Kawashima et al, 1993). This demonstrates that the drug release could not always be correlated to the tensile strengths of the formulations.

8.1.3 Diametral-compression test

The current study was based on the diametral-compression test to assess the tensile strength of tablets as described by Fell and Newton (1968,1970). For the tensile strength to be calculated, a particular state of stress needed to be established within the tablets which dimensions are known. When a tablet is placed between the plates of a loading system, tensile, shear and compressive stresses develop within the sample. The initial failure during tablet breaking has to be caused by tensile stress and this is facilitated by a reduction in the shear and compressive stresses below the loading area. Once this occurs, the maximum length of the load has to be subjected to a constant tensile stress in order to obtain a tensile failure of constant magnitude and a reproducible result. When the tablets are softer and there is some spreading of the load at contact point, shear and compressive stresses are reduced and the failure will still be due to tensile stress, therefore it would still be reproducible. However, when the initial failure is due to shear or compressive stresses as would occur in tablets with high elastic modulus, a soft pad could be utilised between the plates and the tablets. This would permit the distribution of the load over a wider area which would reduce the shear and compressive stresses.

The diametral-compression test was applied to compressed tablets prepared with various fatty acids and lactose (York and Pilpel, 1973). A relationship was found whereby as the melting point of the fatty acid increased, the tensile strength fell. This was attributed to the melting of the asperities at the contact points between the binary particles during compression which resulted in different amounts of bonding. A fatty acid with a lower melting point such as palmitic acid would be able to form more bonds due to greater melting thus increasing the tensile strength, than higher melting fatty acids such as stearic or behenic acids.

In this chapter, the mechanical properties of the samples were evaluated in order to observe possible changes brought about by ageing. Any differences in the ageing effects due to the incorporation of the different drugs was also looked at and a possible association with the drug release profiles can be ascertained.

8.2 Materials and Methods

Moulded tablets were fabricated as described in Chapter 4. The tablets were equilibrated in a silica gel desiccator for 24 hours before being analysed or stored. Their weights were taken (to ±0.0001g) before and after storage to establish whether any loss or uptake in mass occurred. Samples stored at 20°C or 37°C were taken out and equilibrated over silica gel for 24 hours before analysis. The diameters and thickness of the tablets were measured to ±0.001cm using a travelling microscope (Griffin and George Ltd., Great Britain) so as not to compress the tablets and change their dimensions. The average of four measurements (equivalent to the diameters measured along the North-South, East-West, Northeast-Southwest, Northwest-Southeast axes of the tablets) for both dimensions was taken.

The tablets were placed between the two parallel platens of a diametral compression tester (CT40 Engineering Systems, Nottingham) and the maximum loads at which the tablets broke in tension were recorded. The tensile strength can be calculated from the equation (Fell and Newton, 1970):

$$\sigma = \frac{2P}{\pi D t} \qquad \text{....Equation 8.1}$$

where σ = tensile strength ($Kg.cm^{-2}$), P = load (Kg), D = tablet diameter (cm) and t = tablet thickness (cm).

The way the tablets broke during compression was also recorded. This was because only the tablets which broke due to tensile stress were taken into account, seen as tablets which broke along the diameter into two halves. If the breakage was due to compression or shear stresses, the tablet would fracture in non-uniform manner into several fragments. 12 tablets of each sample were analysed for their tensile strength after freshly prepared and 7, 30, 90 and 180 days stored at either 20°C or 37°C. One-way ANOVA was used to statistically compare the samples within each storage condition.

8.3 Results and Discussions

8.3.1 Pure G50/13 tablets

Table 8 shows the tensile strength values of the samples after storage at 20°C or 37°C. Its value decreased for pure G50/13 samples after storage at 20°C ($p<0.005$) and even though after 180 days the tensile strength was lower than for freshly prepared samples, there was no obvious trend of continuously decreasing values in the period between 0 and 180 days storage. Similarly, samples stored at 37°C showed a decrease in the tensile strength values ($p<10^{-4}$), also with the lack of trend. The fluctuation in the values could indicate the movements of segregated gelucire components which eventually reached an equilibrium state, as demonstrated by the two samples aged at different temperatures finally reaching a similar value after 180 days.

A decrease in the values for G50/13 was also found by Sutananta et al (1994) and was attributed to the changes in the distribution of the glyceride component relative to the PEG ester component. That study also found that the G50/13 tablets prepared by slow cooling the melt had a similar value to the tablets prepared by ambient cooling after storage at room

Table 8: Tensile strength values of pure G50/13, 10% paracetamol and 10% caffeine dispersion samples after ageing at 20°C and 37°C ($Kg.cm^{-2}$).

Pure G50/13	***20°C***	***37°C***
fresh	4.15 ± 0.50	
7 days	3.53 ± 0.47	3.30 ± 0.39
30 days	3.76 ± 0.45	3.36 ± 0.71
90 days	3.30 ± 0.53	3.16 ± 0.43
180 days	3.54 ± 0.58	3.75 ± 0.49

10% paracetamol dispersion in G50/13	***20°C***	***37°C***
fresh	-	
7 days	-	7.99 ± 1.59
30 days	6.37 ± 1.57	7.10 ± 1.16
90 days	6.42 ± 1.11	6.38 ± 0.62
180 days	4.02 ± 0.47	5.84 ± 0.44

10% caffeine dispersion in G50/13	***20°C***	***37°C***
fresh	4.15 ± 0.38	
7 days	4.56 ± 0.55	4.90 ± 0.37
30 days	5.67 ± 0.78	4.44 ± 0.61
90 days	5.23 ± 0.88	5.04 ± 0.37
180 days	3.81 ± 0.61	4.69 ± 0.47

temperature for 135 days. In addition, in the current study, the pure G50/13 samples had a more matt appearance than the other samples and also showed a degree of brittleness with some matrix on the surface flaking off.

8.3.2 10% paracetamol dispersion in G50/13 tablets

Tensile strength values could not be assessed for the freshly prepared 10% paracetamol dispersion in G50/13 samples and also those stored for 7 days at 20°C. This was because the tablets were extremely soft and simply deformed under the load. Putting a soft padding in the area of contact between the tablet and the platen, as was proposed by Fell and Newton (1970) did not work in this case as the failure to break under tension was not due to the tablets having a high elastic modulus but most likely due to having a high proportion of LMF and some uncrystallised matrix. Those tablets which still have a high degree of uncrystallised melt will simply shear when load is applied.

Referring back to Chapter 3 on the Hot Stage Microscopy studies, it was found that some of the paracetamol was solubilised in the molten G50/13 during fusion but unlike caffeine which crystallised out separately from the base, the solubilised paracetamol recrystallised within the base and formed mixed crystals with the carrier. This altered or disrupted the G50/13 crystalline structure to the extent that the matrix became very soft either due to an actual change to the molecular arrangements or the retardation of G50/13 crystallisation. Incorporation of base soluble ingredients into fatty suppositories had previously been considered to disturb the gross crystalline structure of the base resulting in a lower viscosity (Coben and Lordi, 1980).

However, when tensile strength values could be established from tablets stored for 30 days and onwards, they were higher than the pure G50/13 samples. The incorporation of the drug had altered the physical make-up of the matrix so that once it had completely recrystallised, it was able to resist the failure due to tensile stress to a greater extent that the pure G50/13 tablets. Fatty acids with lower melting points were found to give higher tensile strength (York and Pilpel, 1973, see Section 8.1.3) and the high amount of LMF in this dispersion may have led to stronger bonding between the new mixed crystals. Nevertheless, like the

pure G50/13 samples, the values decreased with accumulating storage time ($p<10^{-4}$). The samples aged 30 days and onwards could confidently be established to break due to tensile failure as all of the tablets broke cleanly into two equal halves. Some of the tablets showed a little flattening at the bottom after compression, indicating that there was still some softness on the outer layer of the tablets at least. The paracetamol dispersion tablets were also very smooth and not brittle as the pure G50/13 samples.

After storing at 37°C, the tensile strength could be measured for the tablets even after only 7 days compared to 30 days for those stored at 20°C. This suggests that the previous softness of the paracetamol dispersion matrices was due to incomplete crystallisation whereby unsolidified melt was still present within the matrix. Storage at a higher temperature had given it sufficient kinetic energy for the long fatty acid chains to reorientate themselves in a crystalline structure, as had been previously seen in triglyceride suppositories which crystallisation was accelerated when held at a higher temperature (Laine et al,1988). The values were also higher than those stored at the lower temperature condition and after 180 days, the tensile strength value of the tablets stored at 37°C remained significantly higher ($p<0.001$, two-sample Student's t-test). It is evident then that storing at 37°C had not only change the microstructure of the matrix but also the mechanical strength of it. The effect of tensile strength lowering with storage time could also be seen here ($p<10^{-4}$).

8.3.3 10% caffeine dispersion in G50/13

The tensile strength value of the freshly prepared 10% caffeine dispersion in G50/13 was similar to the pure G50/13 sample. However, unlike the tensile strength values of pure G50/13 samples which decrease with ageing, the tensile strength of the caffeine dispersion tablets was first elevated (7 to 90 days storage) and then reduced at 180 days. Student's t-test at 5% significance level of the 180 days aged pure G50/13 sample and 10% caffeine dispersion sample showed that the tensile strength values were not different.

Incorporation of the caffeine must have caused a higher resistance to tensile failure like the paracetamol incorporation but to a lesser degree than the latter. Fat crystals were postulated

to be bonded to each other by Van der Waals/London forces (Haighton, 1976) and it is possible that the drugs promoted this bonding between their crystals and the G50/13 crystals or amongst the gelucire crystals themselves. Nevertheless, between 90 and180 days the mechanical behaviour was dominated by the gelucire components which would probably have undergone similar movements relative to each other as occurred in the pure G50/13 samples. The tablets also showed some signs of flakiness although much less than the pure G50/13 samples.

The overall effect of storing the samples at 37°C was an increase in the tensile strength values ($p<10^{-4}$) even though there was no particular trend to the rise. This elevation for the samples stored at this higher temperature was also seen for the paracetamol dispersion samples, the cause of which may be the greater number of bondings between the bigger amount of G50/13 crystals at this temperature and the drug crystals. Unlike the paracetamol dispersion samples however, these samples did not lessen in the their tensile strength over time.

8.4 Conclusion

Overall, ageing decreased the tensile strength of G50/13 matrices but the extent of this influence depended on the drug incorporated. The addition of drugs to G50/13 increased the strength of the matrices and this effect was sensitive to the storage temperature. The values of both paracetamol and caffeine dispersion samples were higher for those stored at 37°C than those stored at 20°C and in addition, these values were more elevated than for pure G50/13 samples. Therefore, to boost the durability of drug dispersions in G50/13 formulations, the dosage forms could be tempered at this higher temperature. The rise in the kinetic energy of the molecules at the higher temperature promoted an increase in the matrix crystallinity which then translated itself into higher tensile strength values for the drug dispersions.

Pure G50/13 was not affected in its strength by storage at the higher temperature but was adversely affected by the duration of storage instead. This lowering of the values was also shown to a variable extent by the drug dispersions as well and is probably a reflection on

the change in the distribution of the gelucire components within the matrices over time. The highest values were seen for paracetamol dispersions and may be due to the way this drug affected the G50/13 structure including its stabilisation of the lowest melting G50/13 form. The reduction at 180 days for both drug dispersions indicates that the movements of the gelucire components eventually dominate.

CHAPTER 9: DISSOLUTION STUDIES AND KINETICS OF DRUG RELEASE ON AGED G50/13 MATRICES

Modification in the drug release profile is another potential factor that has to be taken into account when considering storage conditions for formulations containing gelucires. Studies related to dissolution testing of aged formulations had been performed extensively as drug release has a direct impact on their functions. Gelucires are frequently utilised as excipients in sustained release dosage forms and alterations to this type of formulations will bring greater consequences compared to conventional forms since they usually contain larger doses of drugs. Many of such studies were centred on assessing the impact of ageing on marketable dosage forms and the feasibility of storing those forms in certain conditions. The objective of this study is not to investigate the stability of a finished product based on G50/13 but to research some of the factors that may affect the drug release characteristics from G50/13 matrices.

9.1 Introduction

The results obtained from previous studies on this subject had been varied with some studies claiming that ageing increases drug release whilst others maintained that release is retarded on storing the formulations. Inevitably, the outcome depends on many parameters such as the type of excipients, drugs, length and conditions of storage. Benzonatate, an oily liquid which is sensitive to light and air, had slightly higher dissolution values when the matrices of gelucire containing this drug were aged for 1 year (Doelker et al, 1986). It was concluded that the matrix crystals underwent a transformation that resulted in the drug being expelled from within the crystallites, which in turn resulted in the higher rate of release. An incorrect combination of the gelucire base and the active drug can lead to the failure of dosage forms on ageing, possibly causing leakage and softening of capsule walls. Preparation conditions will also have an influence on ageing effects. Dispersing a drug at a concentration beyond its solubility into a molten carrier at a high temperature could cause the drug to dissolve but precipitate out upon cooling and storage so that the release profile would not be consistent over time (Chiou and Riegelman, 1971).

9.1.1 Ageing effects on drug release from gelucire matrices

The outcome of ageing processes can rely on the composition of the gelucires as shown by

Sutananta et al (1995). Gelucire 55/18 showed a decrease in viscosity upon ageing, thought to be due to either the hydrolysis of PEG esters into PEG and fatty acids or the breakup of the PEG chains into lower molecular weight fragments. On the other hand, Gelucire 50/13 did not give any evidence of degradation as its viscosity was unaltered even after 220 days. Both bases however, gave higher rates of theophylline release after ageing for 180 days even though only G55/18 was chemically degraded. The higher release rate for G50/13 was thus attributed to the changes in the physical structure rather than chemical modifications. The modification to the gelucire physical structure was also the explanation given to the changes in the release of nifedipine from G53/10 upon ageing (Remuñán et al, 1992). In addition to that, especially due to the presence of high humidity, it was thought that the formation of nifedipine microcrystals also played a part. Another possible alteration to the dispersed drug on storage is the coarsening of the dispersed-phase particles, brought about by the reduction of the interfacial energy when the interface area is reduced such as in particle coarsening (Chiou and Riegelman, 1971). Time and ageing temperature increases would result in more extensive coarsening.

Ageing of ketoprofen dispersions in a carrier composed of a mixture of G50/13 and G50/02 in a 3:1 ratio resulted in an increase rate of drug release with the time for 50% of the drug to be release was reduced from 253 minutes for freshly prepared samples to 161 minutes for samples aged for 28 days at 30°C (Dennis et al, 1990). However, in-vivo studies revealed that no statistically significant difference could be found between the performances of the aged and freshly prepared samples. One of the reasons for the poor correlation could be that in in-vivo conditions, the speed of gastrointestinal transit is important and that the dosage forms used could have passed through before absorption was completed. The lack of correlation between in-vitro data and what was expected in-vivo could also be due the averaging effect that statistical manipulation can have on the results. For example, the mean rates of paracetamol excretion of 4 volunteers over 6 hours from glyceride suppositories were not significantly different between the freshly prepared and aged samples but a closer examination of individual data revealed that there was a significant lowering of the excretion for most of the subjects during the first few hours of the study (Moës and Jaminet, 1976). This then led to the recommendation that those glyceride bases should not be used for suppository formulations due to the unacceptably

low release rate of the drug when immediate action is needed.

9.1.2 Ageing effects on some of gelucire components

The behaviour of individual gelucire based components on ageing can be contradictory to that of the gelucire. No ageing effect was seen for temazepam dispersions formulated into PEG 1500 matrices, the polymer that makes up the PEG component in G50/13 (Dordunoo et al, 1991). When the same drug was formulated into high molecular weight PEGs such as PEGs 4000 and 6000, a reduction of the dissolution profile was observed. This demonstrated that the length of the polymer chain is also an important factor in ageing. In addition, this study proved that different drug dispersions will have contrasting outcomes upon ageing even when incorporated into the same carrier. Another hydrophobic drug, triamterene, was incorporated into several PEGs including the high molecular weight ones but the dispersions did not show any signs of ageing. The authors postulated that the absence of ageing effects was due to the drug not being solubilised in the carrier and remaining as crystals throughout the fusion process.

The stability of formulations based on the higher molecular weight PEGs such as PEGs 4000 and 6000 upon storage was also shown by Bowtle et al (1986) whose formulations of vancomycin in these PEGs were not detrimentally affected by storage of up to 12 months even under challenge conditions of 75% relative humidity or 40°C storage temperature. Again, the choice of drug will have an effect on the ageing behaviour as the incorporation of indomethacin instead of vancomycin into PEG 6000 led to markedly reduced dissolution rates (Ford and Rubinstein, 1979). Other factors such as storage temperature and concentration of drug within the matrices also control the outcome. Storage at a low temperature with low loadings of the drug gave a slower decrease of the rate over time which was continuous even after 1 year whilst storage at a higher temperature with higher loadings of the drug gave an initial large decrease in the release rate followed by a relatively constant rate after only 10 days. When the indomethacin dispersions were in melt granulated tablet form rather than melt discs, a deviation to the ageing effects quoted above was noted. Storage at 25°C and 35°C gave the expected reduction in the release rate but this was then followed by increased dissolution rates on longer storage time (Ford and

Rubinstein, 1980). As it was previously found that the hardness of the tablets had increased on storage and that this factor was expected to lead to an increase in the disintegration efficiency, the authors concluded that for this system, the changes in the dissolution profiles upon ageing must be to an extent, independent of elements such as hardness and disintegration times. The changes in the dissolution rates of chlorpropamide-urea melts upon storage were dependent on the content of the drug within the dispersions (Ford and Rubinstein, 1977). Little change was seen for low loadings of the drug, an initial decrease followed by an increase for the middle loadings and rapid increase followed by a slower increase for the higher loadings. This proved that the results of ageing studies may sometimes be complex and unpredictable. In addition, other factors such as cooling rates and the incorporation of surfactant can also influence the dissolution profiles upon storage (Sjökvist Saers et al, 1993).

Release studies of triglyceride suppositories were often looked at for results of ageing investigations due to the similarity of the chemical composition to most gelucires. It was found that ageing decreased the release rate of drugs from such formulations as was discovered for the release of ampicillin from Witepsol H15 and Novata BD based suppositories which became more retarded as the storage progressed (Hosny et al, 1990). An example of the retardation of release after the storage of fat-based formulations at higher temperatures was demonstrated by Yoshida et al (1991). When indomethacin suppositories in Witepsol were stored at 25-30°C for one month, the release of the drug both in vitro and in vivo was lower than those stored at 4°C, even though the in vivo effect was only slight. Similarly, the release of morphine hydrochloride from Witepsol H15 suppositories after storage for 2 weeks at 30°C (Saito et al, 1994) was also decreased. The main reason for this reduction was cited to be the polymorphic transformation to the more stable forms of the triglyceride components within the base. This increased the Solid Fat Index (SFI) of the base which had been associated with the release behaviour of the suppositories. Such decrease in the release rates from glyceride suppositories upon ageing was also found for paracetamol formulations and this effect was more crucial and apparent in suppositories where the retention time was short (Moës and Jaminet, 1976).

9.2 Materials and Methods

The moulded melt-fused tablets used were manufactured in the same way as described in Chapter 4. 10% paracetamol or caffeine dispersions in G50/13 were used. After fabrication, the tablets were left to set and equilibrate at room temperature in a silica gel desiccator. Some of the tablets were then randomly segregated and kept in a sealed amber glass bottle with silica gel in it, in a temperature controlled incubator set at 37°C. The rest were stored in a similar container but kept in a temperature controlled room set at 20°C. Thus, all the samples used in this study which were stored at different conditions initially came from the same batch.

At the time periods of 0, 7, 30, 90 and 180 days after storage, some of the tablets were taken out from the incubator or the temperature controlled room and allowed to equilibrate to room temperature in a silica gel desiccator for 24 hours. The tablets were then subjected to dissolution studies as described in Chapter 4. Six samples for each storage condition and type of drug dispersion were tested.

9.3 Results and Discussions

The dissolution profiles of the samples stored at either 20°C or 37°C were compared to the dissolution profiles of the samples of the same drug dispersions which had been freshly manufactured. The differences due to the drugs incorporated were also examined.

9.3.1 10% paracetamol dispersion in G50/13

Figure 9.1 shows that even though there was some overlapping of the standard deviation markers especially of the shorter duration stored samples, the overall effect was that increasing the storage time accelerated the release of paracetamol from the G50/13 matrices and it could be clearly seen that the drug release from the 180 days stored samples was significantly higher than from the freshly prepared moulded tablets. From Table 9.3 the time taken for 50% of the drug to be released ($t_{50\%}$) was 7.45 hours for the 180 days stored samples as opposed to13.32 hours for the fresh samples. Therefore, storage of the 10%

Figure 9.1 : Dissolution profiles of 10% paracetamol dispersion in G50/13 samples after storage at 20°C

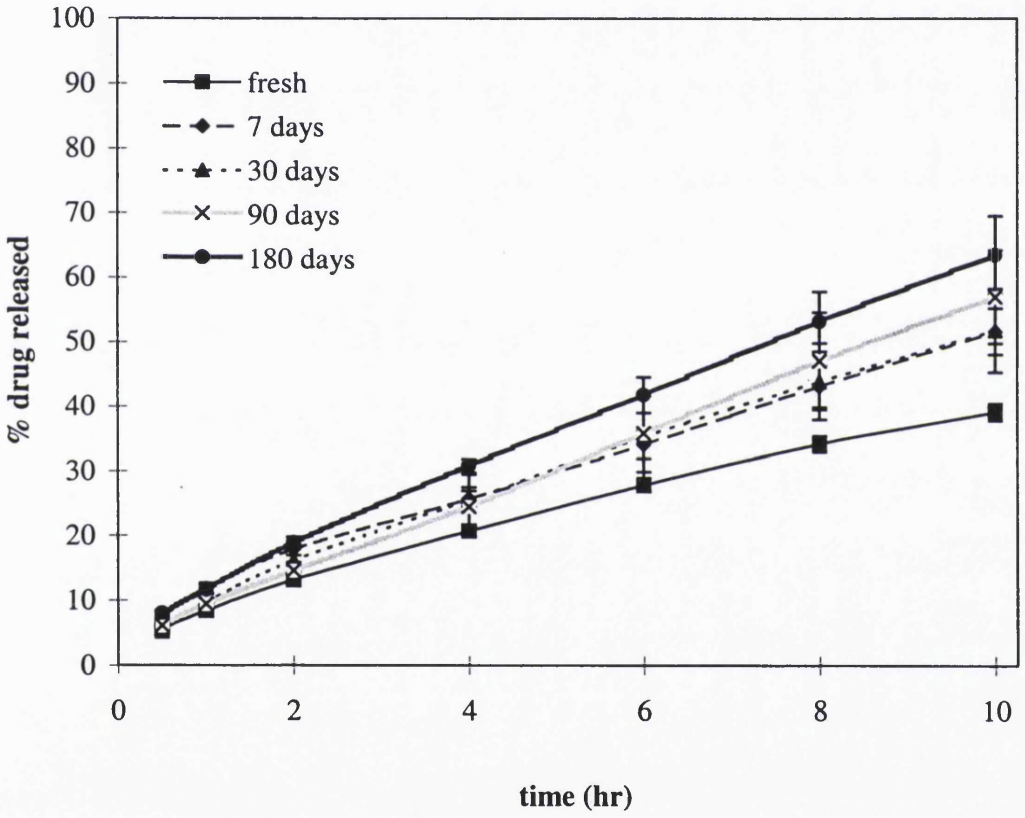

paracetamol dispersion in G50/13 samples at 20°C had increased their dissolution profiles. The increase in the release was evident even after a relatively short period of storage (7 days) but little difference could be seen between the profiles of the samples stored for 7, 30 and 90 days. This suggests that the first few days succeeding the time of manufacture were the most crucial to induce any changes to the release of the drug. Beyond that, the changes became more gradual and only after storage for a longer period of time (180 days) was there another significant change. When the rates of release were plotted against time as in Figure 9.2, it showed that after the initial high rate, there were slight fluctuations on the profiles compared to the freshly prepared sample, but in general the rates were quite uniformed. As expected from the observations above, the rates for the stored samples were also higher than for the freshly prepared samples.

Storage of the samples at 37°C resulted in a more prominent rise in the drug release compared to the freshly prepared samples as revealed in Figure 9.3. The elevation in the drug release profile was also greater for the samples stored at 37°C than those stored at 20°C, as exemplified by the tablets stored for 180 days in Figure 9.5, with the $t_{50\%}$ shown in Table 9.4 reduced to 5.29 hours. As with the samples stored at 20°C, there was a substantial rise in the drug release by the first week of storage followed by little difference between the profiles of samples stored for 7 days and 30 days. However, unlike the samples stored at 20°C, another substantial rise could already be seen after 90 days of storage and further ageing until 180 days did not significantly alter this release profile. This indicates that storage at 37°C not only increased the drug release profile but also quickened the rate of change within the matrices that lead to such increases. In addition, after a certain period of storage, the release behaviour seemed to reach an equilibrium and further ageing did not alter the profile.

From Figure 9.4, the rates of release profiles showed more apparent minimums and maximums for the samples stored at 37°C than those stored at 20°C. From the rates of release data of paracetamol dispersions in G50/13 at different loadings in Section 3 of Chapter 4, it could be seen that they were uniformed. In Section 3 of Chapter 5, the erosion profile of these matrices showed that this process was also uniformed. It could then be postulated that the fluctuating effect was due to inconsistent erosion. As erosion and the

Figure 9.2 : Rate of dissolution profiles of 10% paracetamol dispersion in G50/13 samples stored at 20°C

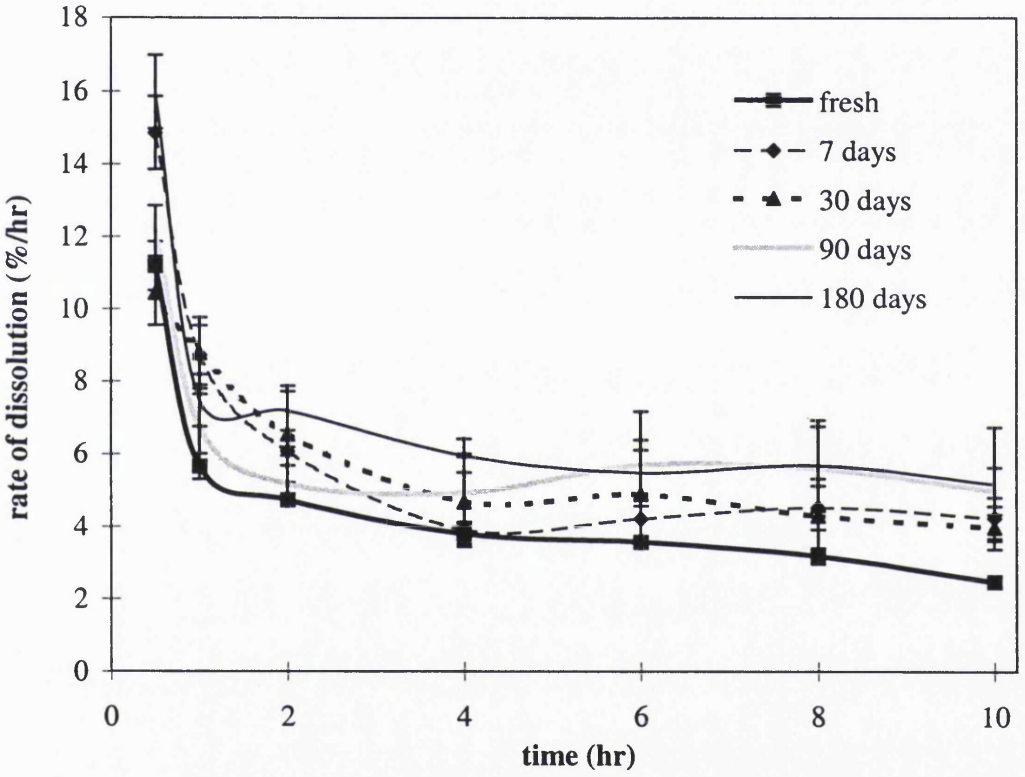

Figure 9.3 : Dissolution profiles of 10% paracetamol dispersion in G50/13 samples stored at 37°C

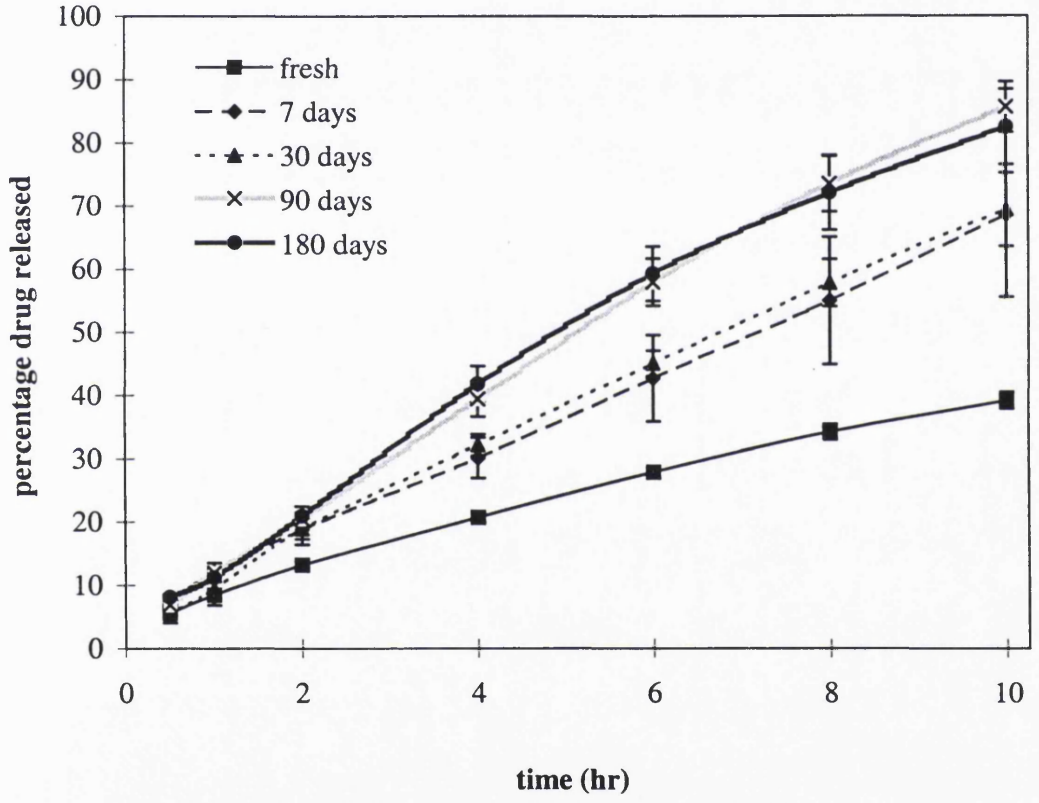

Figure 9.4 : Rates of dissolution profiles of 10% paracetamol dispersion in G50/13 samples stored at 37°C

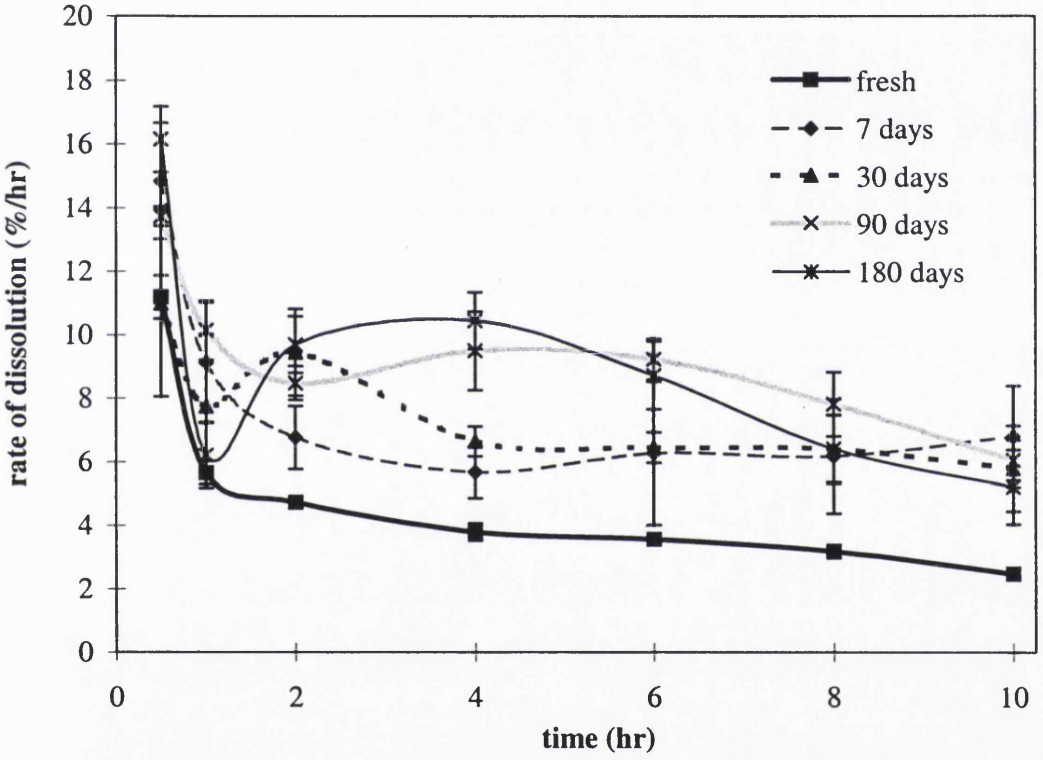

Figure 9.5 : Dissolution profiles of 10% paracetamol dispersion in G50/13 samples aged for 180 days at 20°C and 37°C

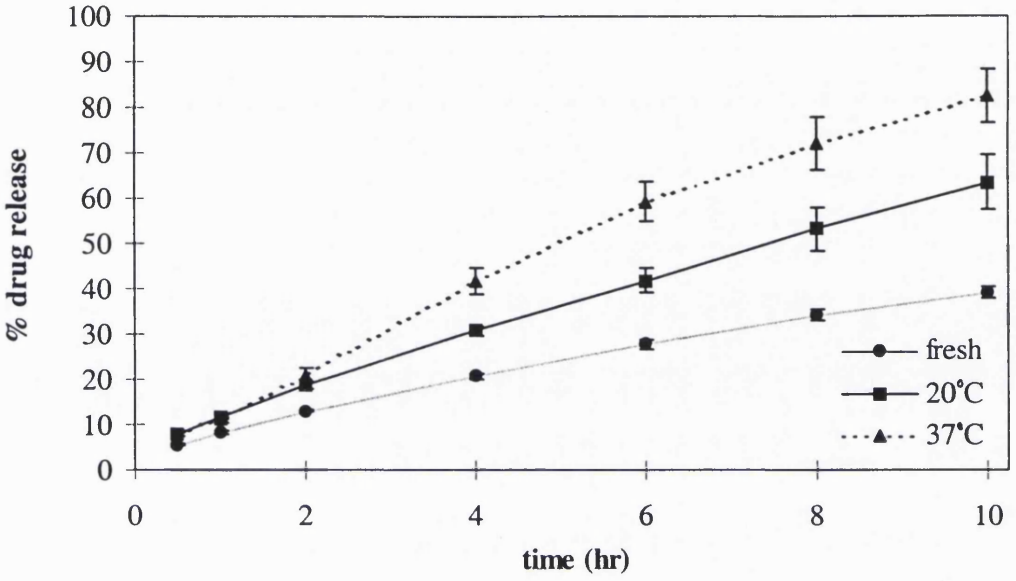

Figure 9.6 : Dissolution profiles of 10% caffeine dispersion in G50/13 stored for 180 days at 20°C and 37°C

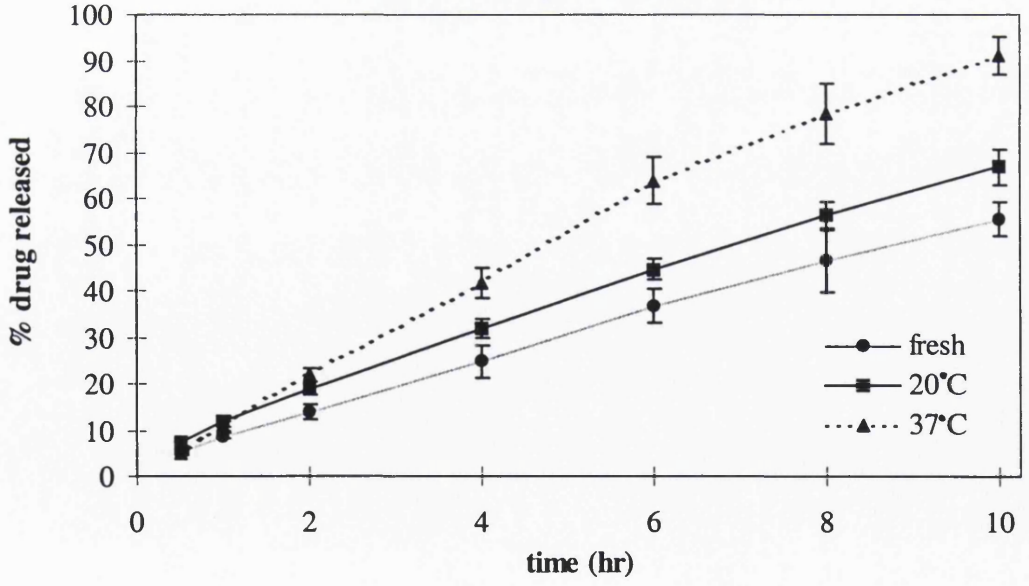

establishments of water-filled micro-networks by which drugs further within the matrix can travel to the surface begun to take place, the rate rose. This was followed by a fall after the depletion of that matrix layer as the next layer began to swell. Such big fluctuations on the rate profiles indicated that storage at 37°C for the paracetamol dispersion samples may not be ideal if uniform rates of release are required.

9.3.2 10% caffeine dispersion in G50/13

The dissolution profiles of the 10% caffeine dispersion samples stored for various periods of time did not show significant changes due to storage at 20°C, as presented in Figure 9.7. With the exception of the 90 days stored samples, there were small and insignificant increases in the release with the duration of storage. Even the release from the180 days stored samples was not appreciably higher than the freshly prepared samples, as was demonstrated by the 10% paracetamol dispersion samples stored at both 20°C and 37°C. The rates of release profiles mirrored the observations above with minimal differences between the rates of the samples except for the 90 days stored sample which showed inexplicably high rates after 6 hours, shown in Figure 9.8.

When the samples were stored at 37°C however, the drug release increased greatly as revealed in Figure 9.9. A trend in the release in relation to the number of storage days could not be established with the profile increasing from 7 days to 90 days storage but decreasing slightly for the 180 days stored samples to be lower than the 90 days stored samples. The accelerated change within the matrix due to storage at this higher temperature, as quoted above for the paracetamol samples stored in the same condition, could be a reason for the close proximity of the stored profiles. This major change could have occurred within the first 7 days of storage and longer storage time brought about only limited changes. An almost complete release was achieved by the longer stored samples after dissolution for 10 hours. As with the paracetamol dispersion samples, a comparison of the caffeine dispersion samples stored for 180 days (Figure 9.6) revealed that storage at 37°C increased the dissolution profiles to a greater extent than those stored at 20°C, with $t_{50\%}$ being 5.02 hours and 6.97 hours respectively compared to 8.70 for freshly prepared samples (Tables 9.9 and 9.10).

Figure 9.7 : Dissolution profiles of 10% caffeine dispersion in G50/13 samples stored at 20°C

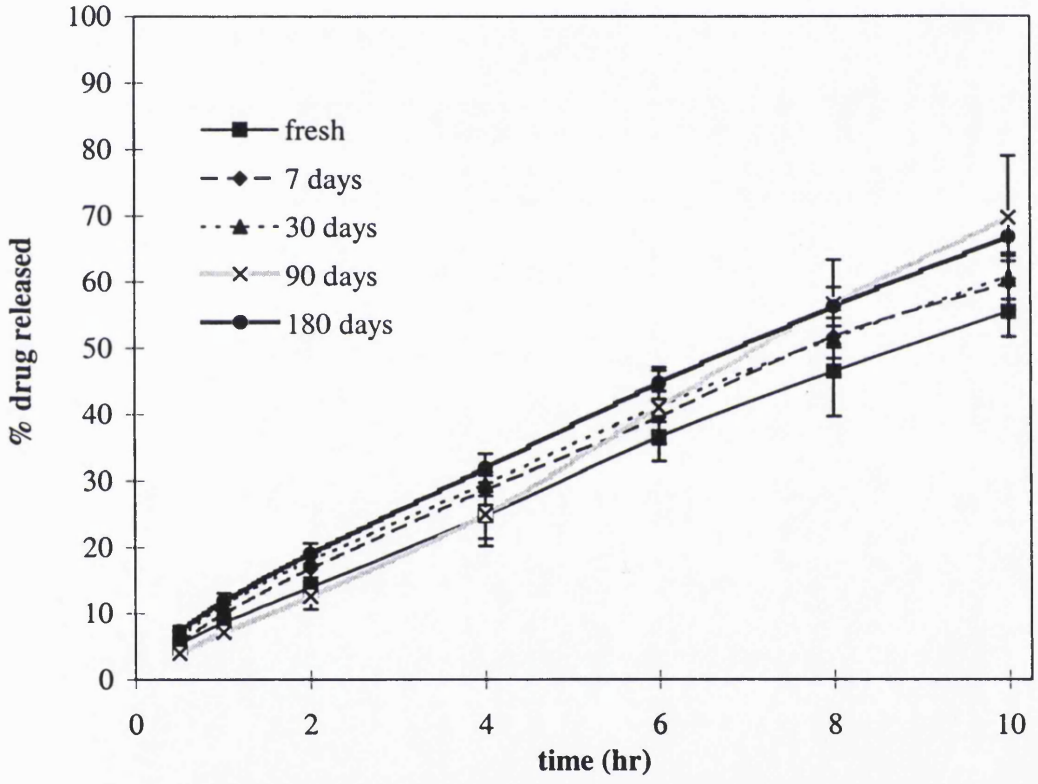

Figure 9.8 : Rates of dissolution profiles of 10% caffeine dispersion in G50/13 samples stored at 20°C

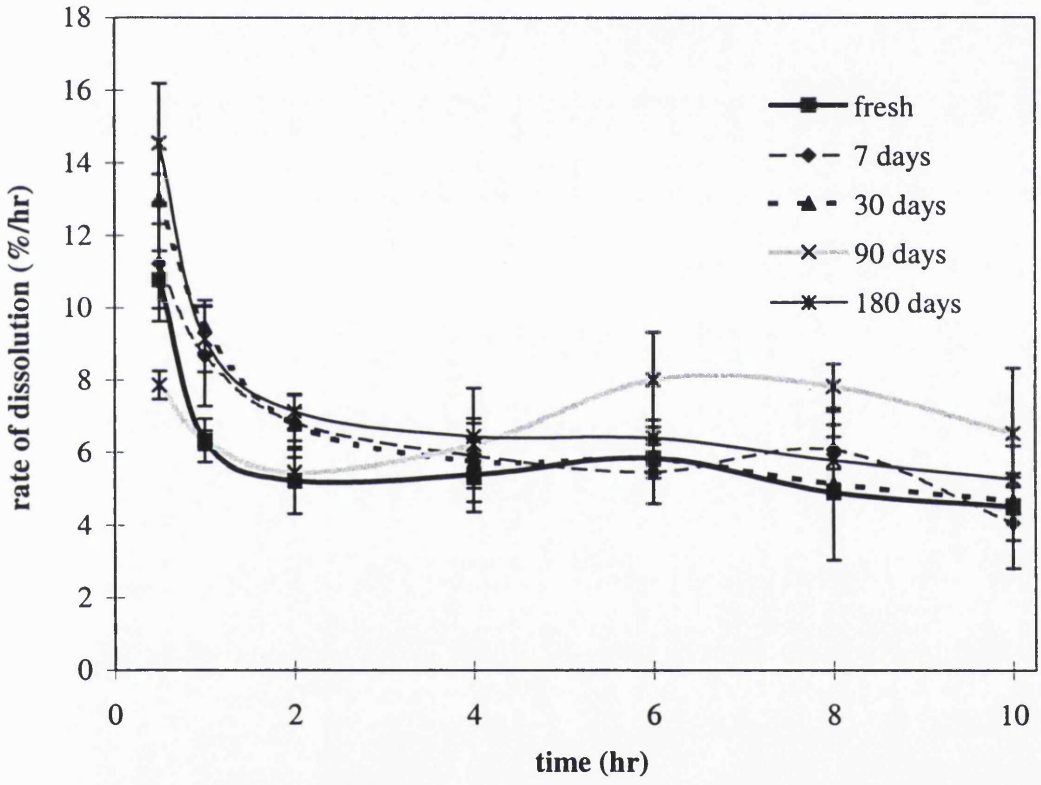

Figure 9.9 : Dissolution profiles of 10% caffeine dispersion in G50/13 stored at 37°C

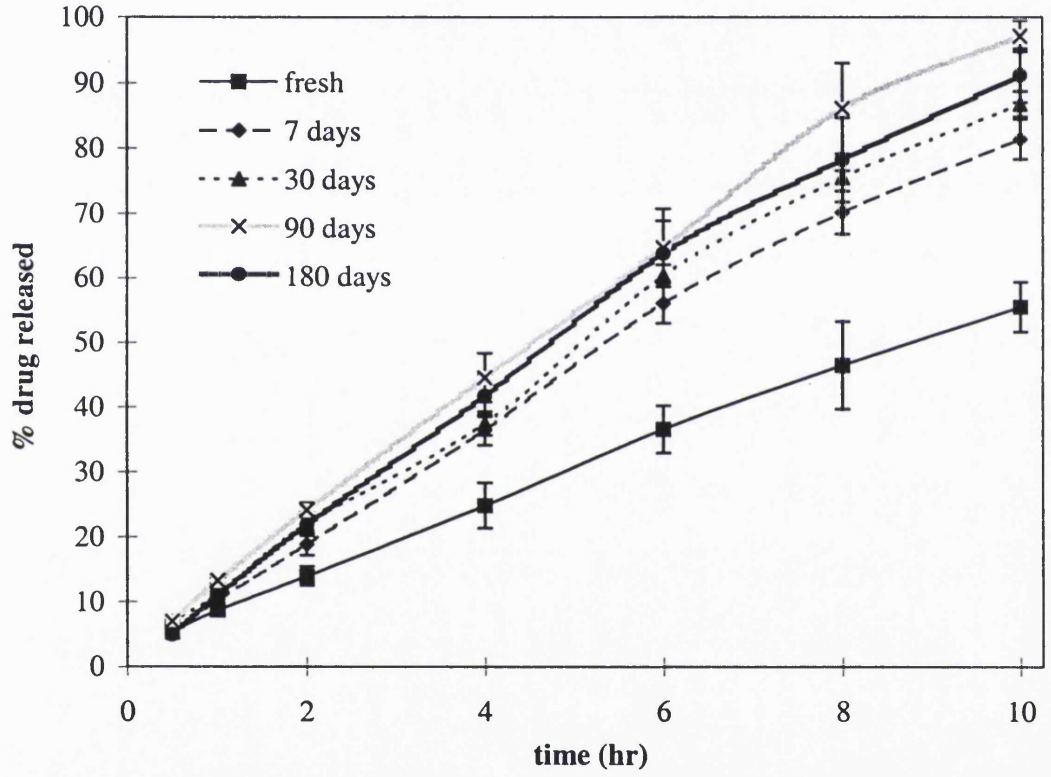

From Figure 9.10, higher rates of release were noted for the samples stored at 37°C compared to the freshly prepared samples although there was little to distinguish between the profiles of the samples stored at different time periods. However, the variations in the rates of release during the dissolution process were so great that the profiles resembled oscillations. One possible explanation could be the erosion of these matrices mimicked such a trend and as the tablets swelled to their limit, extensive erosion followed which gave rise to the high release rate. Therefore, similarly to the paracetamol dispersion samples, storage at 37°C resulted in the matrices giving inconsistent rates of release. This was in contrast to the rate of release from the freshly prepared caffeine dispersion samples which showed a fairly constant profile. A constant profile was also shown by the 180 days stored at 20°C sample but the same sample stored at 37°C fluctuated, consistent with the other caffeine dispersion samples stored at this temperature.

Figure 9.11 compares the effect of storage at 20°C on a 10% paracetamol dispersion in G50/13 to 10% caffeine dispersion samples, both stored for 180 days. The profiles displayed only a minor difference between the two samples. Similarly, it could be seen from Figure 9.12 storage at 37°C resulted in a small difference between the two samples although the releases had increased significantly relative to the samples stored at 20°C. This suggests that it was the G50/13 matrix that was being affected by the different storage conditions, regardless of the drugs incorporated in it. Such postulation is supported by the comparisons of the rates of release of 180 days stored paracetamol and caffeine dispersion samples. Both samples gave constant rates during most of the dissolution process when they had been stored at 20°C, as denoted in Figure 9.13. On the other hand, Figure 9.14 shows that the samples gave high and unpredictable rates of release behaviour when both type of dispersions were stored at 37°C.

9.3.3 Kinetics of release

The temperatures of storage had been shown above to affect the dissolution profiles of the samples. These profiles were then fitted to Equations 4.8, 4.10 and 4.1 (see Chapter 4) which will indicate the kinetics of drug release for the stored samples.

Figure 9.10 : Rate of dissolution profiles of 10% caffeine dispersion in G50/13 samples stored at 37°C

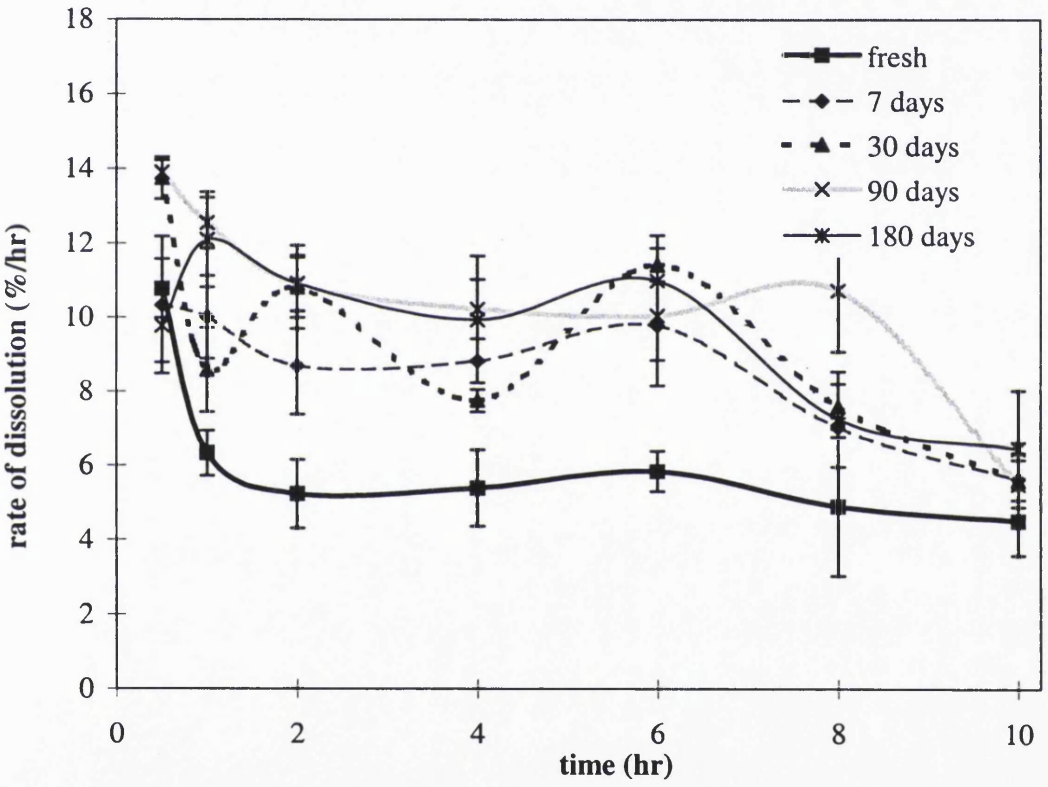

Figure 9.11 : Dissolution profiles of 10% paracetamol and caffeine dispersions in G50/13 samples after aging for 180 days at 20°C

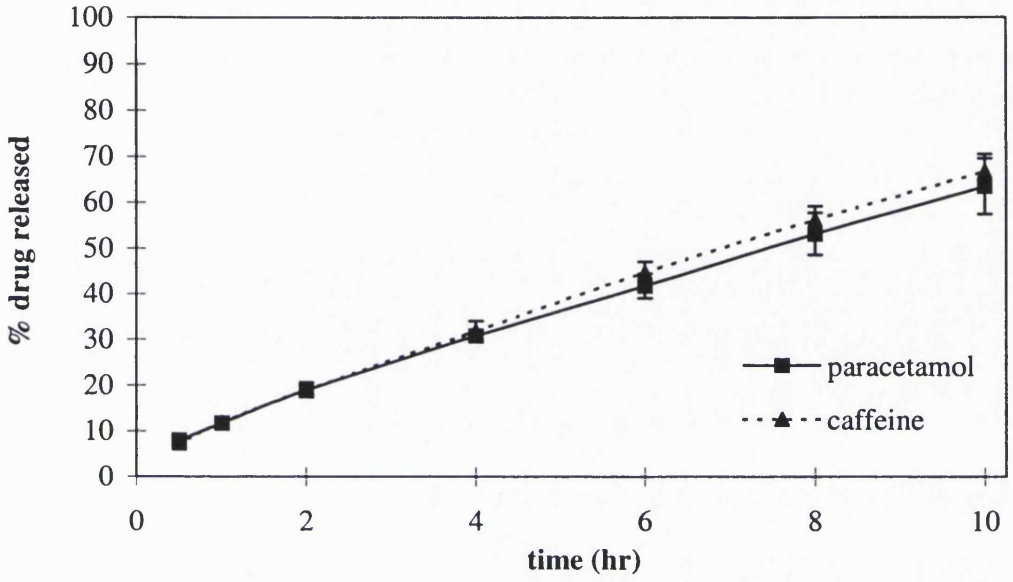

Figure 9.12 : Dissolution profiles of 10% paracetamol and caffeine dispersions in G50/13 samples after storage for 180 days at 37°C

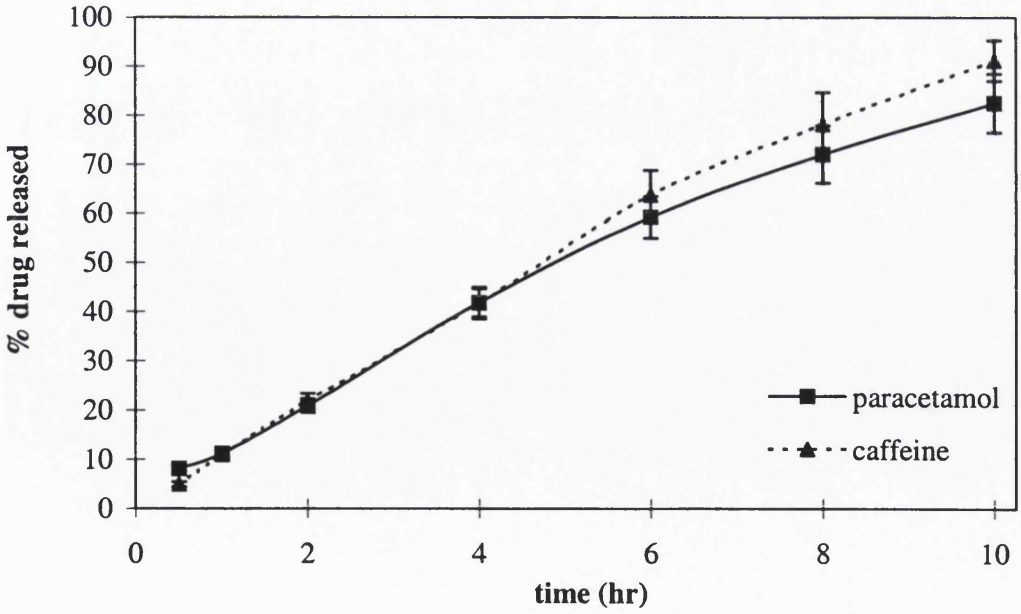

Figure 9.13 : Rate of dissolution profiles of 10% paracetamol and caffeine dispersions in G50/13 samples stored for 180 days at 20°C

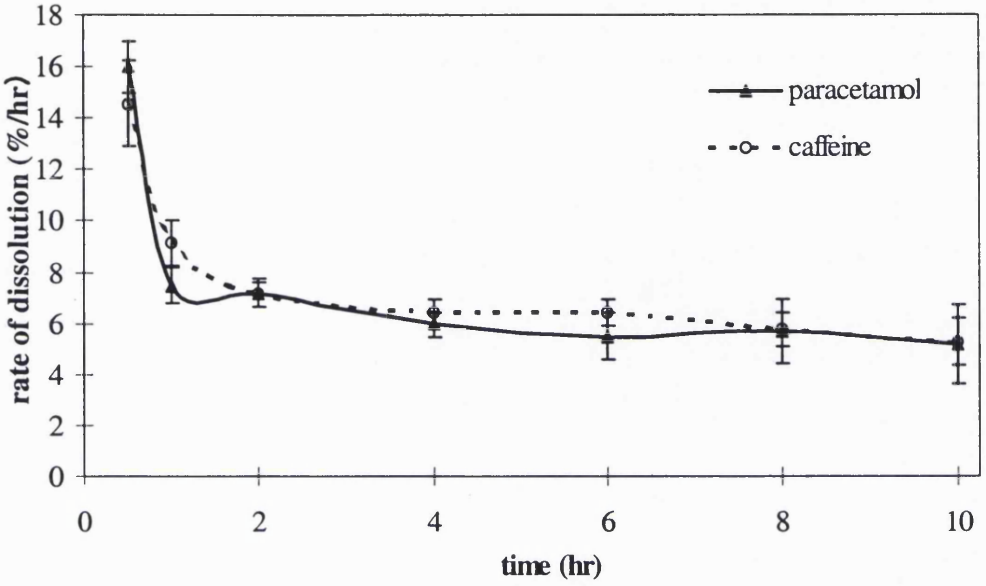

Figure 9.14 : Rate of dissolution profiles of 10% paracetamol and caffeine dispersions in G50/13 samples stored for 180 days at 37°C

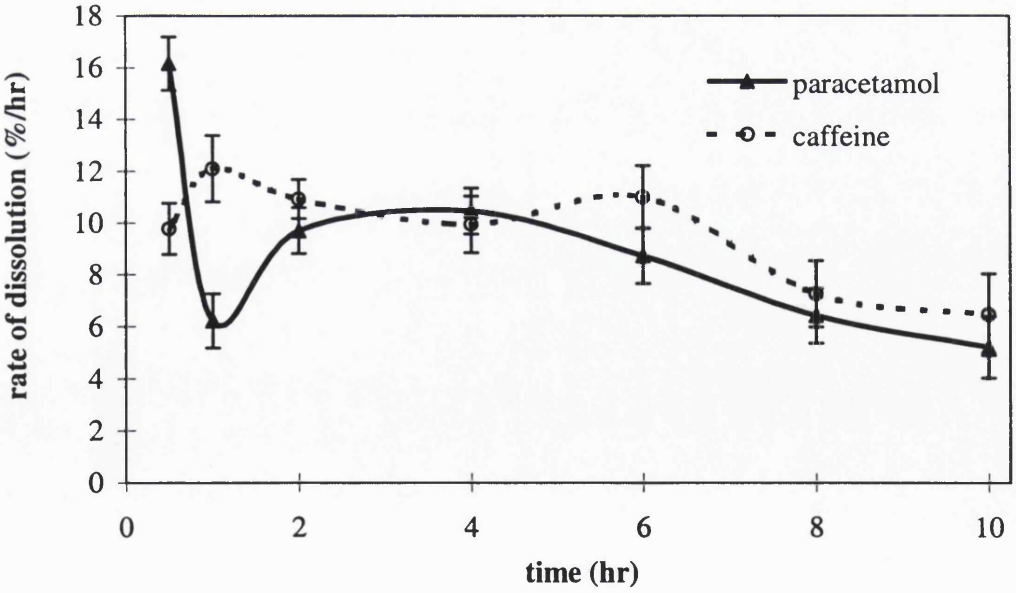

From Table 9.1, it could be seen that paracetamol dispersion samples which were stored at 20°C generally had higher values of the n exponent of Equation 4.8 than freshly prepared samples. Since values closer to 0.5 indicate a more diffusional release and higher values than this indicate a more mixed mechanisms of release, the results suggest that the erosion process played a greater role in the release of paracetamol from the stored samples. The dissolution rate coefficient, k was also higher for the stored samples, consistent to the rate of release profiles (Figure 9.2). Just as the dissolution profiles showed (Figure 9.1), a trend could not be determined with the number of days of storage. Even though the overall effect was that the n and k parameters increased, the actual values did not increase correspondingly with the number of storage days. Table 9.2 showed that storage at 37°C further increased the parameters and the n values higher than 0.8 disclosed a mechanism of release relying very heavily on erosion.

When the data was fitted to Equation 4.10 and the ratio of k_1 to k_2 was calculated for samples stored at 20°C, it was found that the ratio increased for the longer stored samples (Table 9.3). This supported the thought that storage increased the contribution of erosion as a mechanism of release. When the k_1 and k_2 values were looked at individually, it could be seen that the k_2 parameters which are associated with the diffusional process were still quite high but even higher values of k_1 resulted in the ratio being higher than for freshly prepared samples. Thus, although the main mechanism of release was still diffusion, the erosion process was tipping the balance towards itself when the samples were stored. Storing the samples at 37°C substantially increased the ratio in comparison with the freshly prepared samples or the samples stored at 20°C, again indicating the expanded importance of erosion (Table 9.4).

From Table 9.5, the lower r^2 values for the fitting of the paracetamol dispersion stored at 20°C data to Equation 4.1 implied that there were additional mechanisms besides diffusion that were responsible for the release of the drug, as the $t^{½}$ equation was designed to fit release which was diffusional. However, the dissolution rate coefficient, k, increased as storage became longer which could mean that even if the diffusion mechanism was the dominant mechanism, ageing the samples intensified this process. Due to the steady increase in the k values with the number of storage days, this parameter could give a good

Table 9.1: Parameters calculated by fitting dissolution data of 10% paracetamol dispersion in G50/13 samples stored at 20°C to Equation 4.8.

Number of days stored at 20°C	Dissolution rate coefficient, k (%/hr)	Exponent n from Equation	Correlation coefficient, r^2
0	8.55 ± 0.43	0.65 ± 0.01	0.9988
7	11.47 ± 0.72	0.63 ± 0.01	0.9967
30	9.21 ± 0.89	0.75 ± 0.03	0.9985
90	9.47 ± 0.79	0.75 ± 0.03	0.9934
180	12.16 ± 0.62	0.70 ± 0.01	0.9969

Table 9.2: Parameters calculated by fitting dissolution data of 10% paracetamol dispersion in G50/13 samples stored at 37°C to Equation 4.8.

Number of days stored at 37°C	Dissolution rate coefficient, k (%/hr)	Exponent n from Equation	Correlation coefficient, r^2
0	8.55 ± 0.43	0.65 ± 0.01	0.9988
7	11.82 ± 1.49	0.73 ± 0.02	0.9959
30	9.84 ± 2.14	0.85 ± 0.10	0.9989
90	12.03 ± 0.49	0.86 ± 0.01	0.9987
180	12.74 ± 0.81	0.83 ± 0.01	0.9917

Table 9.3: Parameters calculated by fitting dissolution data of 10% paracetamol dispersion in G50/13 samples stored at 20°C to Equation 4.10.

Number of days stored at 20°C	Exponent k_1 from Equation	Exponent k_2 from Equation	Correlation coefficient, r^2	k_1 / k_2	$t_{50\%}$ (hr)
0	2.00 ± 0.05	6.42 ± 0.28	0.9999	0.31 ± 0.02	13.32 ± 0.58
7	2.34 ± 0.27	8.65 ± 0.28	0.9972	0.27 ± 0.04	9.80 ± 1.04
30	3.14 ± 0.43	6.55 ± 0.93	0.9991	0.48 ± 0.14	9.55 ± 1.71
90	4.33 ± 0.78	4.22 ± 0.14	0.9983	1.02 ± 0.22	8.67 ± 1.46
180	3.85 ± 0.77	7.83 ± 0.62	0.9997	0.49 ± 0.06	7.45 ± 0.80

Table 9.4: Parameters calculated by fitting dissolution data of 10% paracetamol dispersion in G50/13 samples stored at 37°C to Equation 4.10.

Number of days stored at 37°C	Exponent k_1 from Equation	Exponent k_2 from Equation	Correlation coefficient, r^2	k_1 / k_2	$t_{50\%}$ (hr)
0	2.00 ± 0.05	6.42 ± 0.28	0.9999	0.31 ± 0.02	13.32 ± 0.58
7	4.82 ± 1.47	6.02 ± 0.64	0.9978	0.80 ± 0.16	7.07 ± 1.55
30	5.39 ± 0.18	5.08 ± 0.91	0.9991	1.06 ± 0.23	6.81 ± 0.56
90	7.06 ± 0.28	5.47 ± 0.63	0.9974	1.29 ± 0.20	5.29 ± 0.35
180	6.15 ± 0.53	7.65 ± 0.38	0.9925	0.80 ± 0.11	5.29 ± 0.46

Table 9.5: Parameters calculated by fitting dissolution data of 10% paracetamol dispersion in G50/13 samples stored at 20°C to Equation 4.1.

Number of days stored at 20°C	Dissolution rate coefficient, k ($\%/hr^{-1/2}$)	Correlation coefficient, r^2	t_{lag} (hr)
0	13.45 ± 0.42	0.9926	0.37 ± 0.01
7	17.45 ± 1.27	0.9852	0.37 ± 0.01
30	18.80 ± 2.79	0.9921	0.51 ± 0.02
90	20.58 ± 3.25	0.9720	0.59 ± 0.03
180	22.52 ± 2.18	0.9851	0.49 ± 0.04

indication of the positions of the release profiles relative to each other towards the end of the dissolution study. t_{lag} is the extrapolation of the fitted line to the x-axis which gives an indication on the length of time taken to establish the linear proportion of the fitted profile and is also dependant on k. For example, the raised value of t_{lag} for the 90 days stored tablets demonstrated that the main diffusional process for this sample happened later than the other samples but more quickly as shown by the steepness of the fitted line. Again, the k values were higher for the 37°C stored samples indicating faster rates of release (Table 9.6).

Fitting the caffeine dispersion stored at 20°C to Equation 4.8 showed that no great differences in the k or n parameters were seen amongst the samples stored for various periods of time nor with the freshly prepared samples, as presented in Table 9.7. However, the higher storage temperature of 37°C vastly increased the n value, indicating that a lot of erosion had occurred in order to release the drug (Table 9.8). The increase in the k value reflected the higher rate of dissolution. This was supported by the fitting of the data to Equation 4.10 presented in Table 9.10 which showed high ratio values. By looking at the k_1 and k_2 parameters separately, it could be seen that the diffusional values of k_2 were still quite low like the freshly prepared samples but the k_1 values were very high. Unlike the paracetamol dispersion samples, the diffusion mechanism had been taken over by erosion as the dominant process here.

No significant changes in the dissolution rate coefficient, k was seen for the caffeine dispersion samples stored at 20°C when fitted to Equation 4.1, either in comparison to the freshly prepared samples or amongst the stored samples themselves, as disclosed in Table 9.11, and this was in agreement with their rates of release profiles (Figure 9.8). Storage at 37°C nevertheless greatly increased the k values and this rise corresponded to the number of storage days until 90 days storage whereby further storage until 180 days did not affect the rate significantly, as revealed in Table 9.12. Looking at the rates of release profile (Figure 9.10), it was difficult to compare the rates for the different samples due to the fluctuations in the profiles. The k values of Equation 4.1 thus provided a clearer indication of the rates and probably represented the average rate throughout the duration of the dissolution process. However, the rates of release profiles are still useful to be plotted

Table 9.6: Parameters calculated by fitting dissolution data of 10% paracetamol dispersion in G50/13 samples stored at 37°C to Equation 4.1.

Number of days stored at 37°C	Dissolution rate coefficient, k ($\%/hr^{-1/2}$)	Correlation coefficient, r^2	t_{lag} (hr)
0	13.45 ± 0.42	0.9926	0.37 ± 0.01
7	24.21 ± 4.75	0.9734	0.55 ± 0.05
30	26.05 ± 1.24	0.9874	0.63 ± 0.04
90	32.95 ± 1.87	0.9850	0.66 ± 0.01
180	31.93 ± 2.46	0.9891	0.61 ± 0.01

Table 9.7: Parameters calculated by fitting dissolution data of 10% caffeine dispersion in G50/13 samples stored at 20°C to Equation 4.8.

Number of days stored at 20°C	Dissolution rate coefficient, k (%/hr)	Exponent n from Equation	Correlation coefficient, r^2
0	9.20 ± 0.69	0.77 ± 0.03	0.9983
7	9.75 ± 1.20	0.79 ± 0.02	0.9996
30	10.92 ± 0.54	0.74 ± 0.01	0.9994
90	7.11 ± 0.68	0.97 ± 0.03	0.9957
180	11.82 ± 1.17	0.74 ± 0.02	0.9989

Table 9.8: Parameters calculated by fitting dissolution data of 10% caffeine dispersion in G50/13 samples stored at 37°C to Equation 4.8.

Number of days stored at 37°C	Dissolution rate coefficient, k (%/hr)	Exponent n from Equation	Correlation coefficient, r^2
0	9.20 ± 0.69	0.77 ± 0.03	0.9983
7	10.00 ± 1.40	0.93 ± 0.05	0.9991
30	11.92 ± 0.73	0.87 ± 0.02	0.9972
90	13.03 ± 0.48	0.89 ± 0.02	0.9994
180	10.45 ± 0.97	0.98 ± 0.01	0.9967

Table 9.9: Parameters calculated by fitting dissolution data of 10% caffeine dispersion in G50/13 samples stored at 20°C to Equation 4.10.

Number of days stored at 20°C	Exponent k_1 from Equation	Exponent k_2 from Equation	Correlation coefficient, r^2	k_1 / k_2	$t_{50\%}$ (hr)
0	4.03 ± 0.87	5.01 ± 0.23	0.9996	0.81 ± 0.21	8.70 ±1.40
7	4.24 ± 0.08	5.80 ± 1.20	0.9988	0.73 ± 0.17	7.95 ± 0.76
30	3.83 ± 0.25	7.26 ± 0.35	0.9997	0.53 ± 0.06	7.78 ± 0.59
90	7.44 ± 0.84	-1.42 ± 0.21	0.9980	-5.25 ± 0.20	7.24 ± 0.95
180	4.41 ± 0.01	7.29 ± 1.06	0.9998	0.60 ± 0.09	6.97 ± 0.51

Table 9.10: Parameters calculated by fitting dissolution data of 10% caffeine dispersion in G50/13 samples stored at 37°C to Equation 4.10.

Number of days stored at 37°C	Exponent k_1 from Equation	Exponent k_2 from Equation	Correlation coefficient, r^2	k_1 / k_2	$t_{50\%}$ (hr)
0	4.03 ± 0.87	5.01 ± 0.23	0.9996	0.81 ± 0.21	8.70 ±1.40
7	7.16 ± 0.15	3.99 ± 1.51	0.9953	1.79 ± 0.75	5.66 ± 0.36
30	7.36 ± 0.24	5.11 ± 1.27	0.9944	1.44 ± 0.33	5.20 ± 0.21
90	8.21 ± 0.65	5.86 ± 0.37	0.9959	1.40 ± 0.20	4.56 ± 0.39
180	7.96 ± 0.17	4.72 ± 1.27	0.9939	1.68 ± 0.53	5.02 ± 0.40

Table 9.11: Parameters calculated by fitting dissolution data of 10% caffeine dispersion in G50/13 samples stored at 20°C to Equation 4.1.

Number of days stored at 20°C	Dissolution rate coefficient, k ($\%/hr^{-1/2}$)	Correlation coefficient, r^2	t_{lag} (hr)
0	19.16 ± 2.81	0.9847	0.53 ± 0.04
7	22.27 ± 1.56	0.9875	0.58 ± 0.03
30	22.06 ± 1.33	0.9894	0.52 ± 0.01
90	26.86 ± 3.56	0.9577	0.79 ± 0.01
180	24.26 ± 1.06	0.9866	0.54 ± 0.03

Table 9.12: Parameters calculated by fitting dissolution data of 10% caffeine dispersion in G50/13 samples stored at 37°C to Equation 4.1.

Number of days stored at 37°C	Dissolution rate coefficient, k (%/hr$^{-1/2}$)	Correlation coefficient, r^2	t_{lag} (hr)
0	19.16 ± 2.81	0.9847	0.53 ± 0.04
7	32.03 ± 0.98	0.9858	0.70 ± 0.03
30	33.76 ± 0.42	0.9818	0.67 ± 0.03
90	37.90 ± 3.10	0.9848	0.67 ± 0.01
180	36.15 ± 2.15	0.9896	0.70 ± 0.01

because they show the behaviour of the matrices and the changes with dissolution time.

Such changes in the kinetic parameters therefore offer some insights into the processes that lead to ageing effects. A previous study (Sutananta et al, 1995) found that although the release rate increased upon storage of theophylline dispersion in G55/18, the n value was unaltered, signalling that for this base at least, the mechanism of release was not affected by ageing. As a viscosity study showed that G55/18 underwent chemical degradation upon storage, it suggested that the mechanism of release would not be altered if the changes upon ageing were due to chemical processes. It was assumed that G50/13 which increase in the dissolution profile was attributed to physical changes to the structure would then show a variation to the mechanism of release upon ageing but this postulation could not be confirmed as the n values were not quoted for this base. A study investigating the effects of ageing on salbutamol dispersions in G35/10, G48/09 and G46/07 also found that the n values remained relatively unchanged after 1 year storage (San Vicente et al, 1998). However, with the exception of the G46/07 formulations, storage reduced the release rates instead.

9.4 Conclusions

It was established that ageing and storage had an effect on the release behaviour from the G50/13 matrices. However, the extent of this effect also depended on the temperature of storage with the samples stored at the higher temperature of 37°C having more profound modifications to their release characteristics. Increasing the duration of storage also appreciated the amount of drug liberated and besides the temperature at which the samples were stored at, this outcome was also affected by the drug dispersed in them. Protracted storage at 20°C increased paracetamol release especially after longer periods of ageing but such occurrence was not demonstrated by the caffeine dispersion samples which did not show any significant changes after similar storage conditions. When stored at 37°C however, both paracetamol and caffeine dispersions showed pronounced elevations of drug release. Holding the samples at this temperature could have altered the structure in an alternative way to the samples held at 20°C or merely accelerated the change that occurred for the 20°C stored matrices.

In samples where storage affected a change in the release behaviour, there appeared to be a limit to the extent of the modification that ageing can bring. After this limit, increasing the number of storage days only brought about insignificant changes to the dissolution behaviour, for example 90 days for paracetamol dispersion samples stored at 37°C or 7 days for caffeine dispersion samples stored at the same temperature. Even though the release characteristics of the shorter or intermediate length of time stored samples were influenced by the type of drug dispersed in the matrices, the longer stored ones (180 days) had similar profiles to each other when they were stored in the same conditions. In view of this, it could be postulated that the release behaviour of aged samples is eventually controlled by the G50/13 only.

The bulk of the change occurred during the first week of ageing and this leads to the assumption that G50/13 matrices need more than 24 hours for the base to set completely. To ensure that the dissolution profiles are not altered further, the matrices could first be stored at 37°C for a few months until all the gelucire modifications have taken place. Most quality control checks for liquid filled hard gelatin capsules are performed after 10 to14 days of manufacture as it was thought that by then, the dissolution would be stable due to changes in polymorphism. This investigation has proven that dissolution studies and thermal analysis studies after ageing at different temperature for various time intervals are necessary to determine and predict whether any further changes would occur after longer periods of storage.

However, samples stored at 37°C gave unpredictable and fluctuating rates of release throughout the duration of the dissolution process. For matrices which are required to give constant rates of release, such tempering process may not be optimal. Ultimately, storage requirements will depend on the factor which is more critical, the availability of the drug at a certain time or a stable rate at which this drug is delivered. Even though there had been at least one previous study which proved that in-vitro results of ageing effects may not be reproduced in-vivo, it may had been due to the very low availability of the drug in the gastrointestinal tract so that the extremely slow release was the rate limiting stage and the dosage form could have passed through the absorption-window without complete absorption (Dennis et al, 1990). For more soluble drugs, ageing effects may be critical as

they have some control over the rate of release.

Finally, the mechanisms of release are also affected by ageing. The parameters which indicate the kinetics of release revealed the tendency towards erosion upon storage and this bias was even more apparent when samples were stored at 37°C. Therefore, ageing induces structural changes to the G50/13 matrix regardless of the drug dispersed within it and these changes lead to a shift in the mechanisms of release, which consequently alters the rate and profile of release. These structural changes are also sensitive to temperature.

CHAPTER 10: CONCLUSIONS

Differential Scanning Calorimetry (DSC) has shown that the G50/13 is composed of several different melting fractions. These fractions are brought about by the interaction between the various components within the gelucire which could be the formation of solid solutions between the multiple fat components and PEG components and their numerous polymorphic forms. The lower melting fraction (LMF) is thought to have a higher proportion of the less stable fat polymorphs and the free PEGs, the higher melting fraction (HMF) of partial glycerides and the middle melting fraction (MMF) of the rest of the components such as triglycerides and PEG esters. The thermal structure of G50/13 can be substantially affected by the drug incorporated. Addition of paracetamol had led to the stabilisation of the lower melting form of the G50/13 and hence the substantial rise in the LMF. Paracetamol could have achieved this by a combination of preventing the transformation of the metastable polymorphs to the more stable versions and forming a eutectic composition with some components in the MMF. However, the incorporation of caffeine did not have a similar effect with the thermal profile of the G50/13 and the SFC being mostly unaltered by the presence of the drug, suggesting that there was minimal interaction between the carrier and caffeine. Varying the loadings of the drug did not seem to have a significant effect on the structure except for the slight increase in the LMF.

Hot-stage microscopy has long been used as a complementary technique to DSC and in these investigations had also provided supportive information to the above. The melting which occurred in stages confirmed that the forms that gave rise to the various peaks existed from the onset of analysis and were not produced through polymorphic transformation during the heating process. The structures of the crystals that corresponded to the melting of the various peaks seen on DSC thermal profiles were different suggesting that the components in each fraction formed mixed crystals with various molecular packing which gave rise to the variance. The morphology of the crystals gave credence to the postulation that each fraction may be richer in some gelucire components than others, with the low melting feathery structure having a bigger proportion of PEGs and the higher melting spherulites having more of the fat components, with the partial glycerides contributing to the last structures seen during melting. More stable polymorphs probably contribute to the higher melting fraction not only due to the peak temperature shown in DSC but also for the larger crystal sizes.

Both paracetamol and caffeine showed a degree of solubilisation in the molten G50/13 which was also detected in DSC thermal analysis. However, the behaviour upon recrystallisation was vastly different with the paracetamol solidifying out as mixed crystals together with G50/13 and the caffeine crystallising out separately as whiskers. This observation supported the findings with DSC that showed the increase in the proportion of LMF in paracetamol dispersions. Under HSM, this is seen as the small and tightly arranged structures which is also indicative of its low melting range. Caffeine produced minimal effect on the G50/13 structure reflecting the DSC thermal profile of its dispersions.

On reflection, the study could have benefited from performing DSC scans on physical mixes of G50/13 and the drugs. This would indicate the effect that actual manufacturing process would have on the carrier and the drugs incorporated during production of dosage forms containing G50/13. From such study, it could be elucidated whether any eutectic was formed in physical mixes. However, eutectic formation in physical mixes could be of less significance in formulations that require the carrier to be melted prior to drug incorporation such as in the current study. Eutectic in physical mixes would be of more importance in compressed tablets made from dry powders. In order to identify the gelucire component(s) which may be forming eutectics with the drugs, DSC studies of the binary mixtures of each constituent such as the fatty acids, PEGs and glycerides with the drugs can be performed. However, this work would be very labourious and may not reflect the true nature of the eutectic as the different components in the gelucire may interact with each other and not be the simple sum of binary mixtures.

DSC scans on physical mixes could have improved the determination of the quantity of drug that is solubilised in the molten carrier. The amount of solubilised drug could be calculated from the difference in the heat of fusion of the drug before and after the holding period during the melt-fusion process. This technique would still not be very accurate due to the slow solubilisation of drug in the molten carrier during scanning itself which could in turn be reduced by increasing the heating rate after the melting of G50/13 in order to minimise the time for slow solubilisation to occur. In addition, the problem of caffeine vaporisation overlapping its melting could be reduced by using special pans designed for volatile substances.

In the dissolution studies, the release of caffeine was found to be slightly higher than paracetamol even after accounting for their solubilities in water. Erosion was also found to be more prominent in the caffeine dispersions than paracetamol dispersions through fitting to mathematical models and this result was supported by the physical measurements conducted. The greater ability of the paracetamol dispersions to swell can be attributed to the formation of mixed crystals as seen under HSM. The increase in the proportion of LMF led to a higher degree of softening in the dissolution medium. This relaxation of the long molecular chains allowed more dissolution medium to be accommodated within the matrices before eroding. The overall effect is then a more sustained release of the paracetamol through the slow dissolution of the swollen layer and diffusion. The pliability of the G50/13 matrices even at temperatures close to the melting range was also demonstrated by Kopcha et al (1991) (see Section 1.1.5, Chapter 1). Therefore, the use of thermal analysis techniques such as DSC and HSM to assess the structure and solidity of G50/13 matrices will facilitate the determination of their release profiles.

Formulations that contain glycerides and fatty acids have polymorphic forms that may alter upon storage so ageing studies were conducted on the G50/13 matrices. DSC thermal profiles revealed that as the ageing period progressed, the level of crystallinity in the matrices correspondingly increased. Gradual polymorphic transformations to the more stable forms seen as the elevation of peak temperatures and higher heat of fusion values due to the contribution of more stable forms occurred during storage. Storage at 37°C had a tempering effect on G50/13 with a substantial portion of the LMF converting to MMF brought about by the more vigorous polymorphic transformation to the more stable forms at this temperature. This postulation was supported by the observations under HSM that there was a dominance of the larger sized crystals indicating more stable forms after such storage. This tempering process brought the greatest modifications to the paracetamol dispersions with the SFC of these samples rising significantly even after only 7 days to diminish the softness previously seen on the freshly prepared matrices. Storage at this temperature could therefore be a useful technique in order to stabilise formulations such as tablets or oral spheres containing G50/13 where softness in the matrix would lead to adherence amongst the dosage forms or alterations to the dimensions of the formulations. The persistence of the lowest melting form even after tempering at 37°C for the caffeine

dispersions could mean that a part of the LMF for these samples was a eutectic composition not affected by storage. Alterations to the matrix due to polymorphism could be further ascertained using X-ray diffraction technique which could reveal changes in the spacings of the crystalline polymorphs. This study was not performed here due to the constrains of time but could be of a future interest.

However, storage also caused the *blooming* effect to be seen on the surfaces of the matrices aided by the use of SEM. The initial stages of this phenomenon could be seen after storage at 20°C with the needle-like structures signalling the movement of the fat towards the surface and the scale-like structures of crystallised stable forms but the most significant blooming occurred after storage at 37°C. This is because polymorphic transformation to the more stable forms which are seen as the bloom was promoted during tempering and also some of the more fluid G50/13 could have travelled through capillary action towards the surface and recrystallised in the more stable form. The incorporation of sorbitan monostearate was found to inhibit the formation of the bloom crystals which may be of importance in dosage forms with coated G50/13. The most substantial change amongst the samples occurred for paracetamol dispersions when the transformation of some LMF into MMF could be seen as the formation of tightly packed large crystals indicating their increased stability. Further work is necessary before it can be established whether the incorporation of SMS can inhibit the formation of these crystals on the surfaces of paracetamol dispersion matrices without affecting their elevated stability.

Ageing had altered the dissolution profiles of the samples but the extent of which depended on the temperature of storage and the drug incorporated. Prolonging the duration of storage at 20°C increased the release of the paracetamol but did not have a significant effect on the caffeine release. This alteration of the paracetamol release could be due to the increasing crystallinity of the matrices as had been shown by the more defined structures under SEM. The paracetamol release was more affected by this slight increase in crystallinity than caffeine due to the high level of LMF caused by the formation of the mixed crystals. In the drug loading dissolution studies, this had been proven to lower the release due to more extensive swelling. Ageing at 37°C however, increased both paracetamol and caffeine releases substantially and this correlated with the rise in crystallinity and the SFC of the

dispersions at the dissolution medium temperature of 37°C. This change in the structure as elucidated by thermal analysis led to a higher degree of erosion which contributed to the increase in the drugs releases. The similarity between the paracetamol and caffeine releases after 180 days ageing at 37°C suggests that the modifications within G50/13 itself that ultimately control the dissolution profiles. This was supported by the observation that the tensile strength of the pure G50/13 decreased as the duration of storage increased and after 180 days, the influence of the carrier dominated as seen in the high drugs releases. The period of time after which the dissolution profiles no longer changes is different for the two drug dispersions. Therefore, it would be recommended that drug dispersions are aged at this temperature for several months in order to obtain formulations which are stable and which dissolution profiles can be predicted from the behaviour of G50/13 only. It could be of future interest to investigate whether these changes to the matrices brought about by ageing would be of significance in-vivo.

Other additional studies which could follow the current series include the storage of the matrices under different humidity conditions in order to investigate the effect of moisture on G50/13. Factors such as the degradation of the gelucire, polymorphic stability, rate of crystallisation and the protective action of the carrier on incorporated drugs could be studied under these environments, thus requirements for any special packing of the formulations could be determined. Furthermore, drugs with very low water solubility could be incorporated into G50/13 to investigate the ability of this gelucire to improve release in relation to its erosional behaviour. These drugs could include those which are novel and have availability problems, as more common low water solubility drugs have been previously investigated in G50/13, for example ketoprofen by Dennis et al (1990). As mentioned before, the study with sorbitan monostearate could be taken much further. The structure of drug incorporated G50/13 matrices with added SMS could be investigated before and after ageing to ascertain beneficial or detrimental changes to the stability together with possible modifications to the release of the drugs due to the emulsifier.

In short, the current study has shown that incorporation of certain drugs into G50/13 can lead to adverse alterations to formulations such as the formation of soft and sticky matrices. Even though studies from other investigators have shown differences in the characteristics

of gelucire matrices due to added drugs, this current study has shown that by manipulating storage conditions, unwanted matrix properties and instability can be overcome. In addition, this can be achieved without having to substitute the chosen gelucire with another type. Variation in dosage forms behaviour during storage can be reduced by tempering so that a stable form with well characterised properties can be obtained in a relatively short time. Emulsifiers such as sorbitan stearates has also been shown by this study to demonstrate a great potential in minimising unfavourable matrix characteristics and would be of great use in the manufacture of dosage forms with gelucires as these emulsifiers are cheap, easily obtainable, convenient to use and compatible with most lipid carriers.

Appendix 1

Specifications for Gelucire 50/13 used in the study (Gattefossé, 1992)

Definition

Steroyl Macrogolglycerides EP. Conforms to the monograph under the same name in the European Pharmacopeia 3rd Edition.

Registrations

INCI Name: Hydrogenated palm glycerides / Polyglycolester.

Solubilities at 20°C (European Pharmacopeia 3rd Edition)

Insoluble in ethanol 96°. Soluble in chloroform and methylene chloride. Dispersible in water. Insoluble in mineral oils.

Description	**Specification limits**
Appearance	Waxy solid
Colour	< 5
Drop point (Mettler)	46.0 to 51.0°C
Acid value	< 2.00 mgKOH/g
Saponification value	67 to 81 mgKOH/g
Iodine value	< 2 gI_2/100g
Hydroxyl value	36 to 56 mgKOH/g
Peroxide value	< 6.0 meqO_2/Kg
Alkaline impurities	< 80 ppm NaOH
Water content	< 0.50 %
Total ashes content	< 0.10 %
Heavy metals	< 10 ppm

Description	**Specification limits**
Free glycerol content	< 3 %
Caprylic acid (C8)	< 3 %
Capric acid (C10)	< 3 %
Lauric acid (C12)	< 5 %
Myristic acid (C14)	< 5 %
Palmitic acid (C16)	40 to 50 %
Stearic acid (C18)	48 to 58 %
Stearic and palmitic acids	> 90 %

Appendix 2

Chemical characteristics of the model drugs used (British Pharmacopeia 1993; The Merck Index, 12th Edition; Therapeutic Drugs, Churchill Livingstone, 1991)

Paracetamol

Chemical structure :

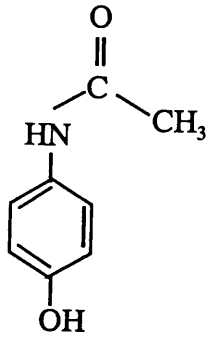

Chemical formula : $C_8H_9NO_2$

Chemical name : N-Acetyl-*p*-aminophenol, 4-hydroxyacetanilide, 4-acetamidophenol

Molecular weight : 151.2

pKa (-OH) : 9.5

Solubility
in alcohol : 1 in 70
in water : 1 in 70

Melting point : 169-170.5°C

Caffeine

Chemical structure :

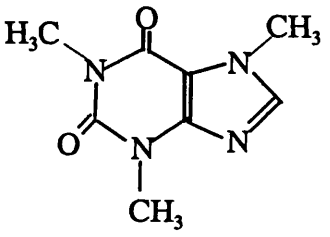

Chemical formula : $C_8H_{10}N_4O_2$

Chemical name : 3, 7-Dihydro-1, 3, 7-trimethyl-1H-purine-2, 6-dione

Molecular weight : 194.2

pKa : 13.9

Solubility
in alcohol : 1 in 130
in water : 1 in 60

Melting point : 234 to 239°C

Sorbitan monostearate

Chemical structure :

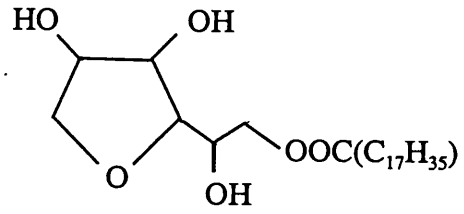

Chemical formula : $C_{24}H_{46}O_6$

Melting point : 49-65°C (Merck Index), 50-55°C (Bri. Phar.)

HLB value : 4.7

Acid value : 5-11

Saponification value : 140-157

Hydroxyl value : 230-260

Solubilities : Soluble in alcohols, carbon tetrachloride, toluene, insoluble in water, acetone and mineral spirits.

Appendix 3

An example of the baseline curve obtained from scanning two empty pans at 2°C/min (refer to Section 2.2.3 in Chapter 2).

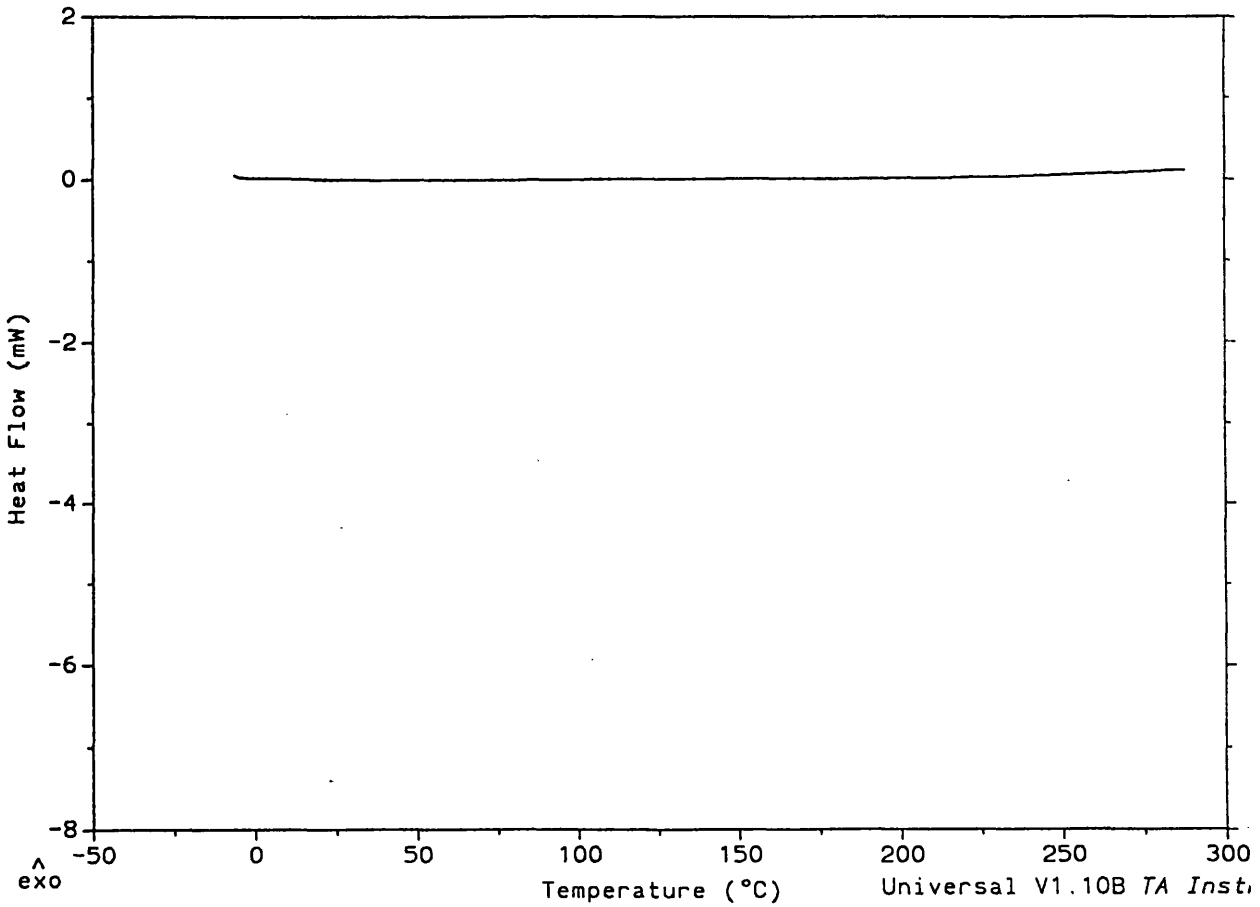

An example of the calculation performed by Universal Analysis software on a 20% paracetamol dispersion in G50/13 sample showing peak temperatures (°C) and heats of fusion (J/g) (refer to Section 2.2.3 in Chapter 2).

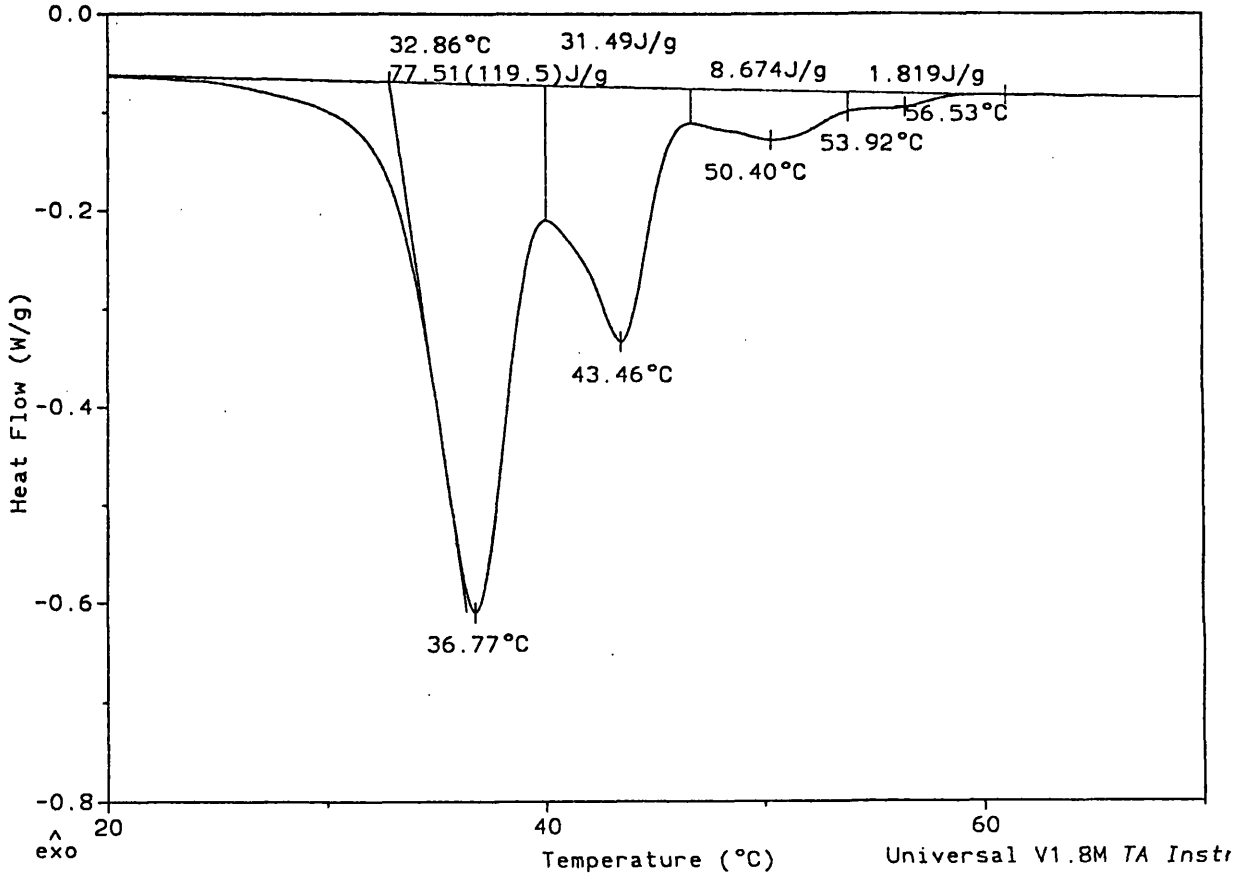

Appendix 4

Diagrammatic example of the calculation of Solid Fat Content (SFC)

(refer to Section 2.2.3 in Chapter 2).

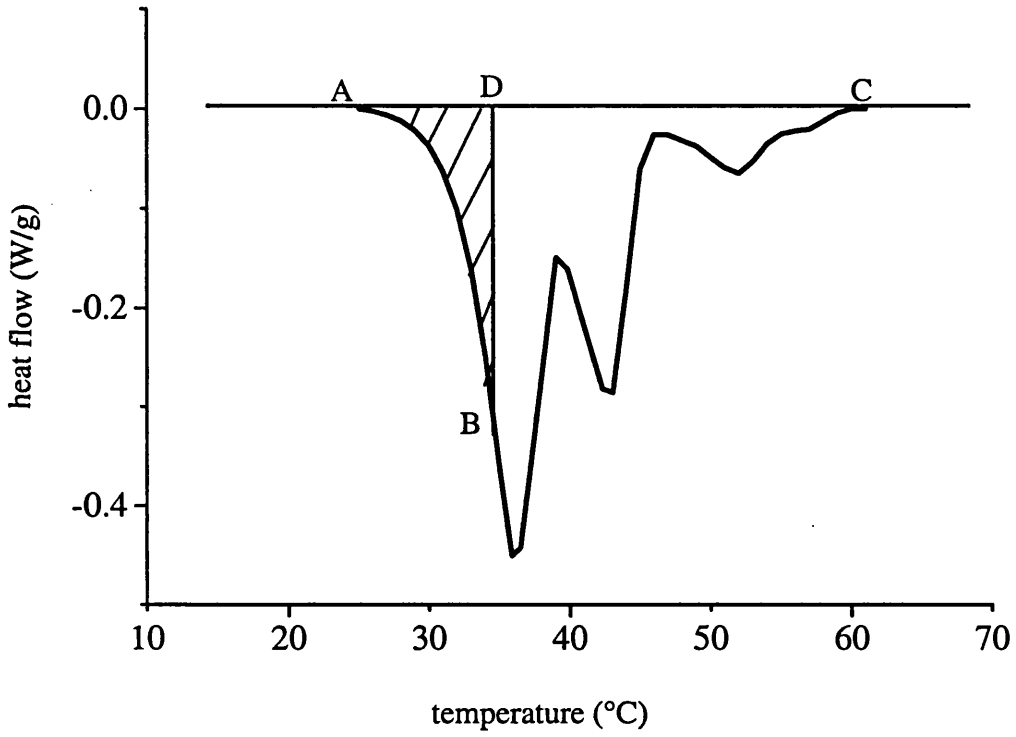

Solid Fat Content (%) at the temperature corresponding to point B is calculated as

$$\frac{\text{Area ABCD - Area ABD (shaded area)}}{\text{Area ABCD}} \times 100$$

Thermal profile of paracetamol (refer to Table 2.8 in Chapter 2)

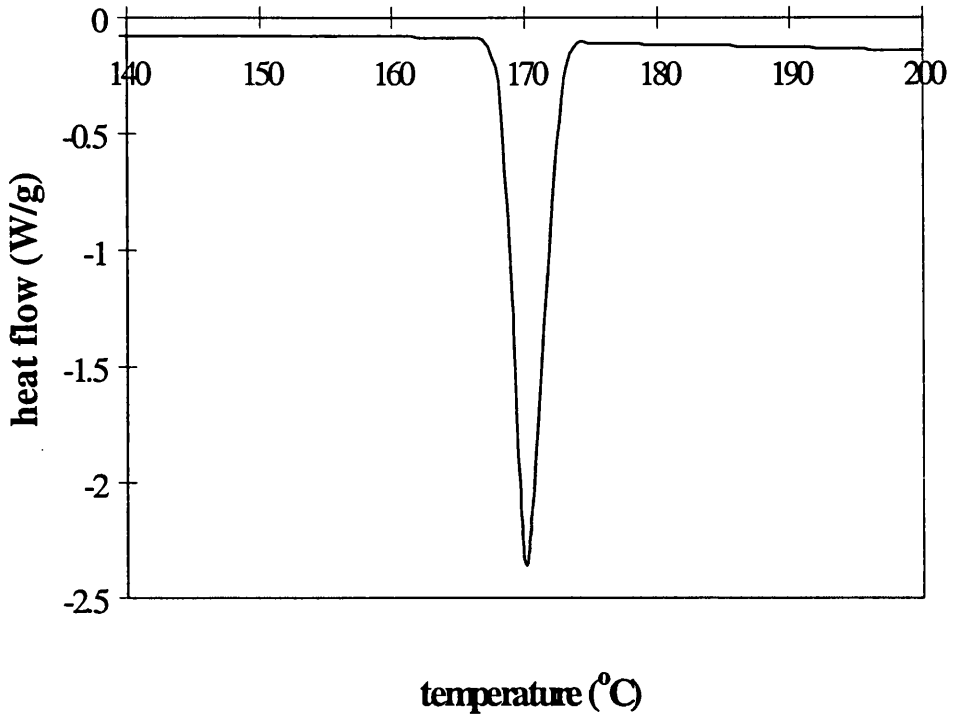

Thermal profile of caffeine (refer to Table 2.12 in Chapter 2)

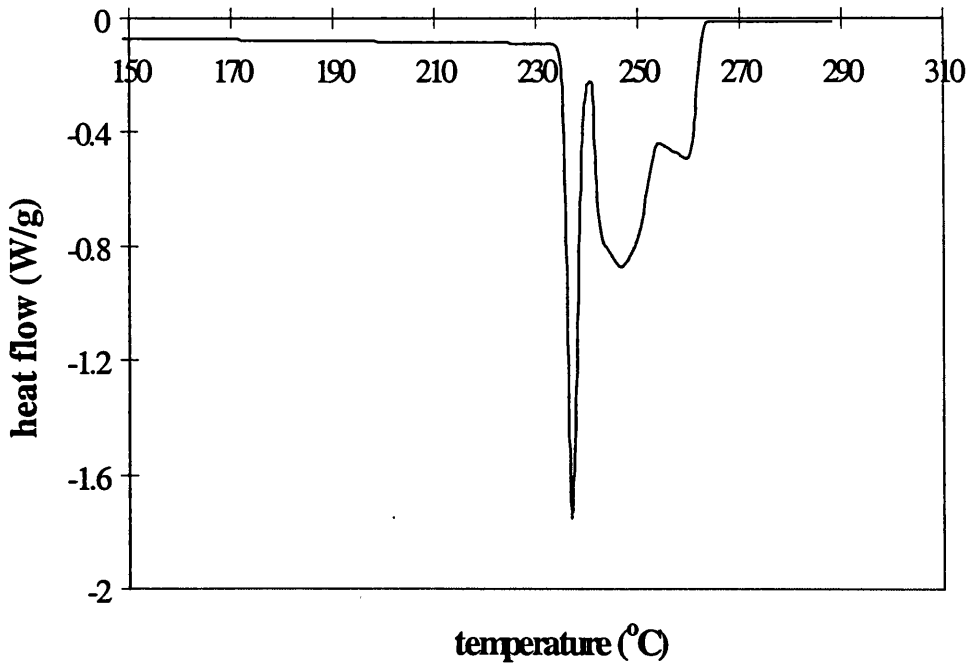

Appendix 5

Particle size analyses of drugs using polarising microscopy method as outlined in US Pharmacopeia No. 24 (optical microscopy for particle characterisation).

Paracetamol

Mean value (μm): 21.5

Confidence interval at 95% confidence level (μm): (20.0,23.0)

1st quartile value (μm): 16.0

Median value (μm): 19.0

3rd quartile value (μm): 24.5

Micrograph showing a sample of paracetamol

Ratio of actual length : length in plate 1:585

Caffeine

Mean value (μm): 24.5

Confidence interval at 95% confidence level (μm): (22.5,26.5)

1st quartile value (μm): 16.0

Median value (μm): 21.0

3rd quartile value (μm): 29.0

Micrograph showing a sample of caffeine

Ratio of actual length : length in plate 1:585

Appendix 6

Tabulated DSC data of aged pure G50/13, 10% paracetamol and 10% caffeine dispersions in G50/13.

Table 1: Peak temperature values (°C) for pure G50/13 after ageing at 20°C (refer to Figure 6.1 in Chapter 6).

	1st peak	*2nd peak*	*3rd peak*	*4th peak*
fresh	36.0 ± 0.2	44.0 ± 0.2	48.7 ± 0.4	55.7 ± 0.1
7 days	38.1 ± 0.2	44.7 ± 0.2	50.2 ± 0.2	55.9 ± 0.4
30 days	37.0 ± 0.2	43.5 ± 0.3	50.3 ± 0.1	54.8 ± 0.2
90 days	38.4 ± 0.2	44.7 ± 0.2	50.4 ± 0.1	55.9 ± 0.3
180 days	38.1 ± 0.2	44.3 ± 0.1	50.4 ± 0.1	55.7 ± 0.1

Table 2: Heat of fusion values (J/g) for pure G50/13 after ageing at 20°C (refer to Figure 6.1).

	1st peak	*2nd peak*	*3rd peak*	*4th peak*	*Total*
fresh	37.7 ± 1.0	99.6 ± 1.4	7.8 ± 0.2	2.4 ± 0.1	147.6 ± 2.2
7 days	49.5 ± 2.7	90.3 ± 3.3	9.0 ± 0.8	2.7 ± 0.2	151.5 ± 6.7
30 days	49.3 ± 0.9	89.4 ± 0.8	10.3 ± 0.4	2.5 ± 0.3	151.5 ± 1.0
90 days	49.4 ± 0.6	90.4 ± 1.2	9.6 ± 0.6	2.9 ± 0.1	152.4 ± 1.1
180 days	48.5 ± 0.6	92.0 ± 0.7	10.0 ± 0.4	3.0 ± 0.2	153.5 ± 1.0

Table 3: Peak temperature values (°C) for pure G50/13 after ageing at 37°C (refer to Figure 6.2).

	1st peak	*2nd peak*	*3rd peak*	*4th peak*
fresh	36.0 ± 0.2	44.0 ± 0.2	48.7 ± 0.4	55.7 ± 0.1
7 days		44.3 ± 0.1	49.4 ± 0.2	55.7 ± 0.2
30 days		46.1 ± 0.1		56.0 ± 0.3
90 days		46.5 ± 0.2	51.6 ± 0.2	56.8 ± 0.2
180 days		47.2 ± 0.1	52.0 ± 0.3	57.3 ± 0.2

Table 4: Heat of fusion values (J/g) for pure G50/13 after ageing at 37°C (refer to Figure 6.2).

	1st peak	*2nd peak*	*3rd peak*	*4th peak*	*Total*
fresh	37.7 ± 1.0	99.6 ± 1.4	7.8 ± 0.2	2.4 ± 0.1	147.6 ± 2.2
7 days		140.8 ± 3.7	7.5 ± 0.5	2.8 ± 0.3	151.0 ± 3.6
30 days		152.5 ± 3.2		3.5 ± 0.1	156.0 ± 3.2
90 days		146.3 ± 2.5	6.7 ± 0.3	5.5 ± 0.7	158.4 ± 2.5
180 days		146.4 ± 0.4	8.0 ± 0.7	5.8 ± 0.2	160.2 ± 0.9

Table 5: Peak temperature (°C) and heat of fusion (J/g) values for untreated G50/13 (refer to Figure 6.3).

	1st peak	*2nd peak*	*3rd peak*	*4th peak*	*Total*
peak temp., (°C)		45.5 ± 0.5	51.7 ± 0.3	57.7 ± 0.3	
heat of fusion, (J/g)	22.4 ± 0.9	118.8 ±1.6	11.7 ± 1.2	2.8 ± 0.1	155.8 ± 2.1

Table 6: Peak temperature values (°C) for 10% paracetamol dispersions in G50/13 after ageing at 20°C (refer to Figure 6.4).

	1st peak	*2nd peak*	*3rd peak*	*4th peak*
fresh	36.4 ± 0.1	42.5 ± 0.1	51.8 ± 0.1	57.0 ± 0.2
7 days	36.4 ± 0.2	42.6 ± 0.4	51.7 ± 0.1	57.0 ± 0.2
30 days	36.8 ± 0.1	43.1 ± 0.2	51.5 ± 0.1	56.6 ± 0.6
90 days	36.6 ± 0.3	42.6 ± 0.4	51.8 ± 0.2	57.0 ± 0.3
180 days	37.6 ± 0.1	44.1 ± 0.1	51.4 ± 0.1	56.7 ± 0.2

Table 7: Heat of fusion values (J/g) for 10% paracetamol dispersions in G50/13 after ageing at 20°C (refer to Figure 6.4).

	1st peak	*2nd peak*	*3rd peak*	*4th peak*	*Total*
fresh	76.6 ± 3.5	38.3 ± 0.8	12.4 ± 0.3	2.3 ± 0.1	129.5 ± 4.5
7 days	70.9 ± 3.6	39.9 ± 0.1	11.4 ± 1.0	2.2 ± 0.3	124.3 ± 5.4
30 days	73.8 ± 0.8	42.7 ± 1.0	11.3 ± 0.5	2.5 ± 0.3	130.2 ± 1.9
90 days	69.2 ± 0.7	42.0 ± 1.0	11.6 ± 0.6	2.2 ± 0.3	124.6 ± 1.7
180 days	78.0 ± 1.9	44.7 ± 0.8	10.4 ± 0.1	2.5 ± 0.2	136.7 ± 3.2

Table 8: Peak temperature values (°C) for 10% paracetamol dispersions in G50/13 after ageing at 37°C (refer to Figure 6.5).

	1st peak	*2nd peak*	*3rd peak*	*4th peak*
fresh	36.4 ± 0.1	42.5 ± 0.1	51.8 ± 0.1	57.0 ± 0.2
	1st peak	*sub1st peak*	*2nd peak*	*3rd peak*
7 days	37.6 ± 0.3	40.9 ± 0.1	44.3 ± 0.3	52.6 ± 0.2
	1st peak	*2nd peak*	*sub2nd peak*	*3rd peak*
30 days	39.9 ± 0.1	44.4 ± 0.1	46.5 ± 0.1	52.8 ± 0.1
90 days		45.4 ± 0.3		53.5 ± 0.2
180 days		45.8 ± 0.1	47.6 ± 0.2	54.1 ± 0.1

Table 9: Heat of fusion values (J/g) for 10% paracetamol dispersions in G50/13 after ageing at 37°C (refer to Figure 6.5).

	1st peak		*2nd peak*	*3rd peak*	*4th peak*	*Total*
fresh	76.6 ± 3.5		38.3 ± 0.8	12.4 ± 0.3	2.3 ± 0.1	129.5 ± 4.5
	1st peak	*sub 1st peak*	*2nd peak*	*3rd peak*	*4th peak*	*Total*
7 days	56.4 ± 2.2	37.2 ± 1.8	21.6 ± 1.5	13.0 ± 0.5	2.9 ± 0.3	131.2 ± 2.8
	1st peak	*2nd peak*	*sub2nd peak*	*3rd peak*	*4th peak*	*Total*
30 days	59.9 ± 0.6	39.4 ± 1.6	25.4 ± 1.5	11.4 ± 0.4	3.8 ± 0.3	139.8 ± 1.3
	1st peak	*2nd peak*		*3rd peak*	*4th peak*	*Total*
90 days	52.2 ± 1.2	72.2 ± 1.3		12.5 ± 0.4	4.7 ± 0.5	141.6 ± 1.5
	1st peak	*2nd peak*	*sub2nd peak*	*3rd peak*	*4th peak*	*Total*
180 days	52.6 ± 2.6	44.9 ± 0.6	28.5 ± 0.5	13.1 ± 0.3	6.3 ± 0.8	145.4 ± 3.9

Table 10: Peak temperature values (°C) for 10% caffeine dispersions in G50/13 after ageing at 20°C (refer to Figure 6.6).

	1st peak	*2nd peak*	*3rd peak*	*4th peak*
fresh	37.0 ± 0.1	43.9 ± 0.1	48.4 ± 0.2	55.0 ± 0.1
7 days	36.8 ± 0.5	42.6 ± 0.3	49.4 ± 0.3	55.5 ± 0.1
30 days	36.9 ± 0.1	43.5 ± 0.2	49.0 ± 0.2	55.4 ± 0.1
90 days	37.4 ± 0.6	43.7 ± 0.1	49.5 ± 0.2	55.6 ± 0.3
180 days	37.7 ± 0.3	44.1 ± 0.3	49.5 ± 0.1	56.0 ± 0.1

Table 11: Heat of fusion values (J/g) for 10% caffeine dispersions in G50/13 after ageing at 20°C (refer to Figure 6.6).

	1st peak	*2nd peak*	*3rd peak*	*4th peak*	*Total*
fresh	39.8 ± 0.5	89.9 ± 0.6	7.1 ± 0.1	2.2 ± 0.2	139.0 ± 0.7
7 days	34.1 ± 2.0	95.0 ± 0.9	9.6 ± 0.7	2.4 ± 0.2	140.5 ± 1.6
30 days	34.2 ± 0.9	95.2 ± 1.3	8.7 ± 0.6	2.5 ± 0.2	140.6 ± 1.2
90 days	30.3 ± 1.4	95.8 ± 0.8	8.0 ± 0.4	2.6 ± 0.2	136.8 ± 2.0
180 days	31.1 ± 1.3	99.2 ± 0.6	8.2 ± 0.2	2.8 ± 0.1	141.3 ± 0.9

Table 12: Peak temperature values (°C) for 10% caffeine dispersions in G50/13 after ageing at 37°C (refer to Figure 6.7).

	1st peak	*2nd peak*	*3rd peak*	*4th peak*
fresh	37.0 ± 0.1	43.9 ± 0.1	48.4 ± 0.2	55.0 ± 0.1
7 days	38.1 ± 0.2	44.6 ± 0.2	50.8 ± 0.2	56.4 ± 0.1
30 days	37.9 ± 0.3	44.8 ± 0.3	51.1 ± 0.2	56.6 ± 0.3
90 days	40.6 ± 0.1	47.4 ± 0.1	52.7 ± 0.1	
180 days	40.9 ± 0.2	47.6 ± 0.1	53.3 ± 0.4	

Table 13: Heat of fusion values (J/g) for 10% caffeine dispersions in G50/13 after ageing at 37°C (refer to Figure 6.7).

	1st peak	*2nd peak*	*3rd peak*	*4th peak*	*Total*
fresh	39.8 ± 0.5	89.9 ± 0.6	7.1 ± 0.1	2.2 ± 0.2	139.0 ± 0.7
7 days	38.8 ± 0.7	87.0 ± 0.4	9.8 ± 0.4	3.0 ± 0.2	138.7 ± 1.0
30 days	35.9 ± 0.9	92.0 ± 0.8	10.7 ± 0.8	3.3 ± 0.3	141.9 ± 0.9
90 days	36.3 ± 1.3	93.4 ± 0.6	13.4 ± 0.2		143.1 ± 1.3
180 days	32.5 ± 0.7	95.2 ± 0.4	16.7 ± 0.3		144.3 ± 1.0

REFERENCES

A

Ainaoui, A., Ouriemchi, E. M., Bidah, D., El Amrani, M. K. and Vergnaud, J. M. (1997) Process of drug release with oral dosage forms with a lipidic gelucire matrix. *J. Polymer Eng.*, **17**, 245-255.

Aïnaoui, A. and Vergnaud, J. M. (1998) Modelling the plasma drug level with oral controlled release dosage forms with lipidic Gelucire. *Int. J. Pharm.*, **169**, 155-162.

Allen, T. (1975) Particle size measurement. *Powder Technology Series.* Chapman and Hall, London.

Armstrong, N. A. (2000) Glyceryl palmitostearate. In *Handbook of pharmaceutical excipients*, Kibbe, A. H. (ed.), American Pharmaceutical Association and Pharmaceutical Press, Washington and London, 228-229.

Aronhime, J. S., Sarig, S. and Garti, N. (1987) Mechanistic considerations of polymorphic transformations of tristearin in the presence of emulsifiers. *J. Amer. Oil Chem. Soc.*, **64**, 529-533.

Aronhime, J. S. (1988) Application of thermal analysis (DSC) in the study of polymorphic transformations. *Thermochimica Acta,* **134**, 1-14.

Aronhime, J. S., Sarig, S. and Garti, N. (1988a) Reconsideration of polymorphic transformations in cocoa butter using the DSC. *J. Amer. Oil Chem. Soc.*, **65**, 1140-1143.

Aronhime, J. S., Sarig, S. and Garti, N. (1988b) Dynamic control of polymorphic transformation in triglycerides by surfactants: The Button Syndrome. *J. Amer. Oil Chem. Soc.*, **65**, 1144-1150.

Aronhime, J. S., Sarig, S. and Garti, N. (1990) Emulsifiers as additives in fats: Effect on polymorphic transformations and crystal properties of fatty acids and triglycerides. *Food Structure,* **9**, 337-352.

Aungst, B. J. and Hussain, M. A. (1992) Sustained propanolol delivery and increased oral bioavailability in dogs given a propanolol laurate salt. *Pharm. Res.*, **9**, 1507-1509.

B

Babar, A., Bellete, T. and Plakogiannis, F. M. (1999) Ketoprofen suppository dosage forms: In vitro release and in vivo absorption studies in rabbits. *Drug Dev. Ind. Pharm.*, **25**, 241-

245.

Bailey, A. E. (ed.)(1950) In *Melting and solidification of fats*. Interscience Publishers, New York, 117-123.

Barnwell, S. G., Gauci, L., Harris, R. J., Attwood, D., Littlewood, G., Guard, P., Pickup, M. E. and Barrington, P. (1994) Greatly enhanced oral bioavailability of propanolol using the HALO™ liver-bypass drug delivery system. *J. Controlled Release,* **28**, 306-309.

Barnwell, S. G., Burns, S. J., Higginbottom, S., Whelan, I., Corness, D., Hay, G., Rosenburg, E. and Attwood, D. (1996) Demonstration of the importance of biphasic oleic acid delivery for enhancing the bioavailability of propanolol in healthy volunteers. *Int. J. Pharm.,* **128**, 145-154.

Basiron, Y. (1996) Palm oil. In *Bailey's Industrial Oil and Fat Products Volume 2*, Hui, Y. H. (ed.), John Wiley and Sons Inc., New York, 271-376.

Baykara, T. and Yüksel, N. (1991) The preparation of prolonged action formulations in the form of semi solid matrix into hard gelatin capsules of oxprenolol 1. Thermocap method. *Drug Dev. Ind. Pharm.,* **17**, 1215-1227.

Behme, R. J., Brooke, D., Farney, R. F. and Kensler, T. T. (1985) Characterisation of polymorphism of gepirone hydrochloride. *J. Pharm. Sci.*, **74**,1041-1046.

Beren, A. R. and Hopfenberg, H. B. (1978) Diffusion and relaxation in glassy polymer powders. II. Separation of diffusion and relaxation parameters. *Polymers,* **19**, 489.

Bernasconi, C., Doelker, E. and Buri, P. (1985) Diffusion and erosion controlled drug release from lipid matrix formulations into hard gelatin capsules. *Proceed. Intern. Symp. Control. Rel. Bioact. Mater., Controlled Release Society, Inc.,* **12**, 272-273.

Bidah, D. and Vergnaud, J. M. (1990) Kinetics of in vitro release of sodium salicylate dispersed in Gelucire. *Int. J. Pharm.,* **58**, 215-220.

Bidah, D. and Vergnaud, J.M. (1991) New oral dosage form with two polymers: Gelucire and Sumikagel. *Int. J. Pharm.*, **72**, 35-41.

Bidah, D., Ouriemchi, E. M. and Vergnaud, J. M. (1992) Diffusion process of drug delivery from a dosage form with a Gelucire matrix. *Int. J. Pharm.*, **80**, 145-149.

Bodmeier, R., Paeratakul, O., Chen, H. and Zhang, W. (1990) Formation of sustained release wax matrices within hard gelatin capsules in a fluidized bed. *Drug Dev. Ind. Pharm.,* **16**, 1505-1519.

Bodmeier, R., Wang, J. and Bhagwatwar, H. (1992) Process and formulation variables in

the preparation of wax microparticles by a melt dispersion technique. I. Oil-in-water technique for water insoluble drugs. *J. Microencapsulation,* **9**, 89-98.

Bowtle, W. J., Lucas, R. A. and Barker, N. J. (1986) Formulation and process studies in semi-solid matrix capsule technology. *Proceedings of the 4th International Conf. of pharmaceutical technology, June 1986, Paris,* **5**, 80-89.

Bradbury, S. and Evennett, P. (eds.)(1996) *Contrast Techniques in Light Microscopy.* Bios Scientific, Oxford.

Bradbury, S. (ed.)(1996) *An introduction to the optical microscope: Royal Microscopical Handbook (01).* Bios Scientific, Oxford.

Brodin, A., Nyqvist-Mayer, A., Wadsten, T., Forslund, B. and Broberg, F. (1984) Phase diagram and aqueous solubility of the lidocaine-prilocaine system. *J. Pharm. Sci.*, **73**, 481-484.

Brossard, C., Ratsimbazafy, V. and Lefort des Ylouses, D. (1991) Modelling of theophylline compound release from hard gelatin capsules containing gelucire matrix granules. *Drug Dev. Ind. Pharm.*, **17**, 1267-1277.

Burns, S. J., Corness, D., Hay, G., Higginbottom, S., Whelan, I., Attwood, D. and Barnwell, S. G. (1996a) An in-vitro assessment of liquid-filled Capill® potato starch capsules with biphasic release characteristics. *Int. J. Pharm.,* **134**, 223-230.

Burns, S. J., Higginbottom, S., Whelan, I., Bowtle, W. J., Rosenberg, E., Corness, D., Hay, G., Attwood, D. and Barnwell, S. G. (1996b) Formulation strategies designed to maintain the biphasic release characteristics of liquid-filled capsules. *Int. J. Pharm.,* **141**, 9-16.

Busfield, W. K. and Proschogo, P. N. (1990) Hydrogenation of Palm Stearine: Changes in chemical composition and thermal properties. *J. Amer. Oil Chem. Soc.,* **67**, 176-181.

C

Cebula, D. J., Dilley, K. M. and Smith, K. W. (1991) Continuous tempering studies on model confectionery systems. *The Manufacturing Confectioner*, **71**, 131-136.

Cebula, D. J., Smith, K. W. and Talbot, G. (1992) DSC of confectionery fats, pure triglycerides. Effects of cooling and heating rate variation. *The Manufacturing Confectioner*, **72**, 135-139.

Chaiseri, S. and Dimick, P. (1995) Dynamic Crystallization of Cocoa Butter. II. Morphological, Thermal and Chemical Characteristics during Crystal Growth. *J. Ame. Oil*

Chem. Soc., **72**, 1497-1504.

Chapman, D. (1962) The polymorphism of glycerides. *Chem. Rev.*, **62**, 433-456.

Charman, W. N. A. and Stella, V. J. (1991) Transport of lipophilic molecules by the intestinal lymphatic system. *Adv. Drug Del. Rev.*, **7**, 1-14.

Chawla, P., deMan, J. M. and Smith, A. K. (1990) Crystal morphology of shortenings and margarines. *Food Structure*, **9**, 329-336.

Chiou, W. L. and Riegelman, S. (1971) Pharmaceutical applications of solid dispersion systems. *J. Pharm. Sci.*, **60**, 1281-1302.

Chiou, W. L. and Niazi, S. (1971) Phase diagram and dissolution-rate studies on sulfathiazole-urea solid dispersions. *J. Pharm. Sci.*, **60**, 1333-1338.

Chow, D. (2000) Suppository bases, hard fat. In *Handbook of pharmaceutical excipients*, Kibbe, A. H. (ed.), American Pharmaceutical Association and Pharmaceutical Press, Washington and London, 550-554.

Coben, L. J. and Lordi, N. G. (1980) Physical stability of semisynthetic suppository bases. *J. Pharm. Sci.*, **69**, 955-960.

Coleman, N. J. and Craig, D. Q. M. (1996) Modulated temperature differential scanning calorimetry: a novel approach to pharmaceutical thermal analysis. *Int. J. Pharm.*, **135**, 13-29.

Colombo, P., Bettini, R., Massimo, G., Catellani, P. L., Santi, P. and Peppas, N. A. (1995) Drug diffusion front movement is important in drug release control from swellable matrix tablets. *J. Pharm. Sci.*, **84**, 991-997.

Corrigan, O. I. (1987) Retardation of polymeric carrier dissolution by dispersed drugs: factors influencing the dissolution of solid dispersions containing polyethylene glycols. In *Controlled Drug Release, Volume 1*, Rubinstein, M. H. (ed.), Ellis Horwood Limited, 88-98.

Craig, D. Q. M. (1996) The physical characterisation of Gelucire 50/13. *Bulletin Technique Gattefossé*, **89**, 39-51.

D

de Blaey, C. J. and Rutten-Kingma, J. J. (1976) Biopharmaceutics of aminophylline suppositories I. Introduction and in-vitro melting behaviour. *Pharm. Acta Helv.*, **51**, 186-192.

Delahaye, N., Duclos, R. and Saiter, J. M. (1997) Characterisation of PEG 6000 phase transitions. Influence of kinetic conditions. *Int. J. Pharm.*, **157**, 27-34.

Delgado-Charro, M. and Vila-Jato, J. (1991) In vitro study of prolonged-release formulations containing amoxicillin and Gelucire 64/02. *S.T.P. Pharm. Sci.*, **1**, 300-306.

Delgado-Charro, M. B. and Vila-Jato, J. L. (1992) In vivo study of sustained-release formulations containing amoxycillin and Gelucire 64/02. *Int. J. Pharm.*, **78**, 35-41.

Delgado-Charro, M. B., Lopez Rial, I. and Vila-Jato, J. L. (1993) Aging of sustained-release formulations of amoxicillin and gelucire 64/02. *Drug Dev. Ind. Pharm.*, **19**, 473-482.

deMan, J. M. (1961a) Physical properties of milk fat. I. Influence of chemical modification. *J. Dairy Res.*, **28**, 81-85.

deMan, J. M. (1961b) Physical properties of milk fat. II. Some factors influencing crystallisation. *J. Dairy Res.*, **28**, 117-121.

deMan, J., Mostafa, A. and Smith, A. (1985) Thermal Analysis Microscopy for the Study of Phase Changes in Fats. *Food Microstructure,* **4**, 233-239.

deMan, L. and deMan, J. M. (1994) Functionality of palm oil in margarines and shortenings. *Lipid Technol.*, **6**, 5-10.

De Muynck, C. and Remon, J. P. (1992) Influence of fat composition on the melting behaviour and on the in vitro release of indomethacin suppositories. *Int. J. Pharm.*, **85**, 103-112.

Dennis, A. B., Kellaway, I. W. and Davidson, R. (1987) Drug release from a slowly hydrating semi-solid matrix. *J. Pharm. Pharmacol.*, **39**, 40P.

Dennis, A. B. (1988) Sustained drug release from semi-solid capsule formulations. Ph.D. Thesis, University of Wales.

Dennis, A. B., S. J. Farr, Kellaway, I. W., Taylor, G. and Davidson, R. (1990) In vivo evaluation of rapid release and sustained release Gelucire capsule formulations. *Int. J. Pharm.*, **65**, 85-100

Dimick, P. S. and Manning, D. M. (1987) Thermal and compositional properties of cocoa butter during static crystallisation. *J. Amer. Oil Chem. Soc.*, **64**, 1663-1669.

Dimick, P. S. (1991) Principles of cocoa butter crystallisation. *The Manufacturing Confectioner,* **71**, 109-114.

Djimbo, M., Fell, J. T., Kaus, L. and Moës, A. J. (1984) Release of drugs formulated as

hard gelatin filled into hard gelatin capsules. Part 2. In vitro studies. *J. Pharm. Belg.*, **39**, 43-49.

Doelker, C., Doelker, E., Buri, P., Waginaire, L. and Glas, B. (1983) Incorporation of liquid, deliquescent and unstable active ingredients into excipients for hard gelatin capsules. *3rd Int. Conf. Pharm. Technol., Paris, June.*

Doelker, C., Doelker, E., Buri, P. and Waginaire, L. (1986) The incorporation and in vitro release profiles of liquid, deliquescent or unstable drugs with fusible excipients in hard gelatin capsules. *Drug Dev. Ind. Pharm.*, **12**, 1553-1565.

Dordunoo, S. K., Ford, J. L. and Rubinstein, M. H. (1991) Preformulation studies on solid dispersions containing triamterene or temazepam in polyethylene glycols or Gelucire 44/14 for liquid filling of hard gelatin capsules. *Drug Dev. Ind. Pharm.*, **17**, 1685-1713.

Dordunoo, S. K., Ford, J. L. and Rubinstein, M. H. (1996) Solidification studies of polyethylene glycols, gelucire 44/14 or their dispersions with triamterene or temazepam. *J. Pharm. Pharmacol.*, **48**, 782-789.

Dunn, G. A. (1998) Transmitted-light interference microscopy: A technique born before its time. *Proc. Roy. Microsc. Soc.*, **33**, 189-196.

DuRoss, J. W. and Knightly, W. H. (1965) Relationship of sorbitan monostearate and polysorbate 60 to bloom resistance in properly tempered chocolate. *The Manufacturing Confectioner*, **July**, 50-56.

E

Eckert, V. T., Knie, U. and Heers, W. (1982a) Über die bioverfügbarkeit bei gelagerten suppositorien: Untersuchungen am beispiel des naproxen. *Pharm. Ind.*, **44**, 622-624.

Eckert, V. T., Knie, U., van Husen, N. and Heers, W. (1982b) Über die bioverfügbarkeit bei gelagerten suppositorien: Untersuchungen am beispiel des naproxen. *Pharm. Ind.*, **44**, 927-929.

Eldem, T., Speiser, P. and Hincal, A. (1991) Optimization of Spray-Dried and -Congealed Lipid Micropellets and Characterization of Their Surface Morphology by Scanning Electron Microscopy. *Pharm. Res.*, **8**, 47-54.

Eldem, T., Speiser, P. and Altorfer, H. (1991) Polymorphic Behaviour of Sprayed Lipid Micropellets and Its Evaluation by Differential Scanning Calorimetry and Scanning Electron Microscopy. *Pharm. Res.*, **8**, 178-184.

Eraker, S. A., Kirscht, J. P. and Becker, M. H. (1984) Understanding and improving patient compliance. *Ann. Intern. Med.*, **100**, 258-268.

Esquisabel, A., San Vicente, A., Igartua, M., Hernández, R. M., Gascón, A. R., Calvo, M. B. and Pedraz, J. L. (1996) Influence of melting point and hydrophilic/lipophilic balance on the release of salbutamol sulphate from lipid matrices. *S. T. P. Pharma Sci.*, **6**, 365-369.

F

Fassihi, A. R. (1987) Controlled drug release from a compressed heterogenous polymeric matrix: Kinetics of release. In *Controlled Drug Release, Volume 1*, Rubinstein, M. H. (ed.), Ellis Horwood Limited, 64-71.

Fell, J. T. and Newton, J. M. (1968) The tensile strength of lactose tablets. *J. Pharm. Pharmacol.*, **20**, 657-658.

Fell, J. T. and Newton, J. M. (1970) Determination of tablet strength by the diametral-compression test. *J. Pharm. Sci.*, **59**, 688-691.

Flack, E. and Krog, N. (1990) Emulsifiers in modern food production. *Lipid Technol.*, **2**, 11-13.

Flanders, P., Dyer, G. A. and Jordan, D. (1987) The control of drug release from conventional melt granulation matrices. *Drug Dev. Ind. Pharm.*, **13**, 1001-1022.

Fontan, J. E., Arnaud, P. and Chaumeil, J. C. (1991) Enhancing properties of surfactants on the release of carbamazepine from suppositories. *Int. J. Pharm.*, **73**, 17-21.

Ford, J. L. and Rubinstein, M. H. (1977a) Phase equilibria and stability characteristics of chlorpropamide-urea solid dispersions *J. Pharm. Pharmacol.*, **29**, 209-211.

Ford, J. L. and Rubinstein, M. H. (1977b) The effect of composition and ageing on the dissolution rates of chlorpropamide-urea solid dispersions. *J. Pharm. Pharmacol.*, **29**, 688-694.

Ford, J. L. and Rubinstein, M. H. (1978) Phase equilibria and dissolution rates of indomethacin-polyethylene glycol 6000 solid dispersions. *Pharm. Acta Helv.*, **53**, 327-332.

Ford, J. L. and Rubinstein, M. H. (1979) Ageing of indomethacin-polyethylene glycol 6000 solid dispersion. *Pharm. Acta Helv.*, **54**, 353-358.

Ford, J. L. and Rubinstein, M. H. (1980) Formulation and ageing of tablets prepared from indomethacin-polyethylene glycol 6000 solid dispersions. *Pharm. Acta Helv.*, **55**, 1-7.

Ford, J. L. (1984) The influence of polyethylene glycol molecular weight variation on the

properties of glutethimide-polyethylene glycol solid dispersions. *Pharm. Acta Helv.*, **59**, 280-288.

Ford, J. L. and Timmins, P. (eds.)(1989) *Pharmaceutical Thermal Analysis; Techniques and Applications.* Ellis Horwood, Chichester, 9-18.

Frömming, K. H. and Hosemann, R. (1985) Stability problems under special consideration of solid dispersion of drugs. *STP Pharma*, **1**, 660-665.

G

Garti, N., Schlichter, J. and Sarig, S. (1985) Polymorphism of even monoacid triglycerides in the presence of sorbitan monostearate, studied by the DSC. *Thermochimica Acta*, **93**, 29-32.

Garti, N., Aronhime, J. S. and Sarig, S. (1989) The role of chain length and an emulsifier on the polymorphism of mixtures of triglycerides. *J. Amer. Oil Chem. Soc.*, **66**, 1085-1089.

Gattefossé product information (1983, 1996), St. Priest.

Ginés, J. M., Veiga, M. D., Arias, M. J. and Rabasco, A. M. (1995) Elaboration and thermal study of interactions between cinnarizine and gelucire® 53/10 physical mixtures and solid dispersions. *Int. J. Pharm.*, **126**, 287-291.

Giron, D. (1986) Applications of thermal analysis in the pharmaceutical industry. *J. Pharm. Biomed. Anal.*, **4**, 755-770.

Griffin, V.J. and Laye, P.G. (1992) Differential Thermal Analysis and Differential Scanning Calorimetry. *Thermal Analysis - Techniques and Applications,* Charsley, E. L. and Warrington, S. B. (eds.) The Royal Society of Chemistry, Cambridge. 17-30.

Gunstone, F. D. (ed.)(1967) *An introduction to the Chemistry and Biochemistry of fatty acids and their glycerides,* Chapman and Hall, London.

Gunstone, F. D. (1994) Fatty acid structure. In *The lipid handbook, 2nd edition,* Gunstone, F. D., Harwood, J. L. and Padley, F. B. (eds.), Chapman and Hall, London, 1-2.

Gunstone, F. D. (ed.)(1996) In *Fatty acid and lipid chemistry,* Blackie Academic and Professional, London.

Gurr, M. I. and Harwood, J. L. (1991) Dietary lipids: implications for health and disease. In *Lipid biochemistry,* Chapman and Hall, London, 163-243.

Guth, O. J., Aronhime, J. and Garti, N. (1989) Polymorphic transitions of mixed triglycerides, SOS, in the presence of sorbitan monostearate. *J. Amer. Oil Chem. Soc.*, **66**,

1606-1612.

H

Hachiya, I., Koyano, T. and Sato, K. (1990) Fat polymorphism and chocolate crystallization. *Lipid Technol.*, **2**, 34-37.

Hagemann, J. W. and Rothfus, J. A. (1983) Polymorphism and transformation energetics of saturated monoacid triglycerides from differential scanning calorimetry and theoretical modelling. *J. Amer. Oil Chem. Soc.*, **60**, 1123-1131.

Hagemann, J. W. (1988) Thermal behaviour and polymorphism of acylglycerides. In *Crystallization and polymorphism of fats and fatty acids*, Garti, N. and Sato, K. (eds.), Marcel Dekker Inc., New York, 9-95.

Haighton, A. J. (1976) Blending, chilling and tempering of margarines and shortenings. *J. Amer. Oil Chem. Soc.*, **53**, 397-399.

Haines, P. J. (ed.) (1995) in *Thermal Methods of Analysis: Principles, Applications and Problems,* Blackie Academic and Professional, London, 67-71.

Haines, P. J., Reading, M. and Wilburn, F. W. (1998) Differential thermal analysis and differential scanning calorimetry. In *Handbook of thermal analysis and calorimetry. Vol. 1. Principles and Practice,* Brown, M. E. (ed.), Elsevier, Amsterdam, 279-361.

Harland, R. S., Gazzaniga, A. M., Sangalli, M. E., Colombo, P., Peppas, H. A. (1988) Drug / polymer matrix swelling and dissolution. *Pharm. Res.*, **5**, 488-494.

Harris, D. C. (1997) UV Spectrophotometer. *Exploring Chemical Analysis*. W. H. Freeman and Company, USA.

Hawley, A. R., Rowley, G., Lough, W. J. and Chatham, S. (1992) Physical and chemical characterisation of thermosoftened bases for molten filled hard gelatin capsule formulation. *Drug Dev. Ind. Pharm.*, **18**, 1719-1739.

Heathcock, J. F. (1993) Microscopy of fats. *Lipid Technol.*, **5**, 4-10.

Heller, J. (1984) Biodegradable polymers in controlled drug delivery. *Critical reviews in therapeutic drug carrier systems,* **1**, 39-90.

Hicklin, J. D., Jewell, G. G. and Heathcock, J. F. (1985) Combining microscopy and physical techniques in the study of cocoa butter polymorphs and vegetable fat blends. *Food Microstructure,* **4**, 241-248.

Higuchi, T. (1961) Rate of release of medicaments from ointment bases containing drugs

in suspension. *J. Pharm. Sci.*, **50**, 874-875.

Higuchi, T. (1963) Mechanism of sustained-action medication. Theoretical analysis of rates of release of solid drug dispersed in solid matrices. *J. Pharm. Sci.*, **52**, 1145-1149.

Hoerr, C. W. (1960) Morphology of fats, oil and shortenings. *J. Amer. Oil Chem. Soc.*, **37**, 539-546.

Hopfenberg, H. B. (1976) Controlled release from erodible slabs, cylinders and spheres, in *Controlled release polymeric formulations*, Paul, D. R. and Harris, F. W. (eds.), American Chemical Society, Washington.

Hosny, E. A., Kassem, A. A. and El-Shattawy, H. H. (1990) Influence of aging on the physical characteristics of ampicillin suppositories. *Drug Dev. Ind. Pharm.*, **16**, 1585-1589.

Howard, J. R. and Gould, P. L. (1987) Drug release from thermosetting fatty vehicles filled into hard gelatin capsules. *Drug Dev. Ind. Pharm.*, **13**, 1031-1045.

Huet de Barochez, B., Lapeyre, F. and Cuiné, A. (1989) Oral sustained release dosage forms comparison between matrices and reservoir devices. *Drug Dev. Ind. Pharm.*, **15**, 1001-1020.

J

Jacobsberg, B. and Ho, O. C. (1976) Studies in palm oil crystallisation. *J. Amer. Oil Chem. Soc.*, **53**, 609-617.

Ju, R. T. C., Nixon, P. R. and Patel, M. (1997) Diffusion coefficients of polymer chains in the diffusion layer adjacent to a swollen hydrophilic matrix. *J. Pharm. Sci.*, **86**, 1293-1298.

K

Kahela, P., Laine, E. and Antilla, M. (1987) A comparison of the bioavailability of paracetamol from a fatty and a hydrous suppository base and the effect of storage on the absorption in man. *Drug Dev. Ind. Pharm.*, **13**, 213-224.

Kawamura, K. (1979) The DSC thermal analysis of crystallisation behaviour in palm oil. *J. Amer. Oil Chem. Soc.*, **56**, 753-758.

Kawamura, K. (1980) The DSC thermal analysis of crystallisation behaviour in palm oil, II. *J. Amer. Oil Chem. Soc.*, **57**, 48-52.

Kawashima, Y., Takeuchi, H., Hino, T., Niwa, T., Lin, T., Sekigawa, F. and Kawahara, K. (1993) Low-substituted hydroxypropylcellulose as a sustained-release matrix base or

disintegrant depending on its particle size and loading in formulation. *Pharm. Res.*, **10**, 351-355.

Kellaway, I. W. and Marriot, C. (1975) Correlations between physical and drug release characteristics of polyethylene glycol suppositories. *J. Pharm. Sci.*, **64**, 1162-1165.

Kim, H. and Fassihi, R. (1997) A new ternary polymeric matrix system for controlled drug delivery of highly soluble drugs: I. Diltiazem hydrochloride. *Pharm. Res.*, **14**, 1415-1421.

Kopcha, M., Tojo, K. J. and Lordi, N. G. (1990) Evaluation of methodology for assessing release characteristics of thermosoftening vehicles. *J. Pharm. Pharmacol.*, **42**, 745-751.

Kopcha, M., Lordi, N. G. and Tojo, K. J. (1991) Evaluation of release from selected thermosoftening vehicles. *J. Pharm. Pharmacol.*, **43**, 382-387.

Koyano, T., Hachiya, I. and Sato, K. (1990) Fat polymorphism and crystal seeding effects on fat bloom stability of dark chocolate. *Food Structure*, **9**, 231-240.

Kristott, J. U. (1999) Physical properties of edible vegetable oils. In *LFRA Oils and Fats Handbook Series Volume 1, Vegetable oils and Fats*, Rossell, B. (ed.), Leatherhead Food RA, Surrey, PP1-19.

Kuhnert-Brandstätter, M. (ed.)(1971) *Thermomicroscopy in the analysis of pharmaceuticals.* Pergamon Press, Oxford, 34-42.

L

Laine, E., Auramo, P. and Kahela, P. (1988) On the structural behaviour of triglycerides with time. *Int. J. Pharm.*, **43**, 241-247.

Laustsen, K. (1991) The nature of fat bloom in molded compound coatings. *The Manufacturing Confectioner*, 137-144.

Laghoueg, N., Paulet, J., Taverdet, J.L. and Vergnaud, J.M. (1989) Oral polymer-drug devices with a core and an erodible shell for constant drug delivery. *Int. J. Pharm.*, **50**, 133-139.

Lee, R. E. (ed.) (1993) Assembled column of the Scanning Electron Microscopy. In *Scanning Electron Microscope*, Prentice-Hall Inc., New Jersey, 93-118.

Lehrian, D. W., Keeney, P. G. and Butler, D. R. (1980) Triglyceride characteristics of cocoa butter from cacao fruit matured in a microclimate of elevated temperature. *J. Amer. Oil Chem. Soc.*, **57**, 66-69.

Linhardt, R. J. (1989) Biodegradable polymers for controlled release of drugs. In *Controlled*

release of drugs: polymers and aggregate systems, Rosoff, M.(ed.), VCH Publishers Inc., New York, 53-95.

Lipp, M. and Anklam, E. (1998) Review of cocoa butter and alternative fats for use in chocolate-Part B. Analytical approaches for identification and determination. *Food Chemistry,* **62**, 99-108.

Liversidge, G. G., Grant, D. J. W. and Padfield, J. M. (1981) Influence of physicochemical interactions on the properties of suppositories I. Interactions between the constituents of fatty suppository bases. *Int. J. Pharm.,* **7**, 211-223.

Lloyd, G. R., Craig, D. Q. M. and Smith, A. (1997a) An investigation into the melting behaviour of binary mixes and solid dispersions of paracetamol and PEG 4000. *J. Pharm. Sci.,* **86**, 991-996.

Lloyd, G. R., Craig, D. Q. M. and Smith, A. (1997b) An investigation into the production of paracetamol solid dispersions in PEG 4000 using hot stage differential inteference contrast microscopy. *Int. J. Pharm.*, **158**, 39-46.

Loth, H. and Bosché, P. (1996) Solidification of molten hard fats in dependence on the chemical composition and thermal treatment. *Pharm. Ind.*, **58**, 161-166.

Lutton, E. S. (1950) Review of the polymorphism of saturated even triglycerides. *J. Amer. Oil Chem. Soc.*, **27**, 276-281.

Lutton, E. S. and Fehl, A. J. (1970) The polymorphism of odd and even saturated single acid triglycerides, C_8-C_{22}. *Lipids,* **5**, 90-99.

M

Magron, P., Rollet, M., Taverdet, J.L. and Vergnaud, J.M. (1987) Spherical oral polymer-drug device with two polymers for constant drug delivery. *Int. J. Pharm.*, **38**, 91-97.

Manning, D. and Dimick, P. (1985) Crystal Morphology of Cocoa Butter. *Food Microstructure,* **4**, 249-265.

Moës, A. and Jaminet, F. (1976) Influence of aging of suppositories on rectal absorption of paracetamol. *Pharm. Acta Helv.,* **51**, 119-125.

Mouricout, A. M., Gerbaud, D., Brossard, C. and Lefort des Ylouses, D. (1990) Gélules à matrice semi-solide de Gélucire; lyodisponibilité et étude structurale. *S. T. P. Pharma,* **6**, 368-375.

Müller, B. W. (1984) Physicochemical parameters affecting chemical stability and

bioavailability of drugs in suppository bases. In *Rectal Therapy*, Glas, B. and de Blaey, C. J. (eds.), JR Prous, Barcelona, 21-26.

Müller, B. W., Hassan, I. and Heers, W. (1989) Untersuchung des thermischen Verhaltens von Glyceriden (Studies on the thermal conditions of glycerides). *Pharm. Ind.*, **51**, 681-685.

N

Nickless, H. and Sidaway, A. F. (1980) Use of fat in confectionery. In *Fats and oils: Chemistry and technology*, Hamilton, R. J. and Bhati, A. (eds.), Applied Science Publishers Ltd., London, 167-180.

O

Okada, M. (1970) Whisker-like growth of triglyceride. *J. Cryst. Growth*, **7**, 371-374.

Ortigosa, C., Gaudy, D., Jacob, M. and Puech, A. (1991) The role of gelucire in the availability of theophylline in semi-solid matrix capsules. A study of factors: pH, melting point, HLB and paddle rotation speed. *Pharm. Acta Helv.*, **66**, 311-315.

Ouriemchi, E. M., Bouzon, J. and Vergnaud, J. M. (1994) Oral dosage forms with a core and shell with the same polymer containing different drug concentrations. *Int. J. Pharm.*, **102**, 47-54.

Ouriemchi, E. M., Bouzon, J. and Vergnaud, J. M. (1995) Modelling the process of controlled release of drug in in vitro and in vivo tests. *Int. J. Pharm.*, **113**, 231-240.

P

Padawer, J. (1968) The Nomarski interference-contrast microscope. An experimental basis for image interpretation. *J. Roy. Microsc. Soc.*, **88**, 305.

Parab, P. V., Oh, C. K. and Ritschel, W. A. (1986) Sustained release from Precirol (Glycerol palmito-stearate) matrix. Effect of mannitol and hydroxypropylmethylcellulose on the release of theophylline. *Drug Dev. Ind. Pharm.*, **12**, 1309-1327.

Peppas, N., Gurny, R., Doelker, E. and Buri, P. (1980) Modelling of drug diffusion through swellable polymeric systems. *J. Membrane Sci.*, **7**, 241-253.

Peppas, N. A. (1985) Analysis of fickian and non-fickian drug release from polymers. *Pharm. Acta Helv.*, **60**, 110-111.

Peppas, N. A. and Korsmeyer, R (1986) *Hydrogels in Medicine and Pharmacy Volume 3:*

Properties and Application, Peppas, N. (ed.), CRC, Boca Raton, 109-305.

Pike, M. (1980) Growth of importance of palm oil in the 1970's. In *Fats and oils: Chemistry and technology,* Hamilton, R. J. and Bhati, A. (eds.), Applied Science Publishers Ltd., London, 215-247.

Plášek, J. and Reischig, J. (1998) Trasmitted-light microscopy for biology: A physicist's point of view. Part 2. *Proc. Roy. Microsc. Soc.*, **33**, 196-205.

Prapaitakul, W., Sprockel, O. L. and Shivanand, P. (1991) Release of chlorpheniramine maleate from fatty acid ester matrix disks prepared by melt-extrusion. *J. Pharm. Pharmacol.*, **43**, 377-381.

Pryce-Jones, R. H., Grant, K. M. and Eccleston, G. M. (1989) Polymorphism of fatty acid diamides of ethylene diamines and their detection in aged aminophylline suppositories. *J. Pharm. Pharmacol.*, **41**, 106P.

R

Ratsimbazafy, V. and Brossard, C. (1992) Optimisation of the release of theophylline derivatives from gelucire matrices. *Pharm. Acta Helv.*, **67**, 166-171.

Ratsimbazafy, V., Bourret, E. and Brossard, C. (1997) Influence of the manufacturing process on the release of proxyphylline from lipid matrices. *Pharmazie,* **52**, 863-866.

Regdon Sr., G., Gombkötő, S., Regdon Jr., G. and Selmeczi, B. (1994) Formulation and in vitro study of antibacterial vaginal suppositories. *Pharm. Acta Helv.*, **69**, 141-148.

Remuñán, C., Mrhar, A., Primozic, S., Karba, R. and Vila-Jato, J. L. (1992a) Sustained release nifedipine formulations: Moment, modelling and simulation as pharmacokinetic analysis approach. *Drug Dev. Ind. Pharm.*, **18**, 187-202.

Remuñán, C., Bretal, M. J., Núñez, A. and Vila Jato, J. L. (1992b) Accelerated stability study of sustained-release nifedipine tablets prepared with gelucire. *Int. J. Pharm.*, **80,** 151-159.

Ritger, P. L. and Peppas, N. A. (1987) *J. Cont. Rel.*, **5**, 37-42.

Rivarola, G., Segura, J. A., Añón, M. C. and Calvelo, A. (1987) Crystallisation of hydrogenated sunflower-cottoseed oil. *J. Amer. Oil Chem. Soc.*, **64**, 1537-1543.

Roussin, P. and Laforêt, J. P. (1997) Gelucire®44/14: A high performance system to enhance bioavailability of poorly water soluble drugs. *Bull. Tech. Gattefossé*, **No.90**, 51-57.

S

Samsudin, S. and Rahim, M. A. A (1996) Use of palm oil mid-fraction in white chocolate formulation. *J. Sci. Food Agric.*, **71**, 483-490.

Saito, H., Takatori, T., Higashi, T. and Nakamura, Y (1994) Design of novel controlled-release suppositories containing polyglycerol ester of fatty acid. *Chem. Pharm. Bull.*, **42**, 1506-1509.

San Vicente, A., Hernández, M. R., Gascón, A. R., Calvo, B. and Pedraz, J. L. (1998) Influence of ageing on the release of salbutamol sulphate from capsules elaborated with Gelucire 35/10, 48/09 and 46/07. *Proc. 2nd World Meeting APGI/APV, Paris, 25/28 May 1998*, 261-262.

Saraiya, D. and Bolton, S. (1990) The use of Precirol to prepare sustained release tablets of theophylline and quinidine gluconate. *Drug. Dev. Ind. Pharm.*, **16**, 1963-1969.

Sato, K. and Kuroda, T. (1987) Kinetics of melt crystallisation and transformation of tripalmitin polymorphs. *J. Amer. Oil Chem. Soc.*, **64**, 124-127.

Sato, K. and Garti, N. (eds.)(1988) Crystallization and polymorphic transformation: An introduction. In *Crystallization and polymorphism of fats and fatty acids*, Marcel Dekker Inc., New York, 3-7.

Seguine, E. S. (1991) Tempering-The inside story. *The Manufacturing Confectioner*, **71**, 117-125.

Sekiguchi, K. and Obi, N. (1961) Studies on absorption of eutectic mixture. I. A comparison of the behaviour of eutectic mixture of sulfathiazole and that of ordinary sulfathiazole in man. *Chem. Pharm. Bull.*, **9**, 866-872.

Senior, N. (1974) Rectal administration of drugs. *Adv. Pharm. Sci.*, **4**, 363-435.

Serajuddin, A. T. M., Sheen, P. C., Mufson, D., Bernstein, D. F. and Augustine, M. A. (1988) Effect of vehicle amphiphilicity on the dissolution and bioavailaility of a poorly water soluble drug from solid dispersions. *J. Pharm. Sci.*, **77**, 414-417.

Seta, Y., Higuchi, F., Otsuka, T., Kawahara, Y., Nishimura, K., Okada, R. and Koike, H. (1988) Preparation and pharmacological evaluation of captopril sustained release dosage forms using oily semisolid matrix. *Int. J. Pharm.*, **41**, 263-269.

Shah, N. V., Phuapradit, W. and Ahmed, H. (1996) Liquid/ semi-solid filling in hard gelatin capsules: formulations and processing considerations. *Bulletin Technique Gattefossé*, **No. 89**, 27-37.

Shehab, M. A. and Richards, J. H. (1996a) Studies on the in vitro release of theophylline from polyethylene glycol-polyvinyl acetate mixtures liquid filled into hard gelatin capsules. *Drug Dev. Ind. Pharm.*, **22**, 291-298.

Shehab, M. A. and Richards, J. H. (1996b) Studies on the in vitro release of ibuprofen from polyethylene glycol-polyvinyl acetate mixtures liquid filled into hard gelatin capsules. *Drug Dev. Ind. Pharm.*, **22**, 645-651.

Sjökvist, E. and Nyström, C. (1988) Physicochemical aspects of drug release. VI. Drug dissolution rate from solid particulate dispersions and the importance of carrier and drug particle properties. *Int. J. Pharm.*, **47**, 51-66.

Sjökvist Saers, E., Nyström, C. and Aldén, M. (1993) Physicochemical aspects of drug release. XVI. The effect of storage on drug dissolution from solid dispersions and the influence of cooling rate and incorporation of surfactant. *Int. J. Pharm.*, **90**, 105-118.

Skoog, D. A., Holler, F. J. and Nieman, T. A. (eds.) (1998) The Scanning Electron Microscope (SEM). In *Principles of instrumental analysis,* Harcourt Brace College Publishers, Philadelphia, 550-552.

Slayter, E. and Slayter, H. (eds.)(1992) *Light and Electron Microscopy.* Cambridge University Press, Cambridge.

Small, D. M. (ed.)(1986) In *The physical chemistry of lipids, Handbook of Lipid Research No. 4,* Plenum Press, New York.

Smith, P. and Pennings, A. J. (1974) Eutectic crystallisation of pseudo binary systems of polyethylene and high melting diluents. *Polymer,* **15**, 413-419.

Sutananta, W., Craig, D. Q. M. and Newton, J. M. (1994a) An investigation into the effect of preparation conditions on the structure and mechanical properties of pharmaceutical glyceride bases. *Int. J. Pharm.*, **110**, 75-91.

Sutananta, W., Craig, D. Q. M. and Newton, J. M. (1994b) The effects of ageing on the thermal behaviour and mechanical properties of pharmaceutical glycerides. *Int. J. Pharm.*, **111**, 51-62.

Sutananta, W., Craig, D. and Newton, J. (1995a) An Evaluation of the Mechanisms of Drug Release from Glyceride bases. *J. Pharm. Pharmacol.*, **47**, 182-187.

Sutananta, W., Craig, D. Q. M. and Newton, J. M. (1995b) An investigation into the effects of preparation conditions and storage on the rate of drug release from pharmaceutical glyceride bases. *J. Pharm. Pharmacol.*, **47**, 355-359.

T

Taylor, J. B. and Simpkins, D. E. (1981) Aminophylline suppositories in vitro dissolution and bioavailability in man. *Pharm. J.*, **227**, 601-603.

Thoma, K. and Serno, P. (1982) Temperaturabhängigkeit der Schmelzzeitverlängerung von Hartfettsuppositorien (Correlation between storage temperature and the increase in melting time of hard fat suppositories). *Pharm. Ind.*, **44**, 1074-1080.

Timms, R. E. (1980) The phase behaviour and polymorphism of milk fat, milk fat fractions and fully hardened milk fat. *Aust. J. Dairy Technol.*, **35**, 47-53.

Timms, R. E. (1984) Phase behaviour of fats and their mixtures. *Prog. Lipid Res.*, **23**, 1-38.

Trigger, D., Davies, P. and Parker, M. (1988) The relationship of rate and kinetics of release of theophylline from a new matrix tablet formulation with content of release control agent. Drug Dev. Ind. Pharm., **14**, 2631-2647.

U

Urbanski, J. J. (1991) Continuation of tempering after production. *The Manufacturing Confectioner*, **71**, 126-130.

US Pharmacopeia 24, National Formulary 19 (1999), The US Pharmacopeial Convention Inc., Rockville, MD.

V

Vial-Bernasconi, A. C., Aebi, A., Doelker, E., Buri, P., Schulz, P. and Dick, P. (1987) Evaluation of highly dosed sustained release hard gelatin capsule formulations based on lipid matrix systems. *Proceedings of the Third European Congress of Biopharmaceutics and Phamacokinetics, Vol. I,* pp 155-165.

Vial-Bernasconi, A. C., Buri, P., Doelker, E., Beyssac, E., Duchaix, G. and Aiache, J. M. (1995) In vivo evaluation of an indomethacin monolithic, extended zero-order release hard-gelatin capsule formulation based on saturated polyglycolysed glycerides. *Pharm. Acta Helv.*, **70**, 307-313.

Vila-Jato, J. L., Remunan, C. and Martinez, R. (1990) Possible use of Gelucires in controlled-release nifedipine tablets. *S.T.P Pharma.*, **6**, 88-92.

Vila-Jato, J. L. and Delgado-Charro, B. (1990) Influence of melting point and HLB on the release of amoxicillin from granulates containing Gelucire as excipients. *STP Pharma.*, **6**,

287-292.

W

Waginaire, L. and Glass, B. (1981) Gélucire®. *Bull. Tech. Gattefossé*, **74**, 7-12.

Wendlandt, W. W. (ed.) (1986) Differential thermal analysis and differential scanning calorimetry. In *Thermal Analysis,* John Wiley and Sons Inc., New York, 213-298.

Westerberg, M. and Nyström, C. (1993) Physicochemical aspects of drug release. XVII. The effect of drug surface area coverage to carrier materials on drug dissolution from ordered mixtures. *Int. J. Pharm.*, **90**, 1-17.

Wunderlich, B. (ed.)(1990) In *Thermal analysis*, Academic Press Inc, San Diego.

Wuidart, W. (1996) Palm oil and its fractions. In *Oil and Fats Manual Volume 1*, Karleskind, A.(ed.), Lavoisier Publishing, Paris, 233-246.

Y

Yap, P. H., deMan, J. M. and deMan, L. (1989a) Polymorphic stability of hydrogenated canola oil as affected by addition of palm oil. *J. Amer. Oil Chem. Soc.*, **66**, 1784-1791.

Yap, P. H., deMan, J. M. and deMan, L. (1989b) Crystallization characteristics of hydrogenated canola oil as affected by addition of palm oil. *J. Amer. Oil Chem. Soc.*, **66**, 1792-1795.

York, P. and Pilpel, N. (1973) The tensile strength and compression behaviour of lactose, four fatty acids and their mixtures in relation to tableting. *J. Pharm. Pharmacol.*, **25**(Dec suppl.), 1P-11P.

Yoshida, T., Itoh, Y., Gomita, Y. and Oishi, R. (1991) Influence of storage temperature on indomethacin release from fatty base suppositories in vitro and in vivo. *Acta Med. Okayama,* **45**, 37-42.

Yoshino, H., Kobayashi, M. and Samejima, M. (1981) Polymorphic transition rate of semisynthetic fatty suppository bases. Chem. Pharm. Bull., **29**, 2661-2669.

Yoshino, H., Hagiwara, Y., Kobayashi, M. and Samejima, M. (1984) Estimation of polymorphic degree of pharmaceutical raw materials. Chem. Pharm. Bull., **32**, 1523-1536.